

**THE CHEMICAL
INVESTIGATION
OF FOUR MEDICINAL
PLANTS**

By Angela Langlois

**Submitted in partial fulfilment of the
requirements for the degree of**

Master of Science

in the

**Department of Chemistry,
University of Natal, Durban**

2000

TABLE OF CONTENTS

	Page
Preface	i
Acknowledgements	ii
List of Abbreviations	iii
List of Figures	iv
List of Schemes	vi
List of Tables	vii
Foreword to Experimental Sections	viii
Abstract	x
Chapter 1: General Introduction	
1.1 : Introduction to Triterpenoids	1
1.2 : Introduction to Coumarins	15
Chapter 2: Extractives from <i>Agave attenuata</i>	
2.1 : Introduction	21
2.2 : Results and Discussion	24
2.2.1 : Structural Elucidation of Compound I	24
2.2.2 : Structural Elucidation of Compound II	29
2.3 : Experimental	37
2.3.1 : Physical Data for Compound I	38
2.3.2 : Physical Data for Compound II	39
2.4 : References	40

Chapter 3: Extractives from *Balanites maughamii*

3.1	: Introduction	41
3.2	: Results and Discussion	45
3.2.1	: Structural Elucidation of Compound III	45
3.2.2	: Structural Elucidation of Compound IV	49
3.3	: Experimental	51
3.3.1	: Physical Data for Compound III	53
3.3.2	: Physical Data for Compound IV	54
3.4	: References	55

Chapter 4: Extractives from *Astrotrichilia parvifolia*

4.1	: Introduction	56
4.2	: Results and Discussion	58
4.2.1	: Structural Elucidation of Compound V	58
4.3	: Experimental	63
4.3.1	: Physical Data for Compound V	64
4.4	: References	65

Chapter 5: Extractives from *Combretum fragrans*

5.1	: Introduction	66
5.2	: Scanning Electron Microscopy	69
5.3	: Results and Discussion	71
5.3.1	: Structural Elucidation of Compound VI	71
5.3.2	: Structural Elucidation of Compound VII	75
5.3.3	: Structural Elucidation of Compound VIII	78
5.3.4	: Structural Elucidation of Compound IX	82
5.3.5	: Structural Elucidation of Compound X	83
5.3.6	: Structural Elucidation of Compound XI	87

5.4	: Experimental	90
5.4.1	: Physical Data for Compound VI	91
5.4.2	: Physical Data for Compound VII	92
5.4.3	: Physical Data for Compound VIII	93
5.4.4	: Physical Data for Compound IX	94
5.4.5	: Physical Data for Compound X	95
5.4.6	: Physical Data for Compound XI	96
5.5	: References	97

Appendix

List of Spectra	99
-----------------	----

PREFACE

The experimental work described in this thesis was carried out in the Department of Chemistry, University of Natal, Durban, from February 1999 to February 2000 under the supervision of Professor D.A. Mulholland.

This study represents original work by the author and has not been submitted in any other form to another university. Where use was made of the work of others, it has been duly acknowledged in the text.

Signed:

A handwritten signature in blue ink, appearing to read "Langlois", is written over a horizontal dashed line.

A. Langlois BSc. Hons (Natal)

I hereby certify that the above statement is correct.

Signed:

A handwritten signature in blue ink, appearing to read "D.A. Mulholland", is written over a horizontal dashed line.

Professor D.A. Mulholland PhD. (Natal)

ACKNOWLEDGEMENTS

I would like to express my sincere thanks to Professor D.A. Mulholland for her continuous support and guidance throughout the year. Her friendship and encouragement have been greatly appreciated, and her willingness to help with the most trivial of problems has been invaluable. This work would not have been possible without her financial assistance, and for this I am truly grateful.

I would also like to thank Professor C.B. Rogers for his assistance in the past six months. His help and advice has been most appreciated. Thanks must also be extended to Dr. Neil Crouch, Professor Appleton, Dr. M. Randrianarivelojosia and Professor C.B. Rogers for the collection of the plants that I studied. I gratefully acknowledge Dr. P. Boschhoff at the Cape Technikon for the running of the mass spectra, and Professor C. Lauvaud at the Universite de Reims, France for all her help with the elucidation of the structure of compound I.

Special thanks must be extended to Mr. B. Parel for all his help and guidance in the laboratory, Mr. D. Jagjivan for running all my NMR spectra and Mr. E. Makhaza for always keeping our laboratory tidy. I would like to thank all the technical staff not directly involved in the Natural Products Research Department, but have always been in assistance in various ways.

Thank you to my all my colleagues Miss T. Pohl, Miss K. Thornell, Mrs C. Koorbanally, Mr. N. Koorbanally, Mr P. Cheplogoi and Mr. P Coombes for all their advice and friendship in the laboratory and who have made this year so memorable. I also acknowledge the University of Natal and the Foundation for Research and Development for their financial assistance.

Finally, I would like to thank my family for their unfailing love, support and encouragement. Words cannot express how grateful I am for moulding me into the person I am today. I would especially like to thank my husband, Dion, for all the sacrifices he has made and for being my pillar of strength during the past year. You are my life, my love, my everything.

LIST OF ABBREVIATIONS

ADEPT	- distortionless enhancement by polarisation transfer
ADP	- adenosine diphosphate
ATP	- adenosine triphosphate
Brs	- broad singlet
c	- concentration
^{13}C NMR	- carbon-13 nuclear magnetic resonance
COSY	- correlated nuclear magnetic resonance spectroscopy
d	- doublet
dd	- double doublet
ddd	- double double doublet
DMAPP	- dimethylallyl diphosphate
^1H NMR	- proton nuclear magnetic resonance
HETCOR	- heteronuclear shift correlation nuclear magnetic resonance
HMBC	- heteronuclear single bond coherence
HSQC	- heteronuclear multiple quantum coherence
Hz	- Hertz
IPP	- isopentenyl diphosphate
IR	- infra red
m	- multiplet
Me	- methyl group
NADPH	- nicotinamide adenine dinucleotide phosphate
NOESY	- nuclear Overhauser effect
ppm	- parts per million
q	- quartet
s	- singlet
t	- triplet
TLC	- thin layer chromatography
TOCSY	- total correlation spectroscopy

LIST OF FIGURES

	Page
Figure 1.1 : Structures of different classes of triterpenoids	1
Figure 1.2 : Terpenoid groups derived from mevalonic acid	2
Figure 1.3 : The biochemically active isoprene units	3
Figure 1.4 : Inhibiting products of the acetate mevalonate pathway	5
Figure 1.5 : The derivation of phytosterols	13
Figure 1.6 : Structure of caffeic acid	16
Figure 2.1 : Structure of agamanone	22
Figure 2.2 : Compounds isolated from <i>Agave americana</i>	22
Figure 2.3 : Structure of agavasaponin E and agavasaponin H	23
Figure 2.4 : Compound I: timosaponin A III	24
Figure 2.5 : Compound II 3 β -hydroxy-5 α -pregn-16-en-20-one 3-O-tetrasaccharide	29
Figure 2.6 : The structure of three sugars	32
Figure 2.7 : NOESY correlations for the aglycone of compound II	33
Figure 3.1 : The <i>Balanites maughamii</i> tree	41
Figure 3.2 : Structure of yamogenin	42
Figure 3.3 : Structure of balanitin-1, balanitin-2 and balanitin-3	43
Figure 3.4 : Compounds isolated from <i>Balanites aegyptiaca</i>	44
Figure 3.5 : Structure of balanitol	44
Figure 3.6 : Compound III: scopoletin	45
Figure 3.7 : NOE correlations for compound III	47
Figure 3.8 : Compound IV: stigmasterol	49
Figure 4.1 : Compounds isolated from <i>Astrotrichilia asterotricha</i>	56
Figure 4.2 : Structure of voamatins A and B	57
Figure 4.3 : Structure of voamatins C and D	57
Figure 4.4 : Compound V: shoreic acid	58

Figure 5.1	: Cycloartane compounds from <i>Combretum erythrophyllum</i>	67
Figure 5.2	: Combretastatins isolated from <i>Combretum caffrum</i>	68
Figure 5.3	: Developing trichomes on a young leaf shoot	69
Figure 5.4	: Trichomes on a mature leaf	70
Figure 5.5	: Desiccating trichomes on an old leaf	70
Figure 5.6	: Compound VI: lupeol	71
Figure 5.7	: Compound VII: lupenone	75
Figure 5.8	: Compound VIII: lupeol 3 β -docosanoate	78
Figure 5.9	: Compound IX: lupeol 3 β -eicosanoate	82
Figure 5.10	: Compound X: hennadiol	83
Figure 5.11	: Compound XI: 30-hydroxylupenone	87

LIST OF SCHEMES

	Page
Scheme 1.1 : The formation of hydroxymethylglutaryl CoA	3
Scheme 1.2 : The formation of L-mevalonic acid	4
Scheme 1.3 : Phosphorylation of mevalonic acid	4
Scheme 1.4 : Formation and isomerisation of isopentenyl diphosphate	6
Scheme 1.5 : The formation of farnesyl diphosphate	7
Scheme 1.6 : The formation of squalene	8
Scheme 1.7 : Formation of the squalene-2,3-epoxide intermediate	9
Scheme 1.8 : The cyclisation of squalene-2,3-epoxide	10
Scheme 1.9 : Rearrangement of the dammarenyl cation	11
Scheme 1.10 : Formation of lanosterol and cycloartenol	12
Scheme 1.11 : The biosynthesis of coumarins	15
Scheme 1.12 : Formation of scopolin	16
Scheme 1.13 : The biosynthesis of daphnin, cichoriin, aesculetin and aesculin	17
Scheme 1.14 : The biosynthesis of melilotic acid glucoside in sweet clover	18
Scheme 1.15 : The formation of dicoumarol in spoilt hay	19
Scheme 2.1 : The biosynthesis of steroidal glycosides and pregnanes	34
Scheme 3.1 : Extraction of <i>Balanites maughamii</i>	52
Scheme 5.1 : The mass spectrometric fragmentation of compound VIII	80
Scheme 5.2 : The mass spectrometric fragmentation of compound IX	82

LIST OF TABLES

	Page
Table 2.1 : ¹ H NMR data for compound I and literature data for timosaponin A III	26
Table 2.2 : ¹³ C NMR data for compound I and literature data for timosaponin A III	27
Table 2.3 : NMR data for compound II	35
Table 2.4 : NMR data for sugars attached to compound II	36
Table 3.1 : ¹ H NMR data for compound III and literature data for scopoletin	48
Table 3.2 : ¹³ C NMR data for compound III and literature data for scopoletin	48
Table 3.3 : ¹ H NMR data for compound IV and literature data for stigmasterol	50
Table 4.1 : ¹ H NMR data for compound V and literature data for shoreic acid	61
Table 4.2 : ¹³ C NMR data for compound V and literature data for shoreic acid	62
Table 5.1 : ¹ H NMR data for compound VI and literature data for lupeol	73
Table 5.2 : ¹³ C NMR data for compound VI and literature data for lupeol	74
Table 5.3 : ¹ H NMR data for compound VII and literature data for lupenone	76
Table 5.4 : ¹³ C NMR data for compound VII and literature data for lupenone	77
Table 5.5 : ¹ H NMR data for compound VIII and literature data for lupeol	80
Table 5.6 : ¹³ C NMR data for compound VIII and literature data for lupeol	81
Table 5.7 : ¹ H NMR data for compound X and literature data for hennadiol	85
Table 5.8 : ¹³ C NMR data for compound X	86
Table 5.9 : ¹ H NMR data for compound XI and literature data for 30-hydroxylupenone	88
Table 5.10 : ¹³ C NMR data for compound XI and literature data for 30-hydroxylupenone	89

FOREWORD TO EXPERIMENTAL SECTIONS.

As the following techniques are common to chapters 2 – 5, they are described here:

Nuclear Magnetic Resonance (NMR) Spectroscopy

All the NMR spectra were recorded using a 300 MHz Varian Gemini spectrometer and a Varian Unity Inova 400 MHz spectrometer. The spectra were obtained using the solvents deuterated chloroform (CDCl_3) and deuterated methanol (CD_3OD).

Infra Red (IR) Spectroscopy

The infra red spectra were recorded using a Nicolet Impact 400 D spectrometer. In all cases the dissolved sample was dropped onto a NaCl disc and the spectrometer was calibrated against air.

High Resolution Mass Spectrometry

Gas chromatography/Mass spectrometry spectra were obtained using a Finnigan 1020 GC/MS spectrometer using both injection and solid probe methods. High resolution mass spectra were recorded on a Kratos 9/50 HRMS instrument by Dr. P. Boshoff at Cape Technikon.

Melting Points

A Kofler micro-hot stage melting point apparatus was used to record the melting points of all the crystalline compounds isolated in this work. All values are uncorrected.

Column Chromatography

Columns ranging from 1cm to 4cm in diameter were used in the separation procedure. Merck 9385 silica gel was used as the solid phase while elution was allowed to proceed via gravity. Solvents used included hexane, dichloromethane, ethyl acetate and methanol in varying proportions depending on the polarity of compounds being isolated.

Thin Layer Chromatography (TLC)

The progress of column chromatography was monitored using thin layer chromatographic plates. Aluminium backed plates (Merck Art 5554) coated with silica gel (0.2 mm thick) and containing a fluorescent indicator (F254) were used. The plates were developed using anisaldehyde spray reagent consisting of anisaldehyde, conc. H_2SO_4 and methanol in a ratio of 1:2:97, followed by heating of the plates.

Acetylations

Compounds V, XI and XII were acetylated. Approximately 20 mg of the compound was placed in a stoppered round-bottomed flask with pyridine (1 cm^3) and acetic anhydride (1 cm^3). The contents of the flask were allowed to react at room temperature for 24 hours. Thereafter, methanol ($3 \times 10 \text{ cm}^3$) was added to remove the excess acetic anhydride, and the pyridine was removed by the addition of toluene ($3 \times 10 \text{ cm}^3$). The final traces of toluene were removed by further addition of methanol ($3 \times 10 \text{ cm}^3$). All solvents were removed on a rotor evaporator.

ABSTRACT

This thesis describes a phytochemical investigation of four medicinal plants, namely, *Agave attenuata* (Agavaceae), *Balanites maughamii* (Balanitaceae), *Astrotrichilia parvifolia* (Meliaceae) and *Combretum fragrans* (Combretaceae).

Investigations of *A. attenuata* and *B. maughamii* were undertaken as biological studies have shown that these plants possess anti-bilharzial properties. Schistosomiasis is an important public health issue in South Africa and attempts to deal with infected rural communities have forced scientists to focus their attention on snail control using plant molluscicides. *A. attenuata* yielded two glycosides, timosaponin A III (**compound I**) and 5 α -pregn-16-en-20-one-3 β -O-tetrasaccharide (**compound II**), while a coumarin, scopoletin (**compound III**) and a sterol, stigmasterol (**compound IV**) were isolated from *B. maughamii*

A dammarane, shoreic acid (**compound V**) was isolated from *A. parvifolia*, this formed part of an ongoing investigation into the Meliaceae of Madagascar.

Plants of the family Combretaceae are widespread in Africa and are used by traditional healers for a wide range of illnesses. The leaves and bark are used abundantly, however, the winged fruits are never eaten as they are highly toxic to animals and humans. The leaf surface is covered with epidermal scale-like trichomes through which acidic triterpenoid mixtures are secreted. Six lupane-type triterpenoids were isolated from *C. fragrans*, namely, lupeol (**compound VI**), lupenone (**compound VII**), lupeol 3 β -docosanoate (**compound VIII**), lupeol 3 β -eicosanoate (**compound IX**) hennadiol (**compound X**) and 30-hydroxylupenone (**compound XI**).

All the above compounds were isolated by column chromatography and the structures were elucidated by means of NMR spectroscopy, mass spectrometry and infra red spectroscopy.

CHAPTER 1

General Introduction

1.1 Introduction to Triterpenoids

In this investigation several triterpenoids and a coumarin were isolated and therefore their biosynthesis will be discussed. The terpenes are amongst the most widespread groups of natural products and are derived from a common biosynthetic pathway based on mevalonate as parent. Terpenes are typically found in higher plants, lower animals (coelenterates, molluscs and arthropods), fungi, algae and lichens¹. Members of this class form the basis of mammalian sex hormones, pheromones and plant hormones.

Despite being structurally diverse, terpenoids are composed of a single unifying feature, the C₅ isoprene unit (1). In 1953 Ruzicka² proposed the “Isoprene Rule” which stated that all terpenoids are formed by the head-to-tail linkage of isoprene units. This rule was later improved and extended to the “Biogenetic Isoprene Rule” which included different types of terpenoids derived from a single parent compound unique to that class i.e. geraniol (2) (C₁₀), farnesol (3) (C₁₅), geranylgeraniol (4) (C₂₀), and squalene (5) (C₃₀) (Figure 1.1), involving tail-to-tail or head-to-tail cyclisation and/or rearrangement.

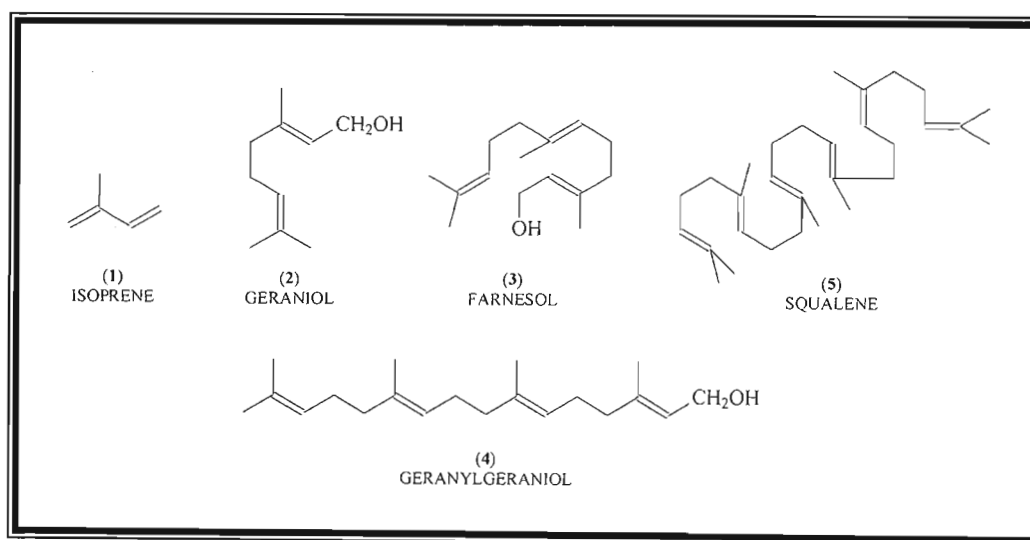


Figure 1.1 Structures of different classes of triterpenoids.

Terpenoids are grouped according to the number of isoprene units they contain i.e. hemiterpenoids, C_5 ; monoterpenoids, C_{10} ; sesquiterpenoids, C_{15} ; diterpenoids, C_{20} ; triterpenoids, C_{30} ; and carotenoids, C_{40} (Figure 1.2).

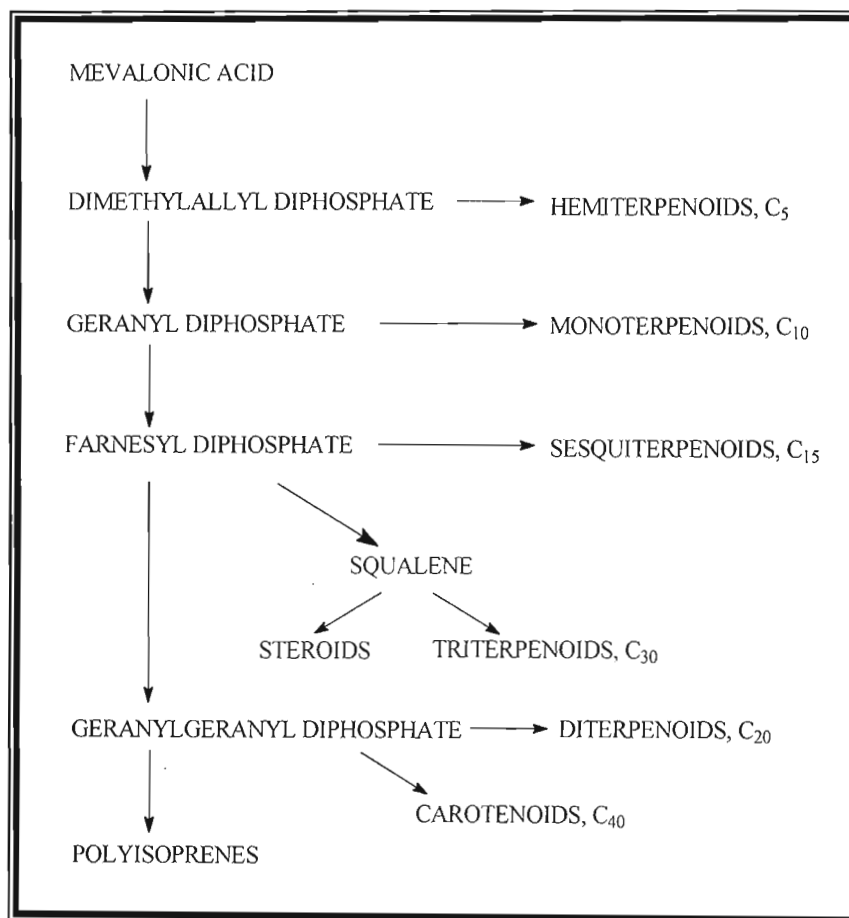


Figure 1.2 Terpenoid groups derived from mevalonic acid³.

However isoprene is not the biogenetic precursor of terpenoids and is only rarely found in nature⁴. The biochemically active isoprene units are the diphosphate esters, dimethylallyl diphosphate (DMAPP) (6) and isopentenyl diphosphate (IPP) (7)¹ (Figure 1.3)

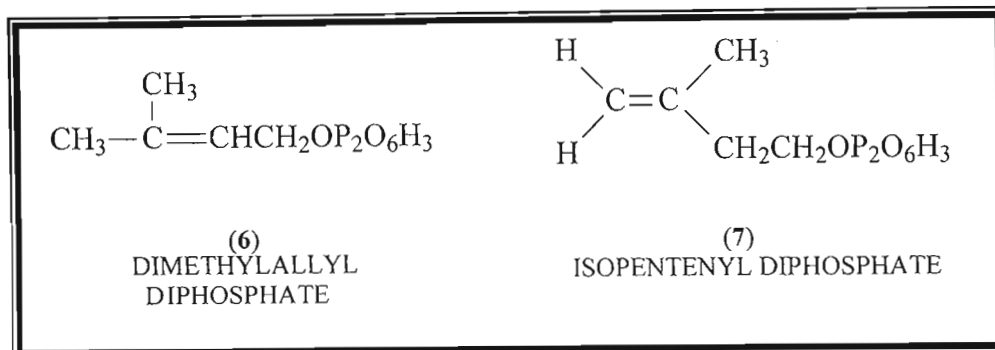
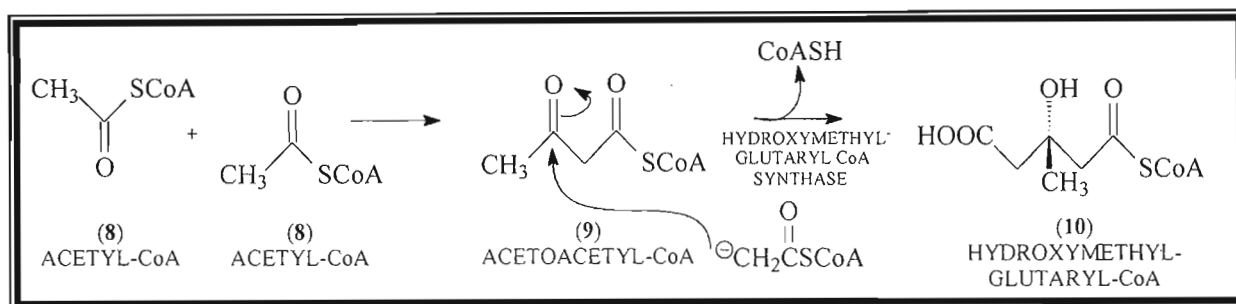


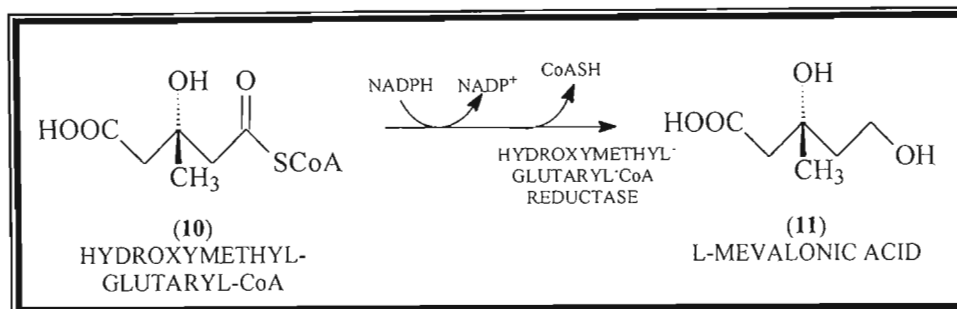
Figure 1.3 The biochemically active isoprene units.

The triterpenoids form a very diverse group of naturally occurring compounds, which are widely distributed throughout the plant kingdom. The starting material for the synthesis of triterpenoids is acetyl-CoA (8) (Scheme 1.1).



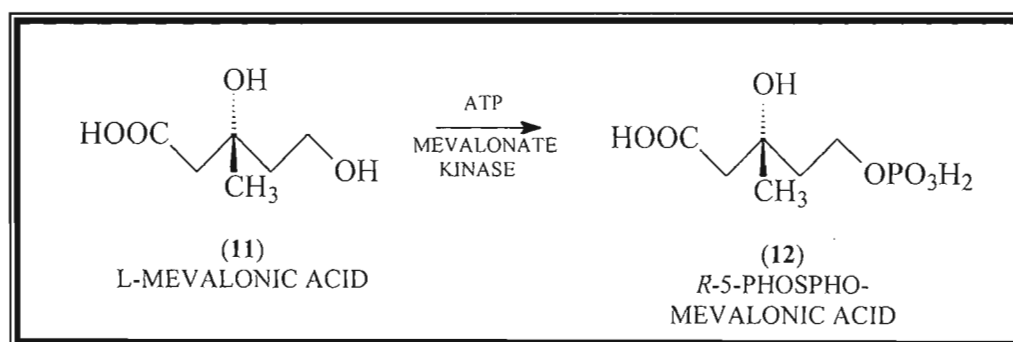
Scheme 1.1 The formation of hydroxymethylglutaryl-CoA¹.

Two molecules of acetyl-CoA combine in a Claisen condensation to form acetoacetyl-CoA (9). A third molecule of acetyl-CoA is incorporated via a stereospecific aldol addition¹ to form (3S)-3-hydroxy-3-methylglutaryl-CoA (HMG-CoA) (10), these reactions being catalysed by acetyl-CoA acetyltransferase and HMG-CoA synthase, respectively. Acetoacetyl-CoA is more acidic than the third acetyl-CoA molecule and thus serves as the nucleophile. NADPH then reduces HMG-CoA to (3R)-mevalonic acid (11) in higher plants (Scheme 1.2), the enzyme catalysing this reaction being hydroxymethylglutaryl-CoA reductase⁵. The conversion of HMG-CoA into mevalonic acid is irreversible, and hence, mevalonic acid has no metabolic future except in terpene formation⁴.



Scheme 1.2 The formation of L-mevalonic acid^{1,5}.

Mevalonic acid is the primary precursor of all the terpenoids biosynthesised by plants^{3,4}. The catalytic phosphorylation of mevalonate to form *R*-5-phosphomevalonic acid (12) (Scheme 1.3) occurs via the enzyme mevalonate kinase and is ATP dependent. Only the *R* form is utilised by organisms for producing terpenes as the *S* form is metabolically inert².



Scheme 1.3 Phosphorylation of mevalonic acid^{1,5}.

This phosphorylation is a primary point at which control of terpenoid biosynthesis operates, as mevalonic acid kinase activity has been found to be inhibited by such products of the acetate-mevalonate pathway as geranyl (13), farnesyl (14), geranylgeranyl (15) and phytyl (16) diphosphates³ (Figure 1.4).

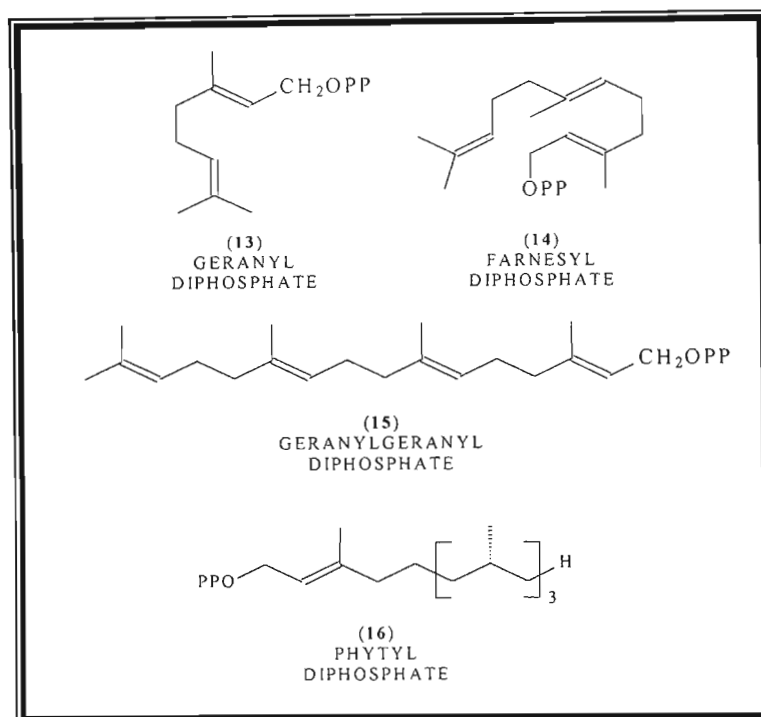
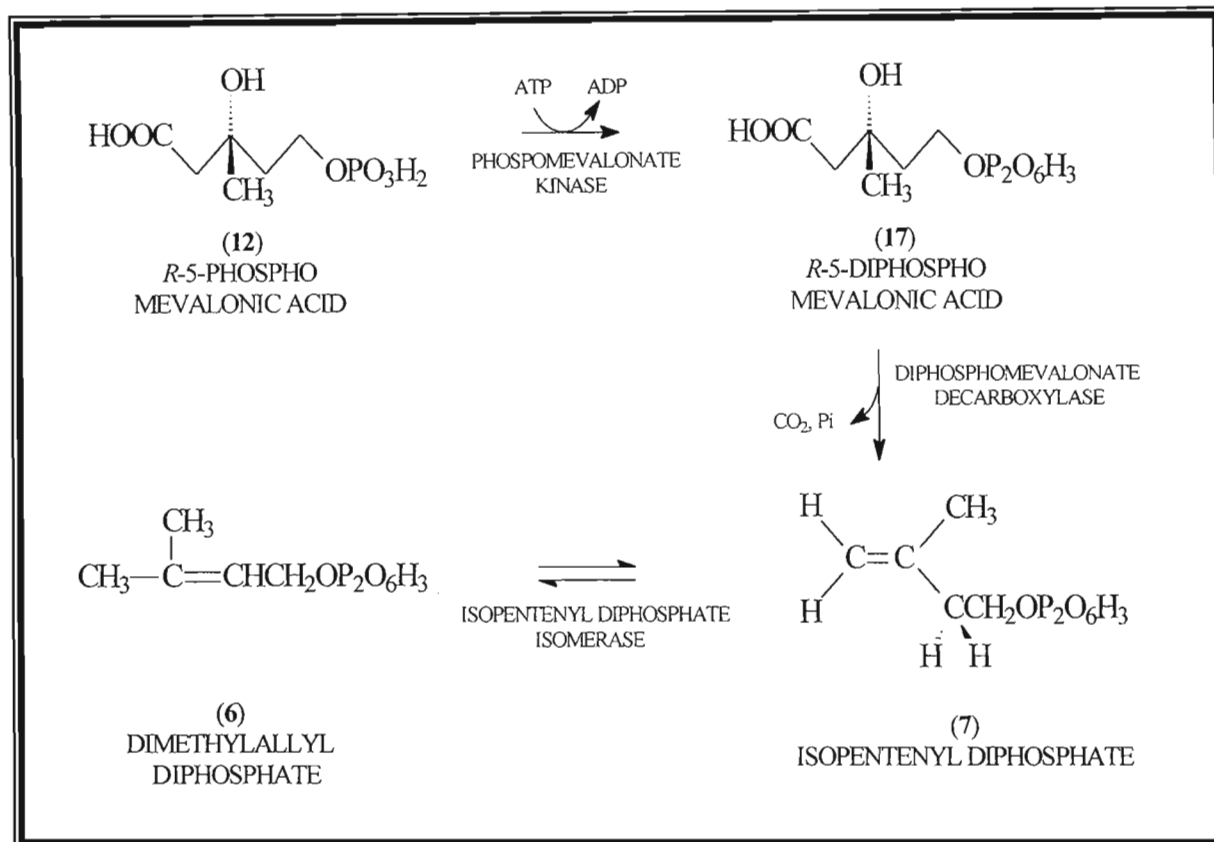


Figure 1.4 Inhibiting products of the acetate mevalonate pathway.

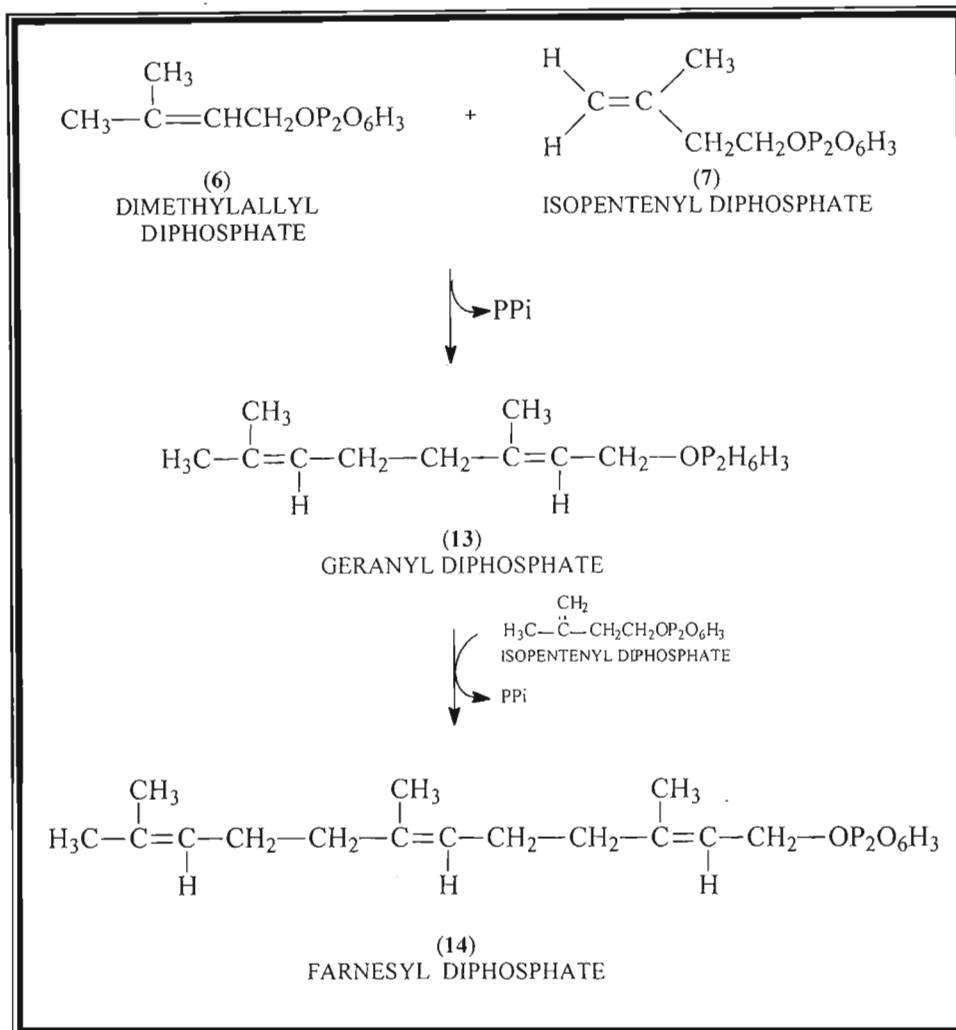
The conversion of *R*-5-phosphomevalonic acid into *R*-5-diphosphomevalonic acid (17) (Scheme 1.4) is catalysed by phosphomevalonate kinase. A concerted decarboxylation-dehydration of *R*-5-diphosphomevalonic acid gives isopentenyl diphosphate (7), the biogenic isoprene unit, and is catalysed by the enzyme diphosphomevalonate decarboxylase, a highly stereospecific enzyme involved in the *trans* elimination of the carboxyl and hydroxyl moieties³.

The interconversion of isopentenyl diphosphate (IPP) (7) and dimethylallyl diphosphate (DMAPP) (6) is an equilibrium reaction catalysed by the enzyme isopentenyl-diphosphate isomerase. The isomerisation is reversible, however, the equilibrium lies heavily on the side of DMAPP¹. This generates a reactive electrophilic DMAPP and a nucleophilic IPP, due to the terminal double bond.



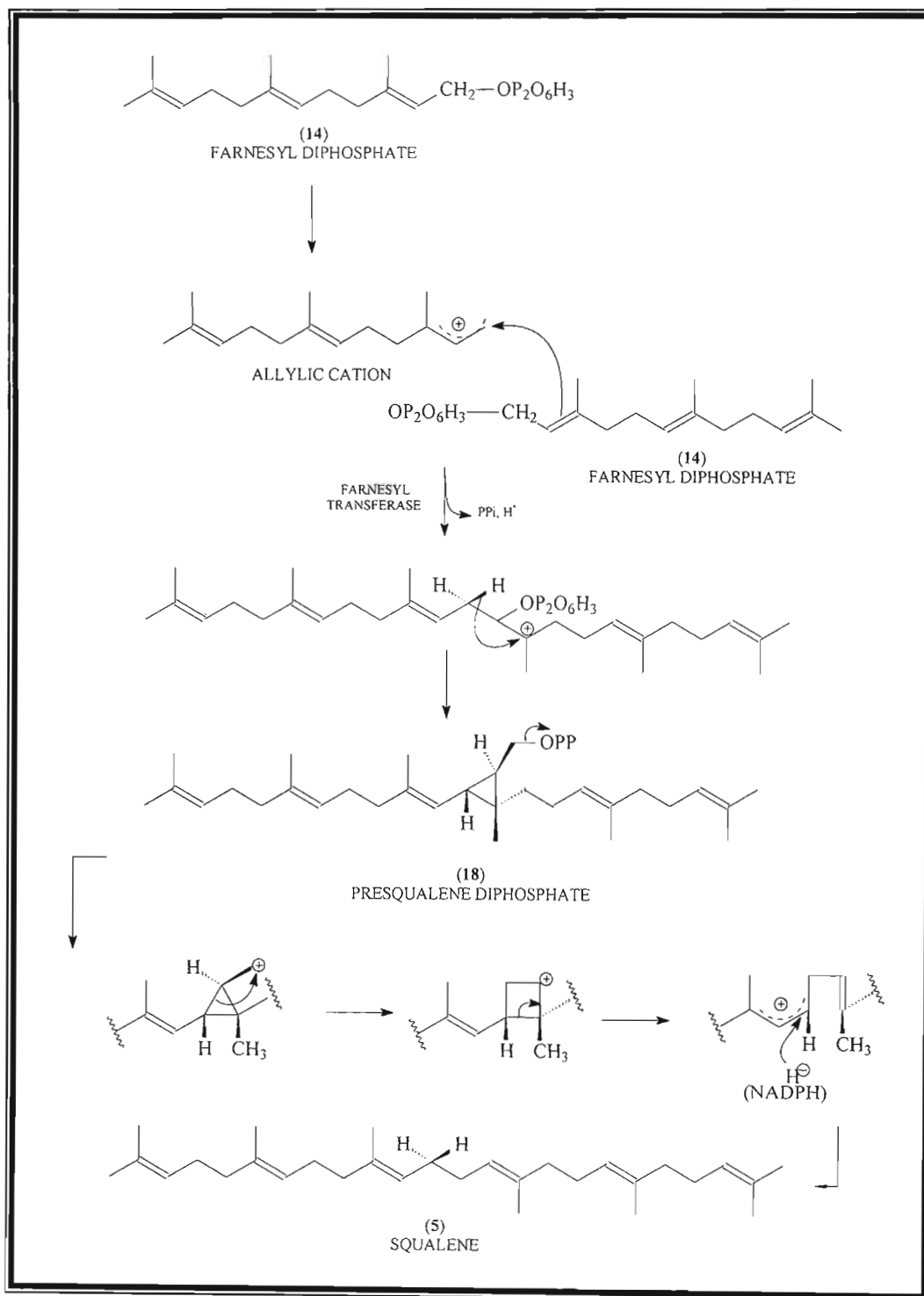
Scheme 1.4 Formation and isomerisation of isopentenyl diphosphate^{1,5}.

Isopentenyl diphosphate condenses with dimethylallyl diphosphate, via the enzyme prenyl transferase to yield geranyl diphosphate (13), which, in turn, condenses with isopentenyl diphosphate to form farnesyl diphosphate (14) (Scheme 1.5). Up till this point the cytosol has been the site of all the reactions, with the exception of those involving HMG-CoA reductase⁵.



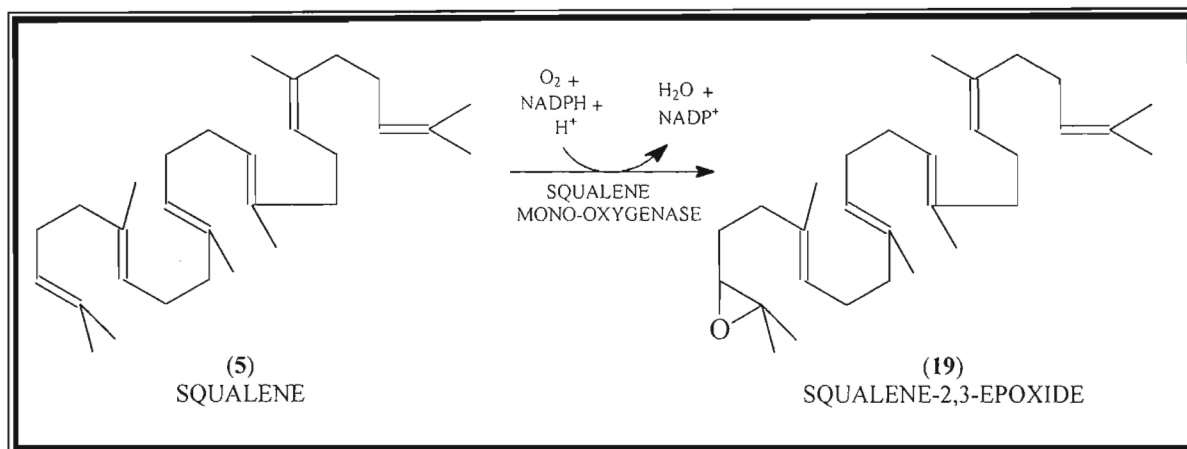
Scheme 1.5 The formation of farnesyl diphosphate⁵.

The NADPH-dependent enzyme farnesyl transferase, bound to membranes of the endoplasmic reticulum, joins two molecules of farnesyl diphosphate, tail-to-tail, to give presqualene diphosphate (18) (Scheme 1.6), which then undergoes diphosphate elimination and rearrangement to yield squalene (5)⁵. This reaction is catalysed by squalene synthase and is NADPH dependent³.



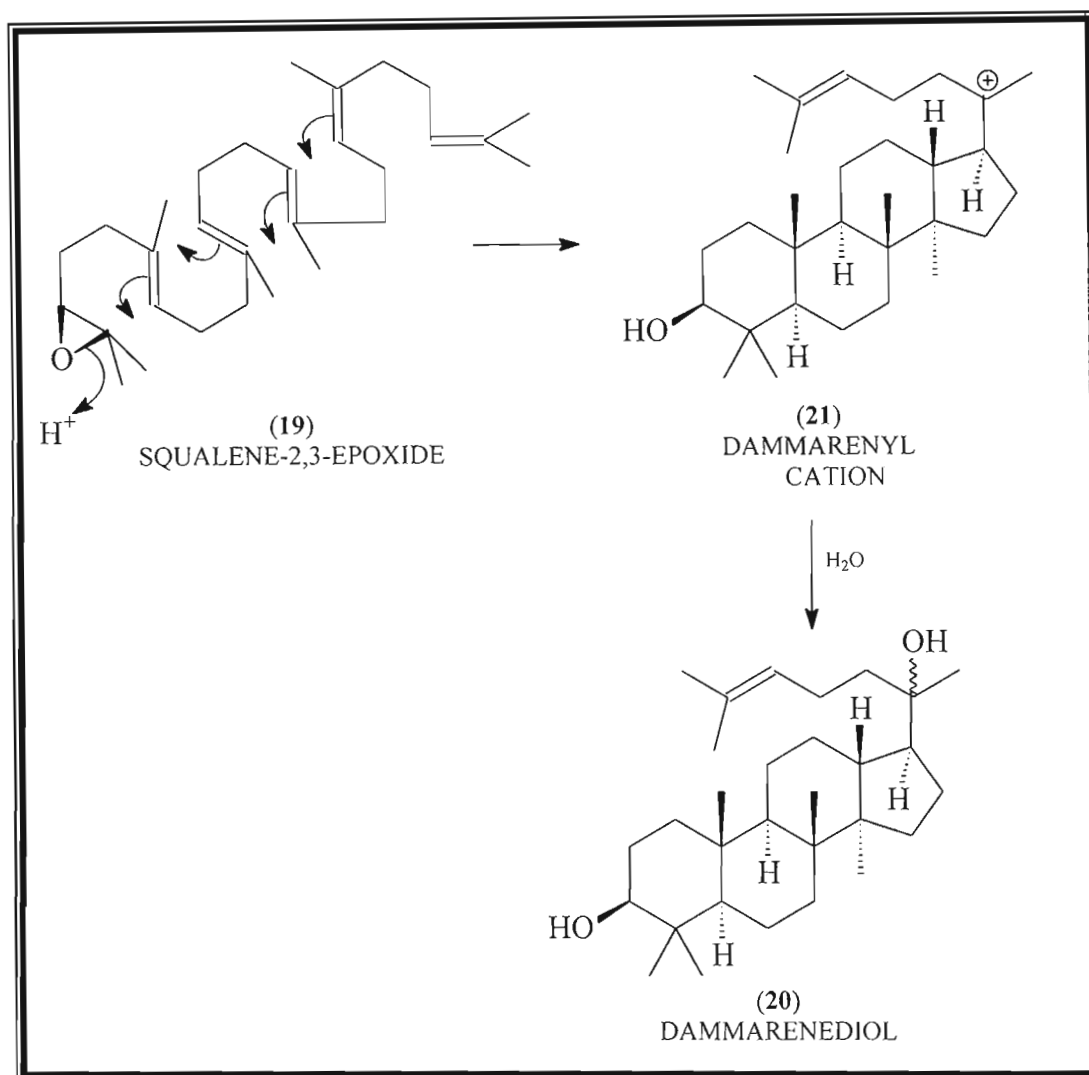
Scheme 1.6 The formation of squalene¹.

Cyclisation of squalene occurs via the intermediate squalene-2,3-oxide (**19**), catalysed by squalene mono-oxygenase, which forms from a reaction involving O_2 and NADPH cofactors^{1,3,6} (Scheme 1.7).



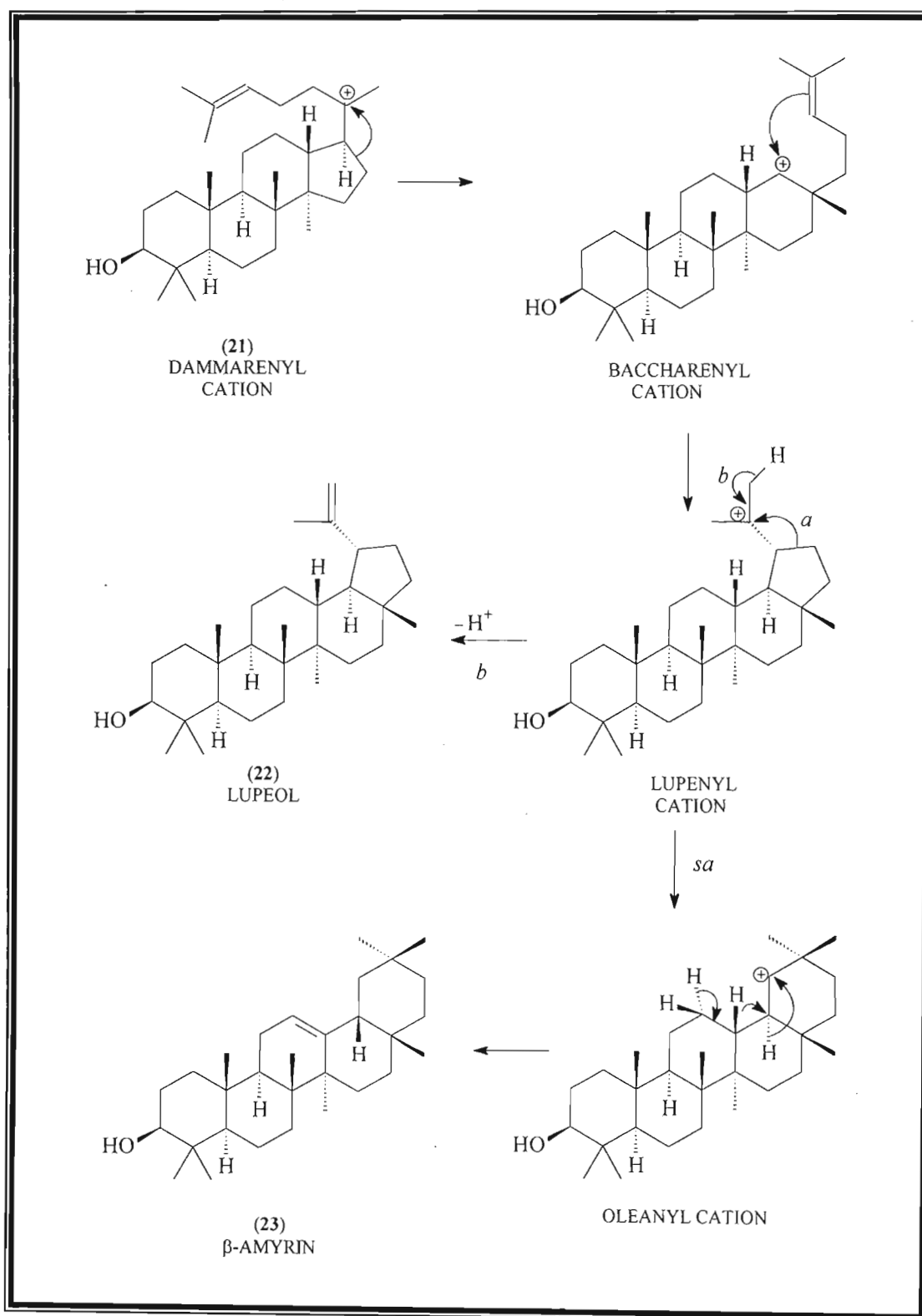
Scheme 1.7 Formation of the squalene-2,3-epoxide intermediate⁵.

One of the simplest cyclisations of squalene-2,3-epoxide, that forming the dammarene derivative, dammarenediol (**20**), via the dammarenyl cation (**21**), is shown in Scheme 1.8. Protonation of the epoxide group initiates a series of 1,2-shifts of methyl groups and hydride ions.



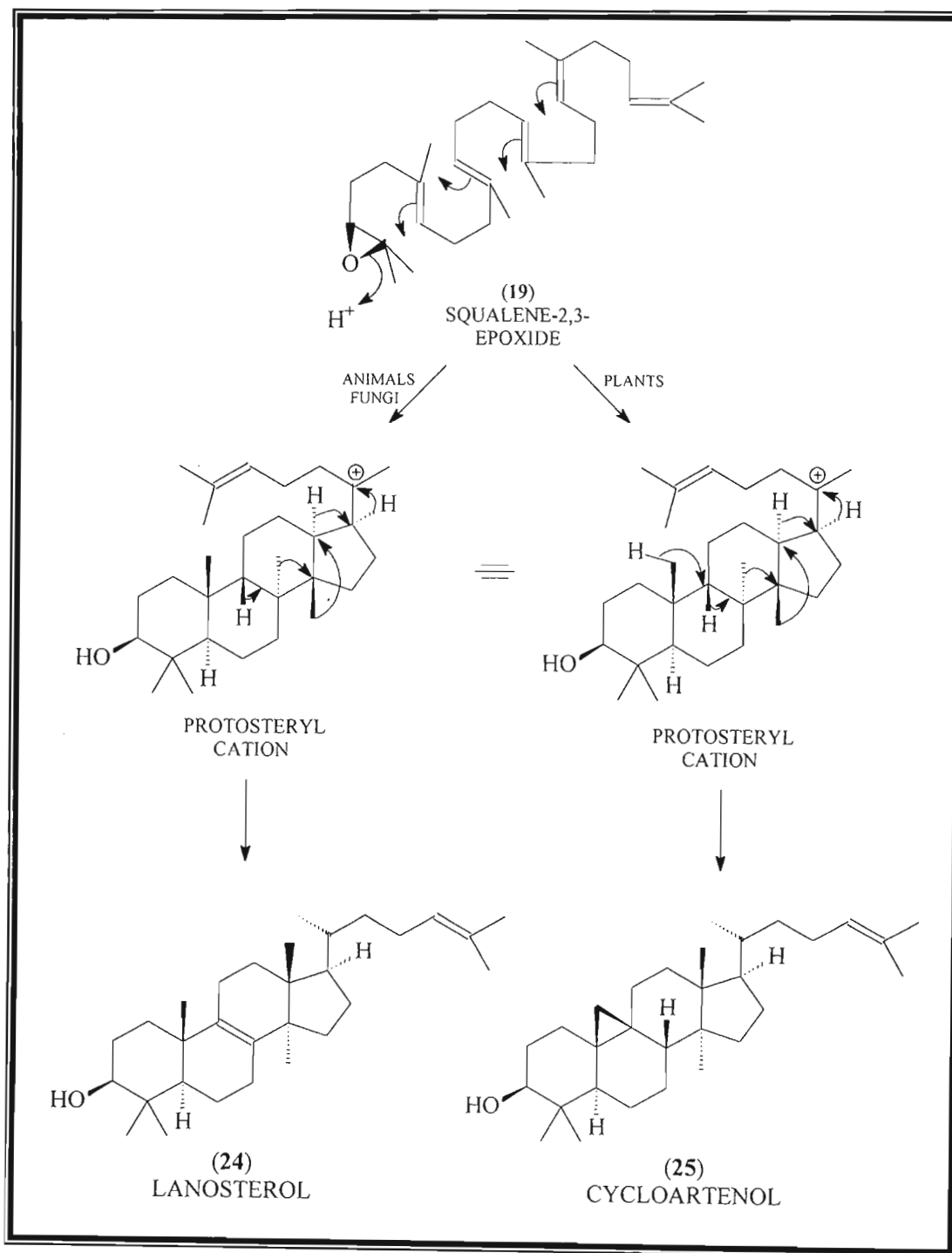
Scheme 1.8. The cyclisation of squalene-2,3-epoxide¹.

The pentacyclic triterpenoids, such as lupeol (**22**) and β -amyrin (**23**) are biosynthesised from a tetracyclic precursor of the dammarene type by a rearrangement resulting in the expansion of ring D and the formation of ring E¹ (Scheme 1.9).



Scheme 1.9 Rearrangement of the dammarenyl cation¹.

In animals, squalene-2,3-epoxide, via the protosteryl cation intermediate, can cyclise to form the lanosterol family of tetracyclic triterpenoids (Scheme 1.10). Lanosterol (**24**) is a typical triterpenoid found in animals and is the precursor for cholesterol biosynthesis.



Scheme 1.10 Formation of lanosterol and cycloartenol¹.

Cycloartenol (**25**), a cyclisation product of squalene in plants, is similarly formed via squalene-epoxide^{1,3,4} (Scheme 1.10). Cycloartenol contains a cyclopropane ring generated by inclusion of the methyl group at C-10. The hydrogen at C-9 migrates to C-8 and the carbocation so formed is quenched by cyclopropane formation and loss of one of the methyl protons.

Through its conversion to 24-methylenecycloartenol or cholesterol, cycloartenol is the precursor of a wide range of compounds collectively termed the phytosterols, which contain varying numbers of carbon atoms, as shown in figure 1.5. Lanosterol, however, is not implicated in the biogenesis of phytosterols⁶.

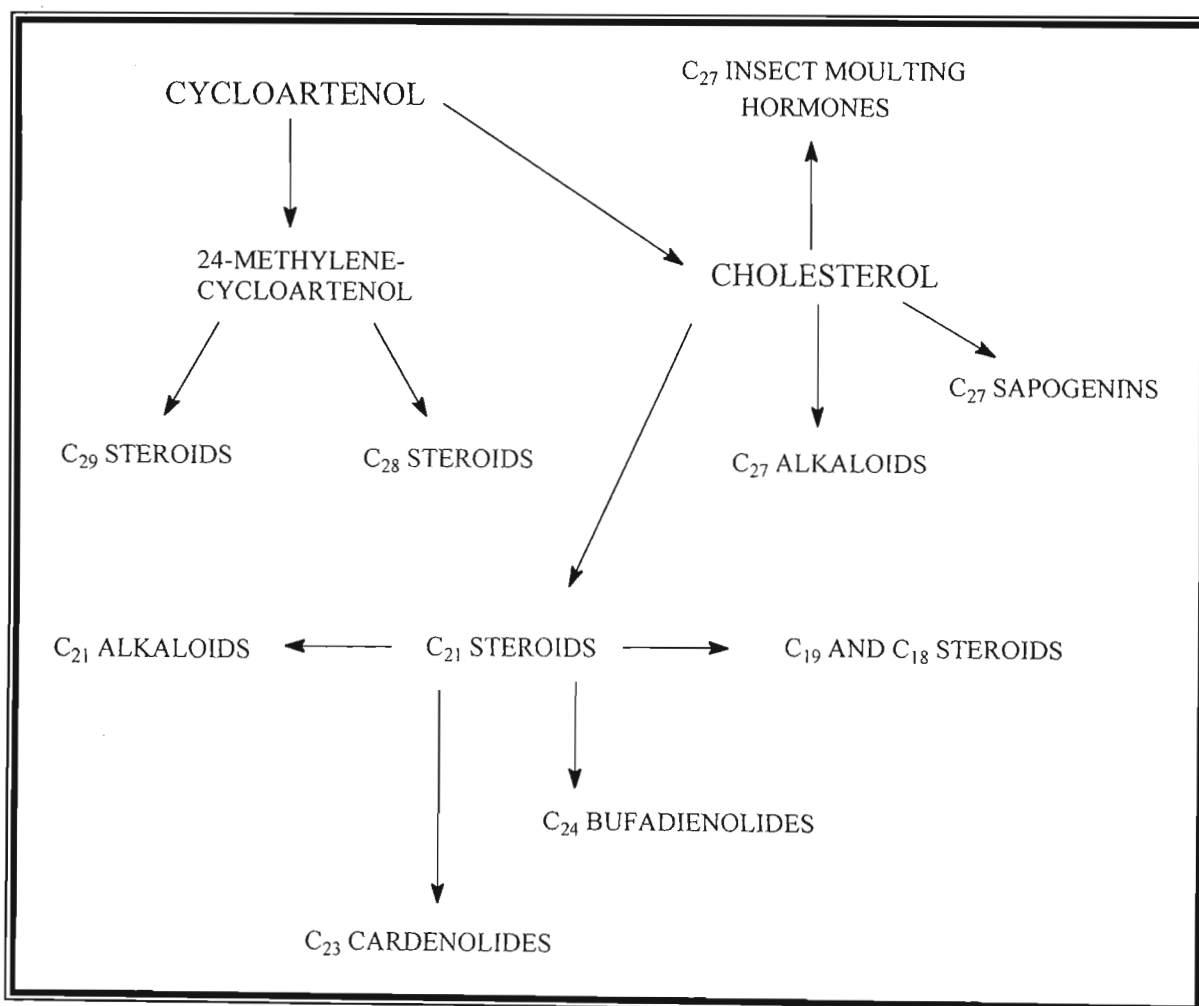


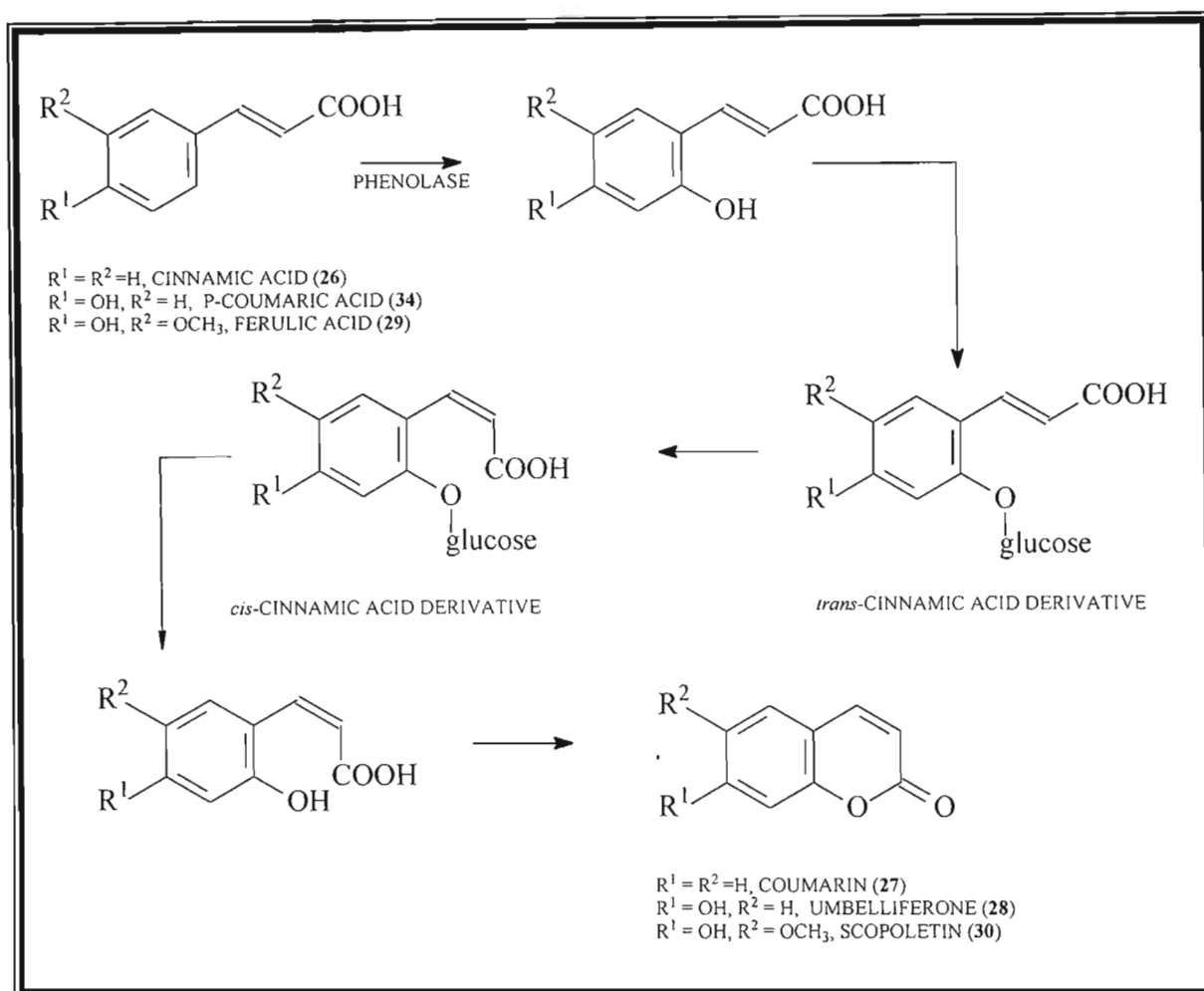
Figure 1.5 The derivation of phytosterols³.

Most natural triterpenoids and steroids are oxygenated at C-3, the original epoxide oxygen from squalene-2,3-oxide, usually as alcohols but some as ketones. Triterpenoids are distinguished from each other by unsaturations, additional hydroxyl groups, and frequently, carboxyl groups⁷.

In plants, the pentacyclic triterpenoids often exist as glycosides, the resulting compounds are termed saponins. Saponins, even at low concentrations, produce frothing in aqueous solutions because they have soap-like properties. Saponins are known to be highly toxic to cold-blooded animals and are lethal if injected as they haemolyse the red blood corpuscles. Medicinally these compounds are used as anti-inflammatory agents, antibiotics, fungicides, and, most importantly, molluscicides³.

1.2 Introduction to Coumarins

Coumarins are an important biologically active class of compounds of plant origin. The biosynthesis of coumarins (Scheme 1.11) involves the hydroxylation of cinnamic acid (**26**) *ortho* to the side-chain, a reaction catalysed by phenolase^{8,9,10}.

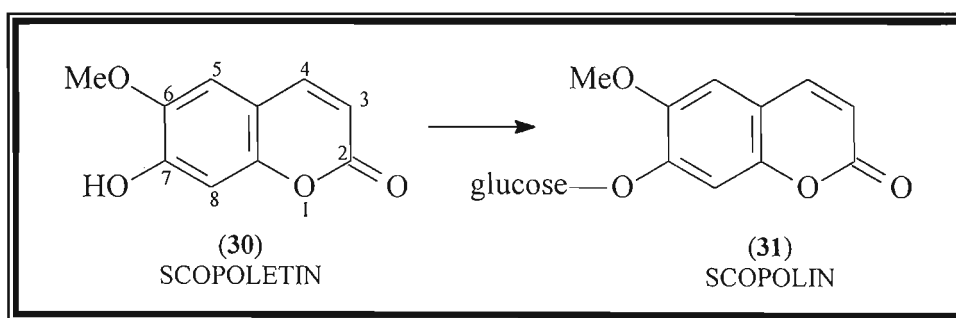


Scheme 1.11 The biosynthesis of coumarins⁸.

The *ortho*-hydroxyl group undergoes glucosylation resulting in isomerisation of *trans*-cinnamic acid derivatives to the less stable *cis*-form. In the case of a single isolated double bond, *cis/trans* isomerisation would be unfavourable, however, cinnamic acid (**26**) has a fully conjugated double bond system which allows this process to occur quite readily⁹. Subsequent hydrolysis of the sugar moiety, via enzymatic cleavage of the

glycoside, leads to spontaneous cyclisation and lactone formation, resulting in the final coumarin (**27**) product. Both *cis/trans* isomerisation and lactonisation are enzyme mediated and light is not necessary for coumarin biosynthesis⁹.

Most naturally occurring coumarins contain an oxygen substituent at the 7-position, introduced by *para*- followed by *ortho*-hydroxylation of cinnamic acid. Umbelliferone (**28**) is regarded as the parent compound of the 7-oxycoumarins. Prior to isomerisation and ring closure, several hydroxyl groups may be introduced and methylated, such as ferulic acid (**29**) giving scopoletin (**30**). Ferulic acid in tobacco tissue cultures converts to scopoletin while the subsequent formation of a glucoside is absent. However, in the intact plant, scopoletin accumulates as the glucoside scopolin⁸ (**31**) (Scheme 1.12).



Scheme 1.12 Formation of scopolin⁹.

Daphnin (**32**) in *Daphne odora* of the family Thymelaeaceae and cichoriin (**33**) in chicory (*Cichorium intybus*, Compositae) are biosynthesised from *p*-coumaric acid (**34**) and not caffeic acid (**35**), the second hydroxyl group being introduced after ring closure⁸, as shown in scheme 1.13.

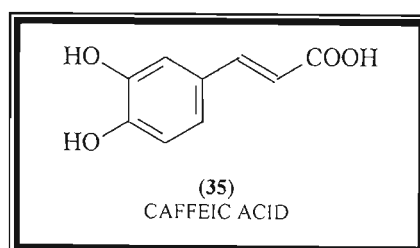
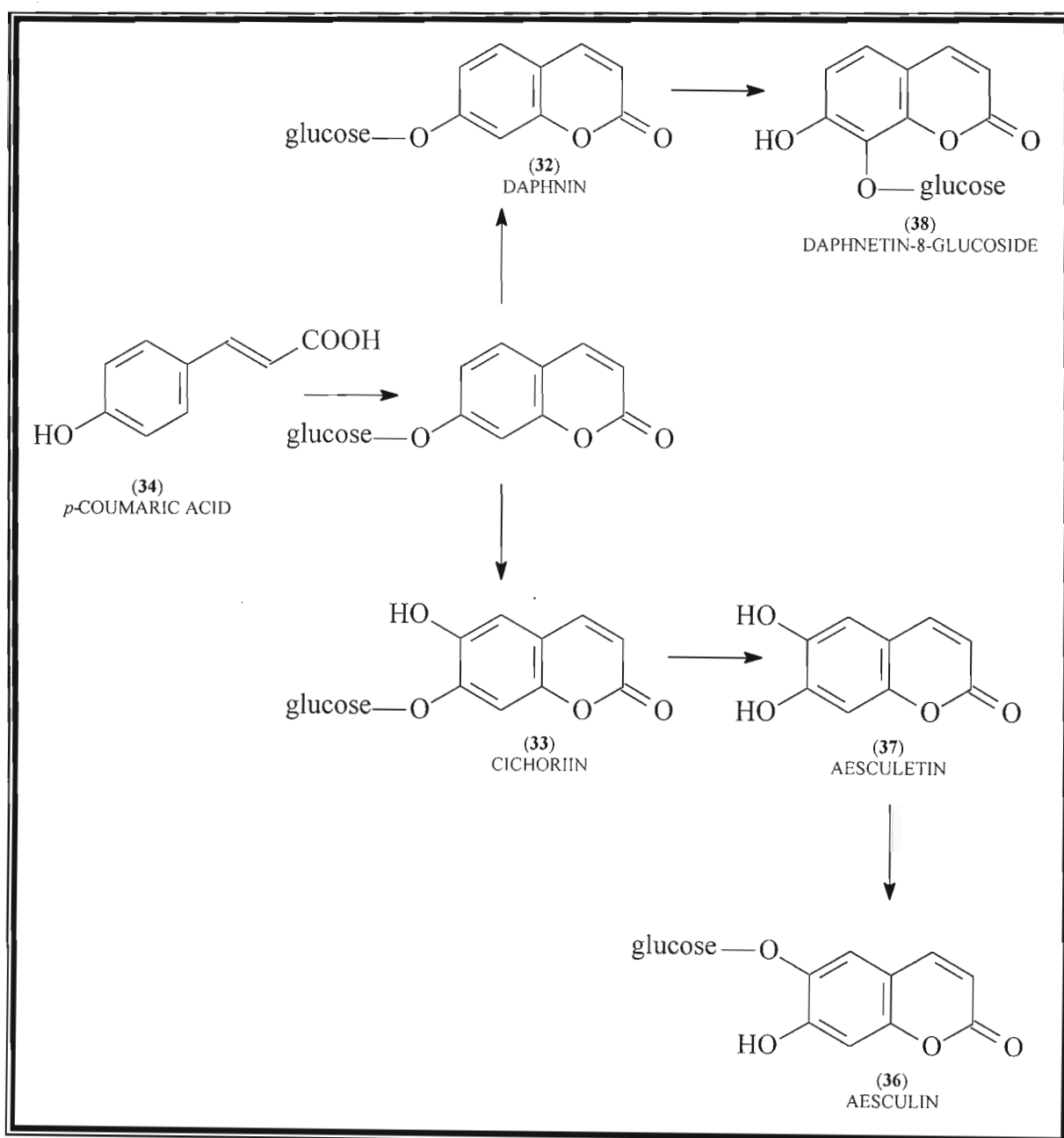


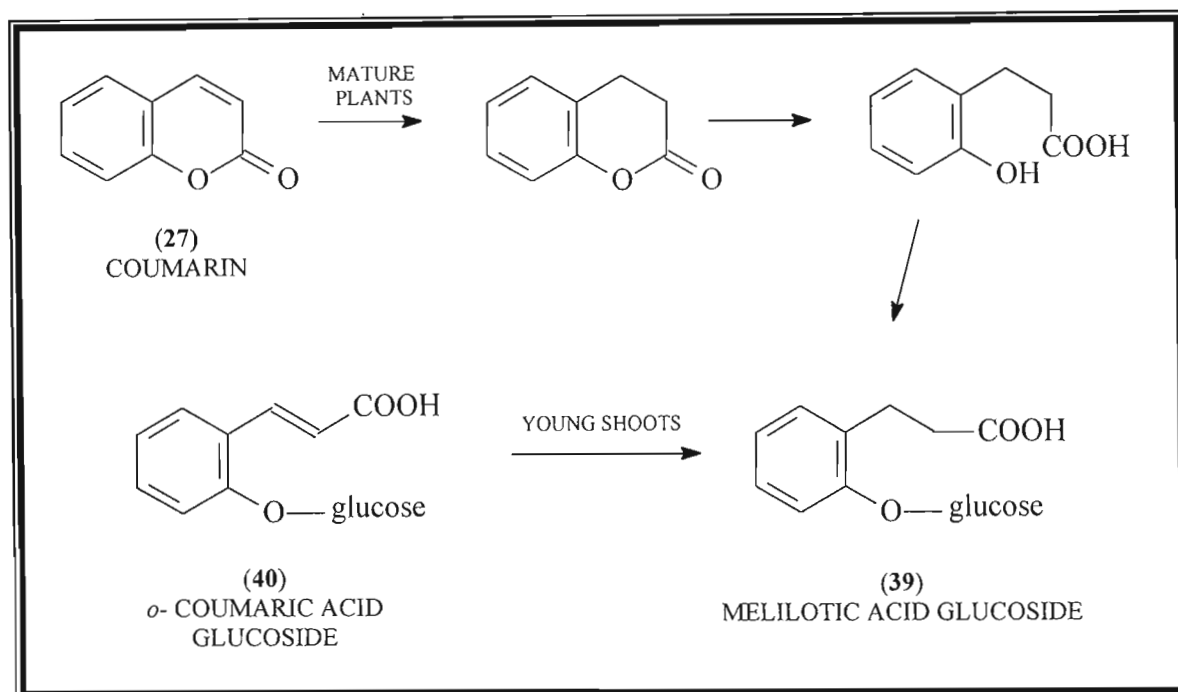
Figure 1.6 Structure of caffeic acid.

Chicory contains an enzyme that catalyses the *trans*-glucosylation of cichoriin to aesculin (36), with aesculetin (37) being an intermediate. A similar enzyme in *Daphne* catalyses the *trans*-glucosylation of daphnin to daphnetin-8-glucoside (38). In both cases the reactions are irreversible and the enzymes responsible are highly specific.



Scheme 1.13 The biosynthesis of daphnin, cichoriin, aesculetin and aesculin⁸.

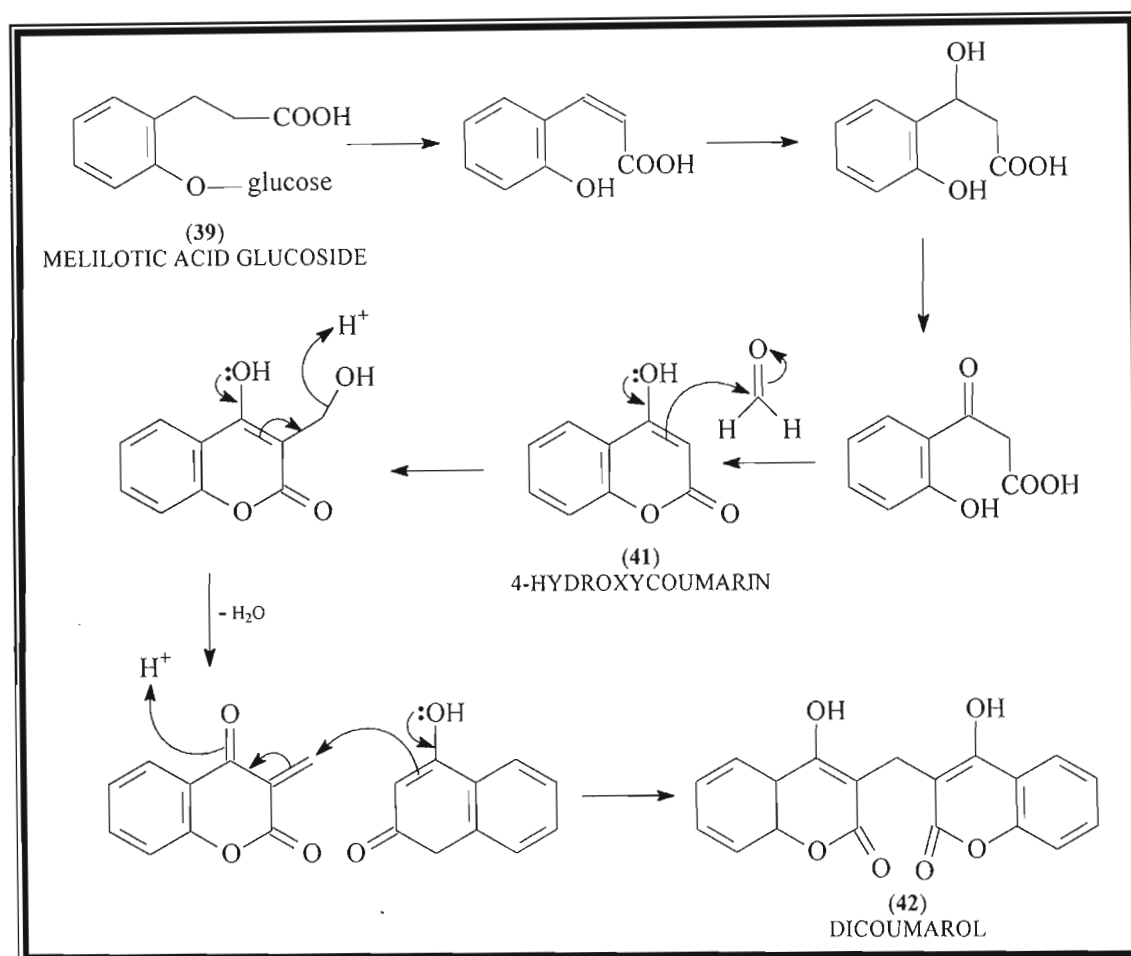
Coumarin (**27**) itself is isolated from *Melilotus alba* (Leguminosae), or commonly known as sweet clover, and gives the scent to newly mown hay. Evidence shows that plants contain the glucosides of *trans*- and *cis*-2-coumaric acid, and that coumarin is only produced through damage during the harvesting process resulting in enzymatic hydrolysis and lactonisation⁹. Melilotic acid glucoside (**39**) is the bound form of coumarin in sweet clover. In mature plants, biosynthesis of the glucoside occurs via reduction of coumarin (**27**) (Scheme 1.14), followed by ring cleavage, and finally glucosylation. In shoots, however, melilotic acid glucoside (**39**) is formed directly from *o*-coumaric acid glucoside (**40**).



Scheme 1.14 The biosynthesis of melilotic acid glucoside in sweet clover⁸.

Fermenting sweet clover produces 4-hydroxycoumarin (**41**), which can react with formaldehyde from microbial degradation reactions to give dicoumarol (**42**) (Scheme 1.15). Dicoumarol has blood anticoagulant properties, which causes intestinal bleeding in livestock, resulting in death¹¹. However, dicoumarol and synthetic analogues can be used therapeutically as anticoagulants, by inhibiting the synthesis of certain proteins concerned with the blood-clotting mechanisms. Vitamin K is a blood-clotting promoter, and

dicoumarol, being an analogue of the vitamin, competes with the enzymes concerned with the synthesis of blood-clotting proteins⁸.



Scheme 1.15 The formation of dicoumarol in spoiled hay⁸.

Characteristically, coumarins fluoresce (usually blue) in ultraviolet light. Those derived from umbelliferone fluoresce with a blue colour when irradiated with visible light, while, if the coumarin has a free 7-hydroxyl group, a green fluorescence is seen in alkaline solution¹².

1.3 References

- 1) Dewick, P.M.; "Medicinal Natural Products, A Biosynthetic Approach", (1997), John Wiley and Sons, New York, Chapter 5, 152-269.
- 2) Manitto, P.; "Biosynthesis of Natural Products", (1981), Ellis Horwood, Ltd. Publishers, Chichester, Chapter 5, 213-313.
- 3) Vickery, M.L. and Vickery, B.; "Secondary Plant Metabolism", (1981), The Macmillan Press, Ltd., London, Chapter 5.
- 4) Herbert, R.B.; "The Biosynthesis of Secondary Metabolites", (1981), Chapman and Hall, London, Chapter 4, 63-95.
- 5) Mathews, C.K. and van Holde, K.E.; "Biochemistry", (1990), The Benjamin/Cummings Publishing Company, Inc., New York, Chapter 18, 604-642.
- 6) Packter, N.M.; "Biosynthesis of Acetate-Derived Compounds", (1973), John Wiley and Sons, London, 164-173.
- 7) Robinson, T.; "The Organic Constituents of Higher Plants, Their Chemistry and Interrelationships", (1963), Burgess Publishing Company, Minneapolis, 132-140.
- 8) Vickery, M.L. and Vickery, B.; "Secondary Plant Metabolism", (1981), The Macmillan Press, Ltd., London, Chapter 6.
- 9) Dewick, P.M.; "Medicinal Natural Products, A Biosynthetic Approach", (1997), John Wiley and Sons, New York, Chapter 4, 109-151.
- 10) Herbert, R.B.; "The Biosynthesis of Secondary Metabolites", (1981), Chapman and Hall, London, Chapter 5, 96-119.
- 11) Manitto, P.; "Biosynthesis of Natural Products", (1981), Ellis Horwood, Ltd. Publishers, Chichester, Chapter 7, 349-364.
- 12) Dean, F.M.; "Naturally Occurring Oxygen Ring Compounds", (1963), Butterworth and Co., Ltd., London, Chapter 6, 176-219.

CHAPTER 2

Extractives from *Agave attenuata*

2.1 Introduction

Plants of the genus *Agave*, belonging to the family Agavaceae, are native to desert regions of the Western Hemisphere. The most common species is the American aloe or century plant (*Agave americana*), which only flowers once between the ages of ten and twenty-five years. The leaves of the *Agave* are large and fleshy, and store large quantities of water. Many species are economically important e.g. fibres from sisal (*Agave sisalana*) are used in the making of rope. The roots of species, known as amoles, yield a pulp, which lathers when wet and is used as a soap. Fermentation of the sap of some *Agave* species produces a drink called pulque, which yields a colourless liquor, mescal, when distilled^{1,2}.

Dried leaf material of a Mexican plant, *Agave attenuata* Salm, Hortus Dyckensis was found to be highly toxic to the target snail, *Bulinus africanus*, which is the intermediate host of *Schistosoma haematobium*, in South Africa. Schistosomiasis is an important public health issue in South Africa and scientists have focussed their attention on snail control using plant molluscicides in an attempt to deal with infected rural communities^{3,4}. The species *A. attenuata* has not yet been studied, however chemical investigations of other *Agave* species have been undertaken because of their traditional use as drugs in the American Indian system of medicine, as a diuretic, antisyphilitic, laxative, emmenagogue and antiscorbutic⁵.

Identification of leaf constituents by earlier researchers has not proved very successful because the leaf chemistry of *Agaves* is complex. However, earlier phytochemical investigations have revealed the presence of glycosides, saponins, sapogenins, sterols, terpenes and vitamins⁶. In recent decades investigations into the chemistry and nutritional value of the *Agaves* have been carried out extensively. The juice of the leaves is rich in sugars and can be used in refreshment drinks when properly treated. A form of the juice

contains fructose sugars, which can be ingested by diabetics and can therefore be used in health foods for diabetics⁶.

Investigations of the aerial parts of *A. americana* yielded a flavanone, agamanone⁵ (5,7-dihydroxy-6,5'-dimethoxy-3',4'-methylenedioxy flavanone) (**43**).

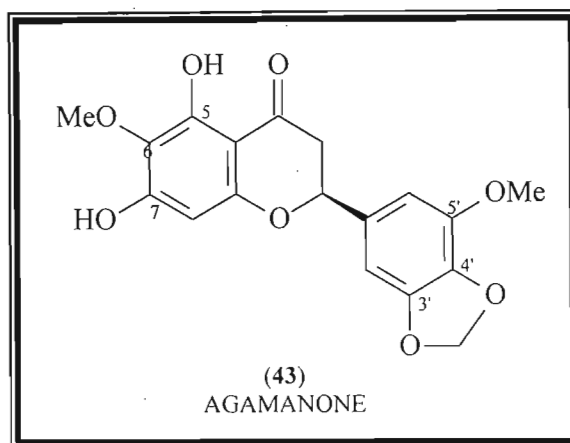


Figure 2.1 Structure of agamanone.

Three related compounds have also been isolated from *A. americana*, namely 5-hydroxy-7-methoxy-2-tritriacontyl-4H-1-benzopyran-4-one (**44**), tetratriacontyl hexadecanoate (**45**) and tetratriacontanol⁷ (**46**). Compounds 45 and 46 exhibited significant antibacterial activity.

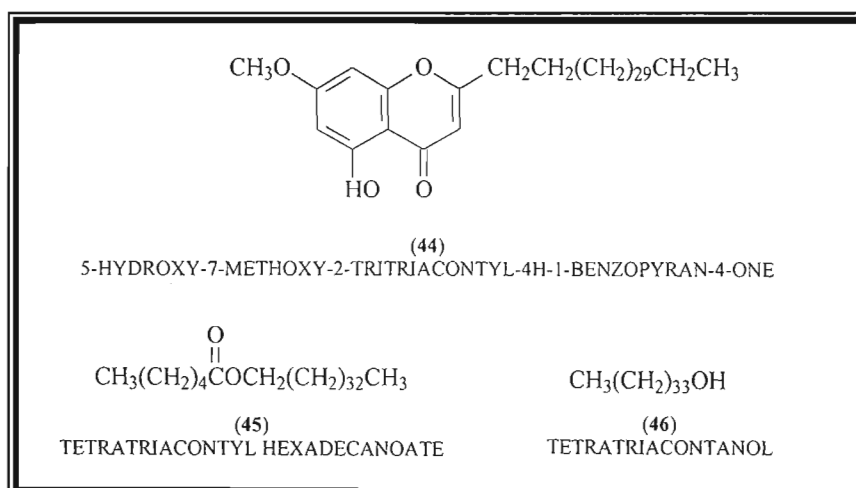


Figure 2.2 Compounds isolated from *Agave americana*.

Two new saponins, agavasaponin E (3 - O - [β - D - xylopyranosyl - (1 \rightarrow 2 glc 1) - α - L - rhamnopyranosyl - (1 \rightarrow 4) - α - L - rhamnopyranosyl - (1 \rightarrow 3 glc 1) - β - D - glucopyranosyl - (1 \rightarrow 4) - β - D - glucopyranosyl - (1 \rightarrow 4) - β - D - galactopyranosyl] - (25R) - 5 α - spirostan - 12 - on - 3 β - ol) (**47**) and agavasaponin H (3 - O - [β - D - xylopyranosyl - (1 \rightarrow 2 glc 1) - α - L - rhamnopyranosyl - (1 \rightarrow 4) - α - L - rhamnopyranosyl - (1 \rightarrow 3 glc 1) - β - D - glucopyranosyl - (1 \rightarrow 4) - β - D - glucopyranosyl - (1 \rightarrow 4) - β - D - galactopyranosyl] - 26 - O - [β - D - glucopyranosyl] - (25R) - 5 α - furostan - 12 - on - 3 β ,22 α ,26 - triol) (**48**) have been isolated from the leaves of *A. americana*⁸. Both are highly complex saponins with the former having six sugars and the latter having seven sugars attached at position 3. Paper chromatography of the sugars obtained from both saponins showed the presence of rhamnose, xylose, glucose and galactose, however in different ratios.

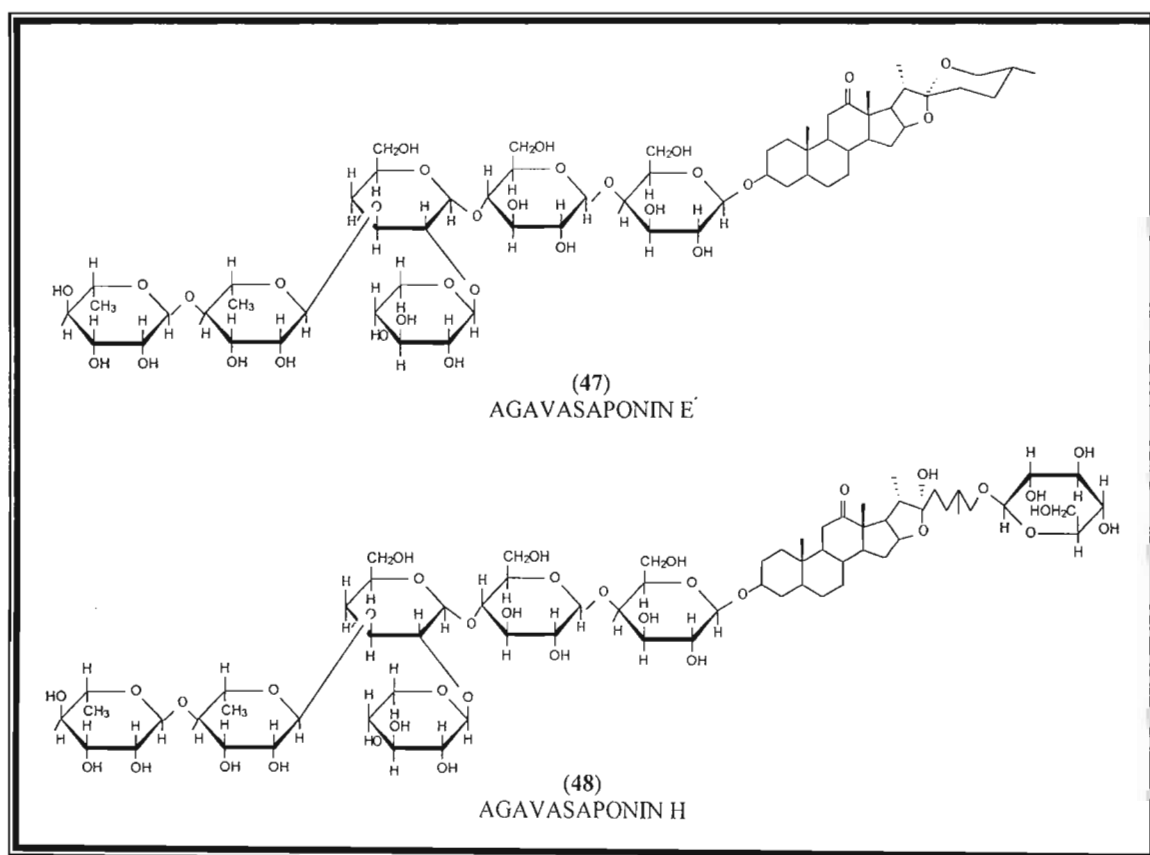


Figure 2.3 Structure of agavasaponin E and agavasaponin H.

2.2 Results and Discussion

Agave attenuata was investigated as this plant has been found to be biologically active as a plant molluscicide. The leaves were extracted, by continuous agitation at room temperature, with hexane, dichloromethane and methanol and column chromatography was used in order to isolate the compounds according to their polarity. No compounds were isolated from the hexane and dichloromethane extracts, however, the methanol extract yielded a glycoside, timosaponin A III (**compound I**), after repeated column chromatography. Compound I had been isolated previously from *Anemarrhena asphodeloides* (Asphodelaceae). Due to the loss of compound I, a second attempt to isolate this compound was undertaken in order to obtain outstanding physical data. Since it was known that this compound was isolated from the methanol fraction, only a methanol extraction was performed. Compound I was not isolated, however, this extract yielded a novel glycoside, 5 α -pregn-16-ene-20-one-3 β -O-tetrasaccharide (**compound II**).

2.2.1 The Structural Elucidation of Compound I

The steroidal glycoside isolated from the leaf extract was a white crystalline material tentatively identified as spirostan-3-O-[[β -D-glucopyranosyl(1 \rightarrow 2)- β -D-galactopyranoside] or commonly known as timosaponin A III (3 β , 5 β , 25S) (**compound I**).

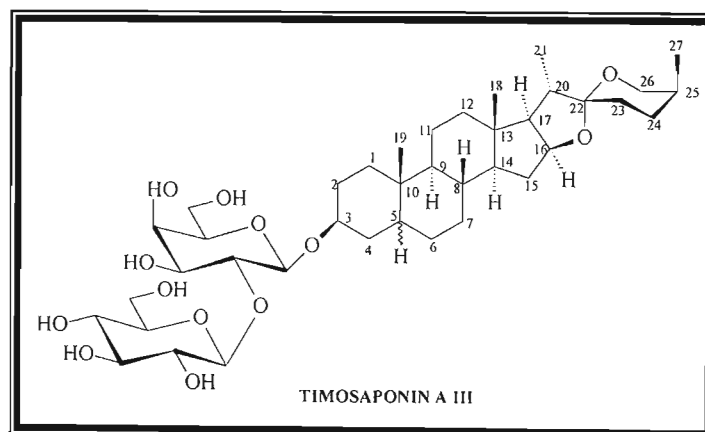


Figure 2.4 Compound I: timosaponin A III.

The ^1H NMR spectrum (Spectrum 1a, pp 102) matched the literature data⁹ for timosaponin A III (Table 1). The two intense singlets at δ 0.76 (3H, s, H-18) and δ 0.96 (3H, s, H-19) were due to tertiary methyl group protons at C-18 and C-19 respectively. The signals ascribed to the protons of the two methyl groups at C-27 and C-21 appeared as doublets at δ 0.97 (3H, d, $J = 7.0$ Hz) and δ 1.06 (3H, d, $J = 7.1$ Hz). The COSY spectrum (Spectrum 1d, pp 105) showed that the H-27 and H-21 methyl protons were coupled to the methine protons H-25 and H-20 respectively.

The anomeric protons of glucose and galactose were seen as doublets at δ 4.63 (1H, d, $J = 7.8$ Hz, H-1'') and δ 4.38 (1H, d, $J = 7.7$ Hz, H-1') respectively. From the HETCOR spectrum (Spectrum 1e, pp 106) these peaks were correlated to the signals at δ 104.1 (d) and δ 101.2 (d) respectively which were seen as methine carbons in the ADEPT spectrum (Spectrum 1c, 104). The resonance at δ 4.06 (1H, brs, H-3) was a broad singlet assigned to H-3 and correlated to a methine signal at δ 75.8 in the ^{13}C NMR spectrum (Spectrum 1b, pp 103).

The ^{13}C NMR spectrum showed the presence of thirty-nine carbon atoms, which supported the suggested structure. The methylene carbon resonance at δ 65.7, the methine carbon resonance at δ 82.1 and the fully substituted carbon signal at δ 110.7 were assigned to C-26, C-16 and C-22 respectively and are characteristic of oxygenated carbons. The methine signal at C-20 was also shifted downfield to δ 43.1 due to being in close proximity to an oxygen atom.

The sample was sent by courier to Reims, France for HMBC spectra to be run, as this facility was not available in Durban at the time, but it was lost *en route*. Fortunately, NMR data obtained in Durban could be used for comparison against literature values⁹, and a COSY and HETCOR spectrum had been run to confirm assignments. Unfortunately, the literature data is given for D-pyridine, whereas compound I was run in deuterated methanol. This led to differences in the proton spectrum, but the ^{13}C NMR data is in good agreement. However, the loss of the sample prevented the confirmation

of the molecular formula by mass spectrometry, a NOESY NMR experiment for confirmation of the stereochemistry, especially that of H-5, and melting points, optical rotation or infra red spectroscopy could not be performed. Without an HMBC spectrum, the places of attachment between the sugars could not be confirmed.

Table 2.1 ^1H NMR data for compound I and literature data for timosaponin A III⁹.

	^1H NMR data for compound I (CD_3OD) (400 MHz)	^1H NMR literature data for timosaponin A III ⁹ (PYRIDINE-D) (500 MHz)
Proton Number	δ_{H} ppm	δ_{H} ppm
Aglycone		
18	0.76 (s)	0.82 (s)
19	0.96 (s)	0.96 (s)
21	1.06 (d, $J = 7.1$ Hz)	1.15 (d, $J = 7.1$ Hz)
27	0.97 (d, $J = 7.0$ Hz)	1.08 (d, $J = 7.0$ Hz)
3	4.06 (brs)	4.30 (brs)
Galactose		
1'	4.38 (d, $J = 7.7$ Hz)	4.88 (d, $J = 7.6$ Hz)
2'	3.82 (m)	4.62 (dd, $J = 9.5, 7.6$ Hz)
3'	3.65 (m)	4.23 (dd, $J = 9.5, 3.1$ Hz)
4'	3.84 (m)	4.53 (d, $J = 3.1$ Hz)
5'	3.46 (m)	4.00 (dd, $J = 7.3, 6.4$ Hz)
6'	3.70 (m)	4.32 – 4.48 (m)
Glucose		
1''	4.63 (d, $J = 7.8$ Hz)	5.24 (d, $J = 7.7$ Hz)
2''	3.17 (m)	4.03 (dd, $J = 8.7, 7.7$ Hz)
3''	3.34 (m)	4.15 (dd, $J = 9.1, 8.7$ Hz)
4''	3.23 (m)	4.26 (dd, $J = 9.4, 9.1$ Hz)
5''	3.28 (m)	3.81 (ddd, $J = 9.2, 4.0, 2.4$ Hz)
6''	3.66 (m)	4.32 – 4.48 (m)

Table 2.2 ^{13}C NMR data for compound I and literature data for timosaponin A III⁹.

	^{13}C NMR data for compound I (CD_3OD) (100 MHz)	^{13}C NMR literature data for timosaponin A III ⁹ (PYRIDINE-D) (125 MHz)
Carbon number	δ_c , ppm	δ_c , ppm
Aglycone		
1	30.7 (CH_2)	30.9 (t)
2	26.9 (CH_2)	27.0 (t)
3	75.8 (CH)	75.4 (d)
4	31.1 (CH_2)	30.9 (t)
5	37.2 (CH)	36.8 (d)
6	26.6 (CH_2)	26.7 (t)
7	26.4 (CH_2)	26.7 (t)
8	36.4 (CH)	35.5 (d)
9	41.0 (CH)	40.2 (d)
10	35.8 (C)	35.2 (s)
11	21.7 (CH_2)	21.1 (t)
12	41.0 (CH_2)	40.3 (t)
13	41.5 (C)	40.9 (s)
14	57.3 (CH)	56.4 (d)
15	32.3 (CH_2)	32.1 (t)
16	82.1 (CH)	81.3 (d)
17	63.3 (CH)	61.9 (d)
18	16.6 (CH_3)	16.6 (q)
19	24.1 (CH_3)	24.0 (q)
20	43.1 (CH)	40.5 (d)
21	14.4 (CH_3)	14.9 (q)
22	110.7 (C)	109.7 (s)
23	27.4 (CH_2)	26.4 (t)
24	27.3 (CH_2)	26.2 (t)
25	28.2 (CH)	27.5 (d)
26	65.7 (CH_2)	65.7 (t)
27	16.0 (CH_3)	16.3 (q)
Galactose		
1'	101.2 (CH)	102.4 (d)
2'	78.5 (CH)	81.6 (d)
3'	74.9 (CH)	75.1 (d)
4'	70.1 (CH)	69.7 (d)
5'	76.1 (CH)	76.5 (d)
6'	62.1 (CH_2)	62.1 (t)

Glucose		
1''	104.1 (CH)	105.9 (d)
2''	75.9 (CH)	76.8 (d)
3''	77.5 (CH)	77.8 (d)
4''	71.6 (CH)	71.6 (d)
5''	78.1 (CH)	78.3 (d)
6''	62.9 (CH ₂)	62.7 (t)

2.2.1 The Structural Elucidation of Compound II

The second glycoside isolated from the leaf extract was a novel compound identified as 5 α -pregn-16-en-20-one-3 β -O-tetrasaccharide (**compound II**).

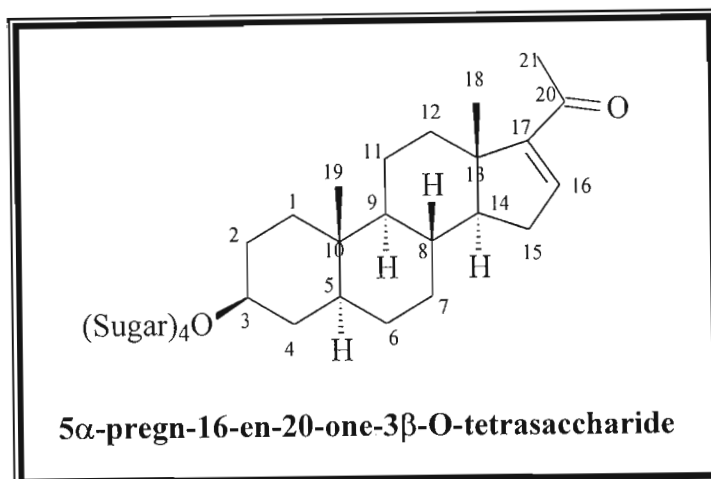


Figure 2.5 Compound II: 5 α -pregn-16-en-20-one-3 β -O-tetrasaccharide.

The infra red spectrum (Spectrum 2h, pp 114) showed a very large broad peak at 3364.2 cm^{-1} which represented the numerous hydroxyl groups present in this tetrasaccharide. The aliphatic C-H stretching vibration could be seen at 2930.8 cm^{-1} . A sharp peak was observed at 1662.9 cm^{-1} , which indicated the presence of an α,β -unsaturated carbonyl group¹⁰. This peak seems small in comparison to the very large hydroxyl peak, however, it is in proportion to the C-H peak

Compound II was found to be a pregnane type compound with sugars attached at C-3 β . Attempts were made to acquire a mass spectrum but these were unsuccessful. However, from the ^1H (Spectrum 2a, pp 107) and ^{13}C (Spectrum 2b, pp 108) NMR spectra it was clear that the aglycone part of the molecule had twenty-one carbon atoms indicating that nine carbons had been lost from a triterpenoid structure. The presence of a keto group, indicated by a resonance at δ 198.1 (C-20) in the ^{13}C NMR spectrum and the presence of a proton singlet at δ 2.23 (3H, H-21) in the ^1H NMR spectrum, suggested the presence of a methyl ketone which indicated that the compound had a two carbon side chain and

could be a pregnane derivative. Two further methyl groups were indicated by resonances at δ 0.98 (H-19) and δ 0.86 (H-18) in the ^1H NMR spectrum, which each integrated to three protons. The presence of a tri-substituted double bond was indicated by a fully substituted carbon resonance at δ 155.2 (C-17) and a methine carbon resonance at δ 146.2 (C-16).

From the 2-D NMR spectra the resonances attributable to the aglycone part of the molecule could readily be distinguished from those due to the sugars. The H-3 resonance was easy to distinguish from the sugar proton resonances as it showed coupling in the COSY (Spectrum 2c, pp 109) and TOCSY (Spectrum 2e, pp 111) spectra with aglycone protons and could be seen to occur as a broad singlet at δ 4.02. The corresponding C-3 resonance could be obtained from the HSQC spectrum (Spectrum 2d, pp 110) and was seen to occur at δ 75.0. The ^{13}C NMR spectrum shows the aglycone part of the molecule had three methyl carbons, eight methylene carbons, six methine carbons and four fully substituted carbons. This supported the idea that this compound was a pregnenolone.

The HMBC spectrum (Spectrum 2g, pp 113) was used to position the alkene double bond. The C-20 carbonyl carbon resonance showed a HMBC correlation with 3H-21. The fully substituted carbon resonance occurring at δ 155.2 (C-17) showed HMBC correlations again with the 3H-21 signal and also the methyl group proton resonance occurring at δ 0.86. Thus the resonance at δ 0.86 was assigned to 3H-18 and the double bond was positioned at Δ^{16} . Placement of this double bond was confirmed by the NOESY spectrum (Spectrum 2f, pp 112). A correlation was seen between the 3H-21 proton resonance and the H-16 resonance at δ 6.87 (brs).

The methyl groups at C-13 and C-10 are in the β -orientation, while H-9 and H-14 are usually α and H-8 is usually β . The stereochemistry of the hydrogen at C-5 could be either α or β , and the NOESY spectrum was used to assign and confirm the stereochemistry of the methine protons. The HMBC spectrum was also used for this purpose. The methine carbon at δ 56.7 was ascribed to C-14 based on its HMBC

correlation with H-16 and 3H-18. The H-14 signal in the ^1H NMR spectrum occurred at δ 1.47. The H-14 resonance showed no correlation in the NOESY spectrum with 3H-18 confirming its stereochemistry to be α . The methine proton resonance occurring at δ 1.64 was assigned to H-8 as it showed correlations with both 3H-18 and 3H-19 proton resonances in the NOESY spectrum confirming its β -orientation. The corresponding carbon resonance occurred at δ 34.3.

The resonance ascribed to H-3 gave a correlation in the NOESY spectrum with a signal occurring at δ 1.86. The HSQC spectrum showed that the methine carbon resonance corresponding to this proton at δ 1.86 occurred at δ 36.5 and the corresponding carbon showed a correlation in the HMBC spectrum to 3H-19, indicating it to be C-5 and the corresponding proton to be H-5. The H-5 resonance showed no correlation in the NOESY spectrum with H-8 or 3H-19, indicating it to be α . This means that the H-3 proton must also be α and the sugars are attached at C-3 β . Although there was some overlap of the H-3 β proton resonance with those due to protons from the sugars, the shape of the H-3 resonance supported this assignment of stereochemistry. The remaining methine proton occurring as part of the multiplet at δ 1.44, with the corresponding carbon resonance at δ 40.7, was assigned to H-9. This assignment was confirmed by correlation between C-9 and 3H-19 in the HMBC spectrum. Thus the structure of the aglycone part of the molecule was confirmed to be 3 β -hydroxy-5 α -pregn-16-en-20-one.

It appeared that there were four sugars attached at C-3 β , however, there were several extra small peaks in the region δ 60 – 110 in the ^{13}C NMR spectrum suggesting that some molecules might have five sugars attached or that different sugars occurred in some of the molecules. As only 8 mg of material was available, it was decided not to perform a hydrolysis to remove the sugars for analysis but to retain the sample for LCMS analysis and 500 MHz NMR analysis during a visit to Professor Hostettman's laboratory later in the year, as they have had considerable success in dealing with molecules of this type.

However, certain deductions could be made about the sugars present. In the region between δ 97 and δ 104 there were four strong signals and a weaker one (possibly due to an impurity). The resonances at δ 100.4 and δ 103.3 were due to methine carbons and the resonances at δ 98.0 and δ 101.9 were due to fully substituted carbon atoms. This means that two of the sugars belonged to the aldohexose class (such as glucose (49) or galactose (50)) and the other two sugars belonged to the ketose class (such as fructose (51) or an isomer of fructose). It was interesting that two of the sugars appear to be fructose as it was earlier stated that leaf juices containing fructose from *Agave* species could be used in health foods for diabetics. The presence of the two distinct doublets at δ 4.63 and δ 4.38 (each 7.7 Hz) confirmed the presence of two cyclised aldohexoses as these were due to the hemiacetal protons, H-1, in the two sugars. The structure of these sugars is given in figure 2.6.

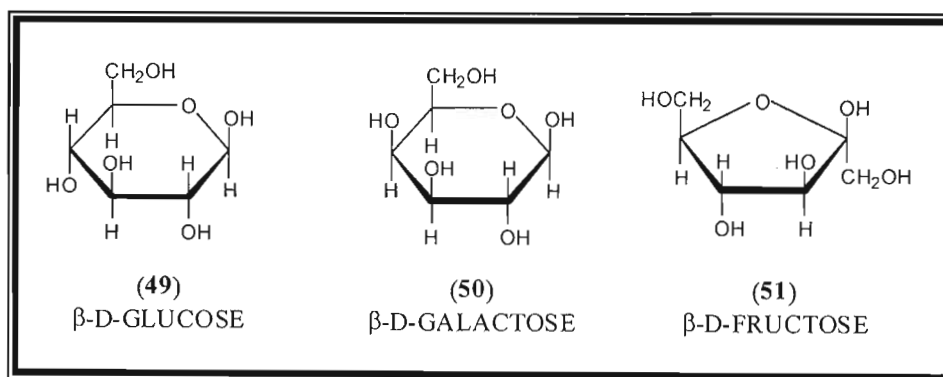


Figure 2.6 The structure of three sugars

Apart from the hemiacetal carbon atoms of glucose or galactose, four methine carbon resonances in the δ 68–85 region and a methylene carbon in the δ 60–65 region are required. Glucose and galactose can be differentiated from each other by coupling constants in their proton spectra. The ketoses, apart from their ketal carbon resonance in the region of δ 100, require a further three methine carbon resonances in the δ 68–85 region, and two methylene carbons in the δ 60–65 region. Thus for two aldohexoses and two ketoses to be present in the molecule, apart from the four resonances occurring in the δ 100 region, a further fourteen methine carbon resonances are necessary and a further

six resonances are required in the methylene region. Fifteen resonances were found in the methine region δ 68-77 (one of these, the one at δ 75.5, is due to C-3) and six methylene carbon resonances were seen in the region δ 61-65.

Due to the fact that there were many smaller peaks present, and overlapping of the proton resonances in the region between δ 3 and δ 4.2 occurred, and also the fact that the COSY and other 2-D spectra were so complex in this region, it was not possible to determine the coupling constants to see which of the aldohexoses were present or to confirm that the ketoses present were fructose, nor to determine how the sugars were connected to each other.

Both compound I and compound II are derived from the same biosynthetic precursor, namely, cholesterol (Figure 2.7)¹¹. Compound II is formed by the hydrogenation of the Δ^5 double bond in pregnenolone, to give the 5α compound. Hydroxylation then occurs at either the C-16 (as in the biosynthesis of compound I) or C-17 position, followed by dehydration to give compound II

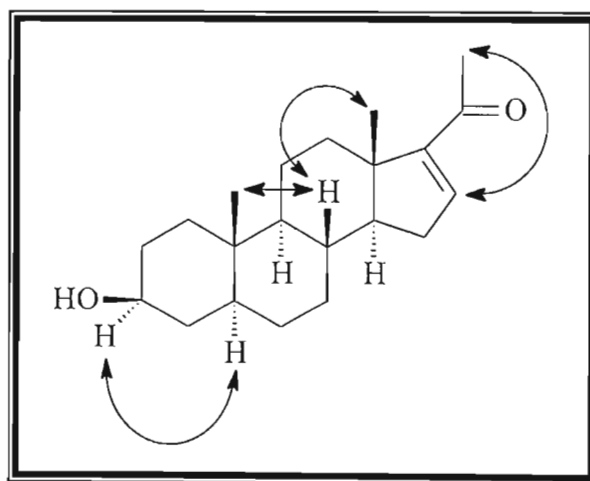
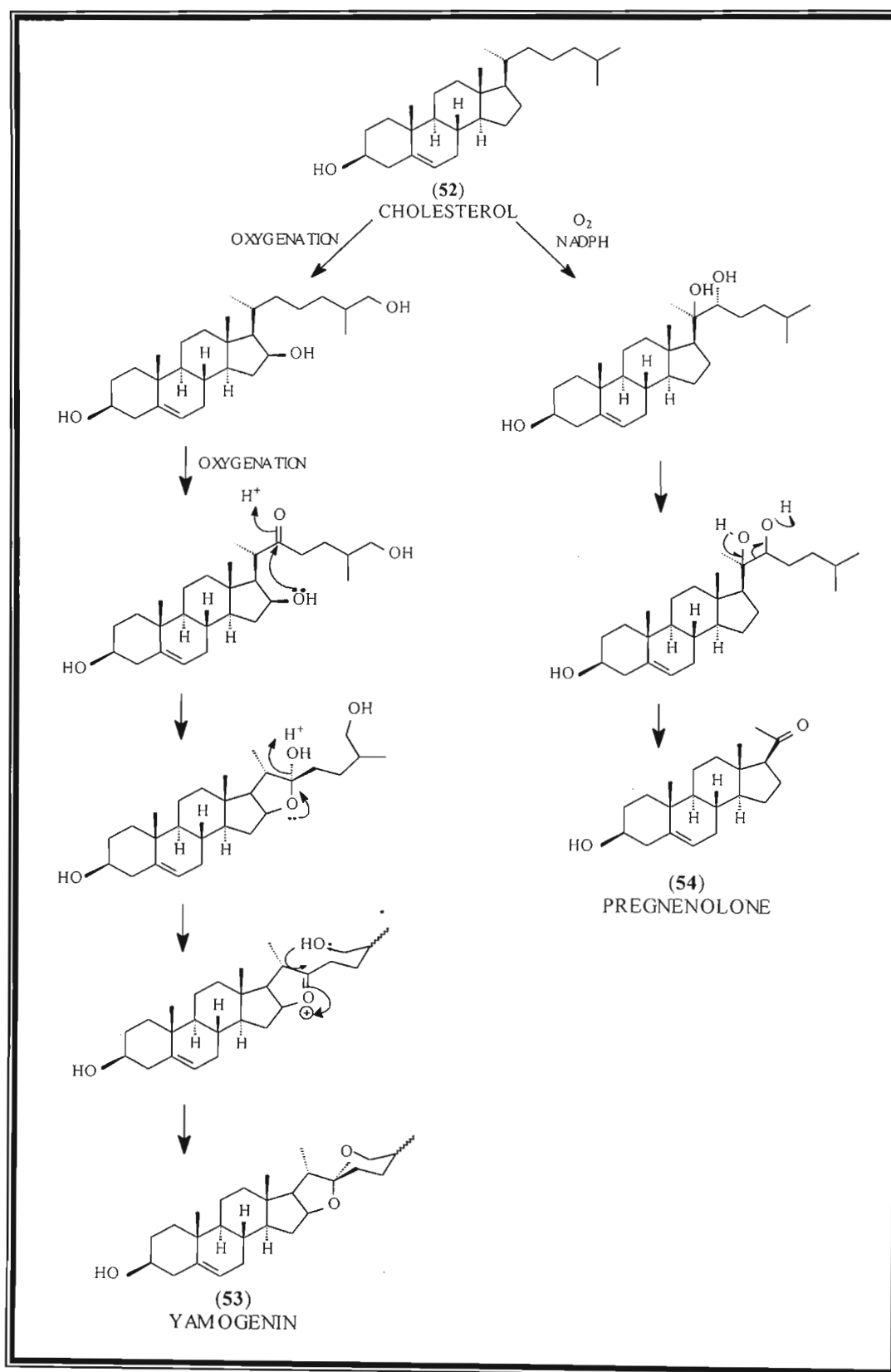


Figure 2.7 NOESY correlations for the aglycone of compound II.



Scheme 2.1 The biosynthesis of steroidal glycosides and pregnanes.

Table 2.3 NMR data for compound II.

Carbon Number	Shift (δ_C ppm)	Type	HSQC (δ_H ppm)	HMBC C \rightarrow H	COSY	NOESY
1	30.0	CH ₂	1.86 (β), 1.52 (α)	3H-19	2H-2	3H-19*
2	26.2	CH ₂	1.66 1.44	-	2H-1, H-3 α	*
3	75.0	CH	4.02 (brs)	*	2H-2, 2H-4	H-5 α
4	30.3	CH ₂	1.44	3H-19	H-3 α , H-5*	*
5	36.5	CH	1.86	3H-19	*	H-7 α ,*
6	26.3	CH ₂	1.46 1.46	-	2H-7	*
7	26.6	CH ₂	1.93 (β) 1.18 (α)	-	2H-6, H-8	H-7 α H-7 β
8	34.3	CH	1.64	3H-19	H-7, H-9*, H-14*,	3H-18, 3H-19, H-11 β *
9	40.7	CH	1.44	3H-19, H-14	*	*
10	35.1	C	-	3H-19	-	-
11	20.9	CH ₂	1.32, 1.44		2H-12, H-9*	
12	35.2	CH ₂	2.31 (β) 1.30 (α)	3H-18, H-14*	H-9, 2H-11	H-12 α H-12 β
13	45.5	C	-	3H-18, H-14, H-16	-	-
14	56.7	CH	1.47	H-16, 3H-18	H-8, 2H-15	*
15	32.2	CH ₂	2.24, 2.03	9/14*	H-14, H-16	Between H-15 α and H-15 β , H-16
16	146.2	CH	6.87 (brs)	2H-15	2H-15	H-15 α
17	155.2	C	-	3H-21, 3H-18, 2H-15	-	-
18	15.2	CH ₃	0.86	H-14	-	H-8, H-12 β
19	23.3	CH ₃	0.98	None	-	H-8,*, H-7 β
20	198.1	C	-	3H-21	-	-
21	26.0	CH ₃	2.23	-	-	H-16

*Correlation seen but not assigned due to overlap of peaks in δ 1.40- δ 1.55 region

Where it was possible to assign the stereochemistry of the methylene protons from NOESY correlations, this has been performed.

All carbon atoms and protons in the aglycone part of the molecule could be assigned using HSQC and HMBC spectra and with comparison of literature ^1H NMR data for the 3β -acetate of compound II¹² and literature ^{13}C NMR data for timosaponin A III. Difficulties were experienced in assigning all the HMBC and NOESY correlations due to the large numbers of protons in the δ 1.4 to δ 1.55 region and sensitivity problems with the 400 MHz NMR spectrometer.

It was not possible to determine coupling constants of protons in the above table due to peak overlap. It is hoped that this problem will be overcome at a later stage when the NMR instrument is set up to perform 1D-TOCSY experiments. This experiment is not available at present.

Table 2.4 ^{13}C NMR data for sugars attached to compound II.

	^{13}C NMR data for compound II	^1H NMR data for compound II		^{13}C NMR data for compound II	^1H NMR data for compound II
	δ_{C} ppm	δ_{H} ppm		δ_{C} ppm	δ_{H} ppm
1	103.3 (CH)	4.63 ($J = 7.7$ Hz)	13	74.1 (CH)	3.64
2	101.9 (C)	-	14	70.8 (CH)	3.22
3	100.4 (CH)	4.38 ($J = 7.7$ Hz)	15	70.6 (CH)	3.76
4	97.9 (C)	-	16	70.1 (CH)	3.80
5	82.1 (CH)	3.72	17	69.2 (CH)	3.80
6	77.7 (CH)	3.82	18	68.2 (CH)	3.76
7	77.2 (CH)	3.23	19	64.7 (CH ₂)	3.44, 3.63
8	76.6 (CH)	3.34	20	63.4 (CH ₂)	3.98, 4.01
9	76.2 (CH)	4.02	21	63.2 (CH ₂)	3.46, 3.60
10	75.2 (CH)	4.02	22	63.1 (CH ₂)	3.68, 3.71
11	75.1 (CH)	3.46	23	62.0 (CH ₂)	3.68, 3.53
12	75.0 (CH)	3.16	24	61.3 (CH ₂)	3.81, 3.65

2.3 Experimental

Oven dried *Agave attenuata* Salm, Hortus Dyckensis leaves (300 g) were collected from Durban and Pietermaritzburg by Professor Appleton of the School of Life and Environmental Science at the University of Natal, Durban. The leaves were extracted at room temperature by continuous agitation for approximately four days using hexane, dichloromethane and methanol successively. A sticky gum-like residue was obtained for all the extracts (1.50 g for hexane, 2.50 g for dichloromethane and 44 g for methanol). Column chromatography (Merck 9385) was used for separation of the compounds, using various ratios of methanol and dichloromethane as solvents. Compound I was the only compound isolated from the methanol extract and was eluted from the column with a 20 % methanol : 80 % dichloromethane solvent system. The hexane and dichloromethane extracts were also examined however no compounds were isolated.

Due to the sample being lost *en route* to Reims, France, a second extraction was attempted using fresh *Agave attenuata* leaves (163.8 g) in order to re-isolate compound I. The leaves, however, were extracted by continual agitation using only methanol as a solvent because compound I was isolated previously from the methanol extract. However, this isolation of compound I proved unsuccessful but rather compound II was isolated as the major component. This could be due to the fact that the initial sample of leaves was collected in December, while the second sample was collected in July.

2.3.1 Physical Data for Compound I

Name: spirostan-3-O- $[\beta$ -D-glucopyranosyl(1 \rightarrow 2)- β -D-galactopyranoside]

Synonyms: timosaponin A III, filiferin B

Physical appearance: white crystals

Yield: 30 mg

^1H NMR: δ_{H} (ppm), CD_3OD .

4.63 (1H, d, $J = 7.8$ Hz, H-1''), 4.38 (1H, d, $J = 7.7$ Hz, H-1'), 4.06 (1H, brs, H-3), 3.84 (1H, m, H-4'), 3.82 (1H, m, H-2''), 3.70 (1H, m, H-6'), 3.66 (1H, m, H-6''), 3.65 (1H, m, H-3'), 3.46 (1H, m, H-5'), 3.34 (1H, m, H-3''), 3.28 (1H, m, H-5''), 3.23 (1H, m, H-4''), 3.17 (1H, m, H-2''), 1.06 (3H, d, $J = 7.1$ Hz, H-21), 0.97 (2H, d, $J = 7.0$ Hz, H-27), 0.96 (3H, s, H-19), 0.76 (3H, s, H-18).

^{13}C NMR: δ_{C} (ppm), CD_3OD .

110.7 (C, C-22), 104.1 (CH, C-1''), 101.2 (CH, C-1'), 82.1 (CH, C-16), 78.5 (CH, C-2'), 78.1 (CH, C-5''), 77.5 (CH, C-3''), 76.1 (CH, C-5'), 75.9 (CH, C-2''), 75.8 (CH, C-3), 74.9 (CH, C-3'), 71.6 (CH, C-4''), 70.1 (CH, C-4'), 65.7 (CH₂, C-26), 63.3 (CH, C-17), 62.9 (CH₂, C-6''), 62.1 (CH₂, C-6'), 57.3 (CH, C-14), 43.1 (CH, C-20), 41.5 (C, C-13), 41.0 (CH, C-9), 41.0 (CH₂, C-12), 37.2 (CH, C-5), 36.4 (CH, C-8), 35.8 (C, C-10), 32.3 (CH₂, C-15), 31.1 (CH₂, C-4), 30.7 (CH₂, C-1), 28.2 (CH, C-25), 27.4 (CH₂, C-23), 27.3 (CH₂, C-24), 26.9 (CH₂, C-2), 26.6 (CH₂, C-6), 26.4 (CH₂, C-7), 24.1 (CH₃, C-19), 21.7 (CH₂, C-11), 16.6 (CH₃, C-18), 16.0 (CH₃, C-27), 14.4 (CH₃, C-21).

2.3.2 Physical Data for Compound II

Name: 5 α -pregn-16-en-20-one-3 β -O-tetrasaccharide

Yield: 8 mg

Physiocl Appearance: colourless gum

Melting Point: amorphous

Infra red Spectrum: ν_{\max} (NaCl) 3364.2, 2930.8, 1662.9 cm^{-1}

Optical Rotation: $[\alpha]_{\text{D}} = -16^{\circ}$ (c, 0.00472 in MeOH)

^1H NMR: δ_{H} (ppm), CD_3OD .

6.87 (1H, brs, H-16), 4.02 (1H, m, H-3), 2.31 (1H, H-12 β), 2.24 (1H, m, H-15A), 2.23 (3H, H-21), 2.03 (1H, H-15B), 1.93 (1H, H-7 β), 1.86 (1H, H-1 β), 1.86 (1H, H-5), 1.66 (1H, H-2A), 1.64 (1H, H-8), 1.52 (1H, H-1 α), 1.47 (1H, H-14), 1.46 (1H, H-6A), 1.46 (1H, H-6B), 1.44 (1H, H-9), 1.44 (2H, H-4), 1.44 (1H, H-2B), 1.44 (1H, H-11A), 1.32 (1H, H-11B), 1.30 (1H, H-12 α), 1.18 (1H, H-7 α), 0.98 (3H, H-19), 0.86 (3H, H-18)

^{13}C NMR: δ_{C} (ppm), CD_3OD .

198.1 (C, C-20), 155.2 (C, C-17), 146.2 (CH, C-16), 75.0 (CH, C-3), 56.7 (CH, C-14), 45.5 (C, C-13), 40.7 (CH, C-9), 36.5 (CH, C-5), 35.2 (CH₂, C-12), 35.1 (C, C-10), 34.3 (CH, C-8), 32.2 (CH₂, C-15), 30.3 (CH₂, C-4), 30.0 (CH₂, C-1), 26.6 (CH₂, C-7), 26.3 (CH₂, C-6), 26.2 (CH₂, C-2), 26.0 (CH₃, C-21), 23.3 (CH₃, C-19), 20.9 (CH₂, C-11), 15.2 (CH₃, C-18)

2.4 References

- 1) <http://encarta.msn.com/index/conciseindex/13/013aa000.htm>
- 2) <http://planetpets.simplenet.com/herbagav.htm>
- 3) Brackenbury, T.D. and Appleton, C.C.; *Acta Tropica*, (1997), **68**, 201-213.
- 4) Clark, T.E., Appleton, C.C. and Drewes, S.E.; *Journal of Ethnopharmacology*, (1997), **56**, 1-13.
- 5) Parmar, V.S., Jha, H.N., Gupta, A.K. and Prasad, A.K.; *Phytochemistry*, (1992), **31**, 2567-2568.
- 6) Gentry, H.S.; "*Agaves of Continental North America*", (1982), The University of Arizona Press, Arizona, Chapter 1, 3-24.
- 7) Parmar V.S., Jha, H.N., Gupta, A.K., Prasad, A.K. and Gupta, S.; *Tetrahedron*, (1992), **48**, 1281-1284.
- 8) Wilkomirski, B., Bobeyko, V.A. and Kintia, P.K.; *Phytochemistry*, (1975), **14**, 2657-2659.
- 9) Saito, S., Nagase, S. and Ichinose, K.; *Chemical Pharmacological Bulletin*, (1994), **42**, 2342-2345.
- 10) Kemp, W.; "*Organic Spectroscopy*", third edition, (1975), The Macmillan Press, Ltd., London, Page 62.
- 11) Dewick, P.M.; "*Medicinal Natural Products, A Biosynthetic Approach*", (1997), John Wiley and Sons, New York, Chapter 5, 152-269.
- 12) Kirk, D.N., Toms, H.C., Douglas, C, White, K.A., Smith, K.E., Latif, S. and Hubbard, R.W.P.; *Journal of the Chemical Society, Perkin Transactions 2*, (1990), 1567-1594

CHAPTER 3

Extractives from *Balanites maughamii*

3.1 Introduction

The genus *Balanites* of the family Balanitaceae consists of spiny shrubs or trees (Figure 3.1). The family is included by many authors in Zygophyllaceae, a family which very often produces steroid or triterpenoid saponins¹. The genus has been found to contain certain toxic saponins. Bark from *Balanites aegyptiaca*, found in the Sudan, is reportedly toxic to fish but not to man. The fruit is used to control snail intermediate hosts of schistosomiasis as it possesses properties lethal to molluscs and bilharzial miracidia and cercaria². *Balanites maughamii* Sprague, which grows in the lowveld of the Eastern and Northern Transvaal, Northern Zululand and East Africa, is a tree extending thirty to sixty feet in height and possesses large thorns for protection. The fruit consists of juicy flesh surrounding a stone with a kernel and is date-like in appearance³.

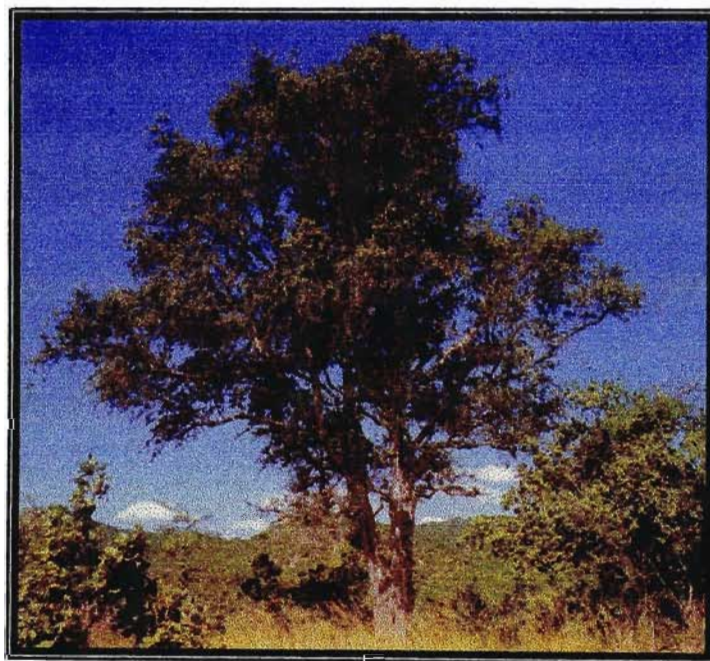


Figure 3.1 The *Balanites maughamii* tree.

Many biological tests have been carried out on the fruits of both *B. aegyptiaca* and *B. maughamii* to determine their effect on snails, tadpoles, fish and mosquito larvae. The fruits were soaked in various quantities of water for various lengths of time and the aquatic fauna were then added. The experiments showed that both species of *Balanites* contained lethal components and to the same extent i.e. snails, tadpoles and fish were affected, however, mosquito larvae were not².

The lethal component is possibly a saponin. Saponins are known to cause a lower surface tension in water and haemolysis of blood corpuscles. Thus it is likely that the aquatic animals' respiratory organs, which come into contact with the toxic solutions, are affected. This would account for the fact that air breathers, the mosquito larvae, are not affected. The fruit is edible and is readily eaten by both man and animals.

Yamogenin (**53**) has been found by Hardman and Sofowora⁴ to be the principle steroidal saponin of *B. aegyptiaca*.

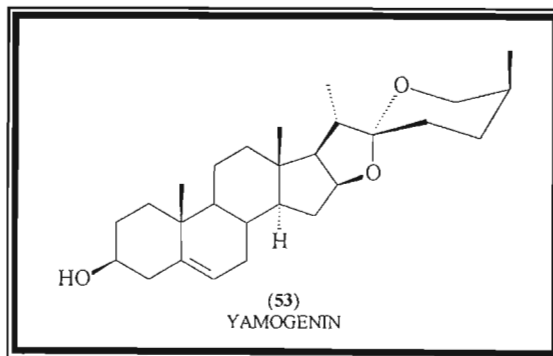


Figure 3.2 Structure of yamogenin.

This was later confirmed by Liu and Nakanishi⁵ who isolated three potent molluscicides balanitin-1 (yamogenin 3-O - α - L - (1 \rightarrow 2) - β - D - glucopyranosyl - (1 \rightarrow 4) - [α - L - rhamnopyranosyl - (1 \rightarrow 2)] - β - glucopyranoside) (**55**), balanitin-2 (yamogenin 3-O - β - D - xylopyranosyl - (1 \rightarrow 6) - β - D - glucopyranosyl - (1 \rightarrow 3) - [α - L - rhamnopyranosyl - (1 \rightarrow 2)] - glucopyranoside) (**56**) and balanitin-3 (yamogenin 3-O - α - L - rhamnopyranosyl - (1 \rightarrow 2) - β - D - glucopyranosyl - (1 \rightarrow 4) - β - D - glucopyranoside)

(57). When biological assays were performed on *B. maughami* the active saponin was assumed to be the same as that for *B. aegyptiaca*³.

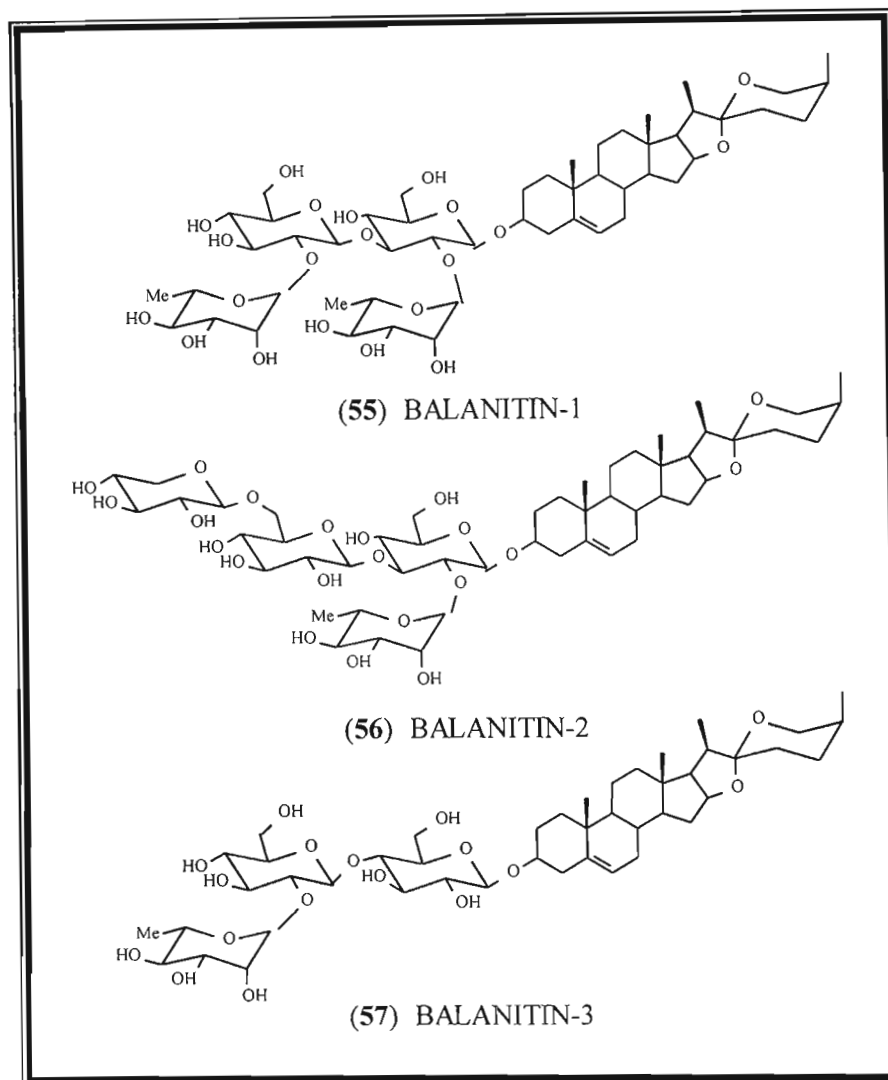


Figure 3.3 Structures of balanitin-1, balanitin-2 and balanitin-3.

The roots and bark of *Balanites maughamii* are used medicinally by Zulu traditional healers in protective rituals against evil spirits. Bark extracts are also used as emetics in certain parts of southern Africa. The fruit, which ripens only between November and January, is consumed by both humans and animals but is highly toxic to aquatic fauna and small fish. The fruit is known to have potent molluscicidal properties, the bark has mild molluscicidal properties while the leaves and seeds have none¹.

No chemical investigations have been reported for *Balanites maughamii*, however much work has been done on *Balanites aegyptiaca*. Previous work on this *B. aegyptiaca* by Kamel and Koskinen⁶ yielded two pregnane glycosides from the mesocarp of the fruit. One was new and identified as pregn-5-ene-3 β ,16 β ,20(R)-triol 3-O-(2,6-di-O- α -L-rhamnopyranosyl)- β -O-glucopyranoside (balagyptin) (**58**), while the other is a known compound and was identified as pregn-5-ene-3 β ,16 β ,20(R)-triol-3-O- β -D-glucopyranoside (**59**).

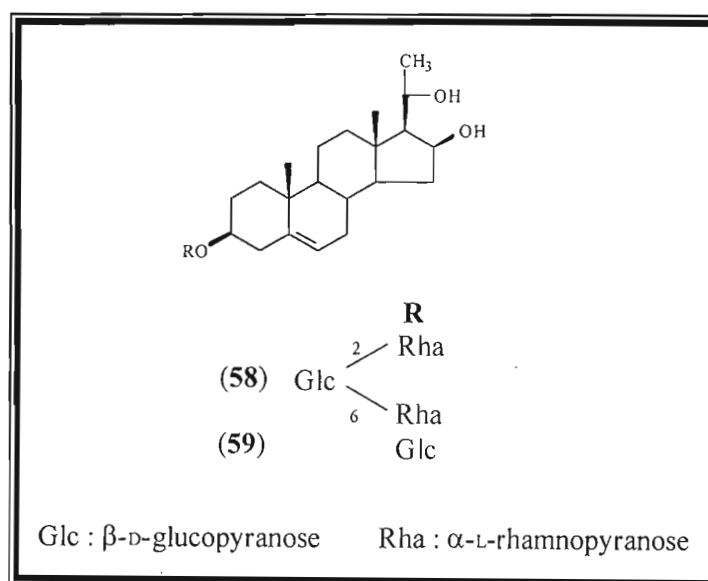


Figure 3.4 Compounds isolated from *Balanites aegyptiaca*.

In 1978, Polonsky *et al.*⁷ isolated (+)-balanitol (**60**), a bicyclic sesquiterpene alcohol, from the bark of *Balanites roxburghii*.

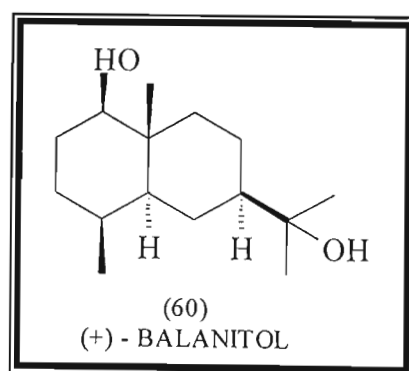


Figure 3.5 Structure of balanitol.

3.2 Results and Discussion

Only the bark from *Balanites maughamii* was investigated due to the fruit only ripening between November and January. The ethanol extract, which was treated with an acid (concentrated hydrochloric acid) and a base (concentrated sodium hydroxide), yielded two compounds from the acidic extract, the coumarin, scopoletin (**compound III**) and the sterol, stigmasterol (**compound IV**). Both of these compounds are known and are common in nature. Scopoletin has been isolated previously from *Atropa belladonna* (Solanaceae) and several Meliaceae species, while stigmasterol has been isolated from many plant sources.

3.2.1 Structural Elucidation of Compound III

The first compound isolated from the stem and bark extract was a coumarin known as 7-hydroxy-6-methoxy-2H-1-benzopyran-2-one or commonly known as scopoletin (**compound III**). It was isolated from the acidic extract as colourless needles. This compound could not be detected by using anisaldehyde spray reagent, instead it fluoresced with a bright blue spot under ultra violet (UV) light at 345 nm. This compound was eluted using a 50% ethyl acetate : 50% hexane solvent system. It is possible to make assignments of the structural class from the colour of the fluorescence. Characteristically 7-alkoxycoumarins show a purple fluorescence while 7-hydroxycoumarins and 5,7-dioxygenated coumarins fluoresce with a blue colour⁸.

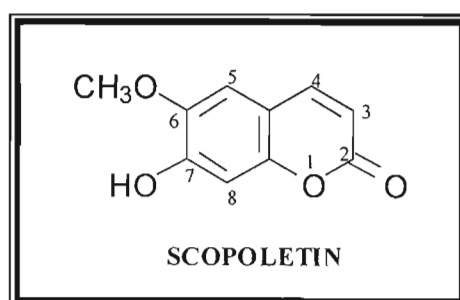


Figure 3.6 Compound III: scopoletin.

Mass spectrometry (Spectrum 3f, pp 120) showed a $[M^+]$ peak at m/z 192.0418 which indicated a molecular formula of $C_{10}H_8O_4$. Characteristic peaks were observed at m/z 177, m/z 149 and m/z 121.

The infra red spectrum (Spectrum 3g, pp 121) showed an intense band at 3342 cm^{-1} due to the O-H stretching vibration. A less intense band at 2927 cm^{-1} was due to aliphatic C-H stretching. The carbonyl stretching vibrations of the α,β -unsaturated lactone was shown as a strong sharp band at 1717 cm^{-1} . The bands at 1576 cm^{-1} and 1526 cm^{-1} indicated that this was an aromatic compound.

The ^1H NMR spectrum (Spectrum 3a, pp 115) showed a signal at δ 3.94 (3H, s, OCH_3) arising due to the methoxyl group protons. The signal at δ 6.10 (1H, s) was ascribed to the hydroxyl group proton while the H-5 (1H, s) and H-8 (1H, s) resonances were observed at δ 6.83 and δ 6.90 respectively. A pair of doublets at δ 7.58 (1H, d, $J = 9.5$ Hz) and δ 6.24 (1H, d, $J = 9.5$ Hz), were assigned to the methine protons at C-4 and C-3 respectively. The coupling constant indicated they were *cis* to each other.

The ^{13}C NMR spectrum (Spectrum 3b, pp 116) only showed resonances for five carbons as the sample was not very concentrated. The resonance at δ 56.4 was due to the methoxyl group carbon. The methine carbon signals at δ 143.3 (C-4), 113.4 (C-3), 107.5 (C-5) and 103.2 (C-8) were assigned, by comparison to literature⁹, to the methine protons, while the quaternary carbons were not observed.

Literature data for the ^1H NMR spectrum of scopoletin was only available using the solvent DMSO-d_6 but ^{13}C NMR data in CDCl_3 was available. The large difference in experimental chemical shift for C-5 compared to literature values, was a cause for concern. Three NOE experiments were performed to confirm the placement of the hydroxyl and methoxyl groups. Irradiation of H-4 (δ 7.58) (Spectrum 3c, pp 117) led to an enhancement of signals at δ 6.83 (d, H-5) and δ 6.24 (d, H-3). Irradiation of the signal at δ 6.83 (d, H-5) (Spectrum 3d, pp 118) led to the enhancements of the resonances at δ 7.58 (d, H-4) and δ 3.94 (OCH_3). Irradiation of the methoxyl group protons (Spectrum 3e, pp 119) only led to an enhancement of the H-5 signal. No NOE was observed between H-8 and the other protons, which confirmed the position of the hydroxyl group at C-7. This confirmed that the structure was scopoletin.

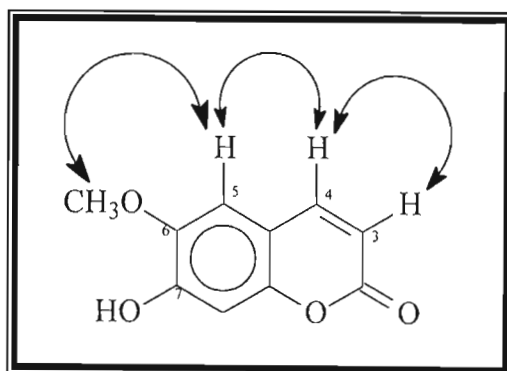


Figure 3.7 NOE correlations for compound III

Table 3.1 ^1H NMR data for compound III and literature data for scopoletin⁹.

	^1H NMR data for compound III (CDCl_3) (400 MHz)	^1H NMR literature data for scopoletin ⁹ ($\text{DMSO}-d_6$) (250 MHz)
Proton Number	δ_{H} ppm	δ_{H} ppm
3	6.24 (d, $J = 9.5$ Hz)	6.18 (d, $J = 9.6$ Hz)
4	7.58 (d, $J = 9.5$ Hz)	7.87 (d, $J = 9.6$ Hz)
5	6.83 (s)	7.18 (s)
8	6.90 (s)	6.73 (s)
OH	6.10 (s)	10.2 (s)
OCH_3	3.94 (s)	3.80 (s)

Table 3.2 ^{13}C NMR data for compound III and literature data for scopoletin⁹.

	^{13}C NMR data for compound III (CDCl_3) (100 MHz)	^{13}C NMR literature data for scopoletin ⁹ (CDCl_3) (62.9 MHz)
Carbon Number	δ_{C} ppm	δ_{C} ppm
2	*	160.3 (s)
3	113.4 (CH)	114.4 (d)
4	143.3 (CH)	143.4 (d)
5	107.5 (CH)	113.9 (d)
6	*	143.3 (s)
7	*	149.8 (s)
8	103.2 (CH)	104.2 (d)
9	*	147.2 (s)
10	*	114.4 (s)
$-\text{OMe}$	56.4	56.3

- Carbon resonances not observed

3.2.2 Structural Elucidation of Compound IV

The second compound isolated was a colourless material identified as 24 β -ethylcholesta-5,22-dien-3 β -ol, commonly known as stigmasterol (**compound IV**)

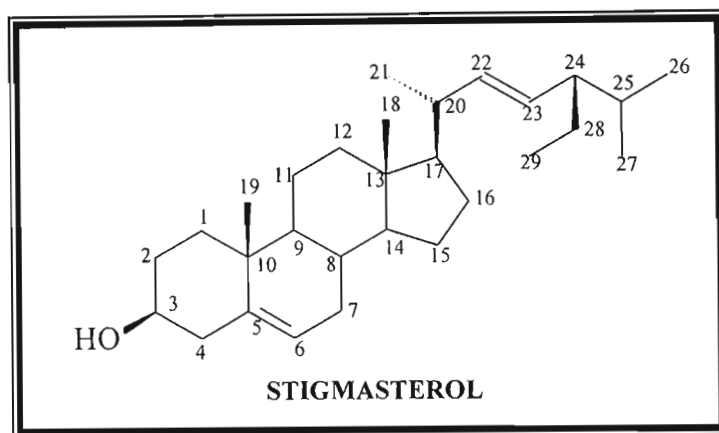


Figure 3.8 Compound IV: stigmasterol.

The ^1H NMR spectrum (Spectrum 4a, pp 122) was typical of that for stigmasterol, which is a Δ^{22} -phytosterol, and the data matched that of literature¹⁰.

The ^1H NMR spectrum showed a broad singlet at δ 5.35 (1H, brs) due to H-6 of the 5,6-double bond. The C-3 β hydroxyl group was indicated by the presence of the multiplet ascribed to H-3 α at δ 3.50 (1H, m, H-3). The signal at δ 5.00 (1H, dd, $J = 7.60$ Hz, $J = 15.38$ Hz, H-22) and δ 5.15 (1H, dd, $J = 11.53$, $J = 15.38$ Hz, H-23) were due to the presence of the 22,23-double bond. The large coupling constant indicated that these protons are *trans* to each other.

The multiplet at δ 2.21 (1H, m, H-24) was due to the methine proton at C-24. The proton NMR spectrum showed the presence of two tertiary methyl groups at δ 0.66 (3H, s) and δ 0.70 (3H, s), which were due to H-18 and H-19 respectively. Secondary methyl groups gave rise to signals at δ 1.00 (3H, d, $J = 6.65$ Hz, H-21), δ 0.90 (3H, d, $J = 6.53$ Hz, H-

26) and δ 0.78 (3H, d, $J=6.35$ Hz, H-27). The resonance at δ 0.80 (3H, t, $J=6.5$ Hz) is a triplet and is ascribed to H-29.

Table 3.3 ^1H NMR data for compound IV and literature data for stigmasterol¹⁰

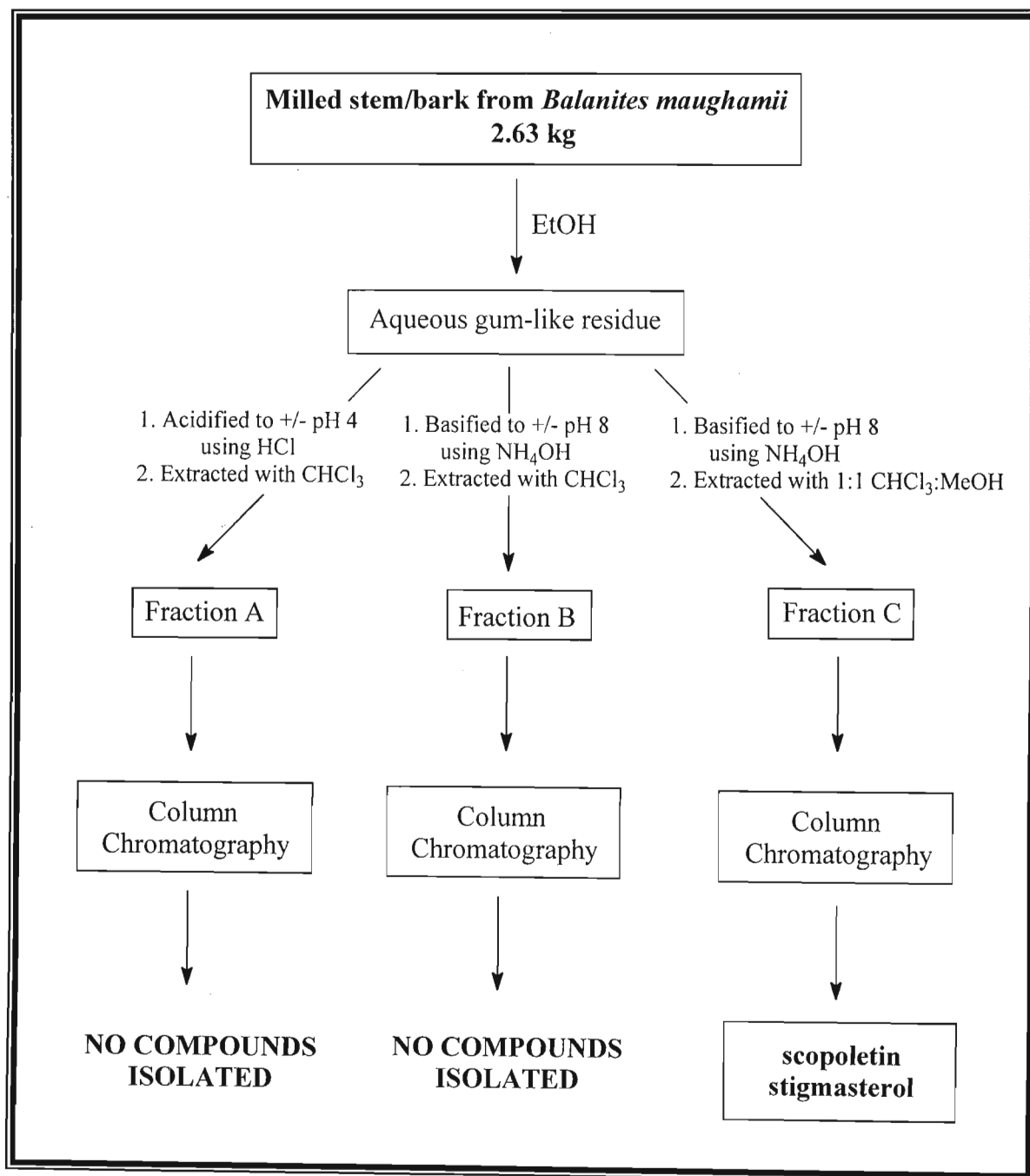
	^1H NMR data for compound IV (CDCl ₃) (300 MHz)	^1H NMR literature data for stigmasterol ¹⁰ (CDCl ₃) (220 MHz)
Proton Number	δ_{H} ppm	δ_{H} ppm
3	3.50 (m)	*
6	5.35 (brs)	*
18	0.66 (s)	0.66 (s)
19	0.70 (s)	0.80 (s)
21	1.00 (d, $J=6.65$ Hz)	1.00 (d, $J=6.5$ Hz)
22	5.00 (dd, $J=7.60$ Hz, $J=15.38$ Hz)	*
23	5.15 (dd, $J=11.53$ Hz, $J=15.38$ Hz)	*
24	2.21 (m)	*
26	0.90 (d, $J=6.53$ Hz)	0.84 (d, $J=6.8$ Hz)
27	0.78 (d, $J=6.35$ Hz)	0.79 (d, $J=6.8$ Hz)
29	0.80 (t, $J=6.5$ Hz)	0.80 (t, $J=7.2$ Hz)

* Data not available

3.3 Experimental

Stem and bark from *Balanites maughamii* Sprague (2.63 kg) was collected from the Botanical Gardens in Durban, Kwazulu-Natal, by Dr. Neil Crouch and a specimen voucher was retained in the Natal Herbarium (*Crouch 787*). The stem and bark were milled together and extracted with ethanol for 48 hours using continuous agitation (Scheme 3.1). A gum like residue was obtained to which was added 50 ml of water. The aqueous extract was acidified with concentrated HCl to pH 4 and extracted with 3 x 200 ml chloroform to produce fraction A (12.3 g). The aqueous extract was then basified to approximately pH 8 using concentrated ammonium hydroxide and extracted with chloroform to yield fraction B (145.6 mg). The remaining basic extract was then extracted with 1:1 chloroform : methanol to produce fraction C (14.2 g). The alkaloid extraction procedure was used in preference to successive extraction with different polarity solvents as the family Zygophyllaceae is known to contain alkaloids. However, this was not a good choice of extraction methods as the genus *Balanites* contains saponins and this method could remove the sugars from the saponins.

Thin layer chromatography was used to find the ideal solvent system for separation of the compounds. Column chromatography was then employed to afford the separation of the compounds. Various ratios of hexane, dichloromethane, ethyl acetate and methanol were used as the mobile phase and the polarity of the solvent system was gradually increased until 100% methanol was used.

Scheme 3.1 Extraction of *Balanites maughamii*.

3.3.1 Physical Data for Compound III

Name: 7-hydroxy-6-methoxy-2H-1-benzopyran-2-one

Synonyms: scopoletin

Physical Appearance: colourless needles

Yield: 10.7 mg

Melting Point: 201°C, lit. value⁹ 204 °C

Mass: $[M^+]$ at m/z 192.0418, $C_{10}H_8O_4$ requires 192.0422

EIMS m/z 192, m/z 177, m/z 149, m/z 121

Infra red Spectrum: ν_{\max} (NaCl) 3342, 2927, 1717, 1576, 1526, 1446 cm^{-1}

¹H NMR: δ_H (ppm), $CDCl_3$.

7.58 (1H, d, $J = 9.5$ Hz, H-4), 6.25 (1H, d, $J = 9.5$, H-3), 6.90 (1H, s, H-8), 6.83 (1H, s, H-5), 6.10 (1H, brs, OH), 3.94 (3H, s, OCH_3)

¹³C NMR: δ_C (ppm), $CDCl_3$.

143.3 (CH, C-4), 113.4 (CH, C-3), 107.5 (CH, C-5), 103.2 (CH, C-8), 56.4 (OCH_3)

3.3.2 Physical Data for Compound IV

Name: 24 β -ethylcholesta-5,22-dien-3 β -ol

Synonyms: stigmasterol

Physical Appearance: colourless crystals

Yield: 10.2 mg

Melting Point: 166 °C, lit. value¹¹ 170 °C

¹H NMR: δ_{H} (ppm), CDCl₃.

5.35 (1H, brs, H-6), 5.15 (1H, dd, $J = 11.53$ Hz, $J = 15.38$ Hz, H-23), 5.00 (1H, dd, $J = 7.60$ Hz, $J = 15.38$ Hz, H-22), 3.50 (1H, m, H-3), 2.21 (1H, m, H-24), 1.00 (3H, d, $J = 6.65$ Hz, H-21), 0.90 (3H, d, $J = 6.53$ Hz, H-26), 0.80 (3H, t, $J = 6.5$ Hz, H-29), 0.78 (3H, d, $J = 6.35$ Hz, H-27), 0.70 (3H, s, H-19), 0.66 (3H, s, H-18)

3.4 References

- 1) Hutchings, A.; “*Zulu Medicinal Plants, An Inventory*”, (1996), University of Natal Press, Pietermaritzburg, 150-151.
- 2) Wager, V. A.; *South African Medical Journal*, (1936), **10**, 10-11.
- 3) Pretorius, S.J., Joubert, P.H. and Evans, A.C.; *South African Journal of Science*, (1988), **84**, 201-202.
- 4) Hardman, R. and Sofowora, E.A.; *Phytochemistry*, (1970), **9**, 645-649.
- 5) Liu, H. and Nakanishi, K.; *Tetrahedron*, (1982), **38**, 513-519.
- 6) Kamel, M.S. and Koskinen, A.; *Phytochemistry*, (1995), **40**, 1773–1775.
- 7) Cordano, G., Merrien, M.A., Polonsky, J., Rabanal, R.M. Varenne, P.; *Journal of the Indian Chemical Society*, (1978), **55**, 1148.
- 8) Murray, R.D.H., Mendez, J. and Brown, S.A.; “*The Natural Coumarins*”, (1982), J. Wiley and Sons, New York, 22.
- 9) Razdan, T.K., Qadri, B., Harkar, S. and Waight, E.S.; *Phytochemistry*, (1987), **26**, 2063-2069.
- 10) Rubinstein, I., Goad, L.J., Clague, A.D.H. and Mulheim, L.J.; *Phytochemistry*, (1976), **15**, 195-200.
- 11) Dictionary of Natural Products (**DNP**) on CD-ROM, **version 6:2**, January 1998 and **version 7:1**, July 1998, Chapman and Hall Electronic Publishing Division, London.

CHAPTER 4

Extractives from *Astrotrichilia parvifolia*

4.1 Introduction

Trees belonging to the genus *Astrotrichilia* (Meliaceae) are endemic to the island of Madagascar. The genus is thought to be closely related to the *Owenia* and distantly related to *Ekebergia* and *Lepidotrichilia*¹. *Owenia* has been found to contain simple limonoids of the havanensin type while *Ekebergia* is distinguished by the occurrence of more complex, highly oxidised methyl angolensate type limonoids and ring C contracted limonoids². The genus *Lepidotrichilia* has not yet been examined chemically.

Previous investigations of *Astrotrichilia asterotricha* have yielded two dammaranes² (**61** and **62**) and a limonoid, astrotrichilin³ (**63**).

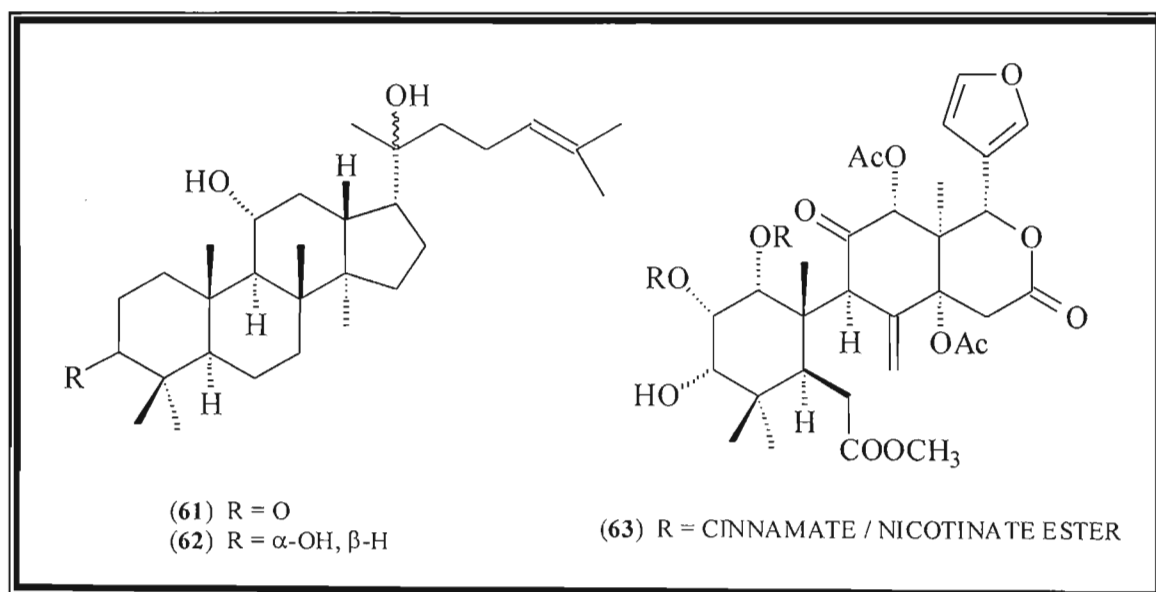


Figure 4.1 Compounds isolated from *Astrotrichilia asterotricha*.

In astrotrichilin, the cinnamate and nicotinate esters are interchangeable. In one case the cinnamate ester was at C-1 and the nicotinate ester was at C-2, in the second case, the

opposite occurred. The presence of the highly oxidised limonoid astrotrichilin, suggested that the genus *Astrotrichilia* was closely related to the genus *Ekebergia*³.

Astrotrichilia voamatata has also been studied and yielded four limonoids, voamatins A (64) and B⁴ (65), and voamatins C (66) and D⁵ (67).

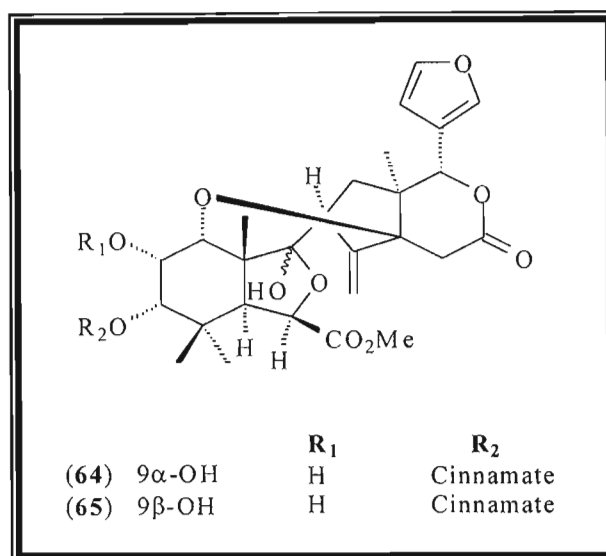


Figure 4.2 Structure of voamatins A and B.

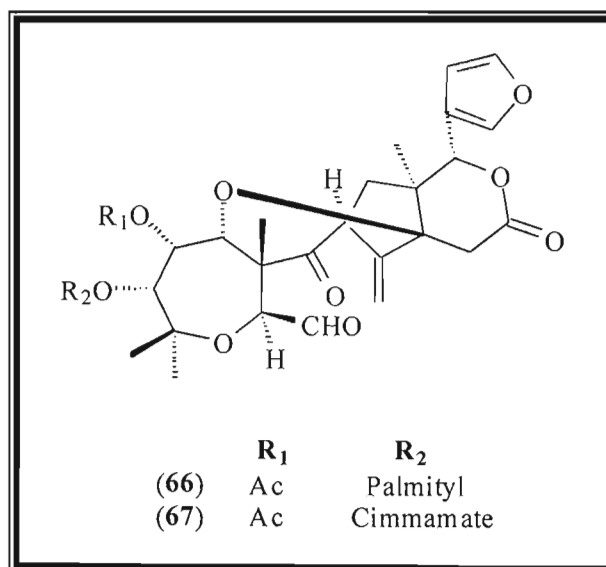


Figure 4.3 Structure of voamatins C and D.

Dammaranes are found sporadically in various genera of the Meliaceae.

4.2 Results and Discussion

The plant *Astrotrichilia parvifolia* J. F. Leroy and Lescot, was studied as previous investigations of the genus *Astrotrichilia* have revealed interesting limonoids. Extraction was achieved by using hexane, dichloromethane, ethyl acetate and methanol as solvents. The hexane fraction yielded a dammarane, shoreic acid (**compound V**), while no limonoids were isolated. No compounds were isolated from the dichloromethane, ethyl acetate and methanol extracts. Shoreic acid had been isolated previously from *Cabralea eichleriana* (Meliaceae)

4.2.1 Structural Elucidation of Compound V

The first compound isolated from the hexane extract was a white crystalline material identified as 20*R*,24*R*-epoxy-25-hydroxy-3,4-seco-5 α -dammar-4(28)-en-3-oic acid or commonly known as shoreic acid (**compound V**).

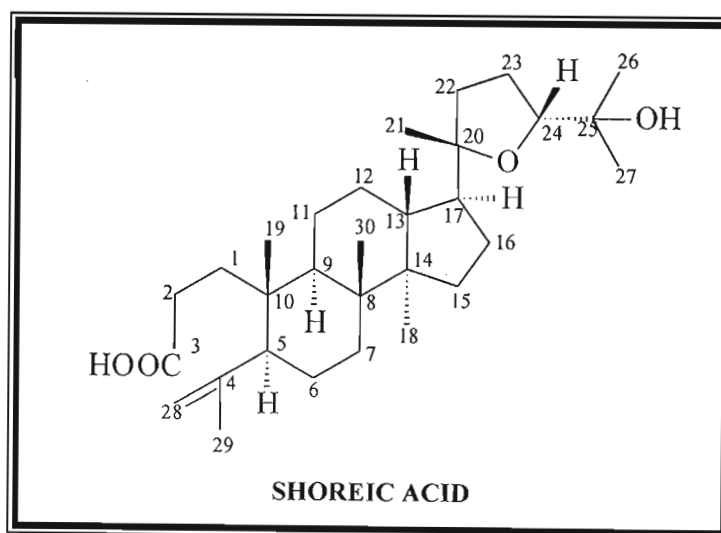


Figure 4.4 Compound V: shoreic acid.

The high resolution mass spectrum (Spectrum 5j, pp 132) showed a molecular ion peak at m/z 474.3674 which supported the proposed structure. Further fragmentation gave rise to

a peak at m/z 459 due to the loss of a methyl group, a peak at m/z 415 due to the loss of the side chain at C-24, and a peak at m/z 397 which indicated the loss of water.

The infra red spectrum (Spectrum 5k, pp 133) showed a broad peak at 3460 cm^{-1} due to –OH stretching and a large peak at 2968 cm^{-1} due to aliphatic C-H stretching. A sharp peak was observed at 1714 cm^{-1} , which indicated the presence of a carbonyl stretching vibration. Methylene group bending was seen at 1460 cm^{-1} and 1391 cm^{-1} .

The two signals at δ 4.64 (1H, brs, H-28A) and δ 4.82 (1H, brs, H-28B) in the proton NMR spectrum (Spectrum 5a, pp 123) were broad singlets ascribed to the two non-equivalent methylene protons on C-28. The two protons correlated to a signal at δ 113.6 (CH₂) in the HSQC spectrum (Spectrum 5e, pp 127), while the resonance at δ 23.5 (CH₃, C-29) was assigned to the vinyl methyl carbon. The COSY spectrum (Spectrum 5d, pp 126) showed coupling of the two vinyl methylene protons to one another as well as to the vinyl methyl protons.

The ¹³C NMR spectrum (Spectrum 5c, pp 125) showed the presence of thirty carbon atoms, which supported the proposed structure. The ¹H NMR spectrum indicated six tertiary methyl groups at δ 0.83, 0.87, 0.99, 1.09, 1.13 and 1.17 (each 3H, s), which were assigned to the methyl protons on C-19, C-18, C-30, C-21, C-26 and C-27 respectively. The methyl groups at C-21, C-26 and C-27 were shifted downfield due to being in close proximity to an oxygen atom. The fully substituted carbon atom at δ 86.8 (C-20), the methine carbon at δ 86.6 (C-24), and the fully substituted carbon at δ 70.6 (C-25), were shifted downfield as they were situated adjacent to an oxygen atom, which could only occur if there was an oxygenated ether ring present in the side chain. Acetylation of compound V (Spectrum 5b, pp 124) confirmed the presence of the ether ring as this compound did not acetylate. If no ether ring was present then the side chain would have to be an open chain containing a hydroxyl group, which would become acetylated, however, this was not the case.

The stereochemistry at C-24 was not known. However, both alternatives, shoreic acid (24*R*) or eichlerianic acid (24*S*), are known and H-21 is the same in both cases, i.e. both β . The NOESY spectrum (Spectrum 5g, pp 129) gave no correlation between the methine proton at δ 3.61 (1H, m, H-24) with that of H-21. However, a model showed that these protons could be quite far apart. Aalbersberg *et al.*⁶ stated that when a β -proton is present at C-24, C-24 resonates at approximately δ 87, while when an α -proton is present at C-24, C-24 resonates at approximately δ 84. The signal assigned to C-24 in compound V resonated at δ 86.6, which indicated the presence of a β -proton at C-24 or *R* stereochemistry. The COSY spectrum shows coupling of H-24 with the two non-equivalent methylene protons on C-23.

Literature data⁶ for shoreic acid matched that for compound V, however, an investigation of the HMBC spectrum (Spectrum 5h, pp 130 and 5I, pp 131) showed the carbon assignments in the literature data were incorrect. For example, the carbon resonance at δ 24.4 in the literature data was ascribed to C-1, however, this signal showed an HMBC correlation with H-27 and cannot therefore be due to C-1. Thus the carbon data was not assigned by comparison with literature, but rather by using the HMBC spectrum. However, it was not possible to assign all the resonances due to overlap of many of the ¹H NMR resonances. The resonances ascribed to H-28A and H-28B showed a three-bond correlation with C-5 at δ 51.1 (CH) and C-29 at δ 23.5 (CH₃), which showed that ring A had to be open at the 3,4-position. Further confirmation of this was that C-3 showed a two-bond correlation with H-2 and a three-bond correlation with H-1, however no correlation was observed with H-5. The protons of the methyl group at δ 1.09 showed a two-bond correlation with C-20, as well as three-bond correlations with C-22 and C-17. The proton signal at δ 1.71 (H-29) showed HMBC correlations with the carbon resonances at δ 113.6 (CH₂, C-28) and δ 51.1 (CH, C-5).

Table 4.1 ^1H NMR data for compound V and literature data for shoreic acid⁶.

	^1H NMR data for compound V (CDCl_3) (400 MHz)	^1H NMR literature data for shoreic acid ⁶ (CDCl_3) (300 MHz)
Proton Number	δ_{H} ppm	δ_{H} ppm
18	0.87 (s)	1.01 (s)
19	0.83 (s)	0.85 (s)
21	1.09 (s)	1.11 (s)
24	3.61 (m)	3.65 (m)
26	1.13 (s)	1.14 (s)
27	1.17 (s)	1.19 (s)
28 A	4.64 (s)	4.66 (s)
28 B	4.82 (s)	4.87 (s)
29	1.71 (s)	1.73 (s)
30	0.99 (s)	1.01 (s)

Table 4.2 ^{13}C NMR data for compound V and literature data for shoreic acid⁶.

Carbon Number	^{13}C NMR data for compound V (CDCl_3) (100 MHz)	^{13}C NMR literature data for shoreic acid ⁶ (CDCl_3) (75 MHz)
	δ_{C} ppm	δ_{C} ppm
1	28.6 (CH_2)	24.4 (t)
2	34.6 (CH_2)	28.1 (t)
3	179.6 (C)	179.2 (s)
4	147.6 (C)	147.2 (s)
5	51.1 (CH)	41.0 (d)
6	*	31.2 (t)
7	34.2 (CH_2)	33.7 (t)
8	40.3 (C)	39.9 (s)
9	41.5 (CH)	49.5 (d)
10	39.5 (C)	38.9 (s)
11	*	22.1 (t)
12	*	25.6 (t)
13	43.2 (CH)	42.7 (d)
14	50.6 (C)	50.2 (s)
15	*	23.8 (t)
16	*	26.7 (t)
17	50.0 (CH)	50.7 (d)
18	16.6 (CH_3)	15.1 (q)
19	20.5 (CH_3)	19.9 (q)
20	86.8 (C)	86.3 (s)
21	27.5 (CH_3)	26.1 (q)
22	*	34.7 (t)
23	*	26.8 (t)
24	86.6 (CH)	86.1 (d)
25	70.6 (C)	70.1 (s)
26	24.3 (CH_3)	26.8 (q)
27	28.1 (CH_3)	27.6 (q)
28	113.6 (CH_2)	113.2 (t)
29	23.5 (CH_3)	22.9 (q)
30	15.7 (CH_3)	16.1 (q)
Unassigned resonances: 35.0 (CH_2), 31.8, (CH_2), 28.6 (CH_2), 27.2 (CH_2), 26.1 (CH_2), 24.9 (CH_2), 22.6 (CH_2)		

- Data could not be assigned due to irresolvable spectra

4.3 Experimental

The stem and bark of *Astrotrichilia parvifolia* J.F. Leroy and Lescot, was collected and identified by Dr M. Randrianarivejosia from Feverive, Madagascar. A voucher specimen was retained at the University of Antananarivo, Madagascar (04.99 MJ/MDUL) The stem and bark (677.27g) were extracted together by continuous agitation at room temperature for approximately four days using hexane, dichloromethane, ethyl acetate and methanol respectively. Column chromatography was used for separating the compounds according to polarity, using various ratios of methanol and dichloromethane as solvents. Compound V was the predominant compound present in this plant and eluted from the hexane extract (17.55g) using a 5% methanol : 95% dichloromethane solvent system. The structural elucidation was determined using NMR spectroscopy. The remaining three extracts were not investigated as crude proton NMRs showed the presence of compound V in high concentrations in the dichloromethane and ethyl acetate extracts, while no interesting signals were observed in the crude proton NMR spectrum of the methanol extract.

4.3.1 Physical Data for Compound V

Name: 20*R*,24*R*-Epoxy-25-hydroxy-3,4-seco-5 α -dammar-4(28)-en-3-oic acid

Synonyms: shoreic acid

Yield: 25.3 mg

Physical Appearance: white crystals

Melting Point: 98 °C, lit. value⁶ 102-104 °C

Mass: [M⁺] at *m/z* 474.3674, C₃₀H₅₀O₄ requires 474.3709, *m/z* 459, *m/z* 415, *m/z* 397

Infra red Spectrum: ν_{\max} (NaCl) 2968, 1714, 1460, 1391, 764 cm⁻¹

Optical Rotation: $[\alpha]_D = +14$ (c, 0.00354 g.ml⁻¹ in CH₂Cl₂), lit. value⁶, +38 in CHCl₃

¹H NMR: δ_H (ppm), CDCl₃

4.64 and 4.82 (each 1H, s, 2 x H-28), 3.61 (1H, m, H-24), 1.71 (3H, s, H-29), 1.17 (3H, s, H-27), 1.13 (3H, s, H-26), 1.09 (3H, s, H-21), 0.99 (3H, s, H-30), 0.87 (3H, s, H-18), 0.83 (3H, s, H-19)

¹³C NMR: δ_C (ppm), CDCl₃

179.6 (C, C-3), 147.6 (C,C-4), 113.6 (CH₂, C-28), 86.8 (C, C-20), 86.6 (C, C-24), 70.6 (C, C-25), 51.1 (CH, C-5), 50.6 (C, C-14), 50.0 (CH, C-17), 43.2 (CH, C-13), 41.5 (CH, C-9), 40.3 (C, C-8), 39.5 (C, C-10), 35.0 (CH₂), 34.6 (CH₂, C-2), 34.2 (CH₂, C-7), 31.8 (CH₂), 28.6 (CH₂, C-1), 28.1 (CH₃, C-27), 27.5 (CH₃, C-21), 27.2 (CH₂), 26.7 (CH₂), 26.1 (CH₂), 24.9 (CH₂), 24.3 (CH₃, C-26), 23.5 (CH₃, C-29), 22.6 (CH₂), 20.5 (CH₃, C-19), 16.6 (CH₃, C-18), 15.7 (CH₃, C-30)

4.4 References

- 1) Pennington, T.D. and Styles, B.T.; *Blumea*, (1975), **22**, 477.
- 2) Mulholland, D.A., Nair, J.J., and Taylor, D.A.H.; *Phytochemistry*, (1994), **35**, 542.
- 3) Mulholland, D.A., Nair, J.J., and Taylor, D.A.H.; *Phytochemistry*, (1996), **42**, 1239.
- 4) Mulholland, D.A., Schwikkard, S.L., and Randrianariveolosia, M.; *Phytochemistry*, (1999), **52**, 705-707.
- 5) Mulholland, D.A., Randrianariveolosia, M., Lavaud, C. Nuzillard, J.-M. and Schwikkard, S.L.; *Phytochemistry*, (2000), **53**, 115-118.
- 6) Aalbersberg, W. and Singh, Y.; *Phytochemistry*, (1991), **30**, 921-926.

CHAPTER 5

Extractives from *Combretum fragrans*

5.1 Introduction

The genus *Combretum* of the family Combretaceae is widespread in Africa and is very dominant with respect to numbers. The genus consists of trees and shrubs and they bear fruits that have wing-like appendages¹. Plants of the genus *Combretum* are sometimes cyanogenic and often accumulate triterpenoids, especially as saponins¹. Many species are highly poisonous and, when ingested, produce symptoms such as stomach pains and severe vomiting. However, many traditional healers all over Africa have used species of Combretaceae to treat a wide range of illnesses. Although traditional medicine shows widespread use of the leaves and bark from *Combretum* species, the abundant winged fruits are never used, as they are highly toxic to humans and animals².

Previous investigations of the Combretaceae have revealed the presence of alkaloids (*Guiera senegalensis*), tannins (*Anogeissus schimperi*), flavonoids (*Combretum micranthum*) and amino acids (*Combretum zeyheri*)². Other isolated metabolites include a large variety of triterpenoid acids and their saponins mainly of the cycloartane (*Combretum molle*) and oleanane (*Combretum imberbe*) types².

Evidence from electron microscopy has revealed the presence of epidermal scale-like trichomes on the surface of the leaves of the *Combretum*, through which acidic triterpenoid mixtures are secreted². Certain isolated metabolites show cytotoxic, anti-inflammatory, anti-HIV, anti-microbial and molluscicidal activity².

Cytotoxic studies were carried out on the fruits of *Combretum* species in order to identify the toxins. Compounds isolated included several acidic triterpenoids and their glycosides, as well as certain combretastatins and their glycosides². Five women in Zimbabwe have reportedly died after inserting the fruit of *Combretum erythrophyllum* into their vaginal orifice to reduce the size. Compounds isolated from this species include unusual

cycloartane dienone lactones³ (**68**) and other cycloartenoids (**69** and **70**) from the leaves and combretastatin glucosides from the roots².

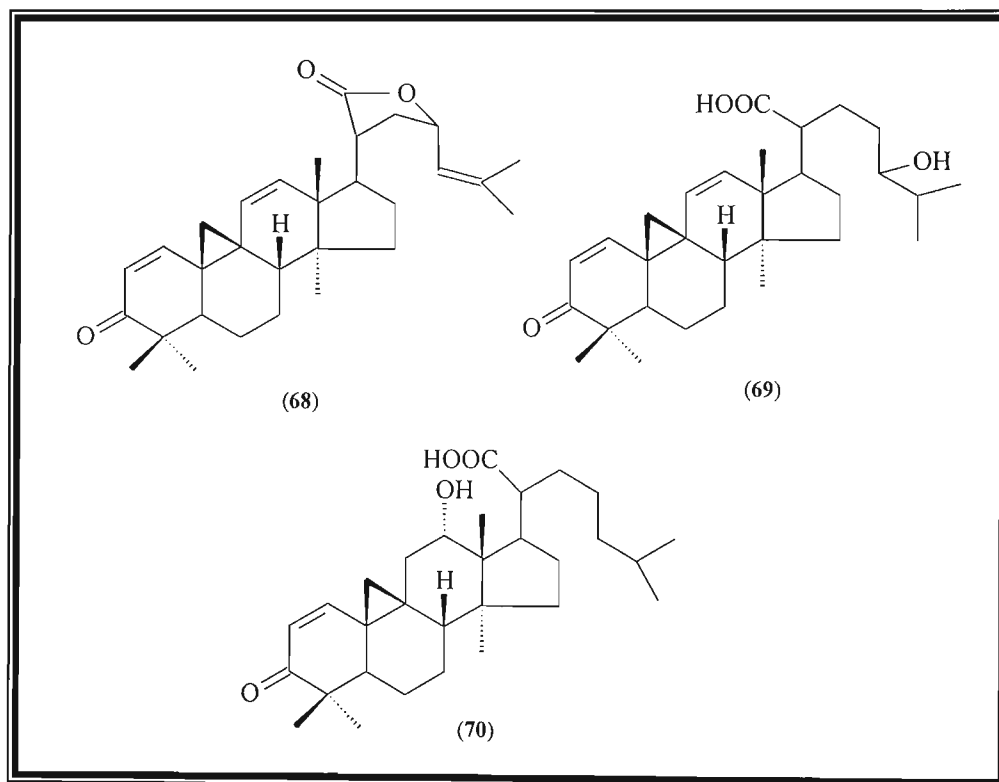


Figure 5.1 Cycloartane compounds from *Combretum erythrophyllum*.

The South African tree *Combretum caffrum* has been found to contain substances that significantly inhibit growth of murine P-388 lymphocytic leukemia (PS system) cell lines and are potent inhibitors of tubulin polymerization. Pettit *et al.* isolated combretastatins A-1⁴ (71), B-1⁴ (72), B-3⁵ (73), B-4⁵ (74) and macrocyclic lactones including combretastatin D-1⁶ (75) from this plant.

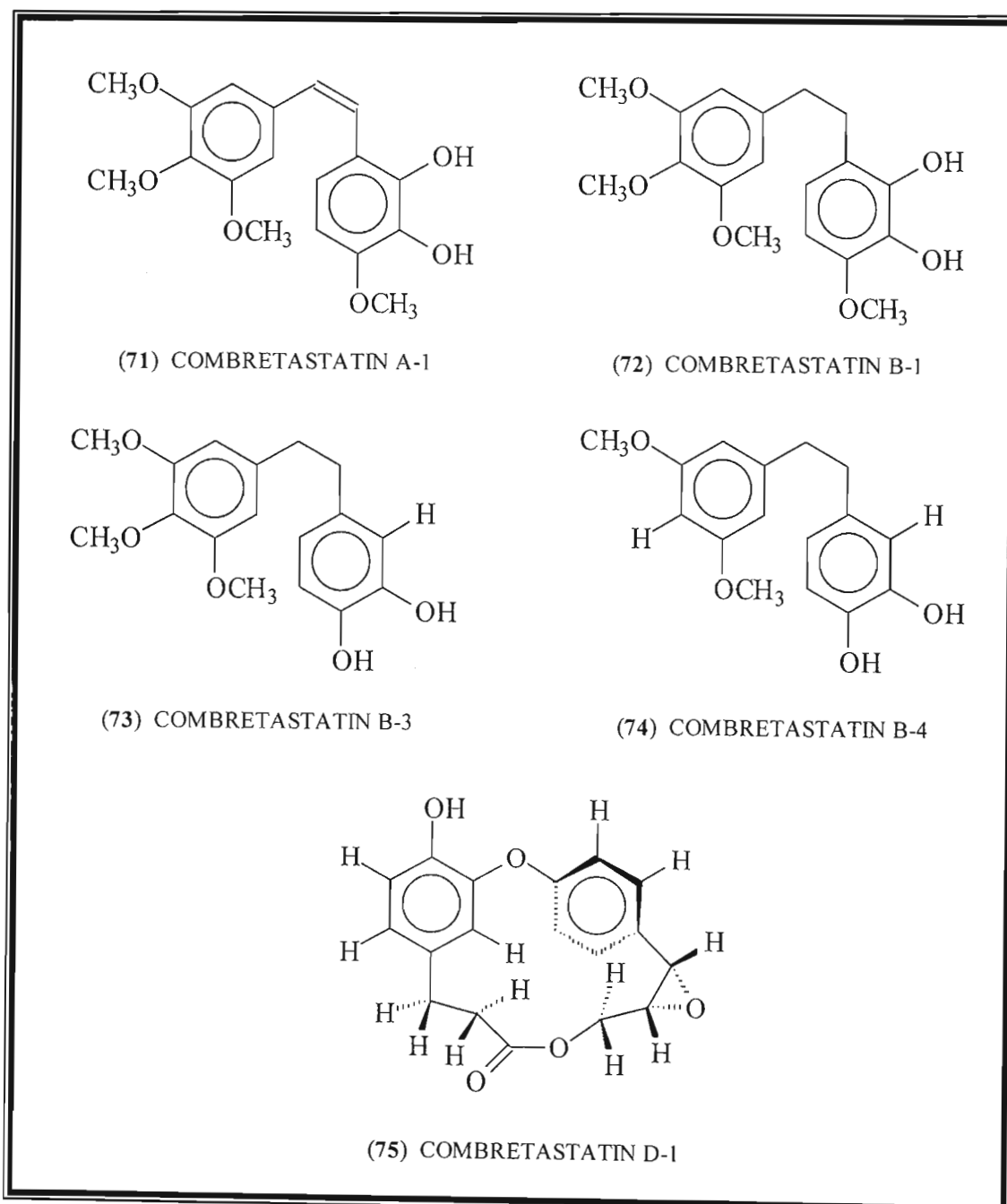


Figure 5.2 Combretastatins isolated from *Combretum caffrum*.

5.2 Scanning Electron Microscopy

The surface of the leaves of all *Combretum* species contain trichomes which secrete acidic triterpenoid mixtures, however, these trichomes are species specific and every species contains its own unique trichome structure². Scanning electron microscopy (SEM) was undertaken in order to determine the structure of the *Combretum fragrans* trichomes.

Three leaves from this species were examined, namely, a young leaf shoot, a mature leaf and an old leaf, in order to determine the structure of the trichomes at various stages of their development. The trichomes of *Combretum fragrans* only occur on the lower epidermal layer, in conjunction with the stomata. Figure 5.3 shows how numerous these trichomes are on the epidermis. These trichomes are in different stages of development as this is a young leaf shoot and most of them have not fully developed yet.

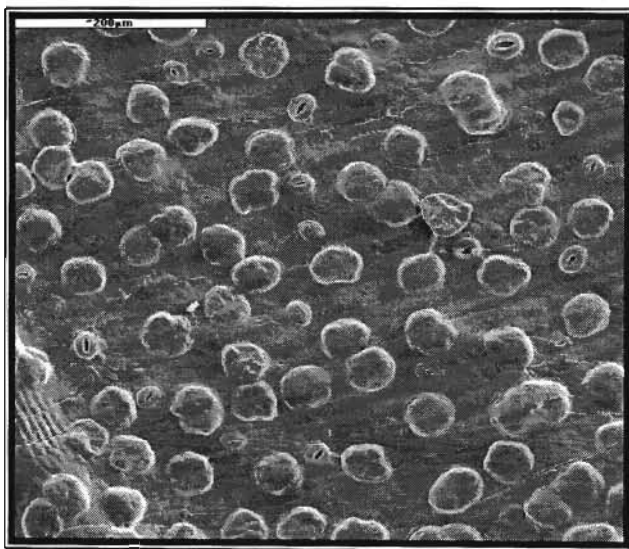


Figure 5.3 Developing trichomes on a young leaf shoot.

Structurally, trichomes consist of a basal cell embedded in the epidermis and a two-celled stalk ending in a one-cell-thick cap. In young trichomes, secretions accumulate in the cap walls and are released when the outer layer of the wall and cuticle break away². Two

fully developed glandular trichomes are shown in figure 5.4. Since these trichomes have relatively small caps and a less complicated cell pattern, plant triterpenoids of the cycloartane group are predicted to occur in this species, while trichomes that are larger and have a complicated arrangement of cap cells, secrete the oleanane group of triterpenoids².



Figure 5.4 Trichomes on a mature leaf.

Figure 5.5 shows the epidermal layer of an old leaf with trichomes that have secreted their triterpenoid mixtures and are now in a stage of desiccation.

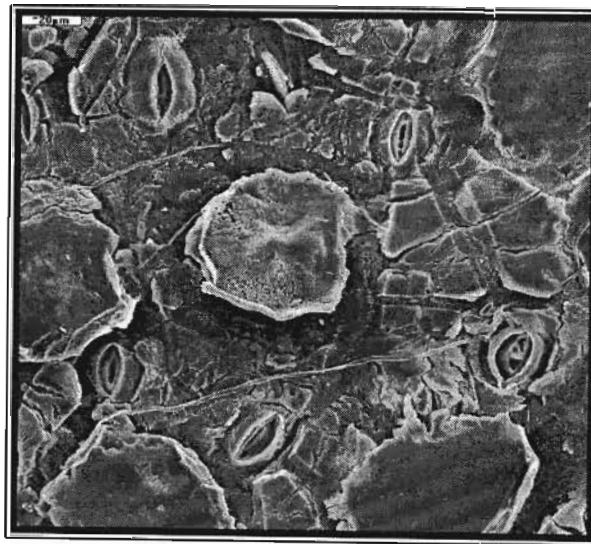


Figure 5.5 Desiccating trichome on an old leaf.

5.3 Results and Discussion

The leaves of *Combretum fragrans* F. Hoffm., were washed with a hot 1% bicarbonate solution and yielded six triterpenoids. Compounds VI-XI are of the lupane-type and are identified as lupeol (**compound VI**), lupenone (**compound VII**), lupeol-3-docosanoate (**compound VIII**), lupeol-3-eicosanoate (**compound IX**), hennadiol (**compound X**) and 30-hydroxylupenone (**compound XI**). Triterpenoids of the lupane type are commonly found in the family Combretaceae.

5.2.1 The Structural Elucidation of Compound VI

The first compound isolated from the surface of the leaves was a white crystalline material identified as 3 β -hydroxylup-20(29)-ene, which is commonly known as lupeol (**compound VI**).

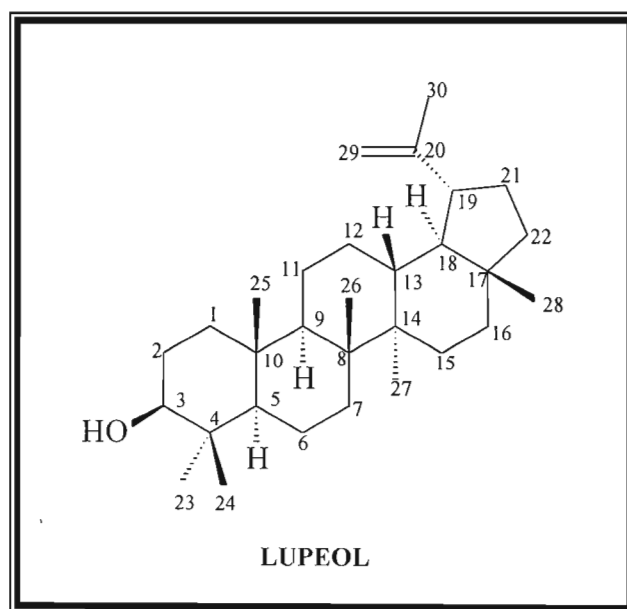


Figure 5.6 Compound VI: lupeol.

A molecular ion peak was observed at m/z 426.3867 in the high resolution mass spectrum (Spectrum 6f, pp 139), which corresponded to a molecular formula of $C_{30}H_{50}O$. Further fragments were observed at m/z 411, m/z 315 and m/z 257, with an intense peak occurring at m/z 218.

The infra red spectrum (Spectrum 6g, pp 140) supported the postulated structure for compound VII. Peaks were observed at 3378 cm^{-1} (O-H stretching), 2929 cm^{-1} (aliphatic C-H stretching). Bending of methylene groups was observed as sharp peaks at 1465 cm^{-1} and 1391 cm^{-1} .

The ^1H NMR spectrum (Spectrum 6a, pp 134) of compound VI suggested that a lupane structure was present. Two broad singlets at δ 4.55 and δ 4.67 (2H, brs, 2 x H-29) were due to the two non-equivalent methylene protons at C-29. This was confirmed by the ^{13}C NMR spectrum (Spectrum 6c, pp 136), which showed signals at δ 109.3 (CH_2) and δ 150.9 (C) due to the C-29 and C-20 carbons of the double bond. A vinyl methyl group was indicated, in the proton spectrum, by a downfield shifted methyl proton resonance at δ 1.66 (3H, s, H-30). The COSY spectrum (Spectrum 6d, pp 137) showed long range coupling between the two broad singlets at δ 4.55 and δ 4.67 and the vinyl methyl group proton resonance at δ 1.66. Six tertiary methyl group proton resonances occurred at δ 0.74, 0.77, 0.81, 0.92, 0.95 and 1.01 (each 3H, s) and were due to H-24, H-28, H-25, H-27, H-23 and H-26 respectively.

Also present in the proton spectrum was a broad double doublet at δ 3.16 (1H, dd, $J = 5.4\text{ Hz}$, $J = 10.9\text{ Hz}$, H-3) ascribed to H-3 and indicating the presence of a β -hydroxyl group at C-3. Deshielding caused by the oxygen atom of the hydroxyl group at C-3 shifted the methine signal downfield to δ 79.02 in the carbon spectrum. Acetylation of compound VII (Spectrum 6b, pp 135) resulted in the H-3 resonance being shifted downfield to δ 4.45 (1H, m). By using the HETCOR spectrum (Spectrum 6e, pp 138), the signals at δ 2.35 (1H, m) and δ 1.90 (1H, m, H-21A) could be ascribed to the proton at C-19 and one of the methylene protons on C-21 respectively.

The ^{13}C NMR spectrum showed the presence of 30 carbon atoms, which supported the proposed structure. The methine group at δ 55.3 ascribed to C-5 and the fully substituted group at δ 38.8 ascribed to C-4 are characteristic of a triterpenoid with two methyl groups attached at C-4.

The triterpenoid, lupeol, is common in nature and has been isolated previously from many species including *Streblus asper* (Noraceae). Thus the data for lupeol was assigned by comparison with literature data⁷.

Table 5.1 ^1H NMR data for compound VI and literature data for lupeol⁷.

	^1H NMR data for compound VI (CDCl_3) (300 MHz)	^1H NMR literature data for lupeol ⁷ (CDCl_3) (400 MHz)
Proton Number	δ_{H} ppm	δ_{H} ppm
3	3.16 (dd, $J = 5.4$ Hz, $J = 10.9$ Hz))	3.18 (dd)
23	0.95 (s)	0.98 (s)
24	0.74 (s)	0.77 (s)
25	0.81 (s)	0.84 (s)
26	1.01 (s)	1.04 (s)
27	0.92 (s)	0.97 (s)
28	0.77 (s)	0.79 (s)
29 A	4.55 (brs)	4.56 (m)
29 B	4.67 (brs)	4.69 (m)
30	1.66 (s)	1.69 (s)

Table 5.2 ^{13}C NMR data for compound VI and literature data for lupeol⁷.

Carbon Number	^{13}C NMR data for compound VI (CDCl_3) (75 MHz)	^{13}C Literature data for lupeol ⁷ (CDCl_3) (100 MHz)
	δ_c ppm	δ_c ppm
1	38.7 (CH_2)	38.6 (t)
2	27.4 (CH_2)	27.3 (t)
3	79.0 (CH)	78.9 (d)
4	38.8 (C)	38.8 (s)
5	55.3 (CH)	55.2 (d)
6	18.3 (CH_2)	18.2 (t)
7	34.2 (CH_2)	34.2 (t)
8	40.8 (C)	40.7 (s)
9	50.4 (CH)	50.3 (d)
10	37.1 (C)	37.1 (s)
11	20.9 (CH_2)	20.9 (t)
12	25.1 (CH_2)	25.0 (t)
13	38.0 (CH)	38.0 (d)
14	42.8 (C)	42.7 (s)
15	29.7 (CH_2)	27.4 (t)
16	35.5 (CH_2)	35.5 (t)
17	43.0 (C)	42.9 (s)
18	48.3 (CH)	48.2 (d)
19	47.9 (CH)	47.9 (d)
20	150.9 (C)	150.8 (s)
21	29.8 (CH_2)	29.8 (t)
22	40.0 (CH_2)	39.9 (t)
23	28.0 (CH_3)	27.9 (q)
24	15.3 (CH_3)	15.3 (q)
25	16.1 (CH_3)	16.1 (q)
26	15.9 (CH_3)	15.9 (q)
27	14.5 (CH_3)	14.5 (q)
28	18.0 (CH_3)	17.9 (q)
29	109.3 (CH_2)	109.3 (t)
30	19.3 (CH_3)	19.2 (q)

5.3.2 The Structural Elucidation of Compound VII

The second compound to be isolated from the leaf surface consisted of white needle-like crystals identified as lup-20(29)-en-3-one and whose common name is lupenone (**compound VII**). Lupenone is a common plant constituent and has been isolated from several sources including *Adenophora axilliflora* (Campanulaceae).

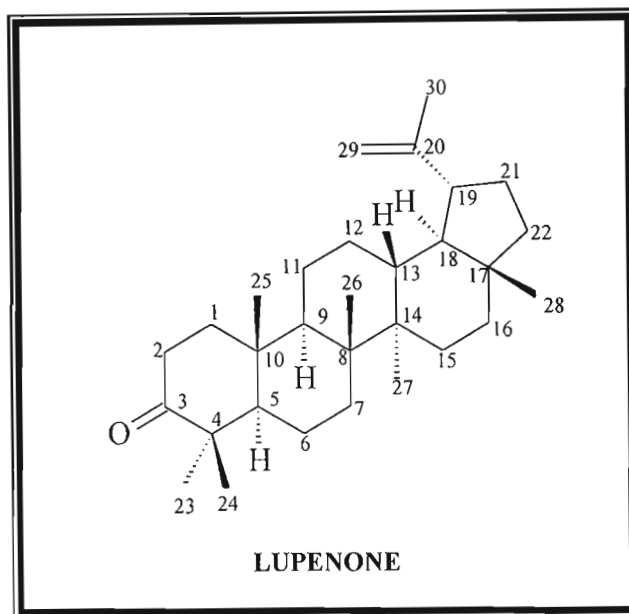


Figure 5.7 Compound VII: lupenone.

The infra red spectrum (Spectrum 7c, pp 143) showed a peak at 2933 cm^{-1} which is characteristic of aliphatic C-H stretching vibrations. An intense peak at 1714 cm^{-1} is due to the carbonyl group stretch. Bending of CH_2 groups give rise to the peaks at 1464 cm^{-1} and 1385 cm^{-1} .

The ^1H NMR spectrum (Spectrum 7a, pp 141) also suggested a lupane-type structure at first inspection. The spectrum showed that the 3-hydroxyl group had been replaced by a ketone. This was confirmed by the presence of a signal at $\delta 218.1$ (C) in the ^{13}C NMR spectrum (Spectrum 7b, pp 142). In the proton spectrum, the H-19 proton signal was merged with the H-2_{ax} proton multiplet at $\delta 2.40$. The two broad singlets at $\delta 4.67$ (1H, brs, H-29A) and $\delta 4.55$ (1H, brs, H-29B) in the proton spectrum suggested the presence

of a double bond and were assigned to the methylene group protons at C-29. The resonance at δ 109.4 (CH₂, C-29) and the fully substituted carbon resonance at δ 150.8 (C-20) confirmed the presence of the 20,29-double bond.

In the proton spectrum the downfield shifted methyl resonance at δ 1.66 (3H, s, H-30) was assigned to the vinyl methyl group at C-30. Six tertiary methyl groups were seen at δ 0.77, 0.91, 0.93, 1.00, 1.05 and 1.23 (each 1H, s) and corresponded to H-28, H-25, H-24, H-27, H-26 and H-23 respectively.

The data for compound VI was assigned by comparison to literature⁸.

Table 5.3 ¹H NMR data for compound VII and literature data for lupenone⁸.

	¹ H NMR data for compound VII (CDCl ₃) (300 MHz)	¹ H NMR literature data for lupenone ⁸ (CDCl ₃) (60 MHz)
Proton Number	δ_{H} ppm	δ_{H} ppm
23	1.23 (s)	1.53 (s) *
24	0.93 (s)	0.92 (s)
25	0.91 (s)	0.89 (s)
26	1.05 (s)	1.04 (s)
27	1.00 (s)	0.99 (s)
28	0.77 (s)	0.76 (s)
29 A	4.67 (brs)	4.66 (brs)
29 B	4.55 (brs)	4.54 (brs)
30	1.66 (s)	1.65 (s)

* This appears to be an error in the literature

Table 5.4 ^{13}C NMR data for compound VII and literature data for lupenone⁸.

Carbon Number	^{13}C NMR data for compound VII (CDCl_3) (75 MHz)	^{13}C NMR data for lupenone ⁸ (CDCl_3) (25.2 MHz)
	δ_c ppm	δ_c ppm
1	39.6 (CH_2)	39.6 (t)
2	34.1 (CH_2)	34.1 (t)
3	218.1 (C)	217.9 (s)
4	47.3 (C)	47.3 (s)
5	54.9 (CH)	55.0 (d)
6	19.6 (CH_2)	19.6 (t)
7	33.5 (CH_2)	33.6 (t)
8	40.7 (C)	40.9 (s)
9	49.7 (CH)	49.8 (d)
10	36.8 (C)	36.9 (s)
11	21.4 (CH_2)	21.5 (t)
12	25.1 (CH_2)	25.2 (t)
13	38.1 (CH)	38.2 (d)
14	42.9 (C)	42.9 (s)
15	27.4 (CH_2)	27.4 (t)
16	36.5 (CH_2)	35.6 (t)
17	42.9 (C)	42.9 (s)
18	48.2 (CH)	48.3 (d)
19	47.9 (CH)	47.9 (d)
20	150.8 (C)	150.7 (s)
21	29.8 (CH_2)	29.9 (t)
22	39.9 (CH_2)	40.0 (t)
23	26.6 (CH_3)	26.6 (q)
24	21.0 (CH_3)	21.0 (q)
25	16.9 (CH_3)	15.8 (q)
26	15.7 (CH_3)	15.9 (q)
27	14.4 (CH_3)	14.4 (q)
28	18.0 (CH_3)	18.0 (q)
29	109.4 (CH_2)	109.2 (t)
30	19.3 (CH_3)	19.3 (q)

5.3.3 The Structural Elucidation of Compound VIII

The third material isolated from the leaves of *Combretum fragrans* was a white fatty material identified as a mixture of two fatty acids joined to lupeol at C-3. The mixture contained lupeol 3 β -docosanoate (**compound VIII**) and lupeol 3 β -eicosanoate (**compound IX**).

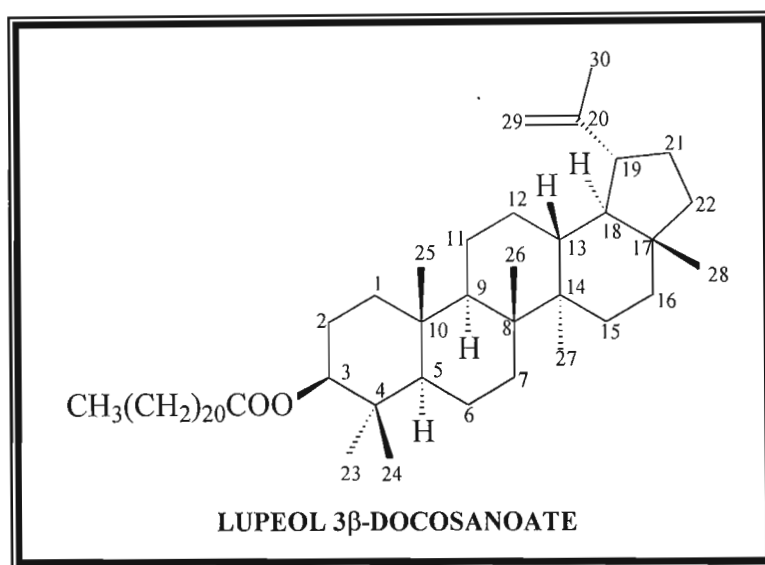


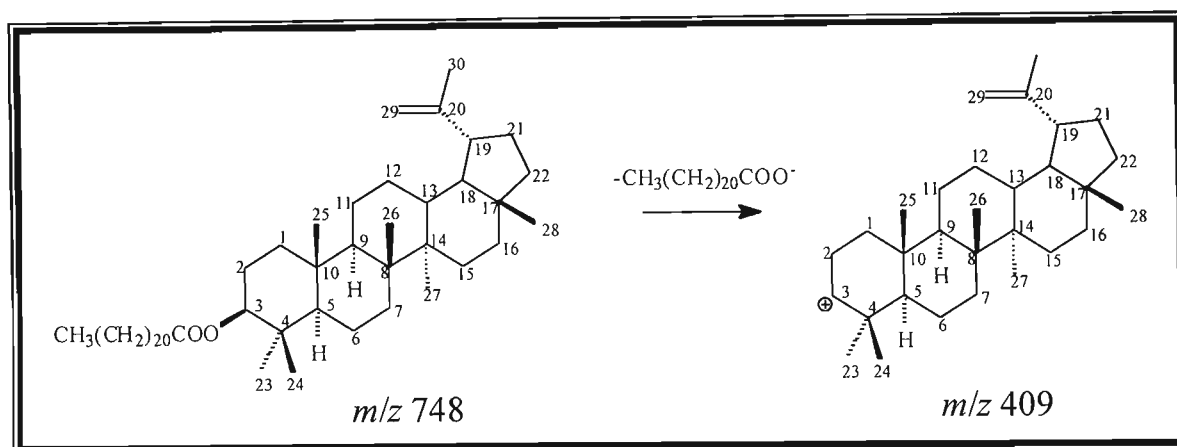
Figure 5.8 Compound VIII: lupeol 3 β -docosanoate.

The ^1H NMR spectrum (Spectrum 8a, pp 144) showed two signals at δ 4.66 (1H, brs, H-29A) and δ 4.54 (1H, brs, H-29B), which were due to the non-equivalent methylene protons at C-29. Resonances at δ 109.3 (CH_2 , C-29) and δ 150.9 (C, C-20) in the ^{13}C NMR spectrum (Spectrum 8b, pp 145) ascribed to the 20,29-double bond served as confirmation. The downfield shifted methyl proton resonance at δ 1.66 (3H, s, H-30) indicated the presence of a vinyl methyl group. The COSY spectrum (Spectrum 8c, pp 146) showed coupling of the H-29 signals with the vinyl methyl group signal. The proton spectrum showed the presence of six tertiary methyl group proton resonances at δ 0.77, 0.81, 0.84, 0.86, 0.91 and 1.01 (each 3H, s), which were due to H-24, H-28, H-25, H-27, H-23 and H-26 respectively.

The HETCOR spectrum (Spectrum 8d, pp 147) showed correlation between the double doublet at δ 4.45 (1H, dd, $J = 6$ Hz, $J = 10$ Hz, H-3) and the methine carbon assigned at C-3. The double doublet was shifted downfield, in comparison to that of lupeol, indicating the presence of an ester at C-3. Literature data was used to assign the lupeol part of the compound.

From the NMR spectra, it was predicted that the structure of this compound was lupeol with a fatty acid attached at C-3, however, the structure of the fatty acid itself could not be determined from the NMR spectra alone and so mass spectrometry was employed to determine the nature of the fatty acid. A hydrolysis reaction was attempted in order to cleave off the fatty acid, however this proved unsuccessful and so the entire sterol ester was sent for mass spectrometry. GC-MS indicated two major esters were present giving compounds VIII and IX.

The high resolution mass spectrum (Spectrum 9a, pp 148) revealed a parent ion peak at m/z 748.7119, which corresponded to a molecular formula of $C_{52}H_{92}O_2$, and was consistent with the proposed structure. In order to determine the molecular formula of the fatty acid, the molecular mass of lupeol was subtracted from the mass of the parent ion, as a comparison with carbon NMR literature data indicated that the sterol backbone of the esters was in fact lupeol. The loss of water upon esterification was taken into account when determining the molecular mass of the fatty acid. Further fragmentation was observed at m/z 409 and was due to the loss of docosanoic acid as shown in scheme 5.1.



Scheme 5.1 The mass spectrometric fragmentation of compound VIII.

Table 5.5 ^1H NMR data for compound VIII and literature data for lupeol⁷.

Proton Number	^1H NMR data for compound VIII (CDCl_3) (300 MHz)	^1H NMR literature data for lupeol ⁷ (CDCl_3) (400 MHz)
	δ_{H} ppm	δ_{H} ppm
3	4.45 (dd, $J = 6$ Hz, $J = 10$ Hz)	3.18 (dd)
23	0.91 (s)	0.98 (s)
24	0.77 (s)	0.77 (s)
25	0.84 (s)	0.84 (s)
26	1.01 (s)	1.04 (s)
27	0.86 (s)	0.97 (s)
28	0.81 (s)	0.79 (s)
29 A	4.54 (brs)	4.56 (brs)
29 B	4.66 (brs)	4.69 (brs)
30	1.66 (s)	1.69 (s)

Table 5.6 ^{13}C NMR data for compound VIII and literature data for lupeol⁷.

Carbon Number	^{13}C NMR data for compound VIII (CDCl_3) (75 MHz)	^{13}C NMR literature data for lupeol ⁷ (CDCl_3) (100 MHz)
	δ_{C} ppm	δ_{C} ppm
1	38.4 (CH_2)	38.6 (t)
2	29.8 (CH_2)	27.3 (t)
3	80.6 (CH)	78.9 (d)
4	40.0 (C)	38.8 (s)
5	55.3 (CH)	55.2 (d)
6	18.2 (CH_2)	18.2 (t)
7	34.2 (CH_2)	34.2 (t)
8	40.8 (C)	40.7 (s)
9	50.3 (CH)	50.3 (d)
10	37.1 (C)	37.1 (s)
11	20.9 (CH_2)	20.9 (t)
12	25.1 (CH_2)	25.0 (t)
13	38.0 (CH)	38.0 (d)
14	42.8 (C)	42.7 (s)
15	27.4 (CH_2)	27.4 (t)
16	35.5 (CH_2)	35.5 (t)
17	43.0 (C)	42.9 (s)
18	48.2 (CH)	48.2 (d)
19	48.0 (CH)	47.9 (d)
20	150.9 (C)	150.8 (s)
21	31.3 (CH_2)	29.8 (t)
22	40.0 (CH_2)	39.9 (t)
23	28.0 (CH_3)	27.9 (q)
24	15.9 (CH_3)	15.3 (q)
25	16.5 (CH_3)	16.1 (q)
26	16.2 (CH_3)	15.9 (q)
27	14.5 (CH_3)	14.5 (q)
28	18.0 (CH_3)	17.9 (q)
29	109.3 (CH_2)	109.3 (t)
30	19.3 (CH_3)	19.2 (q)

5.3.4 The Structural Elucidation of Compound IX

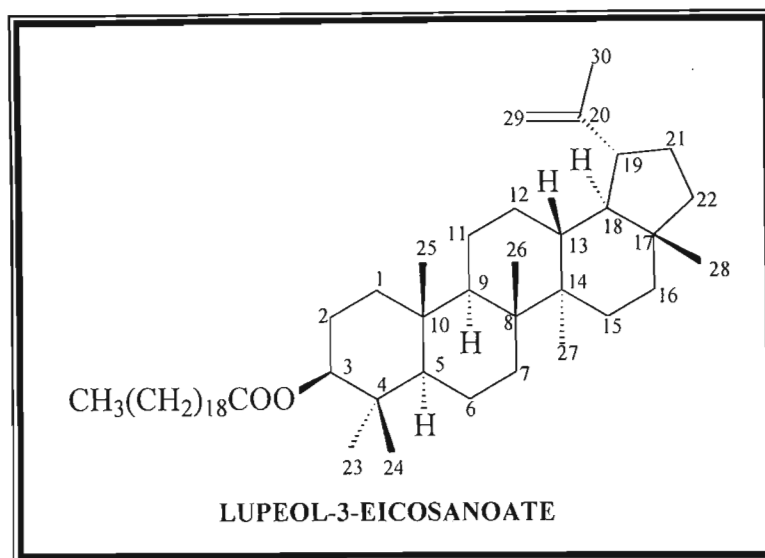
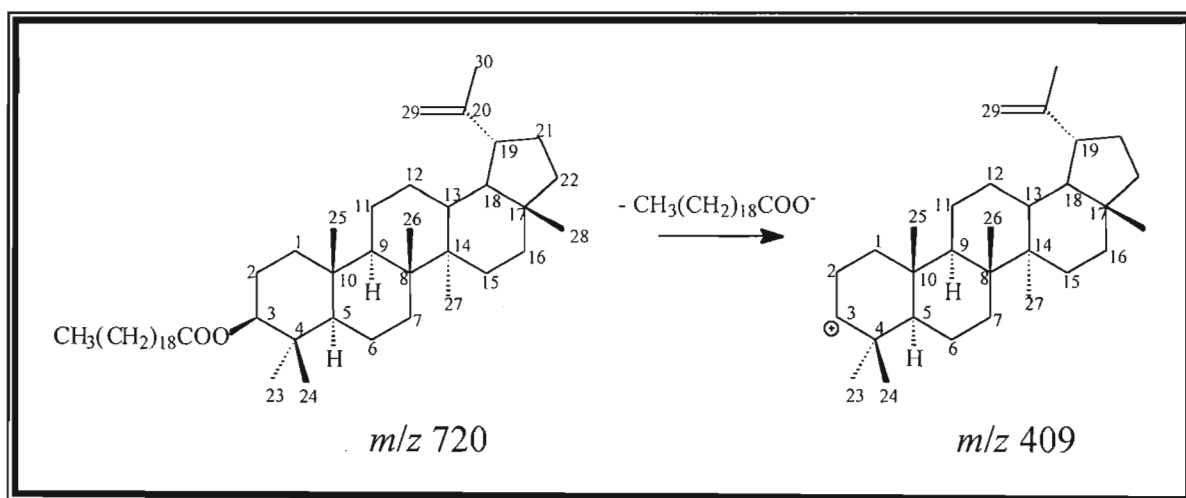


Figure 5.9 Compound IX: lupeol-3-eicosanoate.

The high resolution mass spectrum (Spectrum 9a, pp 148) indicated a molecular ion peak at m/z 720.6728 which corresponded to a molecular formula of $C_{50}H_{88}O_2$. Fragmentation also gave rise to a peak at m/z 409 due to the loss eicosanoic acid (Scheme 5.2). This structure will not be discussed any further as its structural elucidation is identical to that of compound X.



Scheme 5.2 The mass spectrometric fragmentation of compound IX.

5.3.5 The Structural Elucidation of Compound X

The fifth compound to be isolated was a white crystalline material identified as lup-20(29)-ene-3 β ,30-diol or commonly known as hennadiol (**compound X**). Hennadiol has been isolated previously from a number of plant sources including *Mortonia diffusia* (Celastraceae).

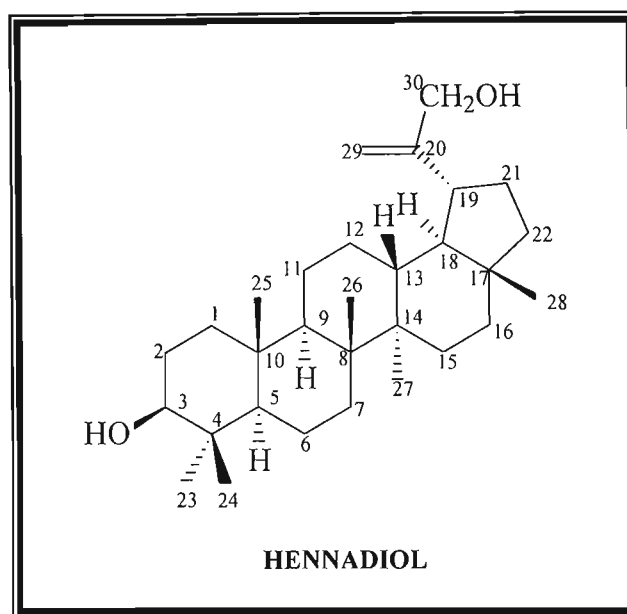


Figure 5.10 Compound X: hennadiol.

High resolution mass spectrometry showed a molecular ion peak at m/z 442.3731 which corresponded to the molecular formula $C_{30}H_{50}O_2$. Fragmentation ions were also observed at m/z 424 and m/z 409 (Spectrum 10j, pp 158), which showed the loss of a water molecule in the former and a loss of a water molecule and a methyl group to form the latter.

The infra red spectrum (Spectrum 10k, pp 159) showed a broad peak at 3412 cm^{-1} characteristic of O-H stretching and a very intense peak at 2928 cm^{-1} which indicated aliphatic C-H stretching.

In the proton NMR spectrum (Spectrum 10a, pp 149), the two signals at δ 4.91 (1H, brs, H-29A) and δ 4.89 (1H, brs, H-29B) were broad singlets due to the non-equivalent H-29 methylene protons of a vinyl group. These signals were shifted further downfield than those for lupeol due to being in close proximity to a deshielding group. The double bond was confirmed by a methylene carbon resonance at δ 107.0 (C-29) in the ^{13}C NMR spectrum (Spectrum 10c, pp 151) and a fully substituted carbon resonance at δ 155.0 (C-20), which indicated the presence of a double bond. The proton spectrum showed no coupling with a vinyl methyl group proton resonance at approximately δ 1.6, as shown in lupeol and lupenone, suggesting modification of the methyl group at C-30 had taken place. Further confirmation of this was that the proton spectrum showed one fewer tertiary methyl group than in lupeol and lupenone. The ^{13}C NMR spectrum showed a methylene signal at δ 65.2, assigned to C-30, which is due to a carbon atom of a $-\text{CH}_2\text{-OH}$ group. The H-30 methylene proton resonance was observed at δ 4.10 (2H, dd, H-30), and correlated to a resonance at δ 65.2 (CH_2) in the ^{13}C NMR spectrum. The coupling constant for the methylene protons in a CH_2OH group is usually about 10 Hz⁹, however in this case the pair of doublets have been shifted close together and so appear as a singlet.

Coupling of the two singlets, H-29A and H-29B, to the H-30 resonances at δ 4.11 and δ 4.09 was shown in the COSY spectrum (Spectrum 10d, pp 152). The TOCSY spectrum (Spectrum 10f, pp 154) showed this isopropenyl group to be a spin system. No coupling to H-19 was observed.

A broad double doublet at δ 3.17 (1H, dd, $J = 5$ Hz, $J = 11.3$ Hz) indicated the presence of a β -hydroxyl group at C-3 and correlated to a methine signal at δ 79.2, as shown in the HSQC spectrum (Spectrum 10e, pp 153). A positive correlation of H-3 with H-5 and H-9 was observed in the NOESY spectrum (Spectrum 10g, pp 155), which showed that the methine hydrogens at C-3, C-5 and C-9 were all in an alpha configuration. The methine proton, H-3, showed a three bond correlation with C-23 and C-24 as shown in the HMBC

spectrum (Spectrum 10h, pp 156 and 10I, pp 157). From this spectrum, the three bond correlations of H-30 with C-29 and H-29 with C-30 were also seen.

After acetylation (Spectrum 10b, pp 150), the double doublet occurring at δ 3.17 in hennadiol was shifted downfield to δ 4.45, while the two H-30 resonances were shifted to δ 4.51(dd) and δ 4.53 (dd). The proton signals at δ 2.10 (3H, s) and δ 2.05 (3H, s) showed that two acetate groups were present, which further proved the presence of the hydroxyl substituents at C-3 and C-30. A very intense signal was observed at δ 1.22, which was due to the methylene groups of the esters. The proton NMR spectrum showed the presence of six tertiary methyl signals at δ 0.74, 0.76, 0.81, 0.92, 0.95 and 1.01 (each 3H, s) ascribed to H-24, H-28, H-25, H-27, H-23 and H-26 respectively.

No carbon literature data was available for hennadiol, however, the data for the acetylated compound X matched that for hennadiol diacetate¹⁰. As the carbon literature data was not available for comparison, resonances were assigned from the HMBC spectrum.

Table 5.7 ¹H NMR data for compound X and literature data for hennadiol¹¹.

	¹ H NMR data for compound X (CDCl ₃) (400 MHz)	¹ H NMR data for hennadiol ¹¹ (CDCl ₃) (270 MHz)
Proton Number	δ_{H} ppm	δ_{H} ppm
3	3.17 (dd, $J = 5$ Hz, $J = 11.3$ Hz)	3.20 (dd)
23	0.94 (s)	0.97 (s)
24	0.74 (s)	0.76 (s)
25	0.81 (s)	0.83 (s)
26	1.01 (s)	1.04 (s)
27	0.92 (s)	0.95 (s)
28	0.76 (s)	0.78 (s)
29 A	4.91 (brs)	4.94 (brs)
29 B	4.89 (brs)	4.91 (brs)
30 A	4.11 (dd)	4.13 (s)
30 B	4.09 (dd)	4.13 (s)

Table 5.8 ^{13}C NMR data for compound X.

	^{13}C NMR data for compound X (CDCl_3) (100 MHz)
Carbon Number	δ_{C} ppm
1	38.9 (CH_2)
2	27.6 (CH_2)
3	79.2 (CH)
4	39.1 (C)
5	55.5 (CH)
6	18.5 (CH_2)
7	34.5 (CH_2)
8	41.0 (C)
9	50.6 (CH)
10	37.4 (C)
11	21.2 (CH_2)
12	26.9 (CH_2)
13	38.2 (CH)
14	43.0 (C)
15	27.6 (CH_2)
16	35.7 (CH_2)
17	43.2 (C)
18	49.1 (CH)
19	44.0 (CH)
20	155.0 (C)
21	28.2 (CH_2)
22	40.1 (CH_2)
23	28.2 (CH_3)
24	15.6 (CH_3)
25	16.3 (CH_3)
26	16.1 (CH_3)
27	14.7 (CH_3)
28	17.9 (CH_3)
29	107.0 (CH_2)
30	65.2 (CH_2)

5.3.6 The Structural Elucidation of Compound XI

The next compound was isolated as white crystals and was identified as 30-hydroxylup-20(29)-en-3-one or commonly known as 30-hydroxylupenone (**compound XI**). This compound has been previously isolated from *Maytenus nemerosa* (Celastraceae)

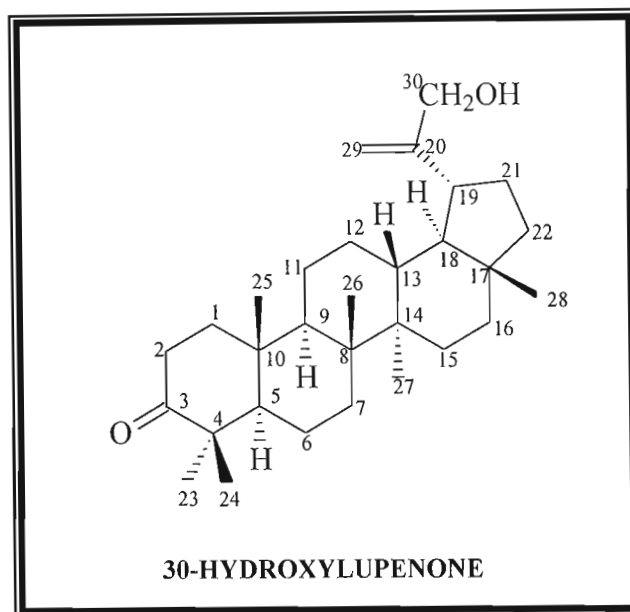


Figure 5.11 Compound XI: 30-hydroxylupenone.

The infra red spectrum (Spectrum 11c, pp 162) showed a broad peak at 3452 cm^{-1} due to the presence of O-H stretching. Aliphatic C-H stretching vibrations were observed at 2942 cm^{-1} and the intense peak at 1711 cm^{-1} was due to the presence of a carbonyl group. Bending of methylene groups was observed at 1465 cm^{-1} and 1391 cm^{-1} .

The proton NMR spectrum (Spectrum 11a, pp 160) showed the presence of two singlets at δ 4.92 (1H, s, H-29A) and δ 4.88 (1H, s, H-29B) ascribed to the two non-equivalent methylene protons on C-29. The presence of a 20,29-double bond was indicated in the ^{13}C NMR spectrum (Spectrum 11b, pp 161) by the signals at δ 107.1 (CH_2 , C-29) and δ 154.9 (C, C-20).

The resonance at δ 4.10 (2H, dd, H-30) in the ^1H NMR spectrum was due to the two methylene protons on C-30, which have a carbon resonance at δ 65.2 (CH_2 , C-30). The data for compound X matched that for hennadiol, however, the multiplet at approximately δ 3.2 was absent in the proton NMR spectrum of compound X. It was therefore postulated that this compound was the 3-ketone derivative of hennadiol.

The ^{13}C NMR spectrum showed 30 carbon signals and they were assigned by comparison to literature¹¹. The signal at δ 218.5 is characteristic of a C-3 ketone group carbon atom. The carbon resonance at δ 34.3 (CH_2 , C-2) and δ 47.5 (C, C-4) are shifted downfield due to being in close proximity to an oxygen atom.

The proton NMR spectrum showed six tertiary methyl group proton signals at δ 1.05, 1.04, 1.00, 0.93, 0.90, 0.77 (each 3H, s) and were assigned to H-23, H-26, H-24, H-27, H-25 and H-28 respectively.

Table 5.9 ^1H NMR data for compound XI and literature data for 30-hydroxylupenone¹².

Proton Number	^1H NMR data for compound XI (CDCl_3) (400 MHz)	^1H NMR literature data for 30-hydroxylupenone ¹² (CDCl_3) (400 MHz)
	δ_{H} ppm	δ_{H} ppm
23	1.05 (s)	1.09 (s)
24	1.00 (s)	1.05 (s)
25	0.90 (s)	0.95 (s)
26	1.04 (s)	1.09 (s)
27	0.93 (s)	0.98 (s)
28	0.77 (s)	0.81 (s)
29A	4.92 (s)	4.99 (s)
29B	4.88 (s)	4.93 (s)
30A	4.10 (d)	4.16 (s)
30B	4.09 (d)	4.16 (s)

Table 5.10 ^{13}C NMR data for compound XI and literature data for 30-hydroxylupenone¹².

Carbon Number	^{13}C NMR data for compound XI (CDCl_3) (100 MHz)	^{13}C NMR literature data for 30- hydroxylupenone ¹² (CDCl_3) (100 MHz)
	δ_{C} ppm	δ_{C} ppm
1	39.8 (CH_2)	39.6 (t)
2	34.3 (CH_2)	34.1 (t)
3	218.5 (C)	218.3 (s)
4	47.5 (C)	47.3 (s)
5	55.0 (CH)	54.9 (d)
6	19.8 (CH_2)	19.7 (t)
7	33.7 (CH_2)	33.6 (t)
8	41.0 (C)	40.8 (s)
9	49.9 (CH)	49.7 (d)
10	37.1 (C)	36.9 (s)
11	21.7 (CH_2)	21.6 (t)
12	26.8 (CH_2)	26.7 (t)
13	38.3 (CH)	38.1 (d)
14	43.0 (C)	42.9 (s)
15	27.6 (CH_2)	27.4 (t)
16	35.6 (CH_2)	35.4 (t)
17	43.2 (C)	43.0 (s)
18	49.0 (CH)	48.8 (d)
19	43.9 (CH)	43.8 (d)
20	154.9 (C)	154.7 (s)
21	31.9 (CH_2)	31.8 (t)
22	40.0 (CH_2)	39.8 (t)
23	26.8 (CH_3)	26.7 (q)
24	21.2 (CH_3)	21.0 (q)
25	16.2 (CH_3)	16.0 (q)
26	16.1 (CH_3)	15.8 (q)
27	14.7 (CH_3)	14.5 (q)
28	17.9 (CH_3)	17.7 (q)
29	107.1 (CH_2)	106.8 (t)
30	65.2 (CH_2)	65.0 (t)

5.4 Experimental

Fresh *Combretum fragrans* F. Hoffm. leaves were collected by Professor B.C. Rogers from Bank Terrace and a voucher specimen was retained in the Ward Herbarium at the University of Natal, Durban-Westville (BCR12). The leaves were washed with a hot 1% sodium bicarbonate solution (volume of solution must be adequate to cover the leaves). The resultant solution was acidified with concentrated hydrochloric acid, as nearly all the acidic triterpenoids produce water-soluble salts. The precipitate that formed was then neutralized by washing with water and then filtered. The extract was left to dry at room temperature. The compounds were separated using column chromatography over silica gel (Merck 9385) and varying ratios of methanol and dichloromethane.

5.4.1 Physical Data for Compound VI

Name: 3 β -hydroxylup-20(29)-ene

Synonyms: lupeol

Physical Appearance: white crystals

Yield: 25.9 mg

Melting Point: 190 °C (MeOH:CHCl₃), lit. value⁷ 210 °C (CHCl₃-petrol)

Mass: HRMS: [M⁺] at *m/z* 426.3867, C₃₀H₅₀O requires 426.3862, *m/z* 411 (11%),
m/z 218 (100%), *m/z* 203 (24%)

Infra red Spectrum: ν_{\max} (NaCl) 3378, 2929, 1465, 1391 cm⁻¹

Optical Rotation: $[\alpha]_D = +41^\circ$ (c, 0.0006 g.ml⁻¹ in CHCl₃), lit. value⁷ +26° in CHCl₃

¹H NMR: δ_H (ppm), CDCl₃.

4.67 and 4.55 (each 1H, brs, 2 x H-29), 3.16 (1H, dd, *J* = 5.4, *J* = 10.9, H-3), 1.66 (3H, s, H-30), 1.01 (3H, s, H-26), 0.95 (3H, s, H-23), 0.92 (3H, s, H-27), 0.81 (3H, s, H-25), 0.77 (3H, s, H-28), 0.74 (3H, s, H-24).

¹³C NMR: δ_C (ppm), CDCl₃.

150.9 (C, C-20), 109.3 (CH₂, C-29), 79.0 (CH, C-3), 55.3 (CH, C-5), 50.4 (CH, C-9), 48.3 (CH, C-18), 47.9 (CH, C-19), 43.0 (C, C-17), 42.8 (C, C-14), 40.8 (C, C-8), 40.0 (CH₂, C-22), 38.8 (C, C-4), 38.7 (CH₂, C-1), 38.0 (CH, C-13), 37.1 (C, C-10), 35.5 (CH₂, C-16), 34.2 (CH₂, C-7), 29.8 (CH₂, C-21), 28.0 (CH₃, C-23), 27.9 (CH₂, C-15), 27.4 (CH₂, C-2), 25.1 (CH₂, C-12), 20.9 (CH₂, C-11), 19.3 (CH₃, C-30), 18.3 (CH₂, C-6), 18.0 (CH₃, C-28), 16.1 (CH₃, C-25), 15.9 (CH₃, C-26), 15.3 (CH₃, C-24), 14.5 (CH₃, C-27).

5.4.2 Physical Data for Compound VII

Name: lup-20(29)-en-3-one

Synonyms: lupenone

Physical Appearance: white needles

Yield: 32.1 mg

Melting Point: 160 °C (MeOH), lit. value⁸ 169-170 °C (MeOH)

Infra red Spectrum: ν_{\max} (NaCl) 2933, 1714, 1464, 1385 cm^{-1}

Optical Rotation: $[\alpha]_{\text{D}} = +36^{\circ}$ (c, 0.00562 $\text{g}\cdot\text{ml}^{-1}$ in CH_2Cl_2), lit. value¹⁰ $+63^{\circ}$ in CHCl_3

¹H NMR: δ_{H} (ppm), CDCl_3 .

4.67 and 4.55 (each 1H, brs, 2 x H-29), 1.66 (3H, s, H-30), 1.23 (3H, s, H-23), 1.05 (3H, s, H-26), 1.00 (3H, s, H-27), 0.93 (3H, s, H-24), 0.91 (3H, s, H-25), 0.77 (3H, s, H-28)

¹³C NMR: δ_{C} (ppm), CDCl_3 .

218.1 (C, C-3), 150.8 (C, C-20), 109.4 (CH_2 , C-29), 54.9 (CH, C-5), 49.7 (CH, C-9), 48.2 (CH, C-18), 47.9 (CH, C-19), 47.3 (C, C-4), 42.9 (C, C-14), 42.9 (C, C-17), 40.7 (C, C-8), 39.9 (CH_2 , C-22), 39.6 (CH_2 , C-1), 38.1 (CH, C-13), 36.8 (C, C-10), 36.5 (CH_2 , C-16), 34.1 (CH_2 , C-2), 33.5 (CH_2 , C-7), 29.8 (CH_2 , C-21), 27.4 (CH_2 , C-15), 26.6 (CH_3 , C-23), 25.1 (CH_2 , C-12), 21.4 (CH_2 , C-11), 21.0 (CH_3 , C-24), 19.6 (CH_2 , C-6), 19.3 (CH_3 , C-30), 18.0 (CH_3 , C-28), 16.9 (CH_3 , C-25), 15.7 (CH_3 , C-26), 14.4 (CH_3 , C-27).

5.4.3 Physical Data for Compound VIII

Name: lupeol 3 β -docosanoate

Yield: 18.7 mg (mixture with compound X)

Physical Appearance: white fatty material

Mass: HRMS: [M^+] at m/z 748.7107, $C_{52}H_{92}O_2$, requires 748.7097, m/z 409

1H NMR: δ_H (ppm), $CDCl_3$.

4.66 and 4.54 (each 1H, brs, 2 x H-29), 4.45 (1H, dd, $J = 6$ Hz, $J = 10$ Hz, H-3), 1.66 (3H, s, H-30), 1.01 (3H, s, H-26), 0.91 (3H, s, H-23), 0.86 (3H, s, H-27), 0.84 (3H, s, H-25), 0.81 (3H, s, H-28), 0.77 (3H, s, H-24)

^{13}C NMR: δ_C (ppm), $CDCl_3$.

150.9 (C, C-20), 109.3 (CH_2 , C-29), 80.6 (CH, C-3), 55.3 (CH, C-5), 50.3 (CH, C-9), 48.2 (CH, C-18), 48.0 (CH, C-19), 43.0 (C, C-17), 42.8 (C, C-14), 40.8 (C, C-8), 40.0 (CH_2 , C-22), 40.0 (C, C-4), 38.4 (CH_2 , C-1), 38.0 (CH, C-13) 37.1 (C, C-10), 35.5 (CH_2 , C-16), 34.2 (CH_2 , C-7), 31.3 (CH_2 , C-21), 29.8 (CH_2 , C-2), 28.0 (CH_3 , C-23), 27.4 (CH_2 , C-15), 25.1 (CH_2 , C-12), 20.9 (CH_2 , C-11), 19.3 (CH_3 , C-30), 18.2 (CH_2 , C-6), 18.0 (CH_3 , C-28), 16.5 (CH_3 , C-25), 16.2 (CH_3 , C-26), 15.9 (CH_3 , C-24), 14.5 (CH_3 , C-27)

5.4.4 Physical Data for Compound IX

Name: lupeol 3 β -eicosanoate

Yield: 18.7 mg (mixture with compound IX)

Physical Appearance: white fatty material

Mass: HRMS: [M⁺] at *m/z* 720.6728, C₅₀H₈₈O₂, requires 720.6784, *m/z* 409

¹H NMR: δ_{H} (ppm), CDCl₃.

4.66 and 4.54 (each 1H, brs, 2 x H-29), 4.45 (1H, dd, *J* = 6 Hz, *J* = 10 Hz, H-3), 1.66 (3H, s, H-30), 1.01 (3H, s, H-26), 0.91 (3H, s, H-23), 0.86 (3H, s, H-27), 0.84 (3H, s, H-25), 0.81 (3H, s, H-28), 0.77 (3H, s, H-24)

¹³C NMR: δ_{C} (ppm), CDCl₃.

150.9 (C, C-20), 109.3 (CH₂, C-29), 80.6 (CH, C-3), 55.3 (CH, C-5), 50.3 (CH, C-9), 48.2 (CH, C-18), 48.0 (CH, C-19), 43.0 (C, C-17), 42.8 (C, C-14), 40.8 (C, C-8), 40.0 (CH₂, C-22), 40.0 (C, C-4), 38.4 (CH₂, C-1), 38.0 (CH, C-13), 37.1 (C, C-10), 35.5 (CH₂, C-16), 34.2 (CH₂, C-7), 31.3 (CH₂, C-21), 29.8 (CH₂, C-2), 28.0 (CH₃, C-23), 27.4 (CH₂, C-15), 25.1 (CH₂, C-12), 20.9 (CH₂, C-11), 19.3 (CH₃, C-30), 18.2 (CH₂, C-6), 18.0 (CH₃, C-28), 16.5 (CH₃, C-25), 16.2 (CH₃, C-26), 15.9 (CH₃, C-24), 14.5 (CH₃, C-27)

5.3.5 Physical Data for Compound X

Name: lup-20(29)-ene-3 β ,30-diol

Synonyms: hennadiol, wallichenol, 30-hydroxylupeol

Physical Appearance: white crystals

Yield: 18.2 mg

Melting Point: 230 °C, lit. value⁹ 236-238 °C (MeOH:CHCl₃)

Mass: HRMS: [M⁺] at 442.3731, C₃₀H₅₀O₂ requires 442.3861, *m/z* 424 (14.2%),
m/z 409 (5.0%), 384 (81.0%)

Infra red Spectrum: ν_{\max} (NaCl) 3412, 2928 cm⁻¹

Optical Rotation: $[\alpha]_D = -17^\circ$ (c, 0.00142 in CHCl₃), lit. value⁹ - 9.5°

¹H NMR: δ_H (ppm), CDCl₃.

4.91 and 4.89 (each 1H, s, 2 x H-29), 4.11 and 4.09 (each 1H, s, 2 x H-30), 3.17 (1H, dd, *J* = 5 Hz, *J* = 11.3 Hz, H-3), 1.01 (3H, s, H-26), 0.94 (3H, s, H-23), 0.92 (3H, s, H-27), 0.81 (3H, s, H-25), 0.76 (3H, s, H-28), 0.74 (3H, s, H-24)

¹³C NMR: δ_C (ppm), CDCl₃.

155.0 (C, C-20), 107.0 (CH₂, C-29), 79.2 (CH, C-3), 65.2 (CH₂, C-30), 55.5 (CH, C-5), 50.6 (CH, C-9), 49.1 (CH, C-18), 44.0 (CH, C-19), 43.2, (C, C-17), 43.0 (C, C-14), 41.0 (C, C-8), 40.1 (CH₂, C-22), 39.1 (C, C-4), 38.9 (CH₂, C-1), 38.2 (CH, C-13), 37.4 (C, C-10), 35.7 (CH₂, C-16), 34.5 (CH₂, C-7), 28.2 (CH₂, C-21), 28.2 (CH₃, C-23), 27.6 (CH₂, C-2), 27.6 (CH₂, C-15), 26.9 (CH₂, C-12), 21.2 (CH₂, C-11), 18.5 (CH₂, C-6), 17.9 (CH₃, C-28), 16.3 (CH₃, C-25), 16.1 (CH₃, C-26), 15.6 (CH₃, C-24), 14.7 (CH₃, C-27)

5.3.6 Physical Data for Compound XI

Name: 30-hydroxylup-20(29)-en-3-one

Yield: 15.0 mg

Physical Appearance: white crystals

Melting Point: 181 °C, lit. value¹³ 183-184 °C

Infra red Spectrum: ν_{\max} (NaCl) 3452, 2942, 1711, 1465, 1391 cm^{-1}

Optical Rotation: $[\alpha]_{\text{D}} = 16.7^{\circ}$ (c, 0.006 in CHCl_3), lit. value¹³ 17.2°

¹H NMR: δ_{H} (ppm), CDCl_3 .

4.92 (1H, brs, H-29A), 4.88 (1H, brs, H-29B), 4.10 (1H, d, H-30A), 4.09 (1H, d, H-30B), 1.05 (3H, s, H-23), 1.04 (3H, s, H-26), 1.00 (3H, s, H-24), 0.93 (3H, s, H-27), 0.90 (3H, s, H-25), 0.77 (3H, s, H-28)

¹³C NMR: δ_{C} (ppm), CDCl_3 .

218.5 (C, C-3), 154.9 (C, C-20), 107.1 (CH_2 , C-29), 65.2 (CH_2 , C-30), 55.0 (CH, C-5), 49.9 (CH, C-9), 49.0 (CH, C-18), 47.5 (C, C-4), 43.9 (CH, C-19), 43.2 (C, C-17), 43.0 (C, C-14), 41.0 (C, C-8), 40.0 (CH_2 , C-22), 39.8 (CH_2 , C-1), 38.3 (CH, C-13), 37.1 (C, C-10), 35.6 (CH_2 , C-16), 34.3 (CH_2 , C-2), 33.7 (CH_2 , C-7), 31.9 (CH_2 , C-21), 27.6 (CH_2 , C-15), 26.8 (CH_2 , C-12), 26.8 (CH_3 , C-23), 21.7 (CH_2 , C-11), 21.2 (CH_3 , C-24), 19.8 (CH_2 , C-6), 17.9 (CH_3 , C-28), 16.2 (CH_3 , C-25), 16.1 (CH_3 , C-26), 14.7 (CH_3 , C-27)

5.4 References

- 1) Hutchings, A.; “*Zulu Medicinal Plants, An Inventory*”, (1996), University of Natal Press, Pietermaritzburg, 213-216.
- 2) Rogers, C.B and Verotta, L.; “*Chemistry and Biological Properties of the African Combretaceae*”, (1996), Proceedings of the International Organisation for Chemical Sciences in Development Working Group on Plant Chemistry, University of Zimbabwe Publications, 121-141.
- 3) Rogers, C.B.; *Phytochemistry*, (1998), **49**, 2069-2076.
- 4) Pettit, G.R., Singh, S.B., Niven, M.L., Hamel, E. and Schmidt, J.M.; *Journal of Natural Products*, (1987), **50**, 119-131.
- 5) Pettit, G.R., Singh, S.B. and Schmidt, J.M.; *Journal of Natural Products*, (1988), **51**, 517-527.
- 6) Pettit, G.R., Singh, S.B. and Niven, M.L.; *Journal of the American Chemical Society*, (1988), **110**, 8539-8540.
- 7) Ahmad, V.U. and Atta-ur-Rahman; “*Handbook of Natural Products Data*”, (1994), Elsevier Science B.V., London, Vol. 2, 1038.
- 8) Ahmad, V.U. and Atta-ur-Rahman; “*Handbook of Natural Products Data*”, (1994), Elsevier Science B.V., London, Vol. 2, 1029-1030.
- 9) Monkhe, T., Mulholland, D. and Nicholls, G.; *Phytochemistry*, (1998), **49**, 1819-1820.
- 10) Ahmad, V.U. and Atta-ur-Rahman; “*Handbook of Natural Products Data*”, (1994), Elsevier Science B.V., London, Vol. 2, 1079-1080.
- 11) Bohlmann, F. and Jakupovic, J.; *Phytochemistry*, (1979), **18**, 1189-1194.
- 12) Tinto, W.F., Blair, L.C., Alli, A., Reynolds, W.F. and McLean, S.; *Journal of Natural Products*, (1992), **55**, 395-398.
- 13) Ahmad, V.U. and Atta-ur-Rahman; “*Handbook of Natural Products Data*”, (1994), Elsevier Science B.V., London, Vol. 2, 1055.

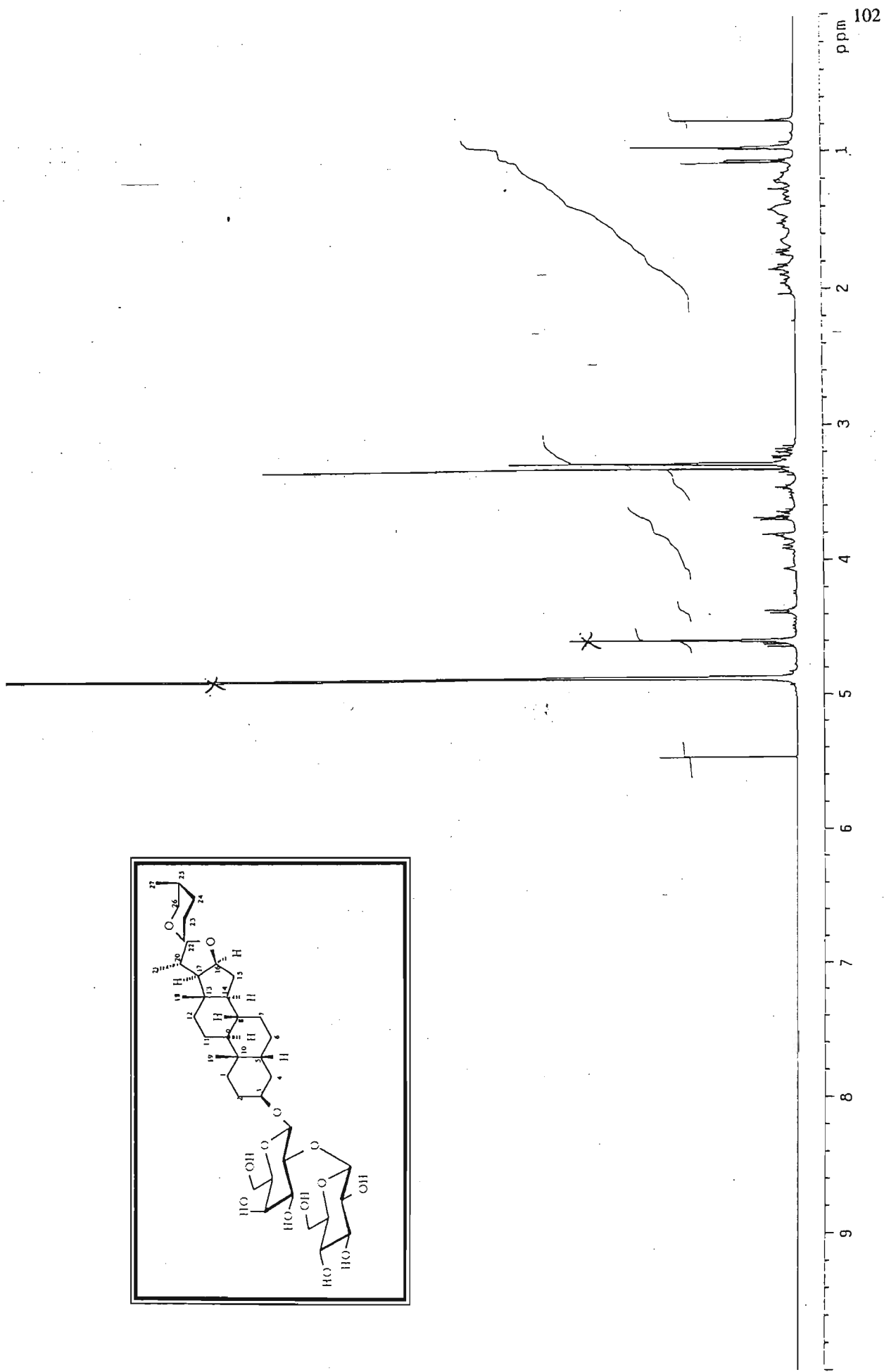
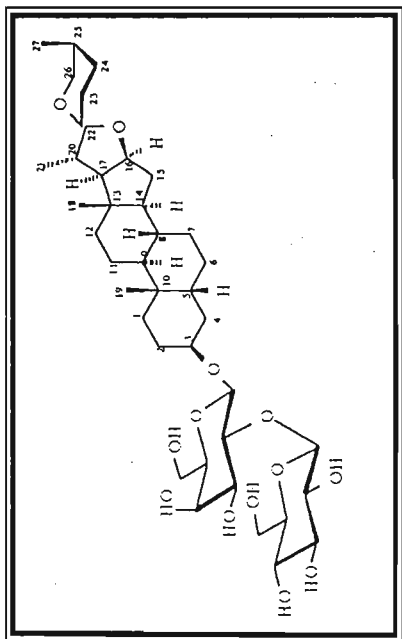
APPENDIX

LIST OF SPECTRA

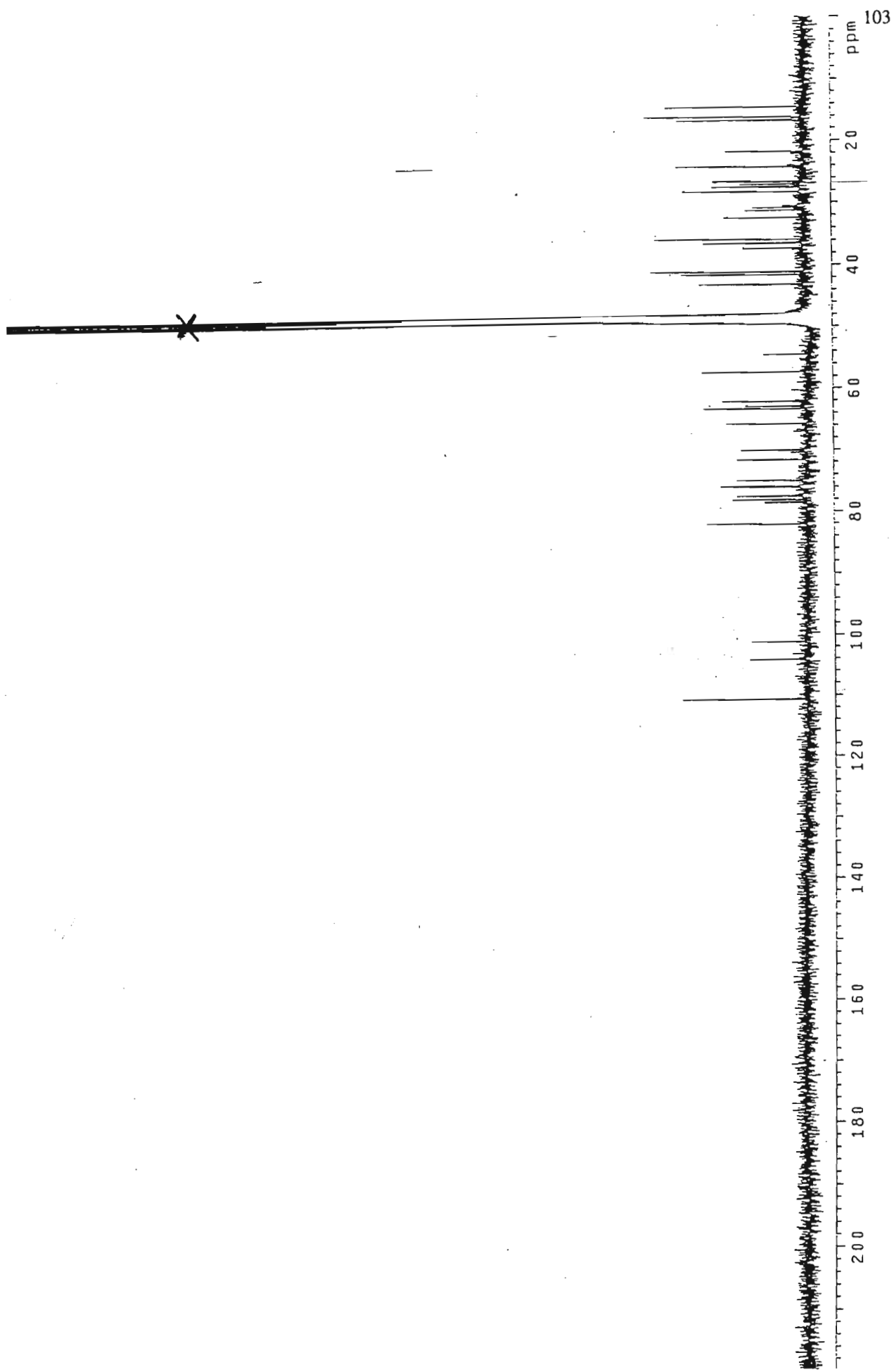
	Page
Spectrum 1a: ^1H NMR spectrum of compound I (CD_3OD) (400 MHz)	102
Spectrum 1b: ^{13}C NMR spectrum of compound I (CD_3OD) (100 MHz)	103
Spectrum 1c: ADEPT spectrum of compound I	104
Spectrum 1d: COSY spectrum of compound I	105
Spectrum 1e: HETCOR spectrum of compound I	106
Spectrum 2a: ^1H NMR spectrum of compound II (CD_3OD) (400 MHz)	107
Spectrum 2b: ^{13}C NMR spectrum of compound II (CD_3OD) (100 MHz)	108
Spectrum 2c: COSY spectrum of compound II	109
Spectrum 2d: HSQC spectrum of compound II	110
Spectrum 2e: TOCSY spectrum of compound II	111
Spectrum 2f: NOESY spectrum of compound II	112
Spectrum 2g: HMBC spectrum of compound II	113
Spectrum 2h: Infra red spectrum of compound II	114
Spectrum 3a: ^1H NMR spectrum of compound III (CDCl_3) (300 MHz)	115
Spectrum 3b: ^{13}C NMR spectrum of compound III (CDCl_3) (75 MHz)	116
Spectrum 3c: NOE spectrum of compound III showing irradiation of H-4	117
Spectrum 3d: NOE spectrum of compound III showing irradiation of H-5	118
Spectrum 3e: NOE spectrum of compound III showing irradiation of the methoxyl group protons	119
Spectrum 3f: Mass spectrum of compound III	120
Spectrum 3g: Infra red spectrum of compound III	121
Spectrum 4a: ^1H NMR spectrum of compound IV (CDCl_3) (300 MHz)	122

Spectrum 5a: ^1H NMR spectrum of compound V (CDCl_3) (400 MHz)	123
Spectrum 5b: ^1H NMR spectrum of acetylated compound V (CDCl_3) (300 MHz)	124
Spectrum 5c: ^{13}C NMR spectrum of compound V (CDCl_3) (100 MHz)	125
Spectrum 5d: COSY spectrum of compound V	126
Spectrum 5e: HSQC spectrum of compound V	127
Spectrum 5f: TOCSY spectrum of compound V	128
Spectrum 5g: NOESY spectrum of compound V	129
Spectrum 5h: HMBC spectrum of compound V	130
Spectrum 5i: Expanded HMBC spectrum of compound V	131
Spectrum 5j: High resolution mass spectrum of compound V	132
Spectrum 5k: Infra red spectrum of compound V	133
Spectrum 6a: ^1H NMR spectrum of compound VI (CDCl_3) (300 MHz)	134
Spectrum 6b: ^1H NMR spectrum of acetylated compound VI (CDCl_3) (300 MHz)	135
Spectrum 6c: ^{13}C NMR spectrum of compound VI (CDCl_3) (75 MHz)	136
Spectrum 6d: COSY spectrum of compound VI	137
Spectrum 6e: HETCOR spectrum of compound VI	138
Spectrum 6f: High resolution mass spectrum of compound VI	139
Spectrum 6g: Infra red spectrum of compound VI	140
Spectrum 7a: ^1H NMR spectrum of compound VII (CDCl_3) (300 MHz)	141
Spectrum 7b: ^{13}C NMR spectrum of compound VII (CDCl_3) (75 MHz)	142
Spectrum 7c: Infra red spectrum of compound VII	143

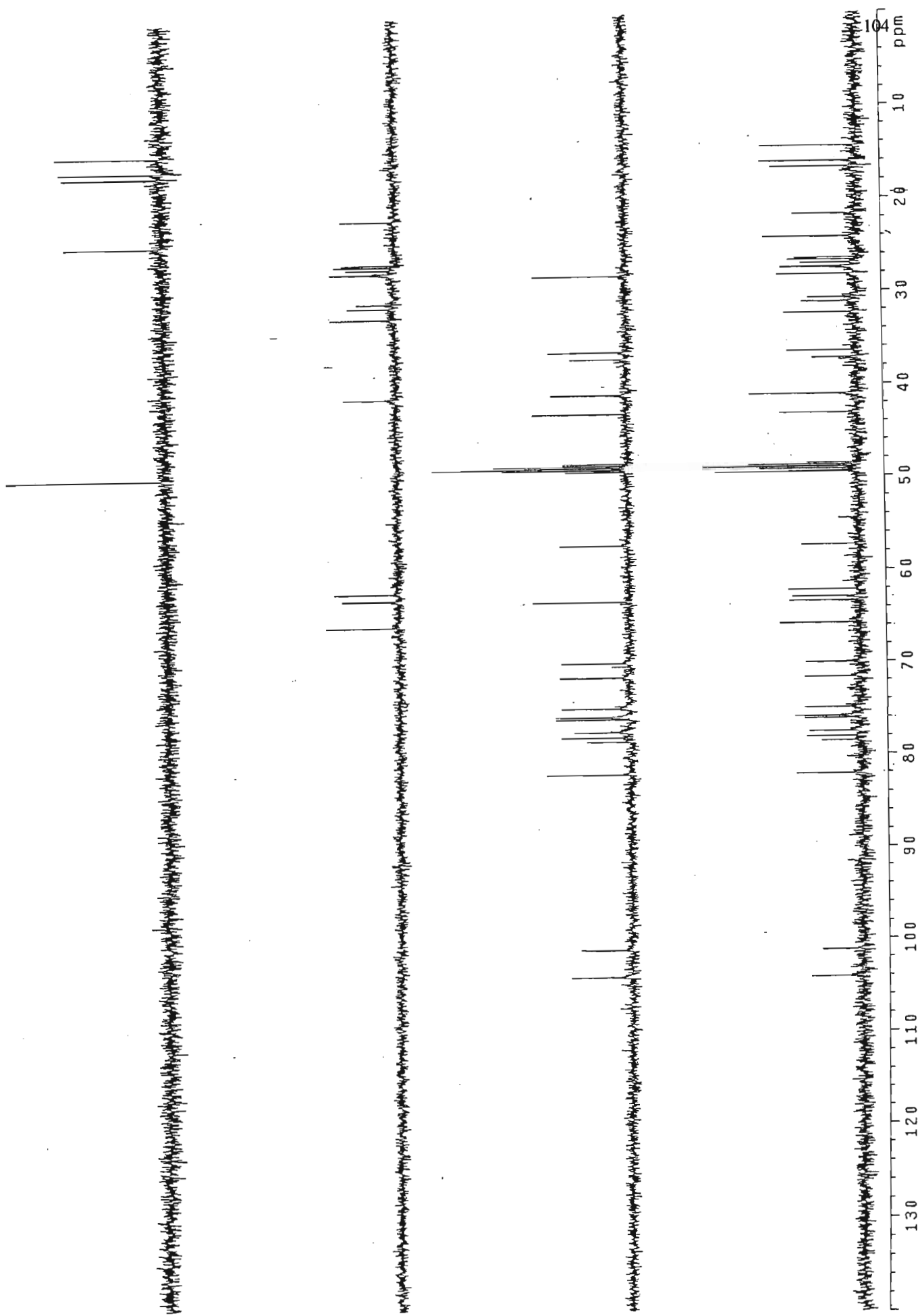
Spectrum 8a: ^1H NMR spectrum of compound VIII and IX (CDCl_3) (300 MHz)	144
Spectrum 8b: ^{13}C NMR spectrum of compound VIII and IX (CDCl_3) (75 MHz)	145
Spectrum 8c: COSY spectrum of compound VIII and IX	146
Spectrum 8d: HETCOR spectrum of compound VIII and IX	147
Spectrum 9a: High resolution mass spectrum of compound VIII and IX	148
Spectrum 10a: ^1H NMR spectrum of compound X (CDCl_3) (400 MHz)	149
Spectrum 10b: ^1H NMR spectrum of acetylated compound X (CDCl_3) (400 MHz)	150
Spectrum 10c: ^{13}C NMR spectrum of compound X (CDCl_3) (100 MHz)	151
Spectrum 10d: COSY spectrum of compound X	152
Spectrum 10e: HSQC spectrum of compound X	153
Spectrum 10f: TOCSY spectrum of compound X	154
Spectrum 10g: NOESY spectrum of compound X	155
Spectrum 10h: HMBC spectrum of compound X	156
Spectrum 10i: Expanded HMBC spectrum of compound X	157
Spectrum 10j: High resolution mass spectrum of compound X	158
Spectrum 10k: Infra red spectrum of compound X	159
Spectrum 11a: ^1H NMR spectrum of compound XI (CDCl_3) (400 MHz)	160
Spectrum 11b: ^{13}C NMR spectrum of compound XI (CDCl_3) (100 MHz)	161
Spectrum 11c: Infra red spectrum of compound XI	162



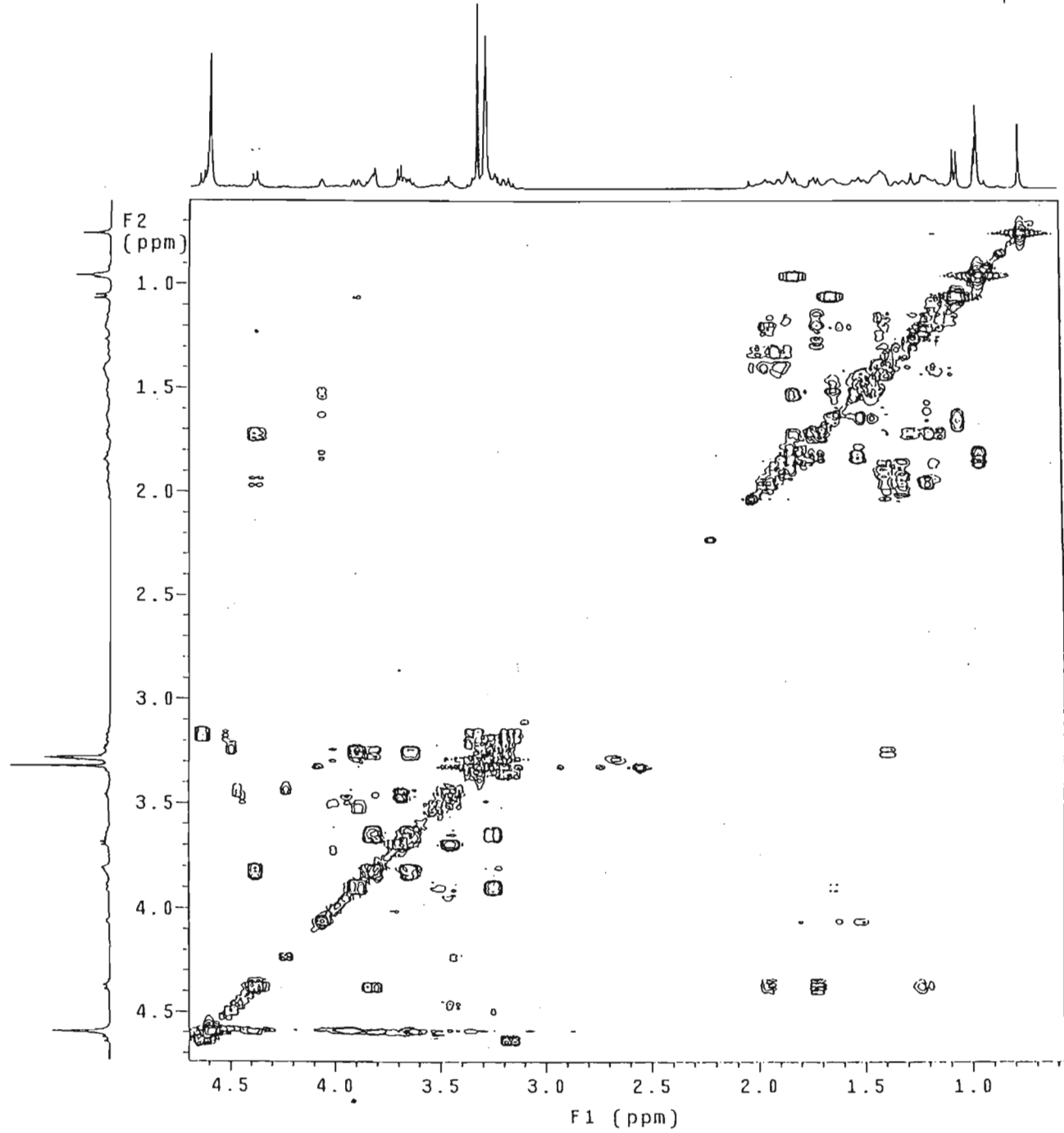
Spectrum 1a: ^1H NMR spectrum of compound 1.



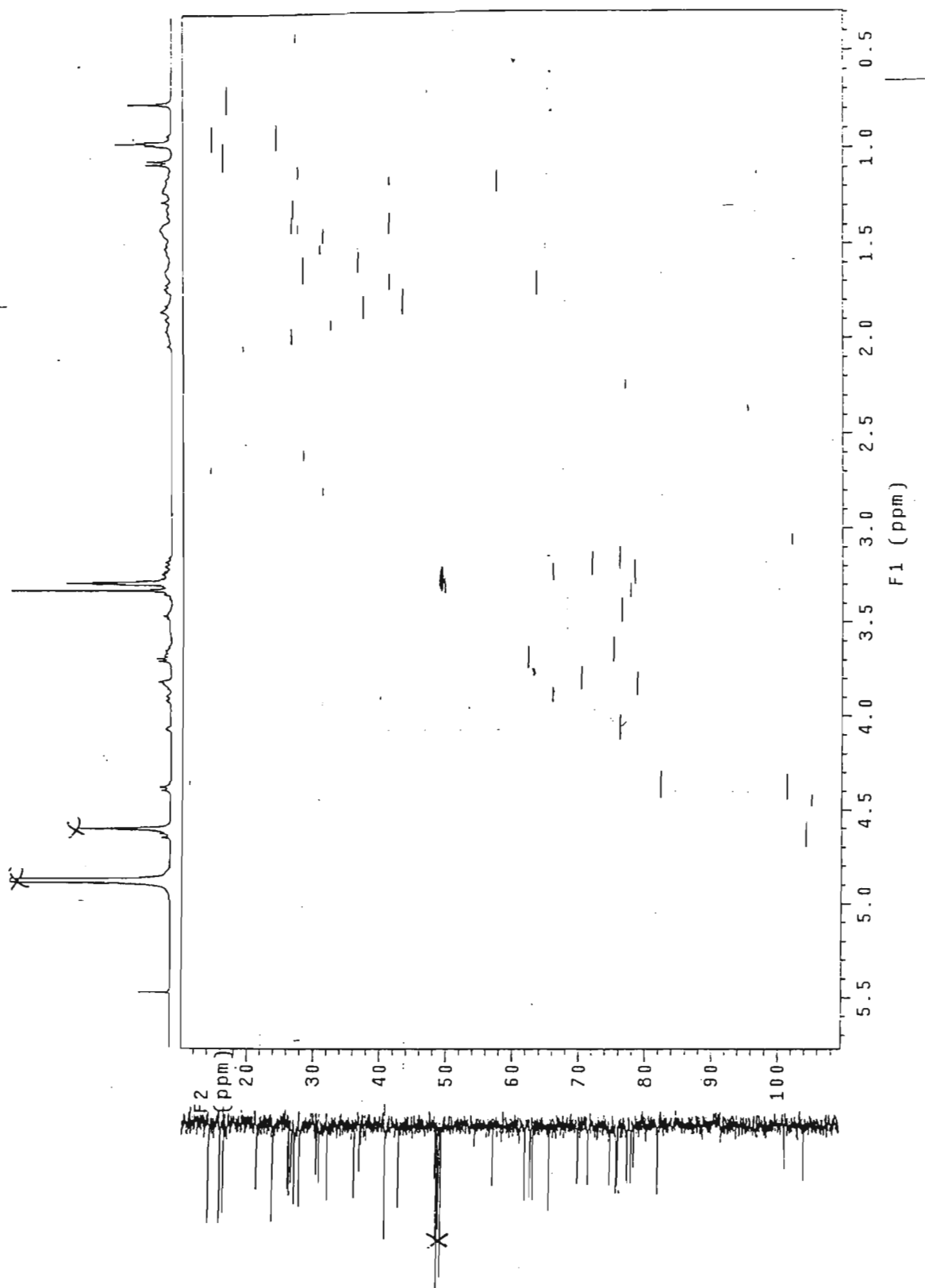
Spectrum 1b: ^{13}C NMR spectrum of compound I.



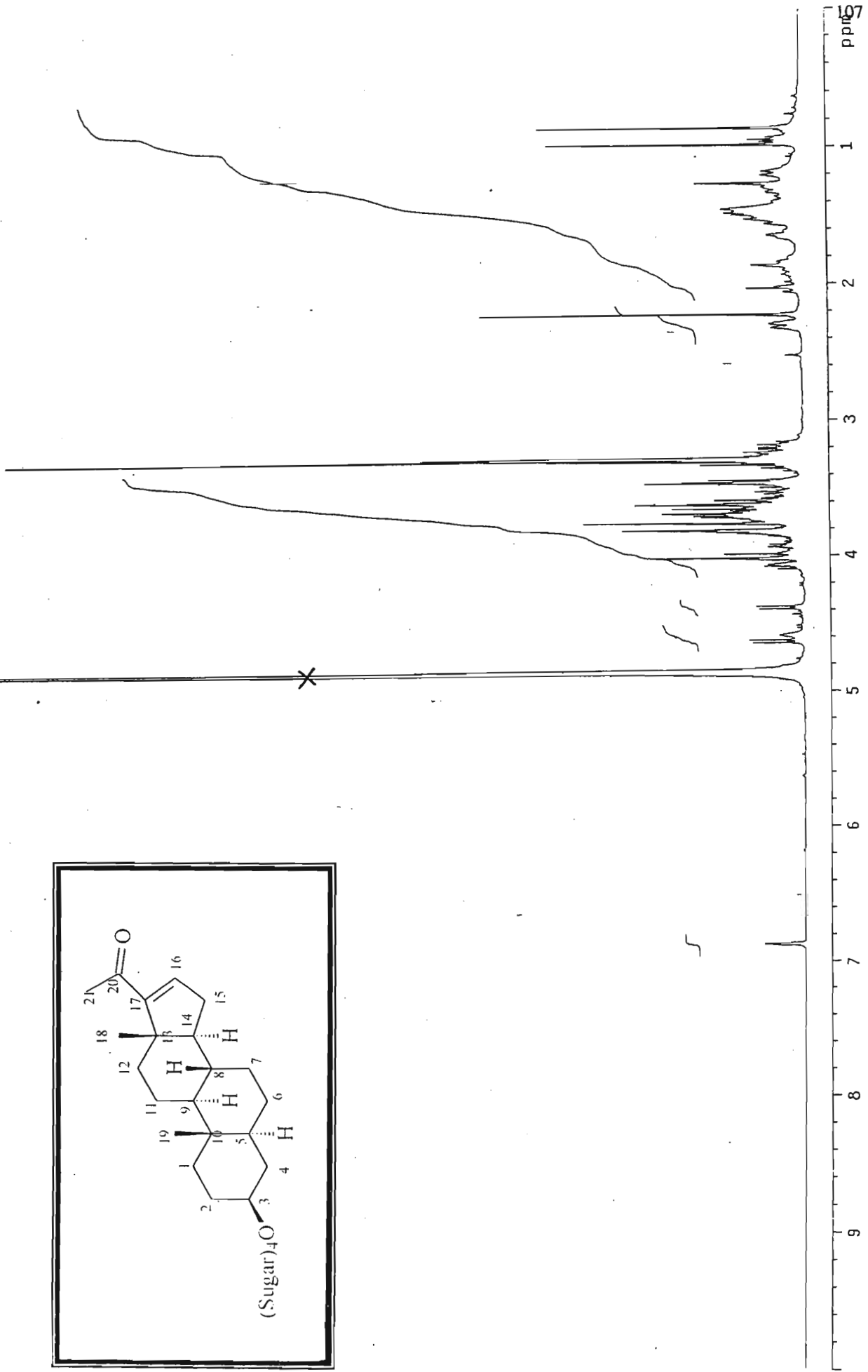
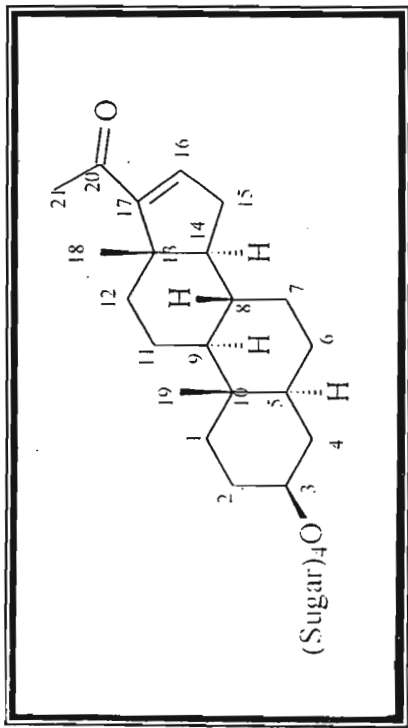
Spectrum 1c: ADEPT spectrum of compound 1.



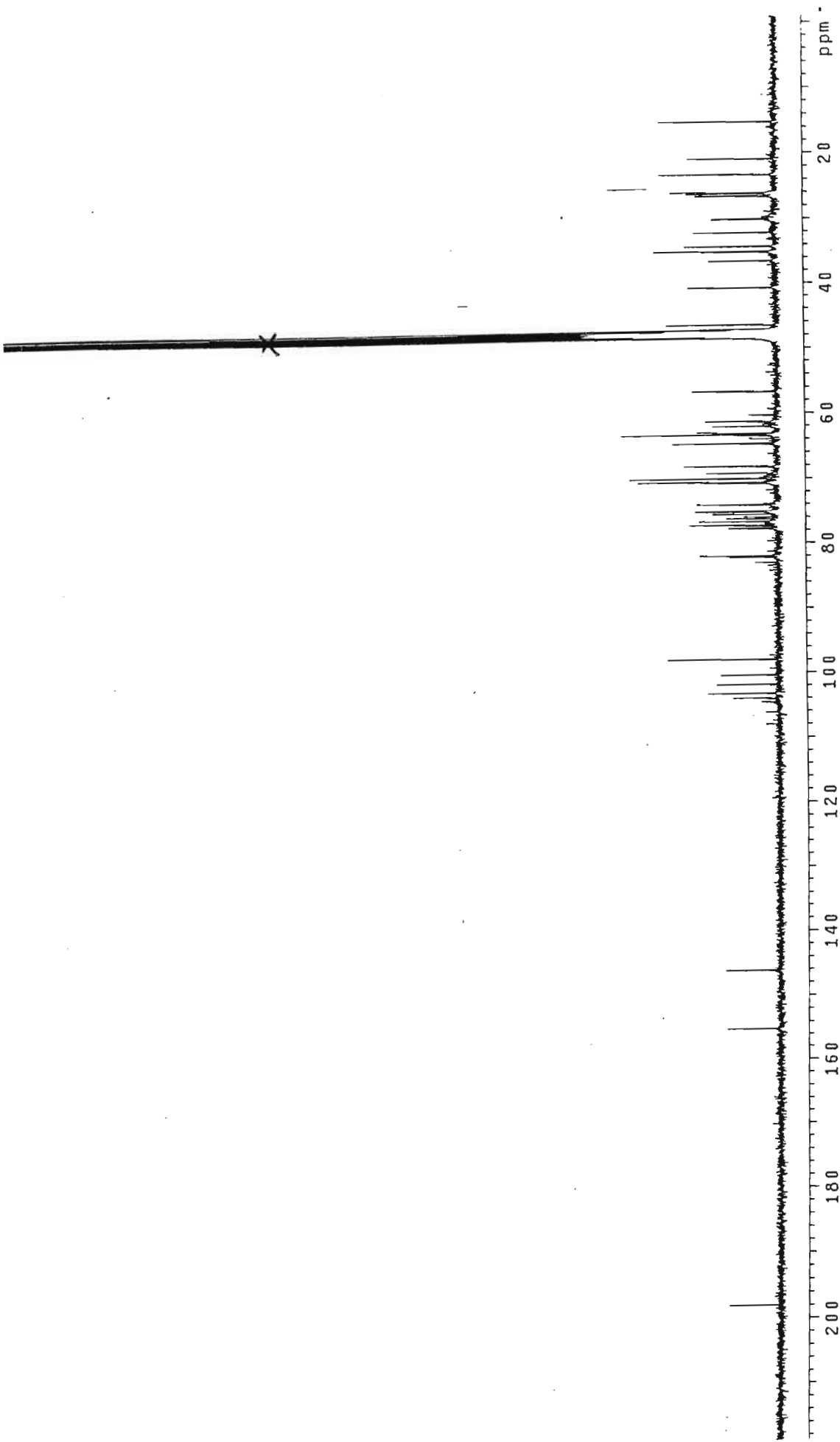
Spectrum 1d: COSY spectrum of compound I.



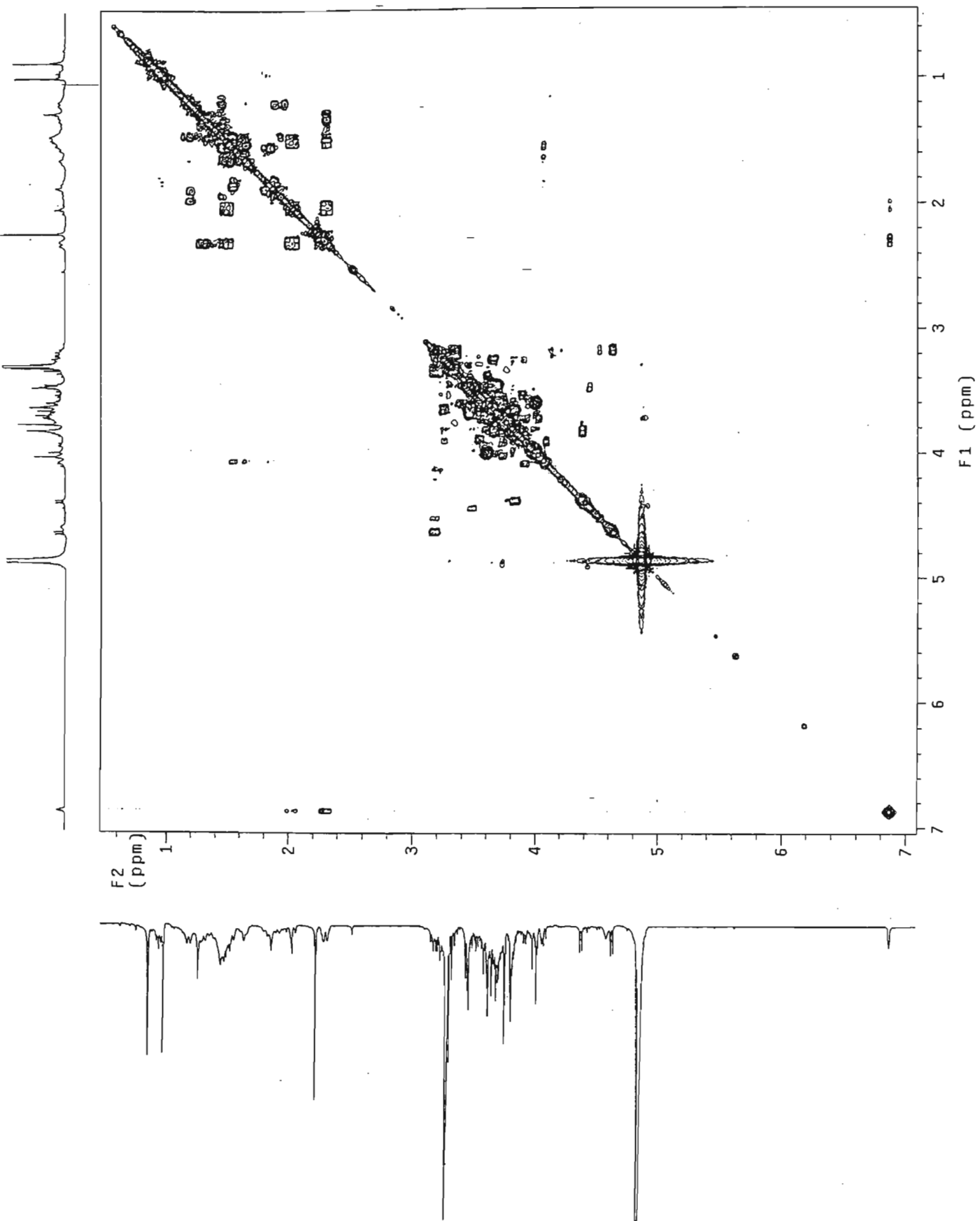
Spectrum 1e: HETCOR spectrum of compound 1e.



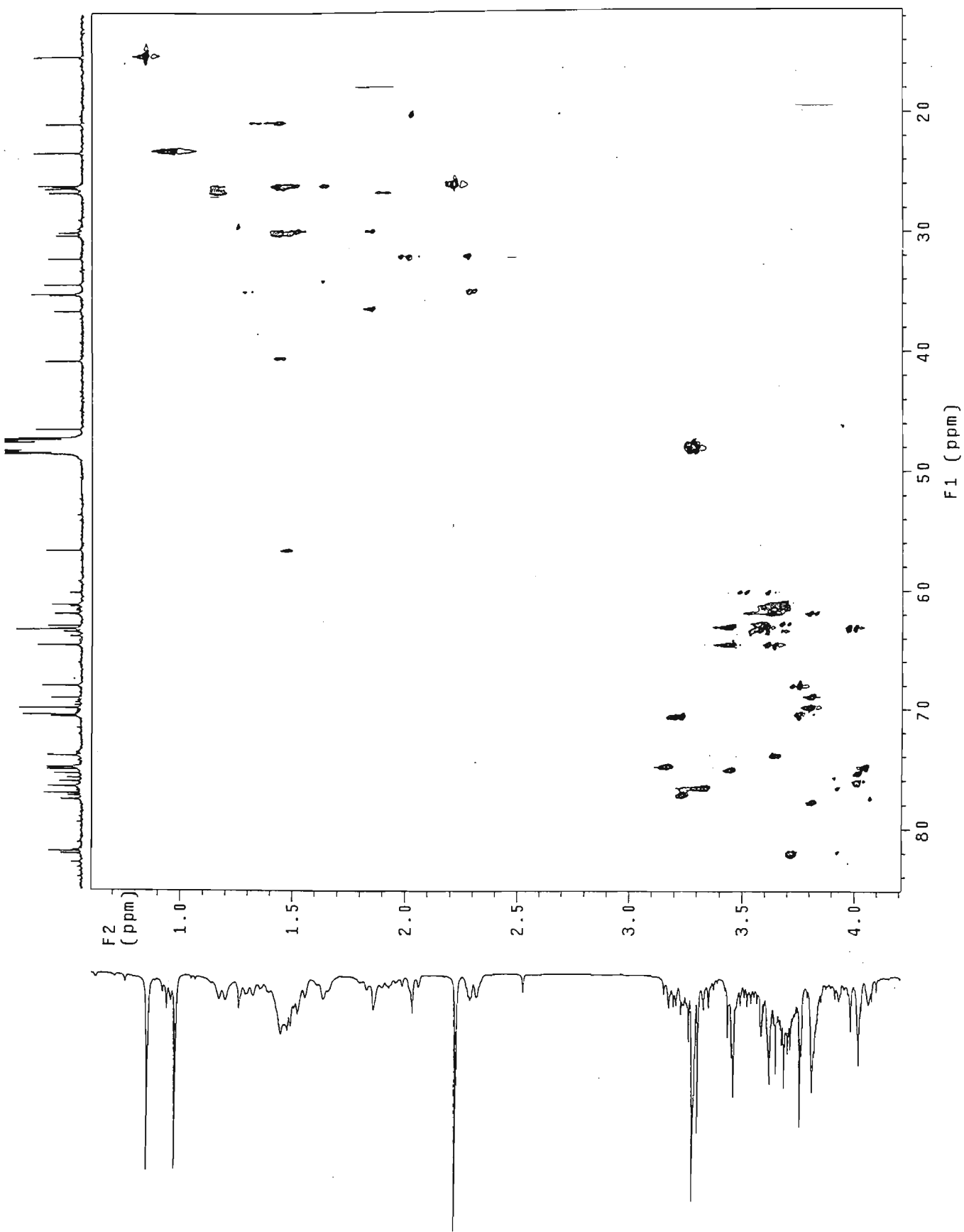
Spectrum 2a: ¹H NMR spectrum of compound II.



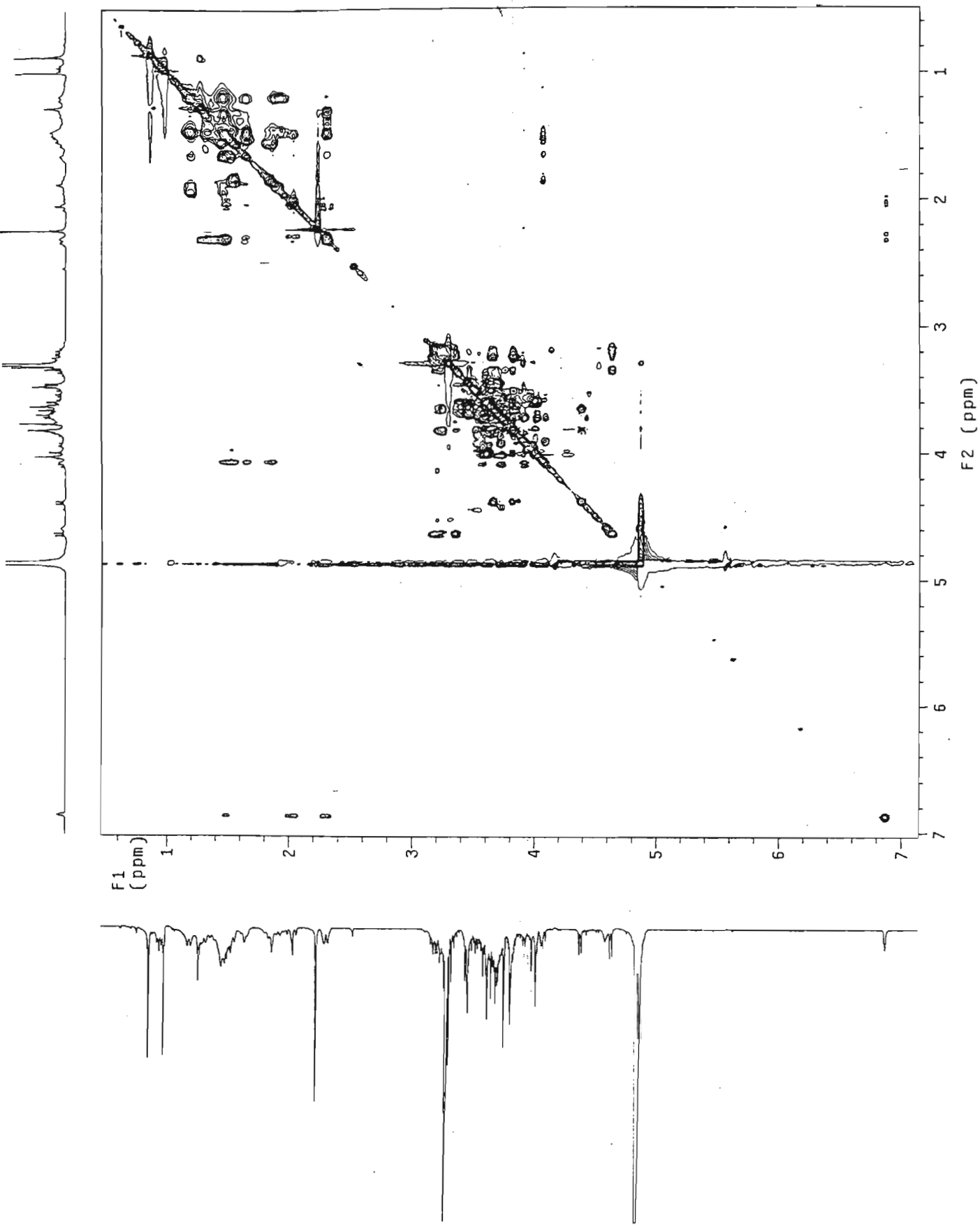
Spectrum 2b: ^{13}C NMR spectrum of compound II.



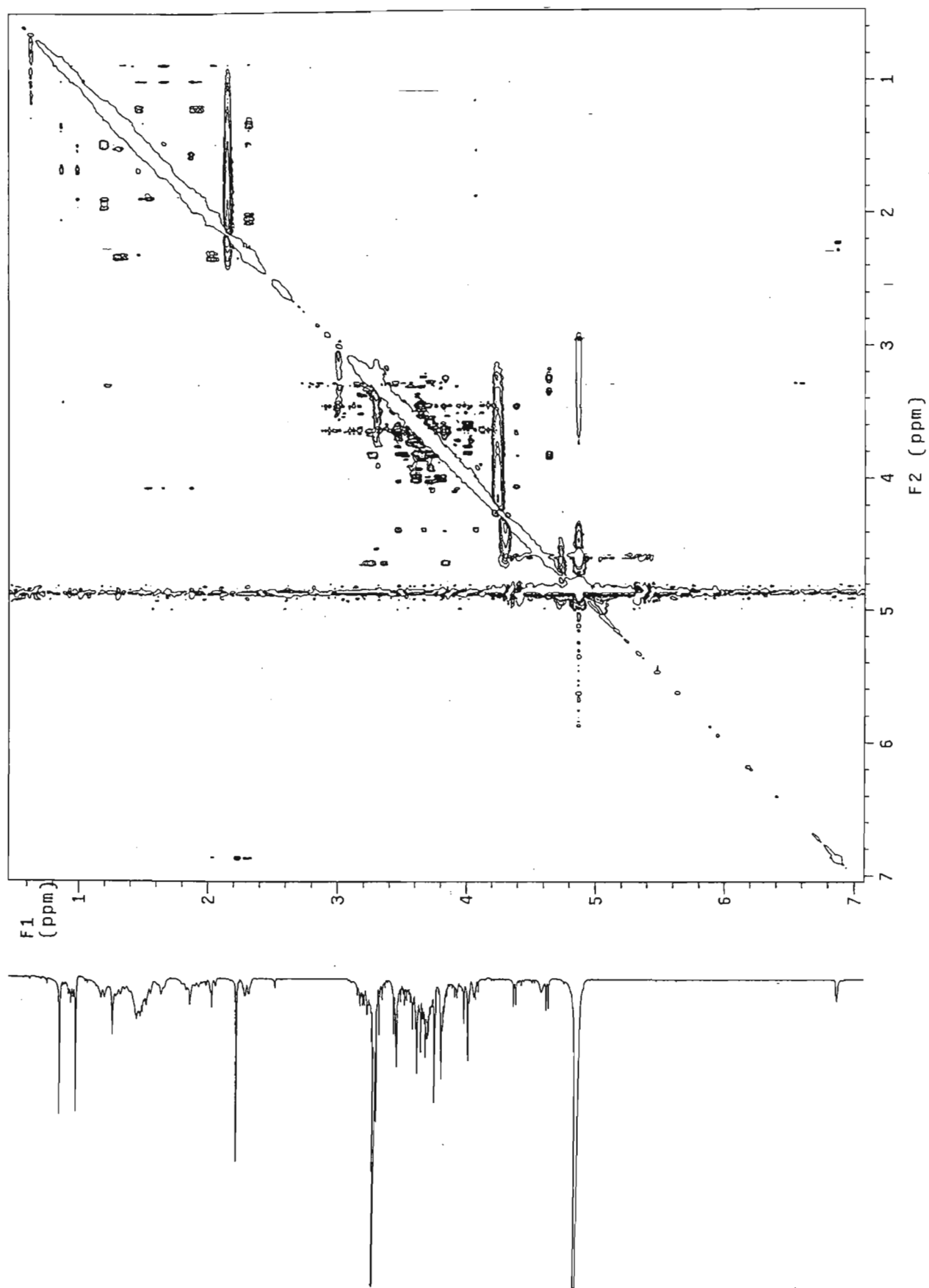
Spectrum 2c: COSY spectrum of compound II.



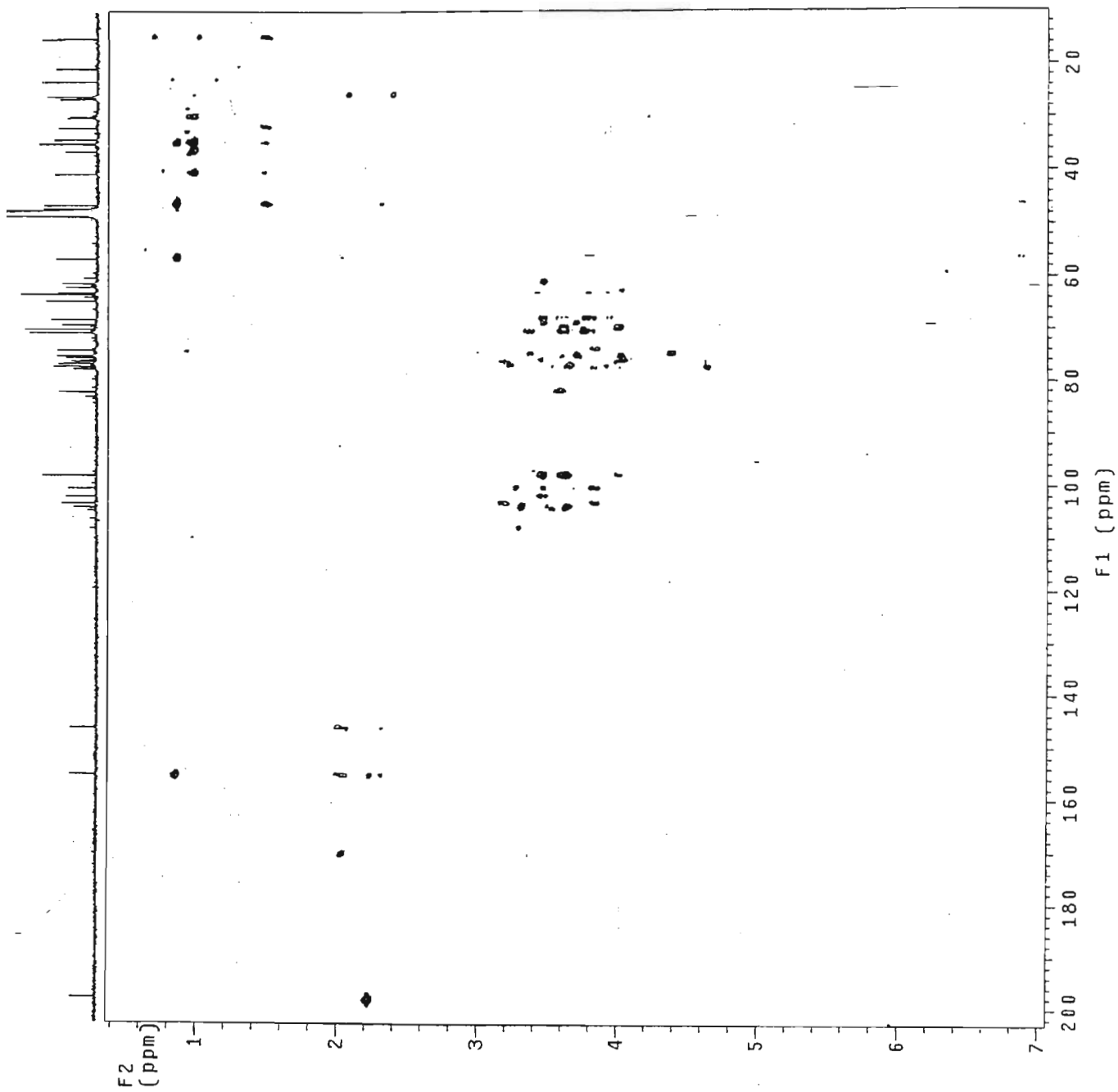
Spectrum 2d: HSQC spectrum of compound II.



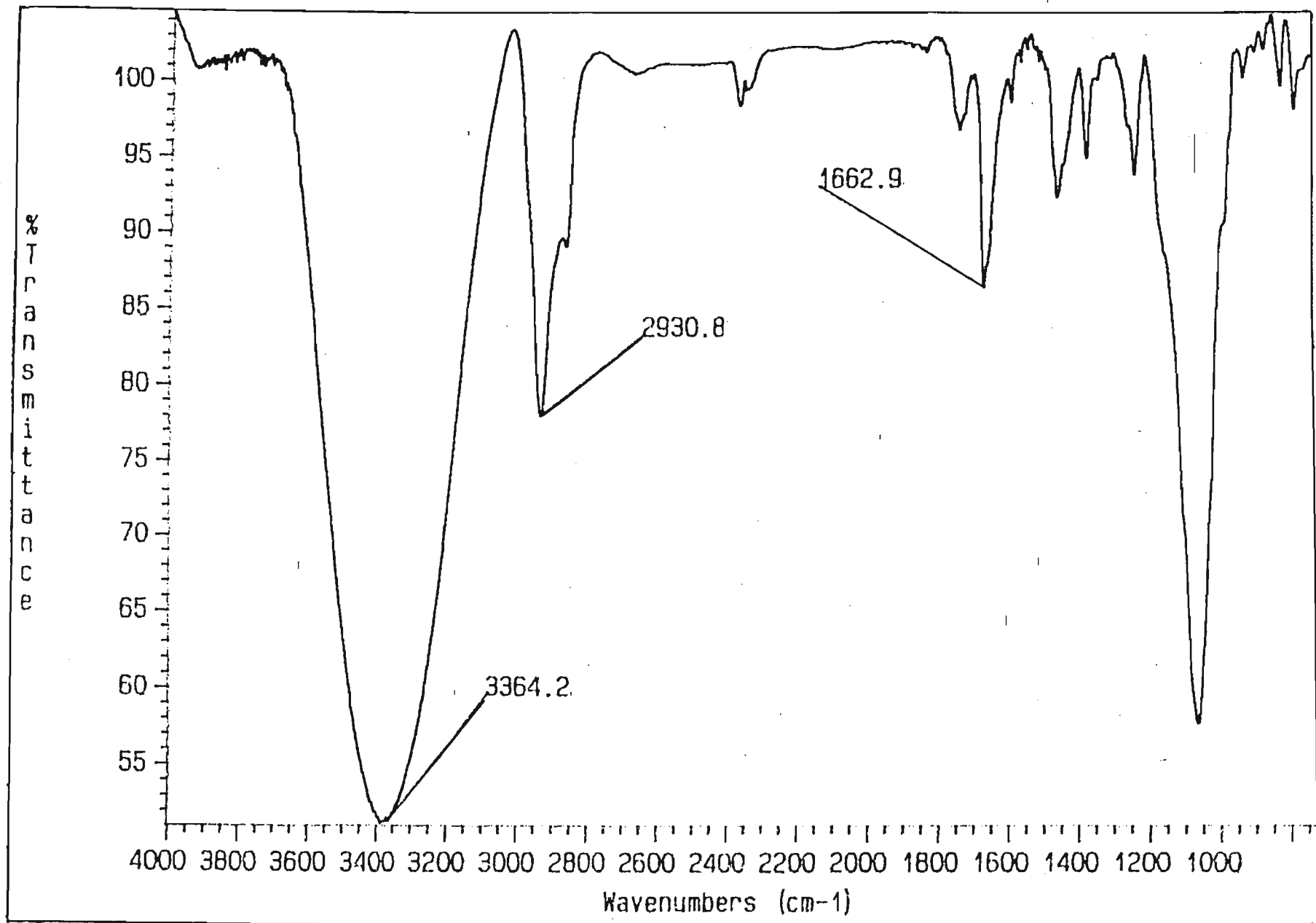
Spectrum 2e: TOCSY spectrum of compound II.



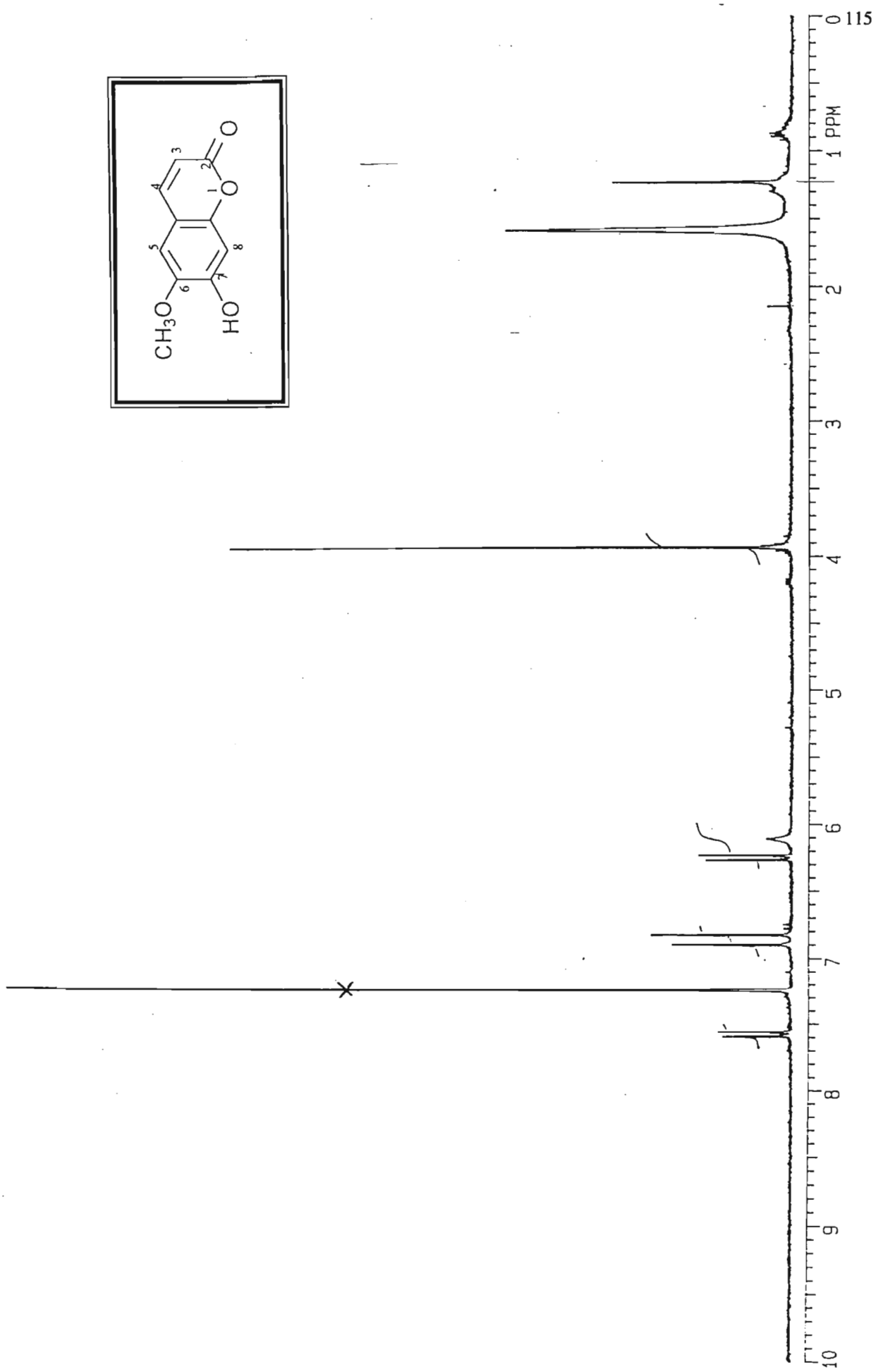
Spectrum 2f: NOESY spectrum of compound II.



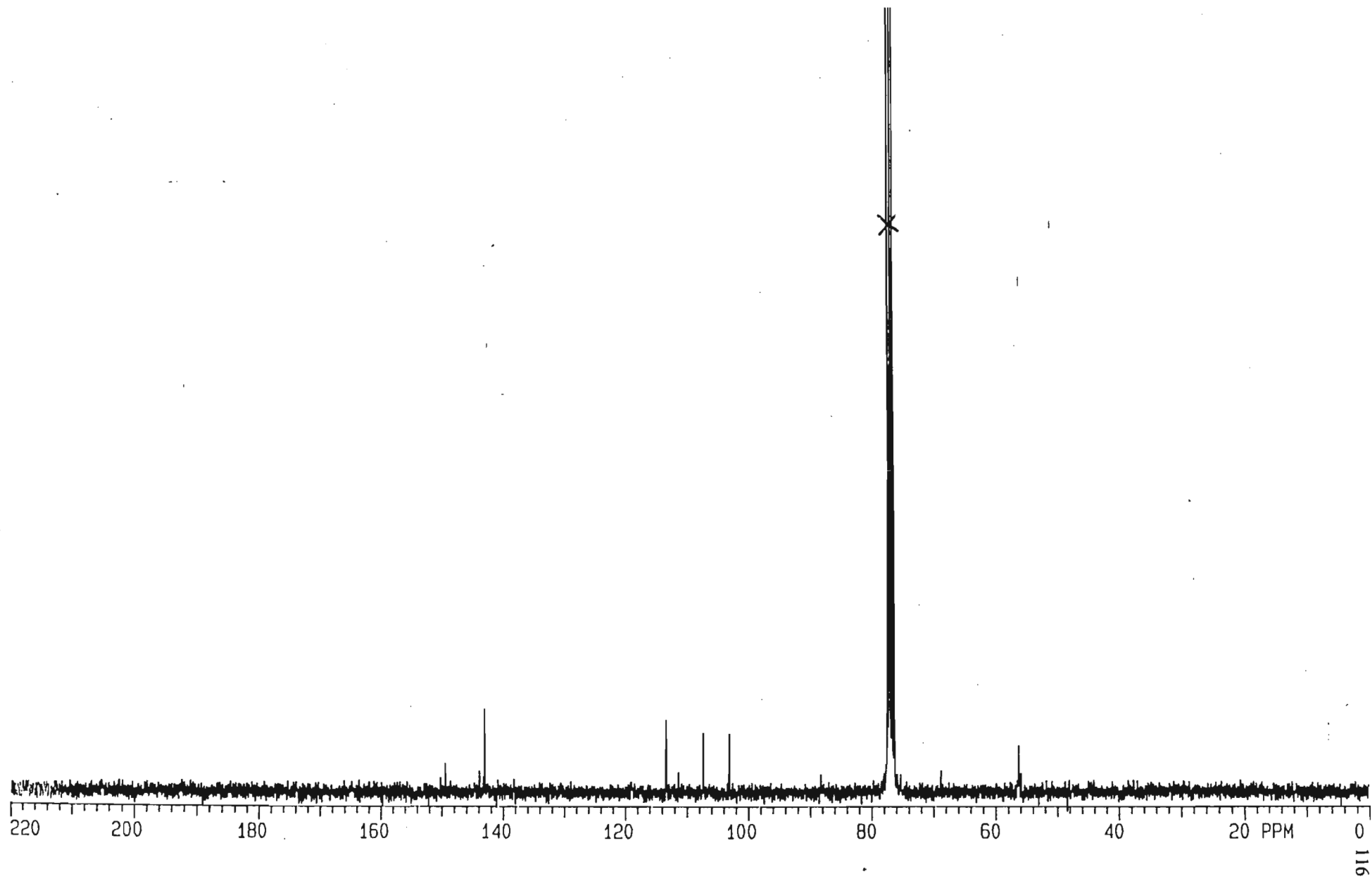
Spectrum 2g: HMBC spectrum of compound II.



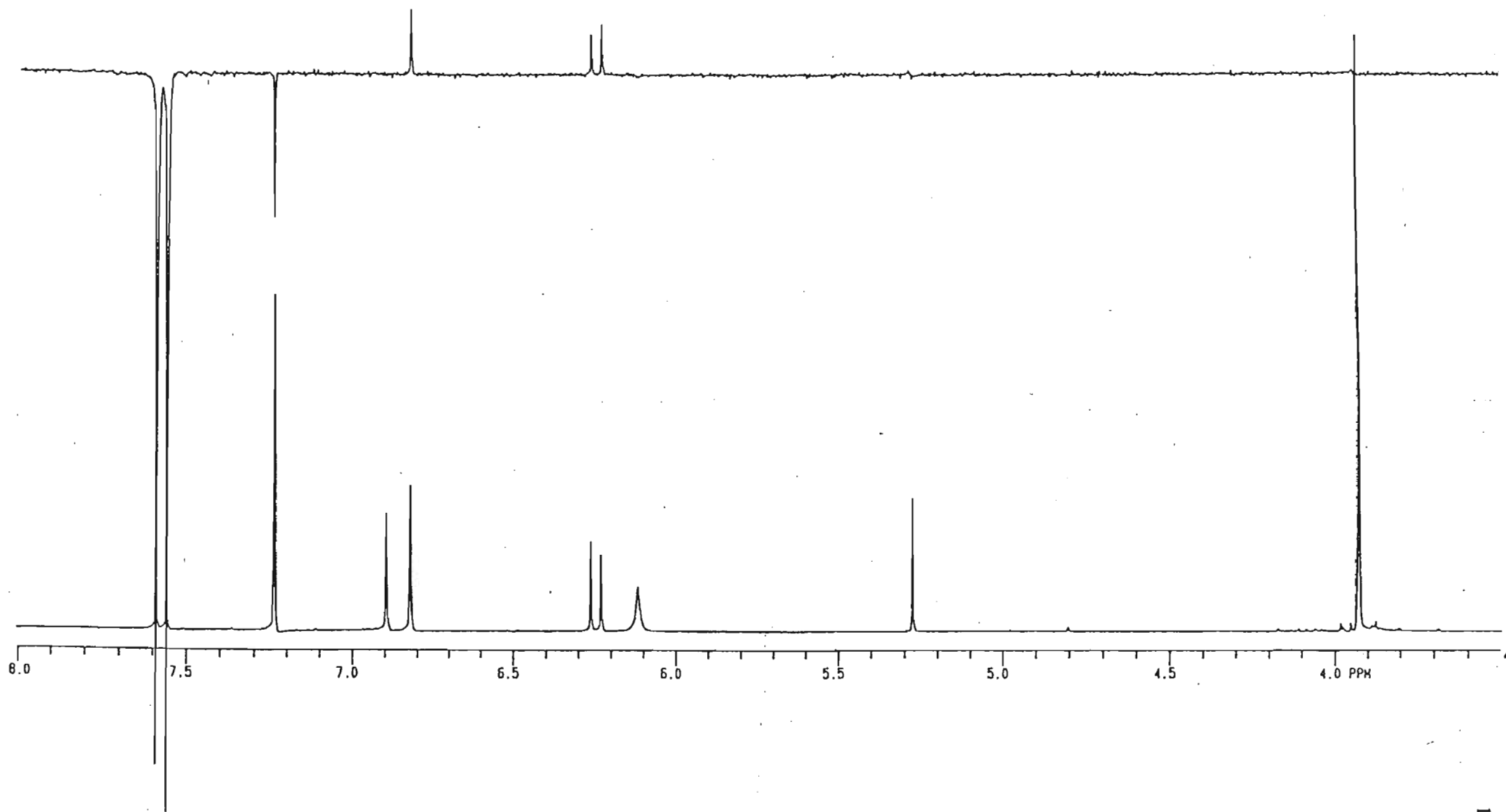
Spectrum 2h: Infra red spectrum of compound II.



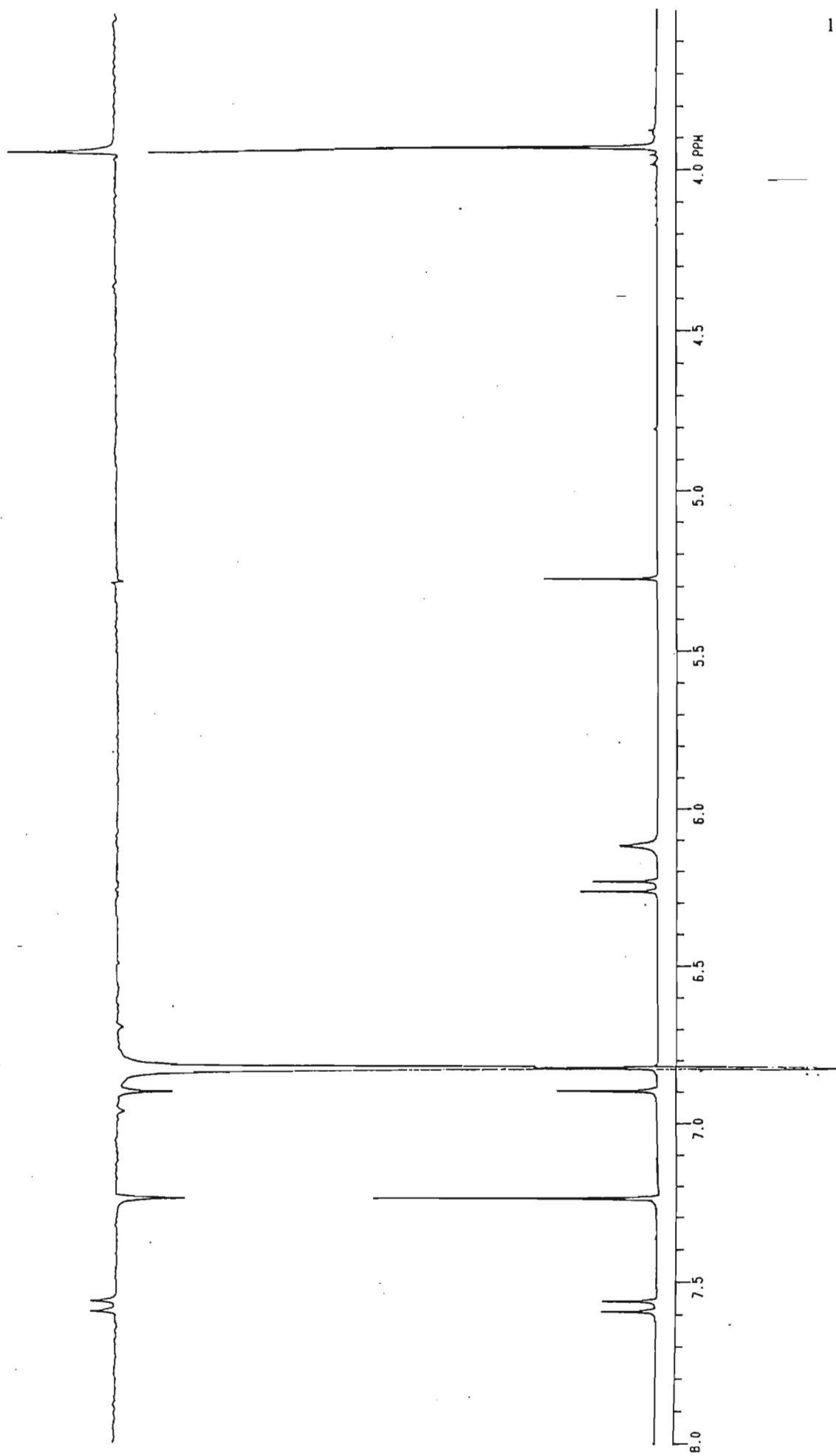
Spectrum 3a: ^1H NMR spectrum of compound III.



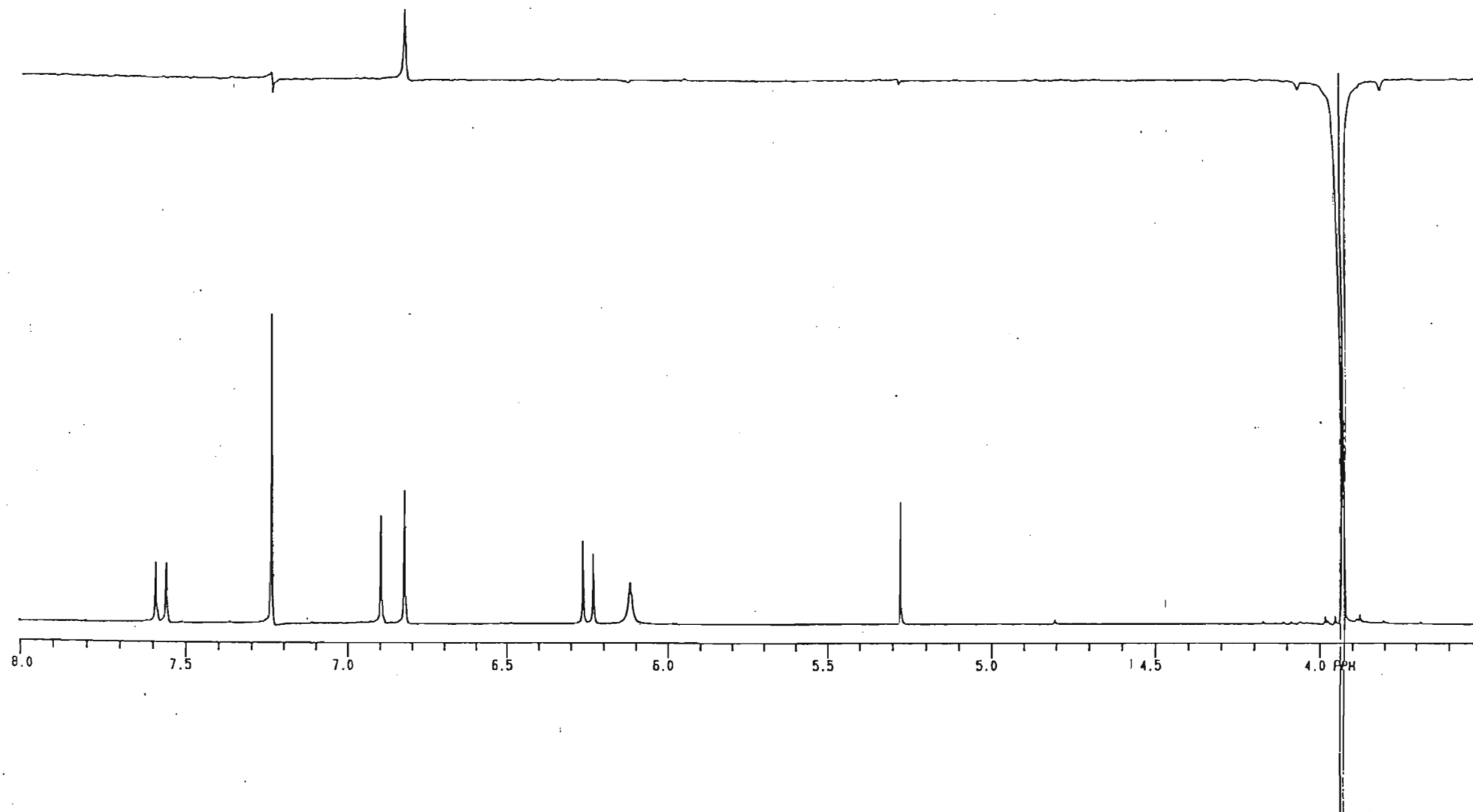
Spectrum 3b: ^{13}C NMR spectrum of compound III.



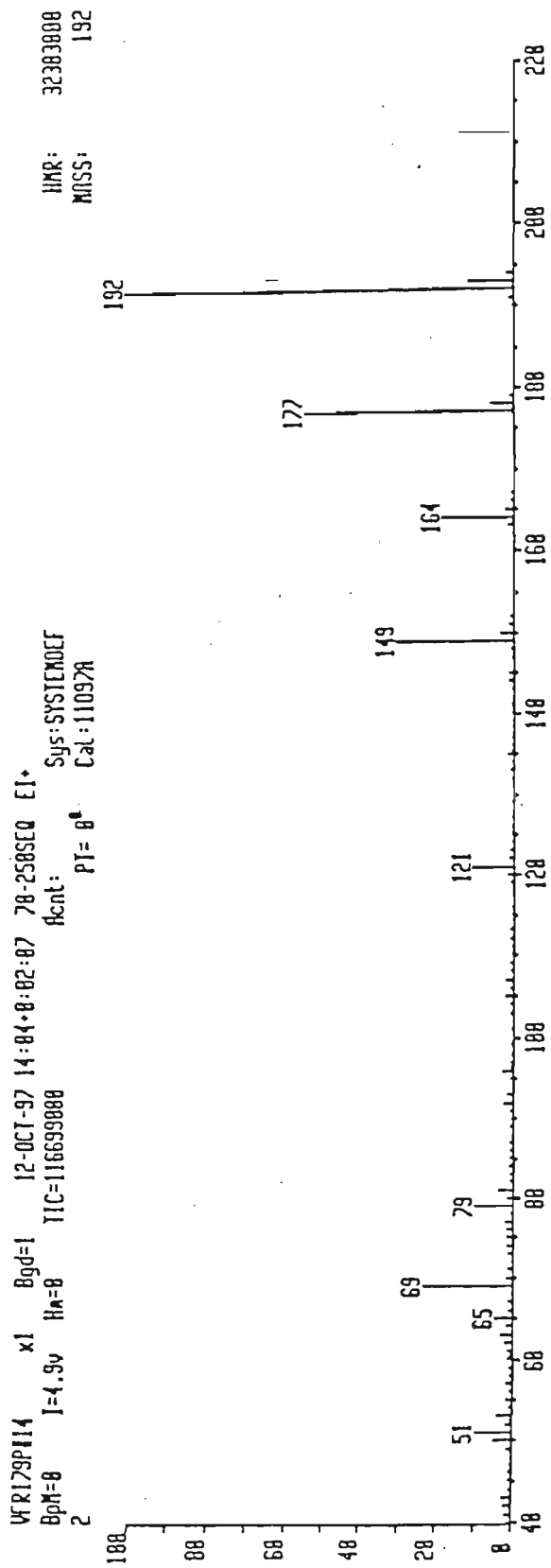
Spectrum 3c: NOE spectrum of compound III showing irradiation of H-4.



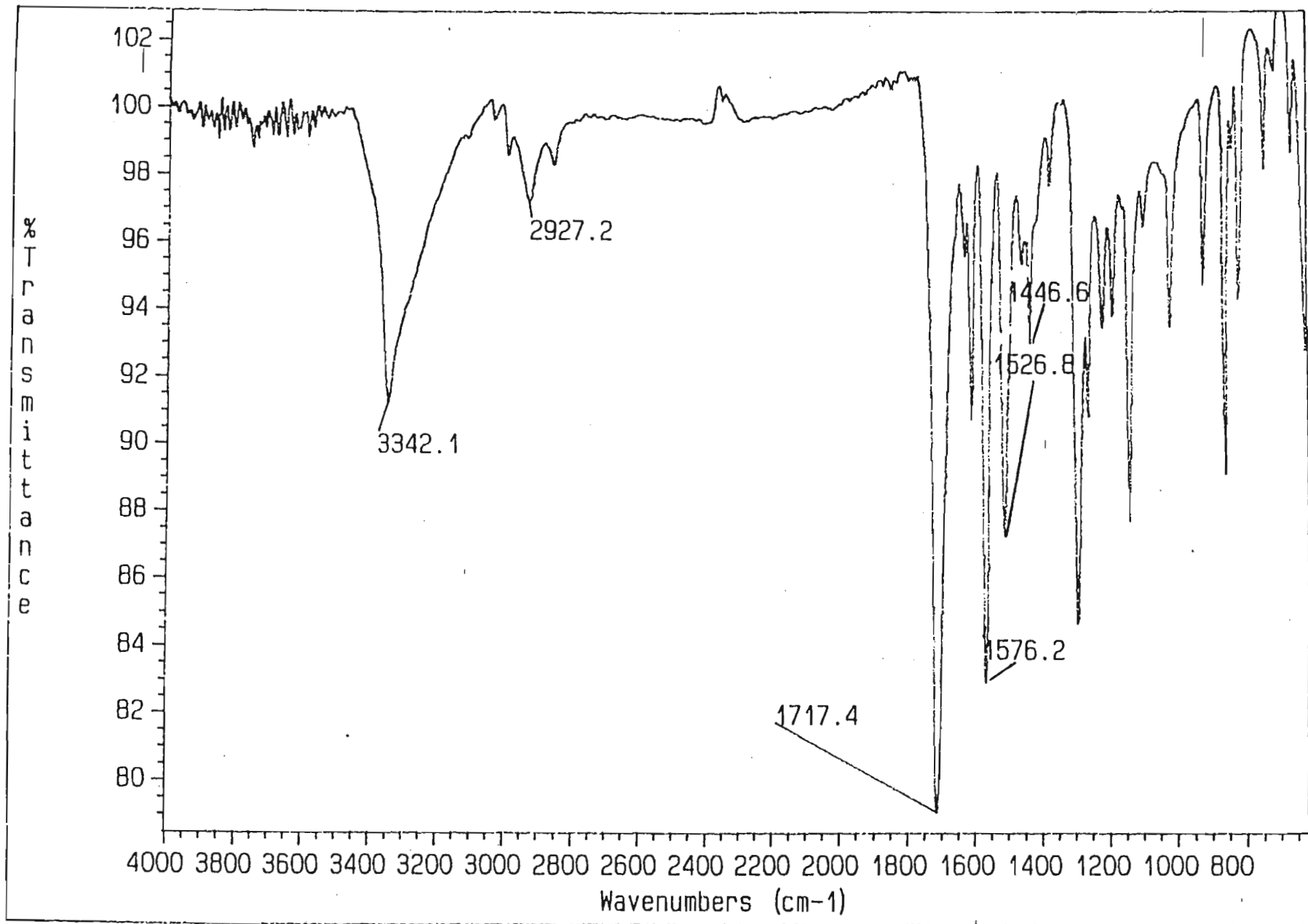
Spectrum 3d: NOE spectrum of compound III showing irradiation of H-5.



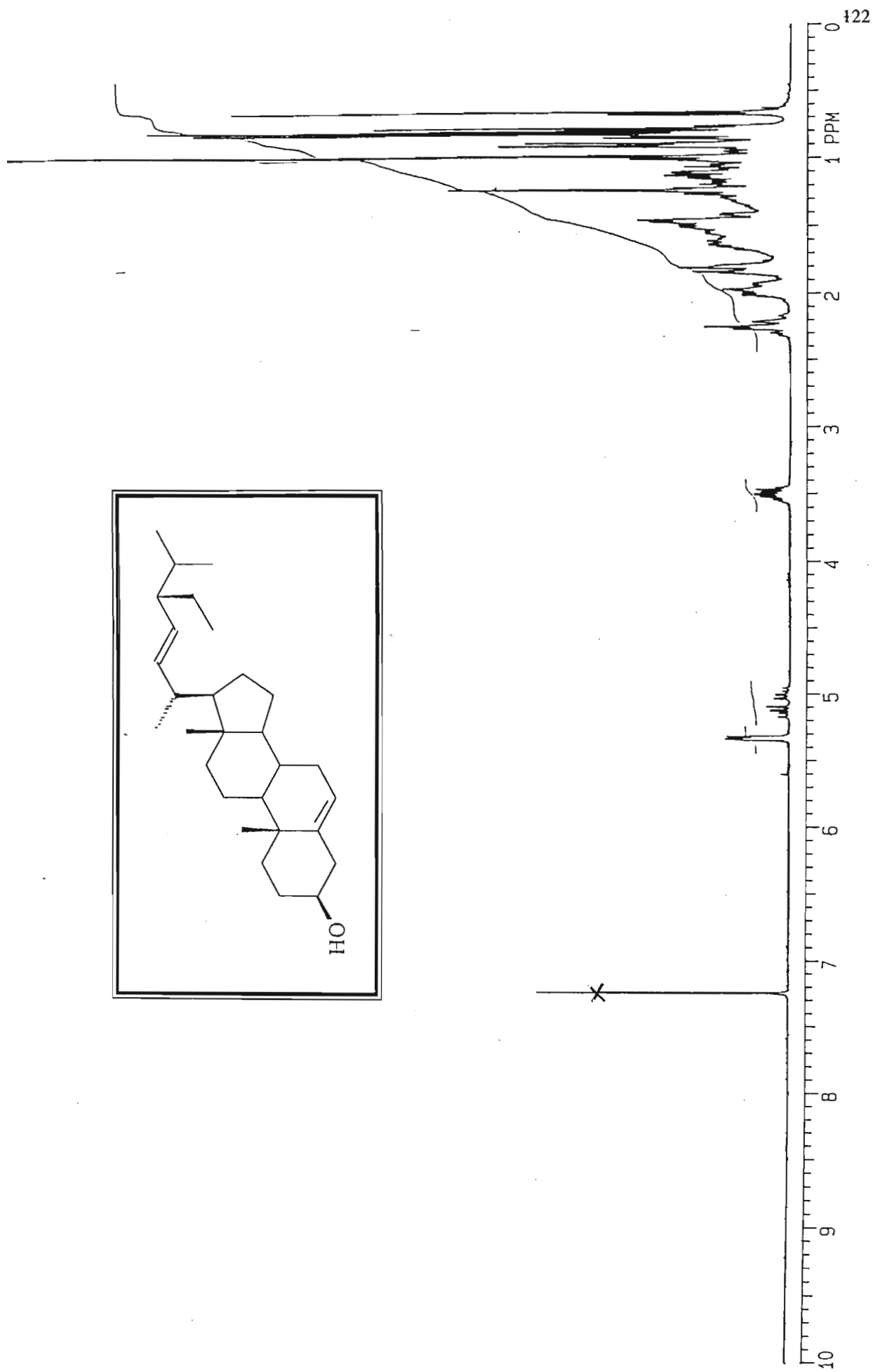
Spectrum 3e: NOE spectrum of compound III showing irradiation of the methoxyl group protons.



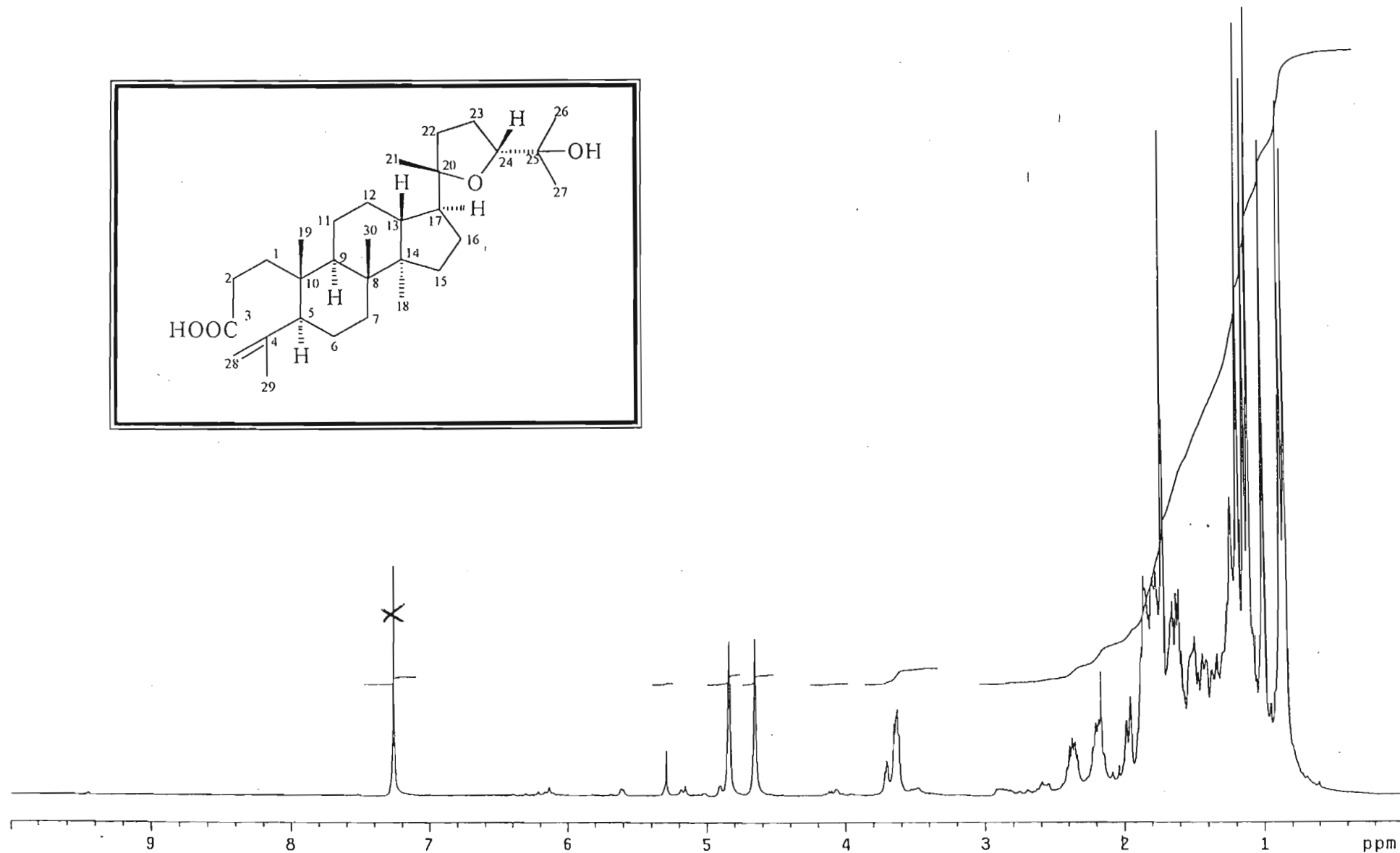
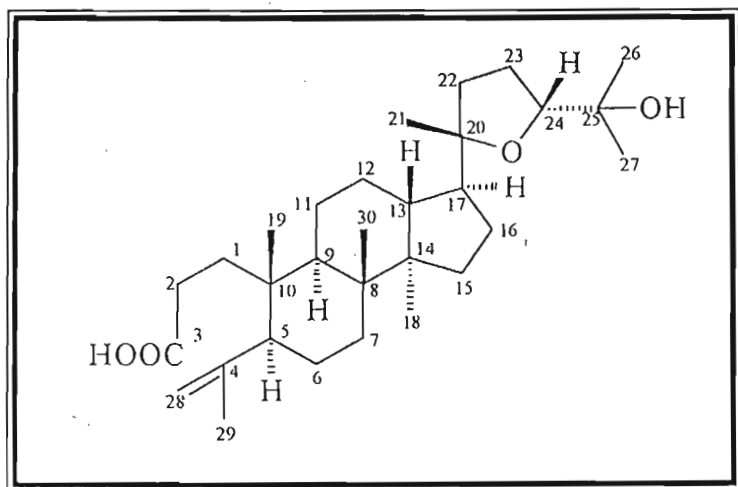
Spectrum 3f: Mass spectrum of compound III.



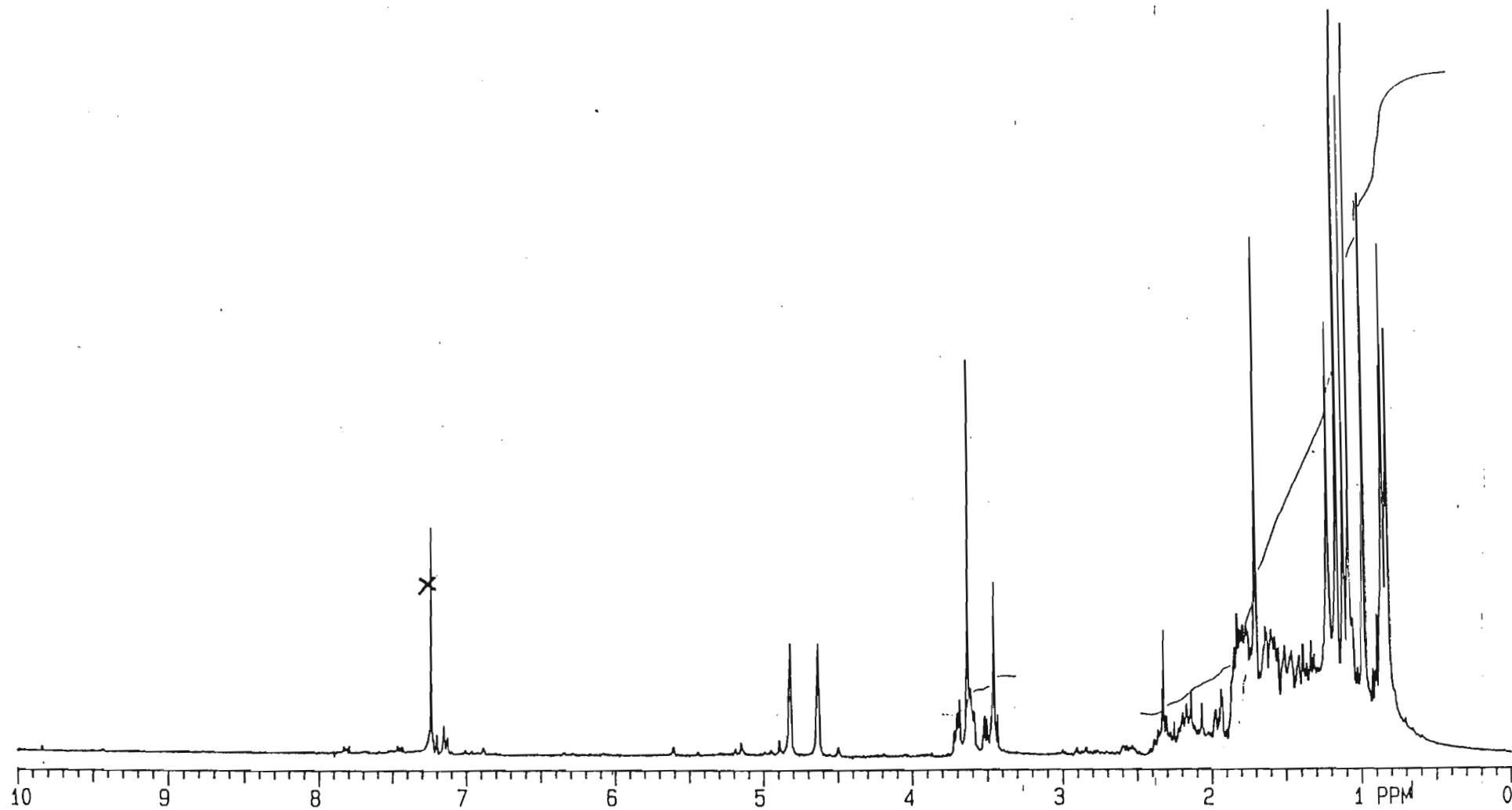
Spectrum 3g: Infra red spectrum of compound III.



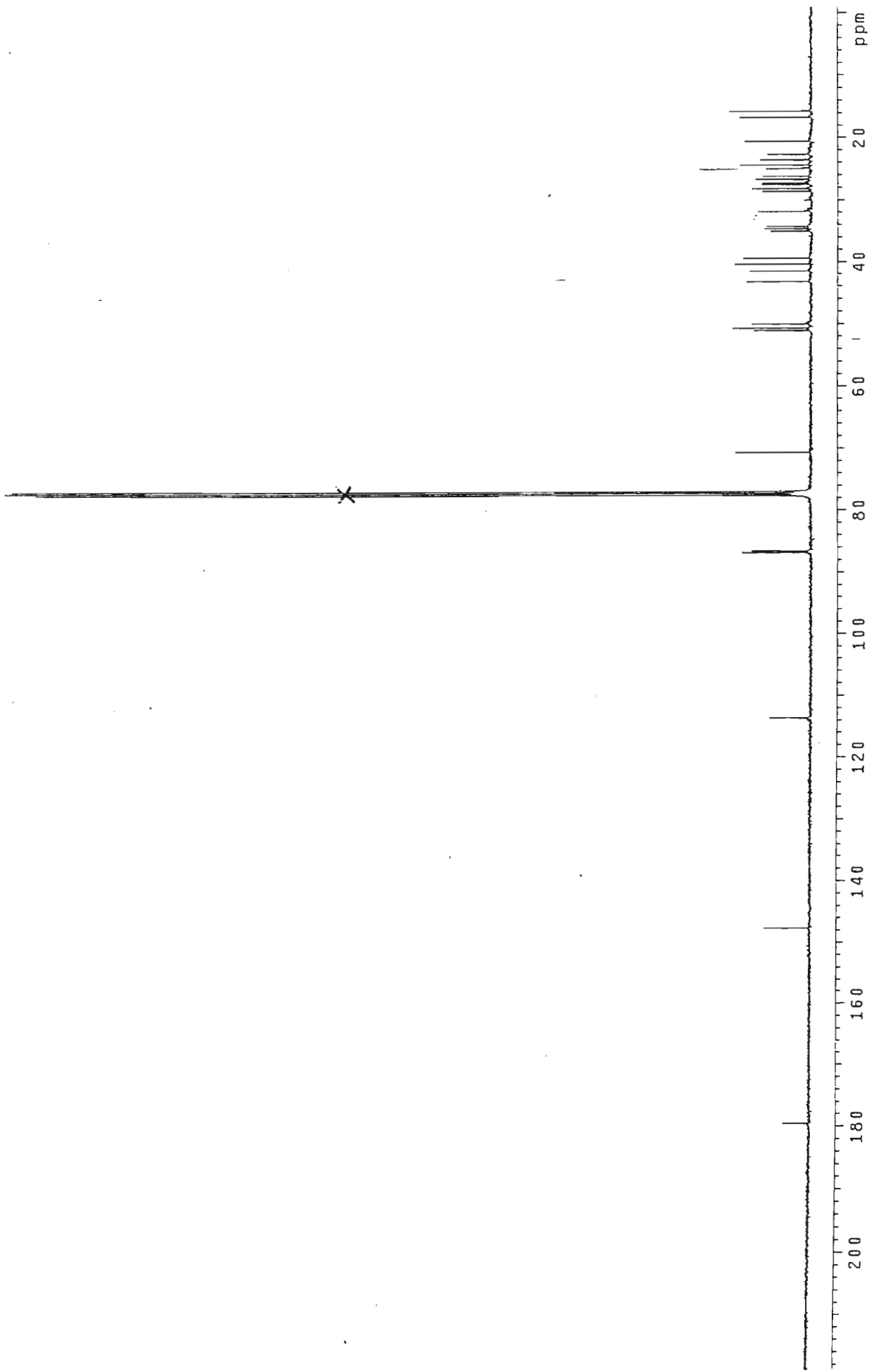
Spectrum 4a: ¹H NMR spectrum of compound IV.



Spectrum 5a: ^1H NMR spectrum of compound V.

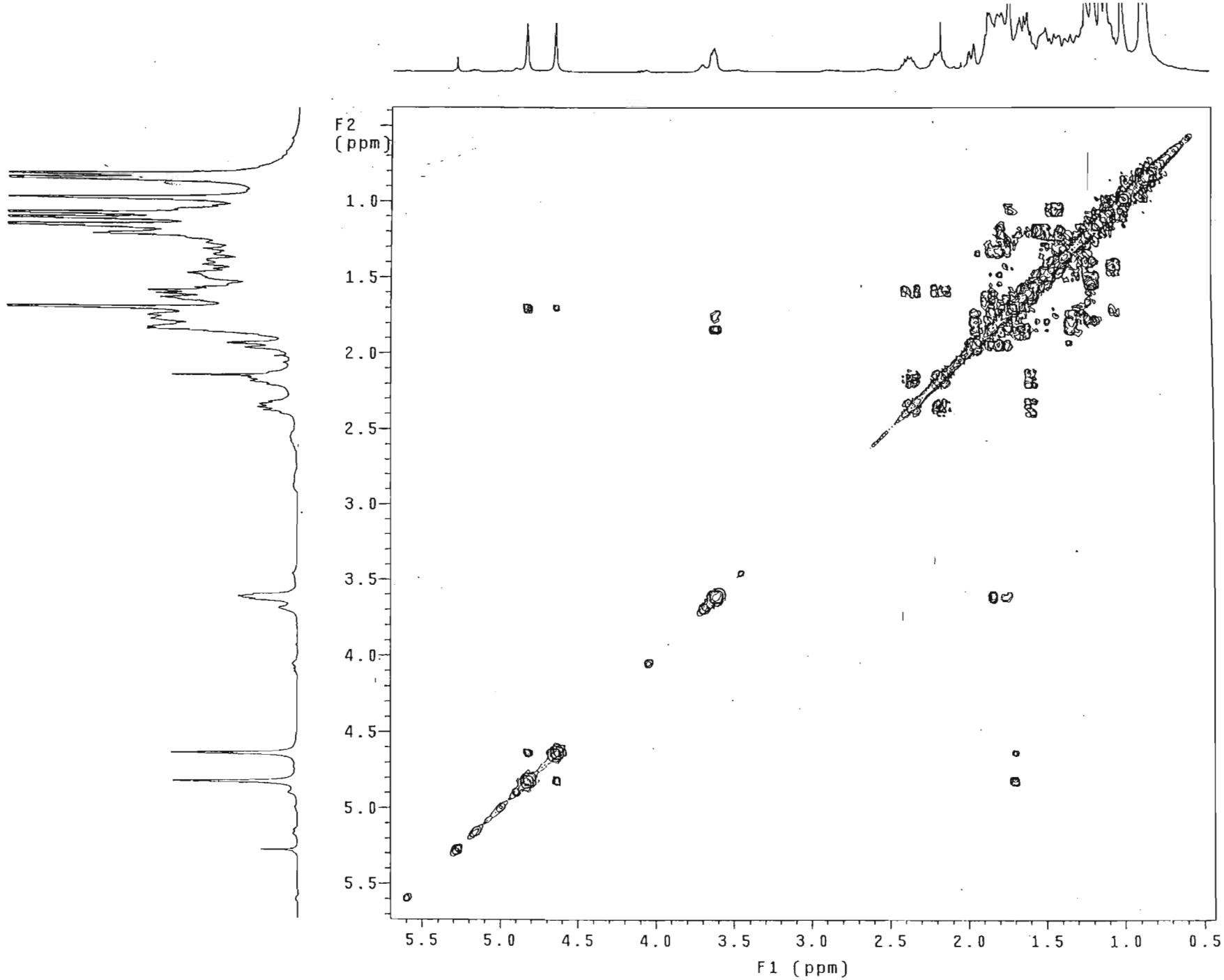


Spectrum 5b: ^1H NMR spectrum of acetylated compound V.

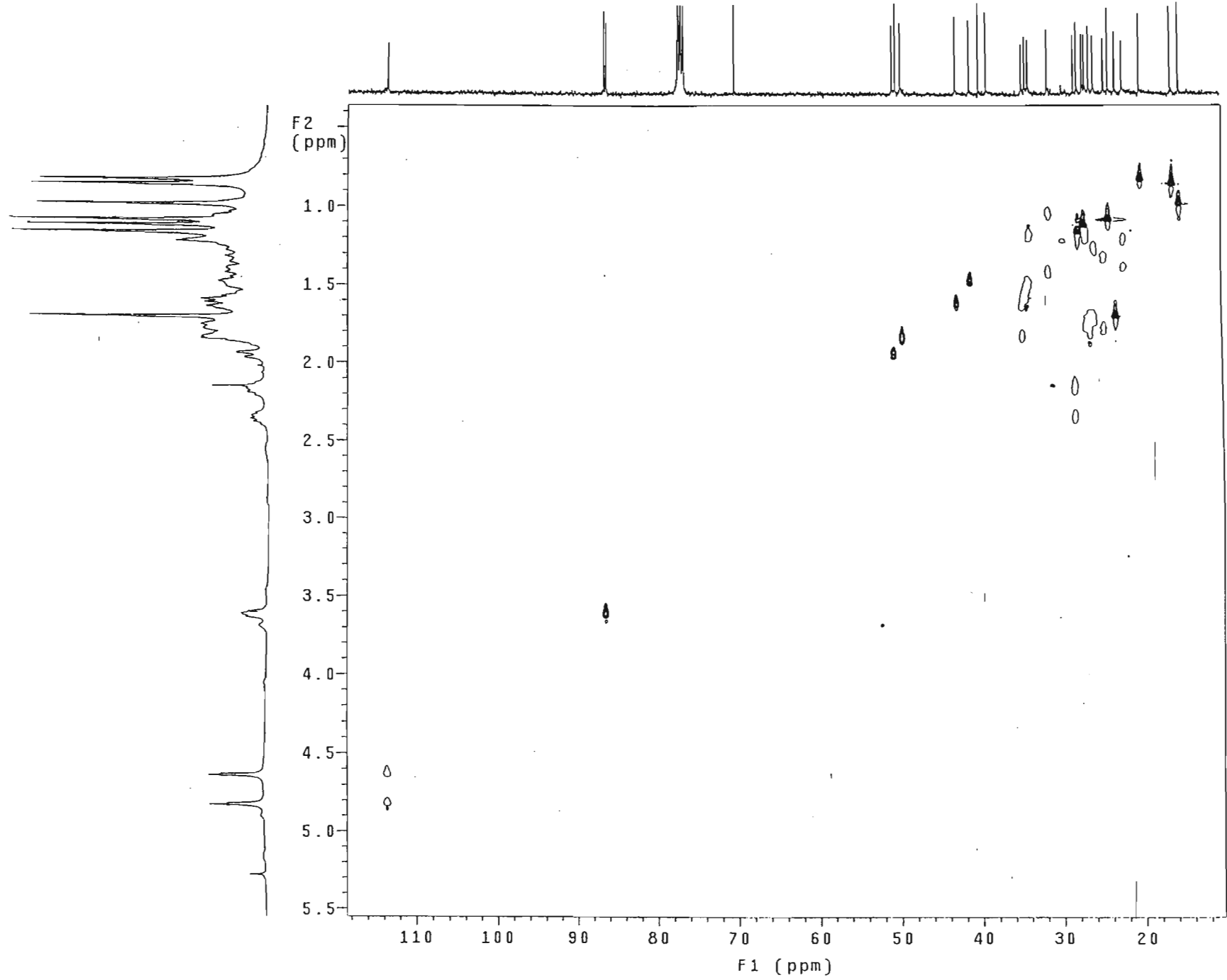


125

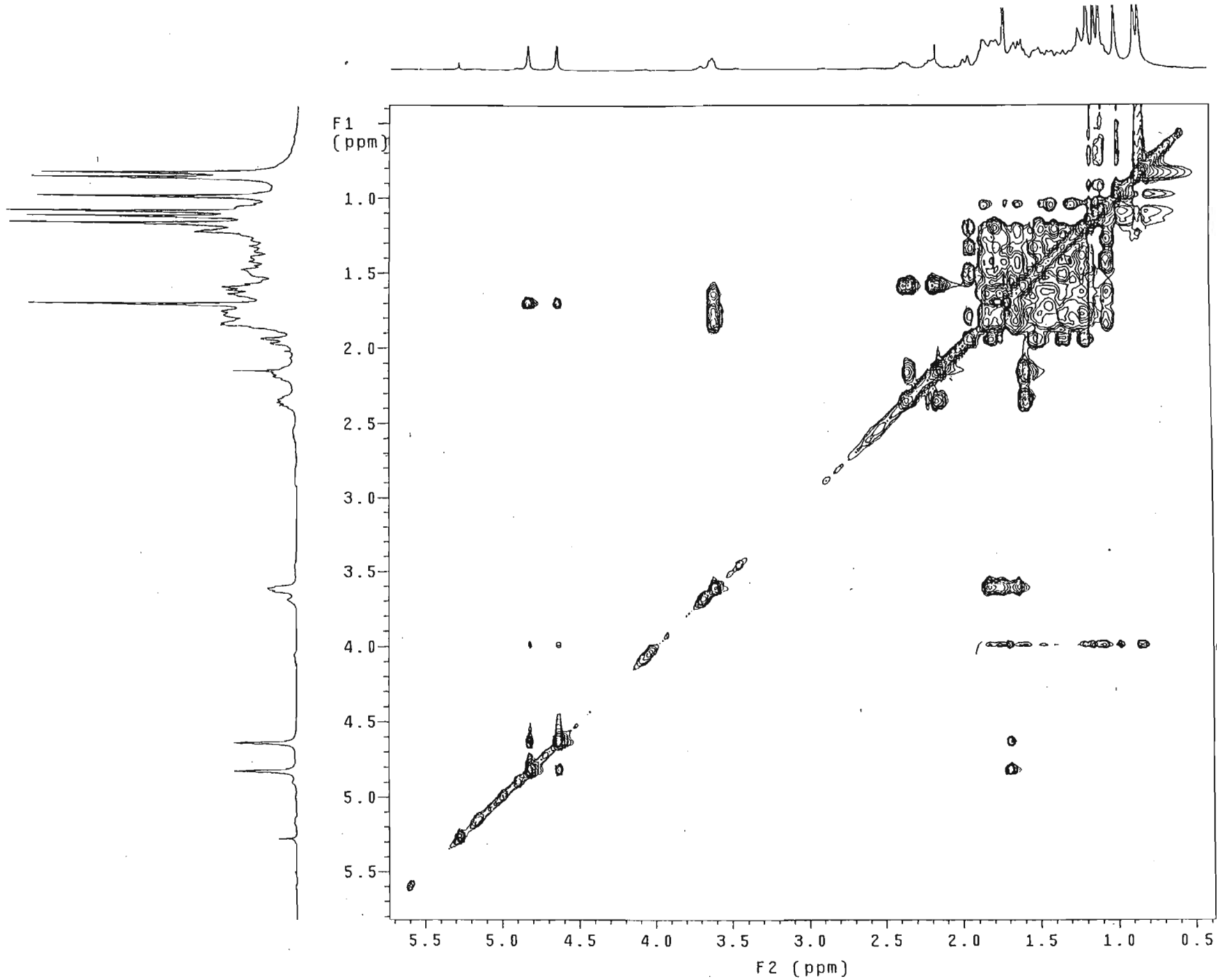
Spectrum 5c: ^{13}C NMR spectrum of compound V.



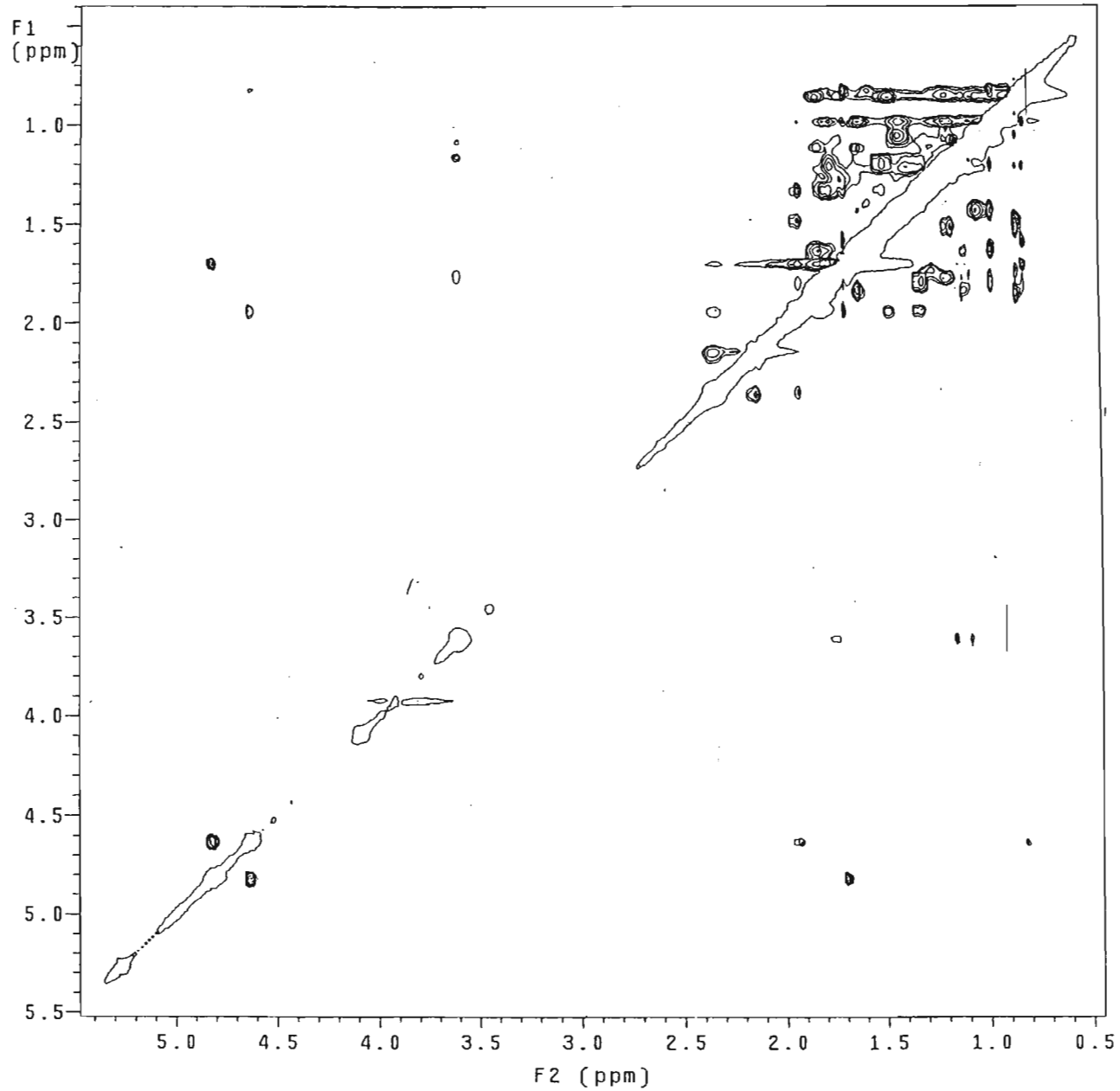
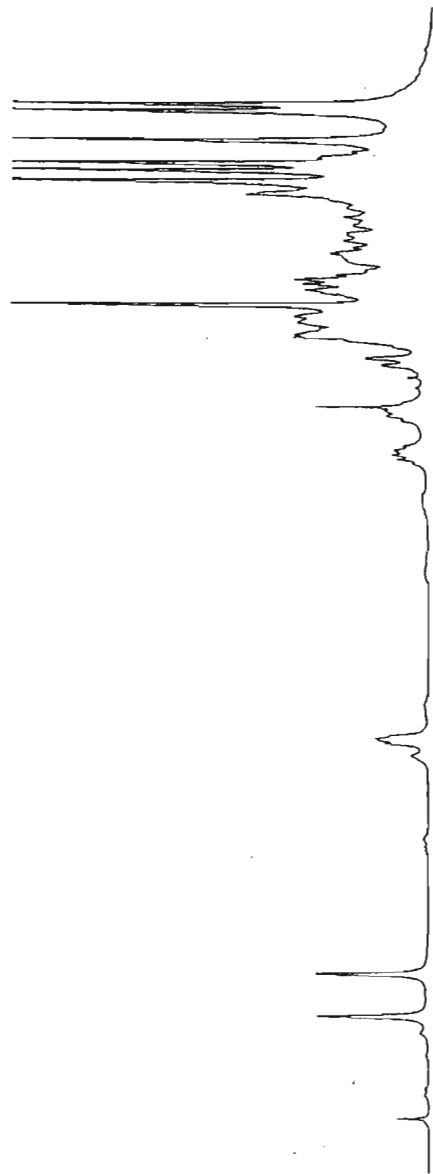
Spectrum 5d: COSY spectrum of compound V.



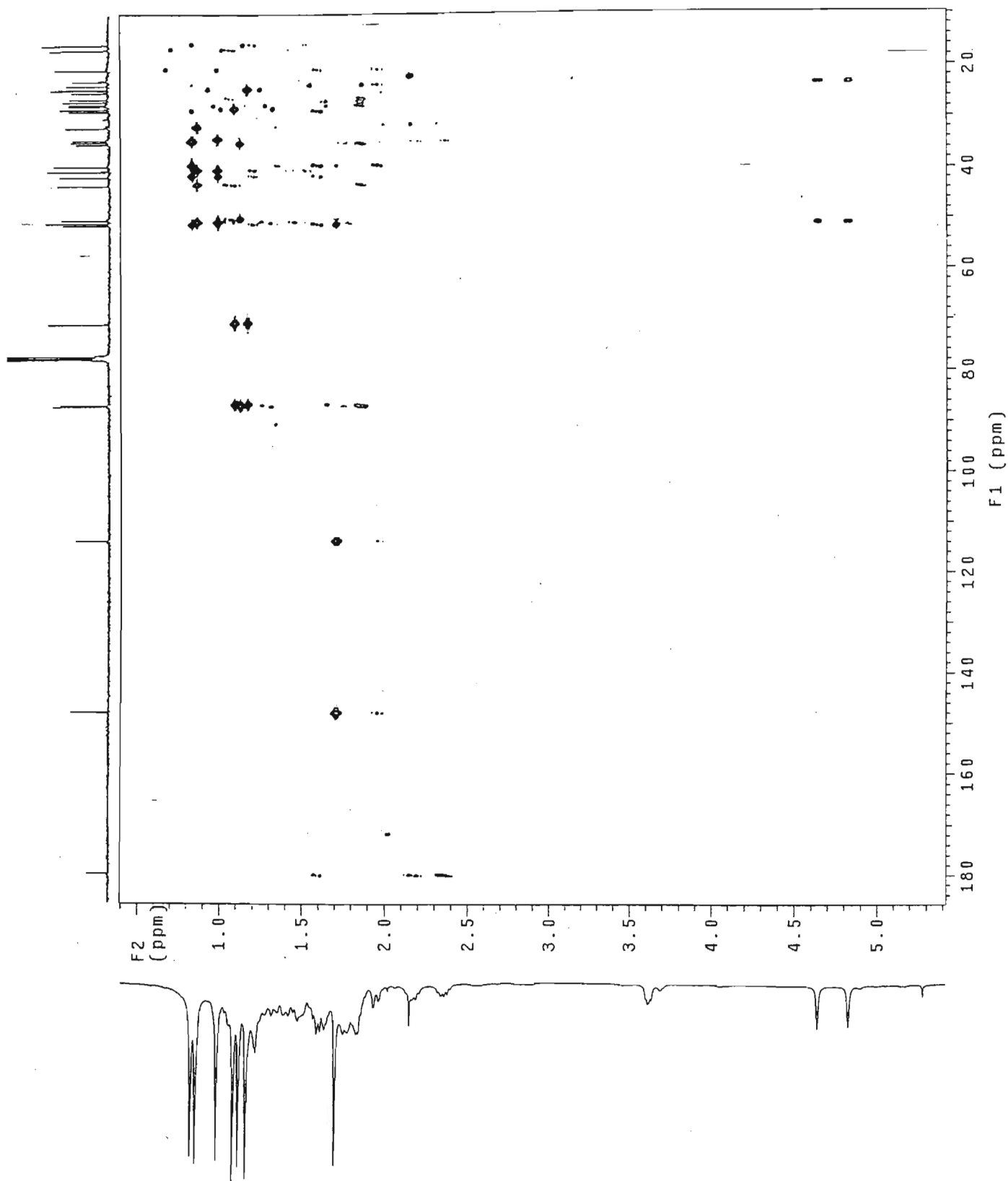
Spectrum 5e: HSQC spectrum of compound V.



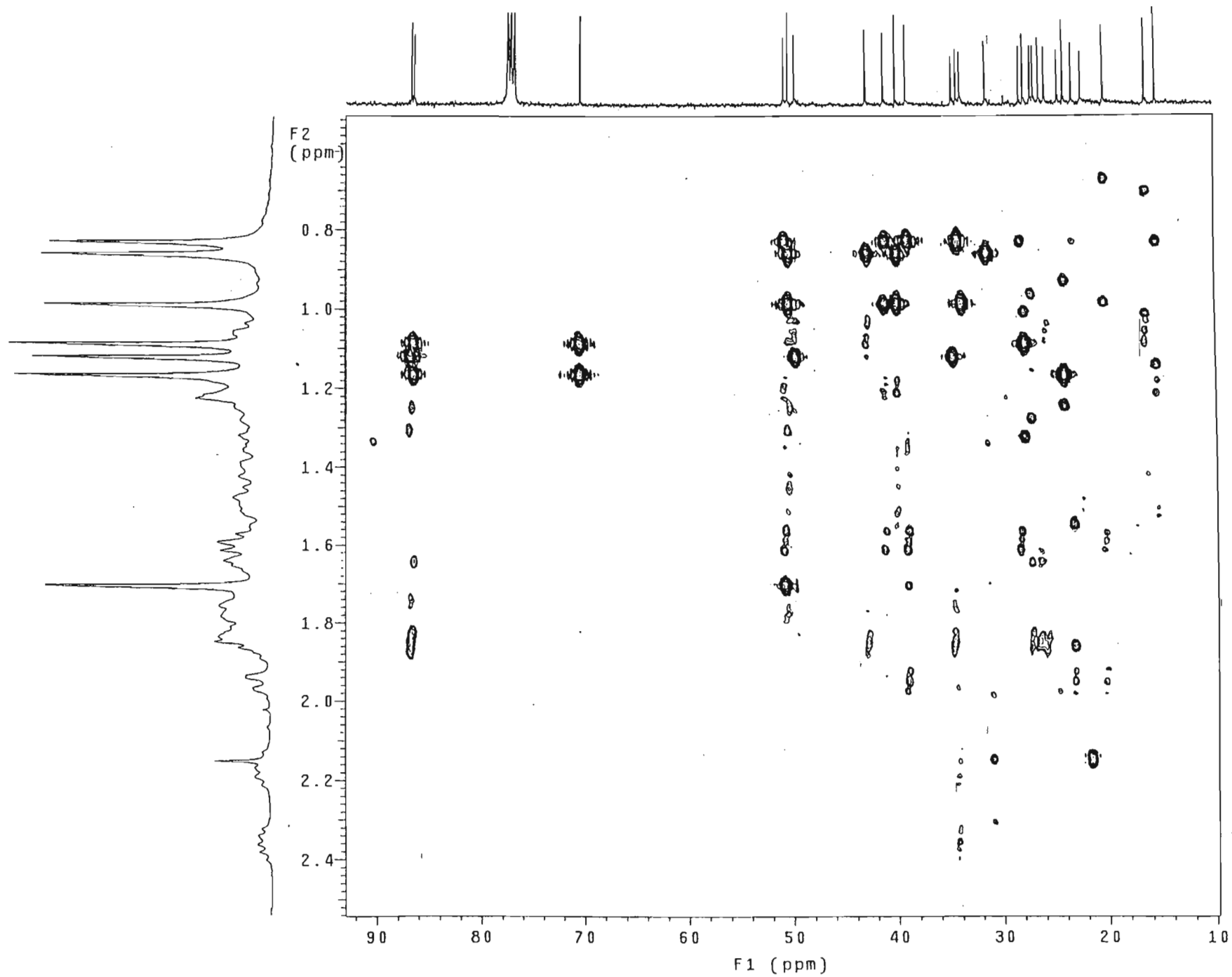
Spectrum 5f: TOCSY spectrum of compound V.



Spectrum 5g: NOESY spectrum of compound V.

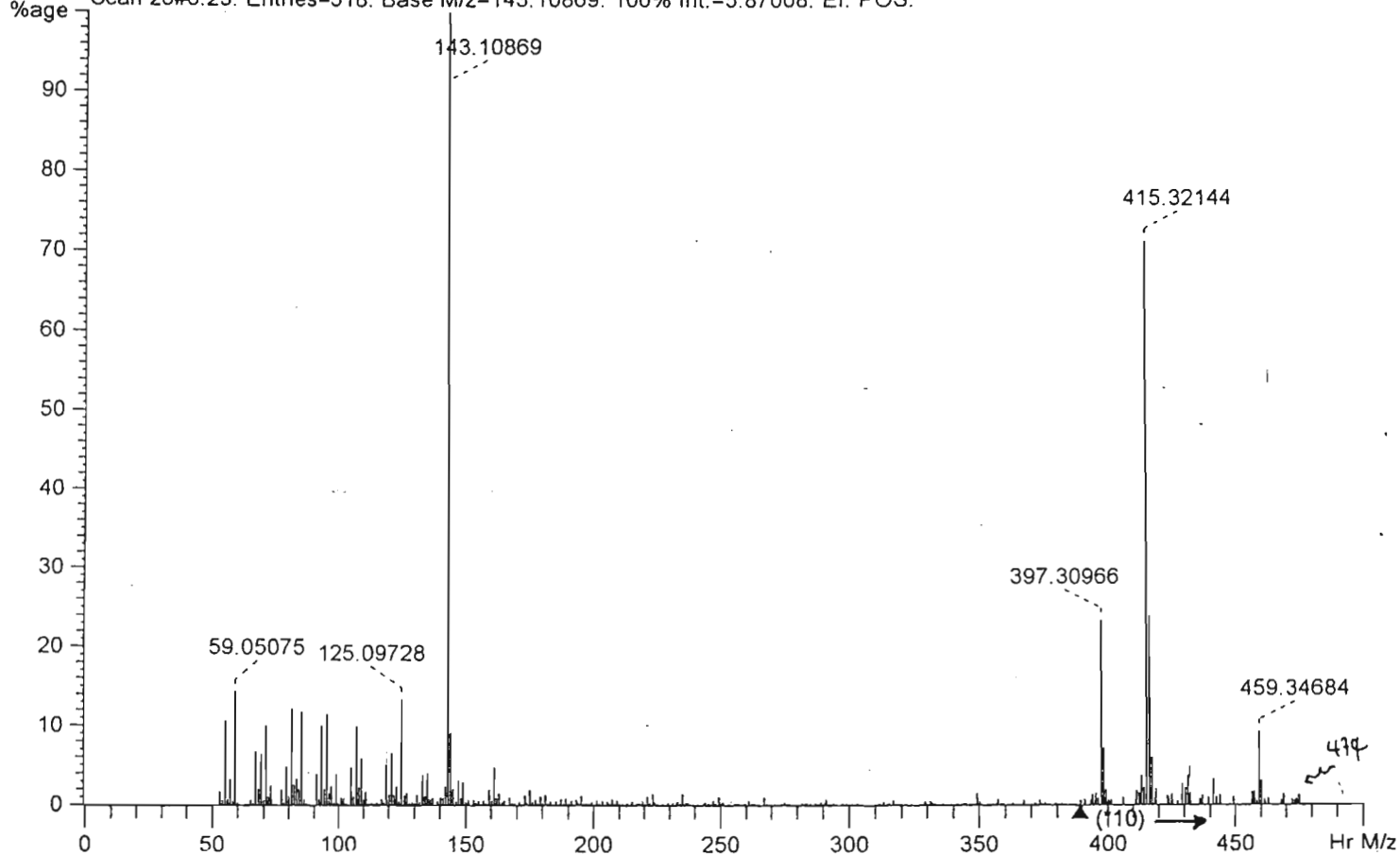


Spectrum 5h: HMBC spectrum of compound V.

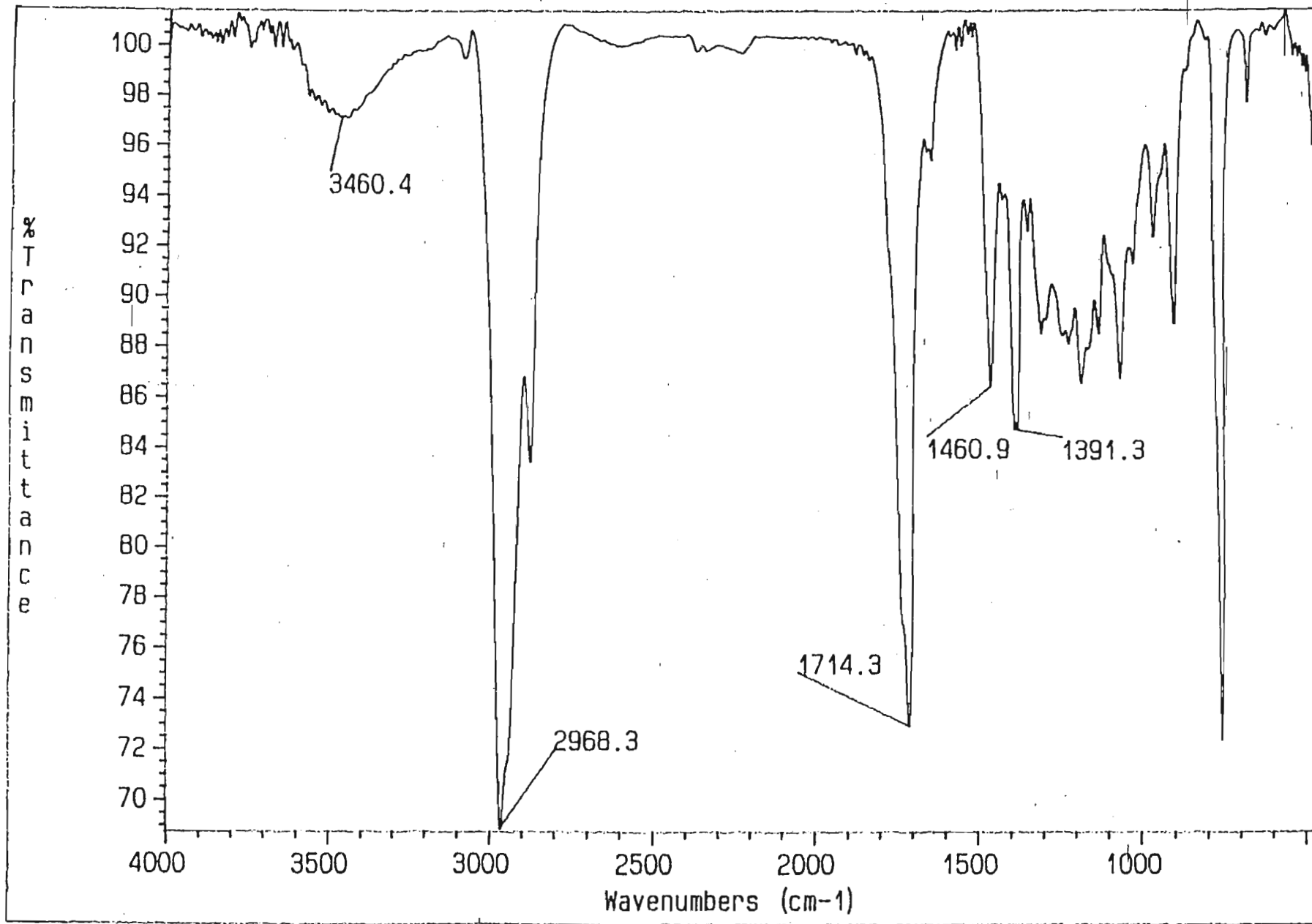


Spectrum 5i: Expanded HMBC spectrum of compound V.

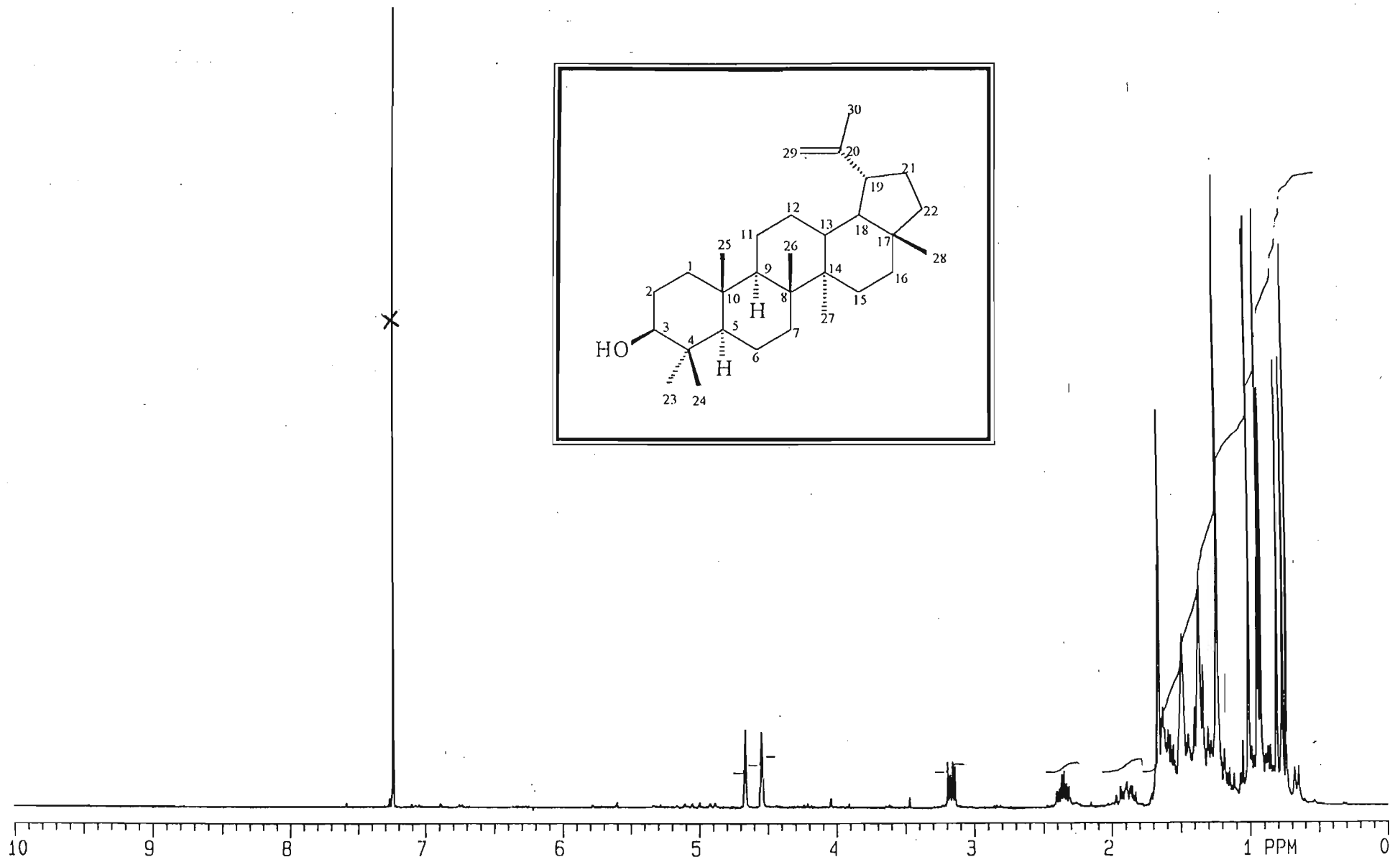
SCAN GRAPH. Flagging=Hr M/z. Filter=[Range:50-476. Excl: Ref/Ex.].
Scan 26#6:23. Entries=518. Base M/z=143.10869. 100% Int.=5.87008. EI. POS.



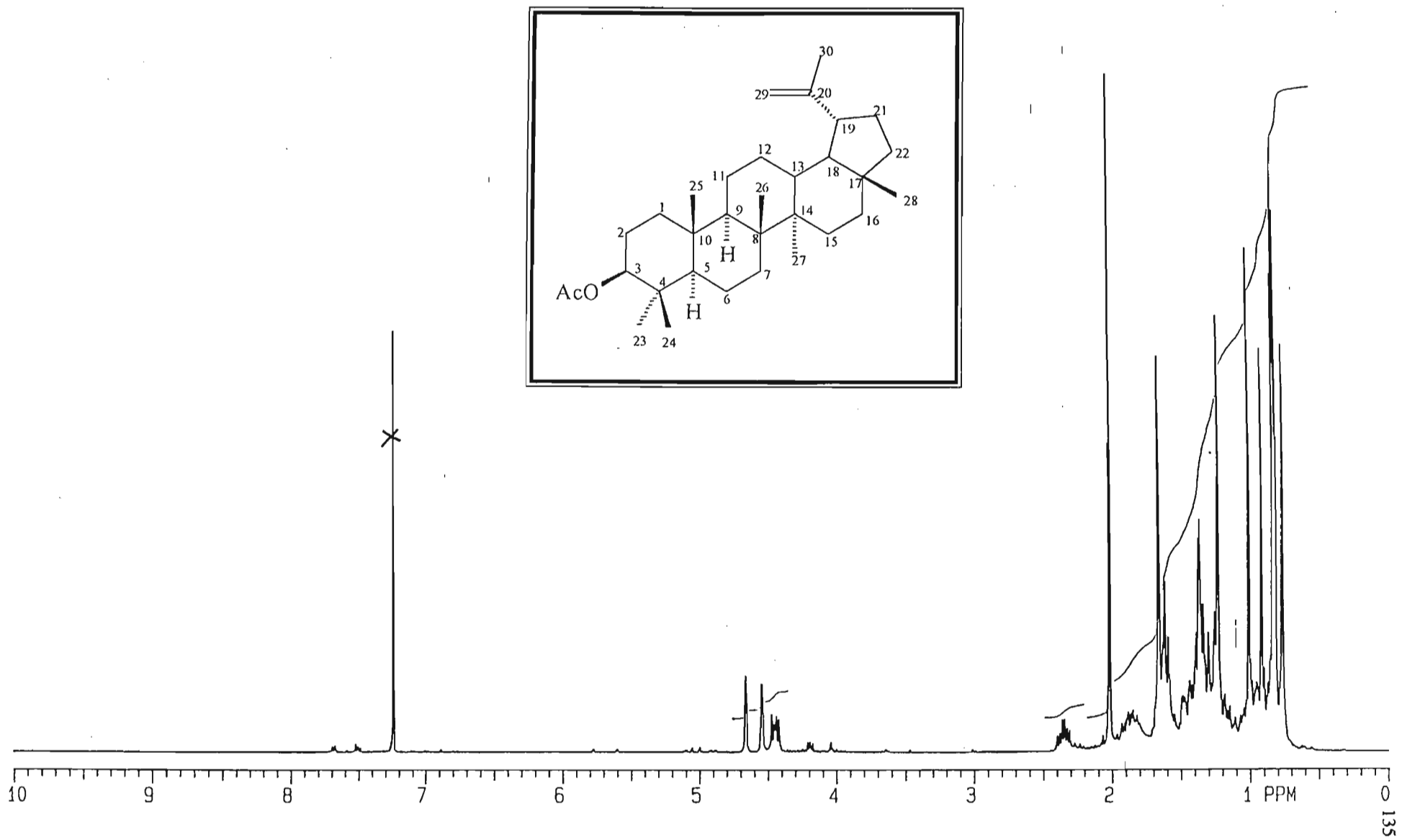
Spectrum 5j: High resolution mass spectrum of compound V.



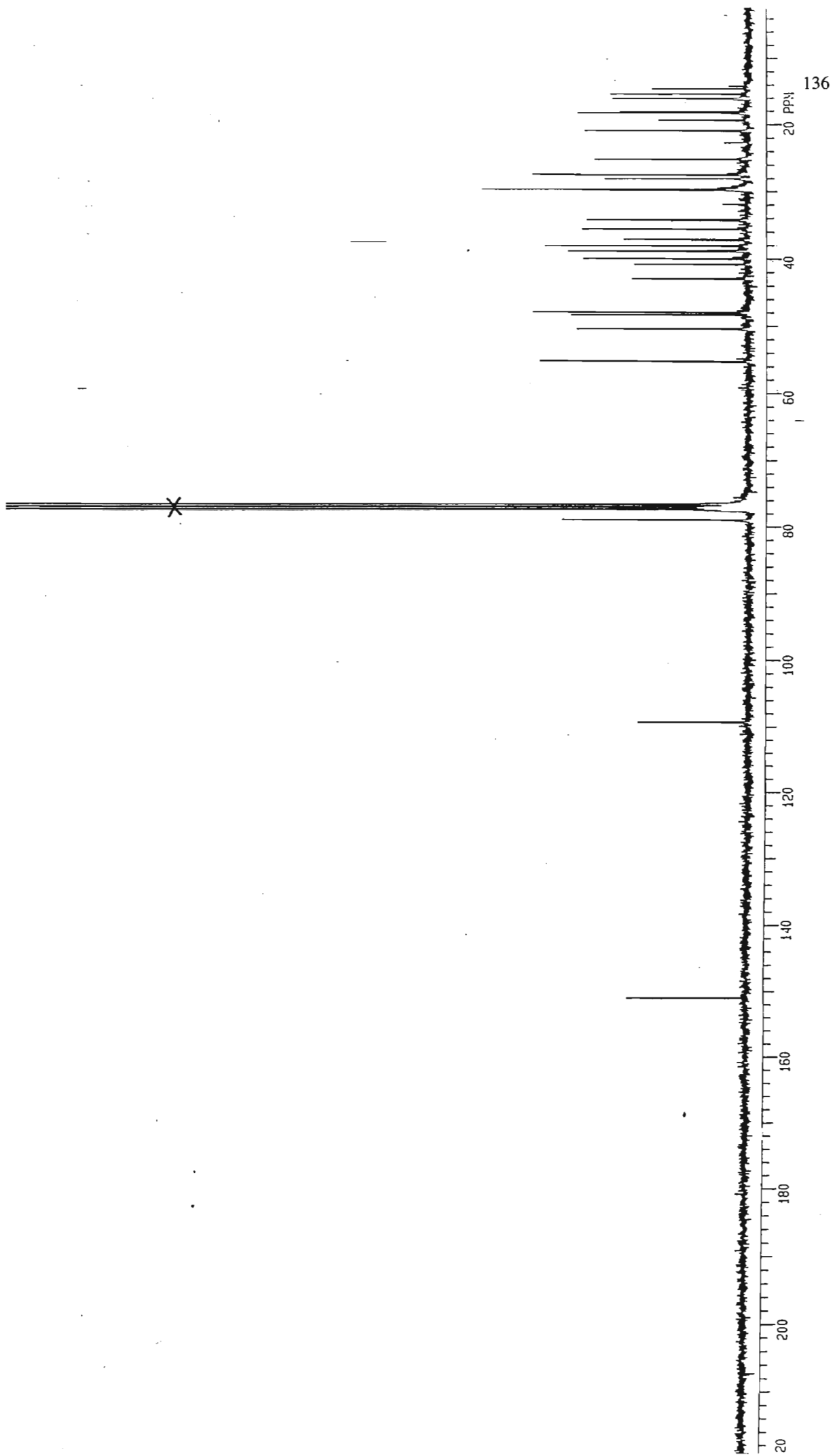
Spectrum 5k: Infra red spectrum of compound V.



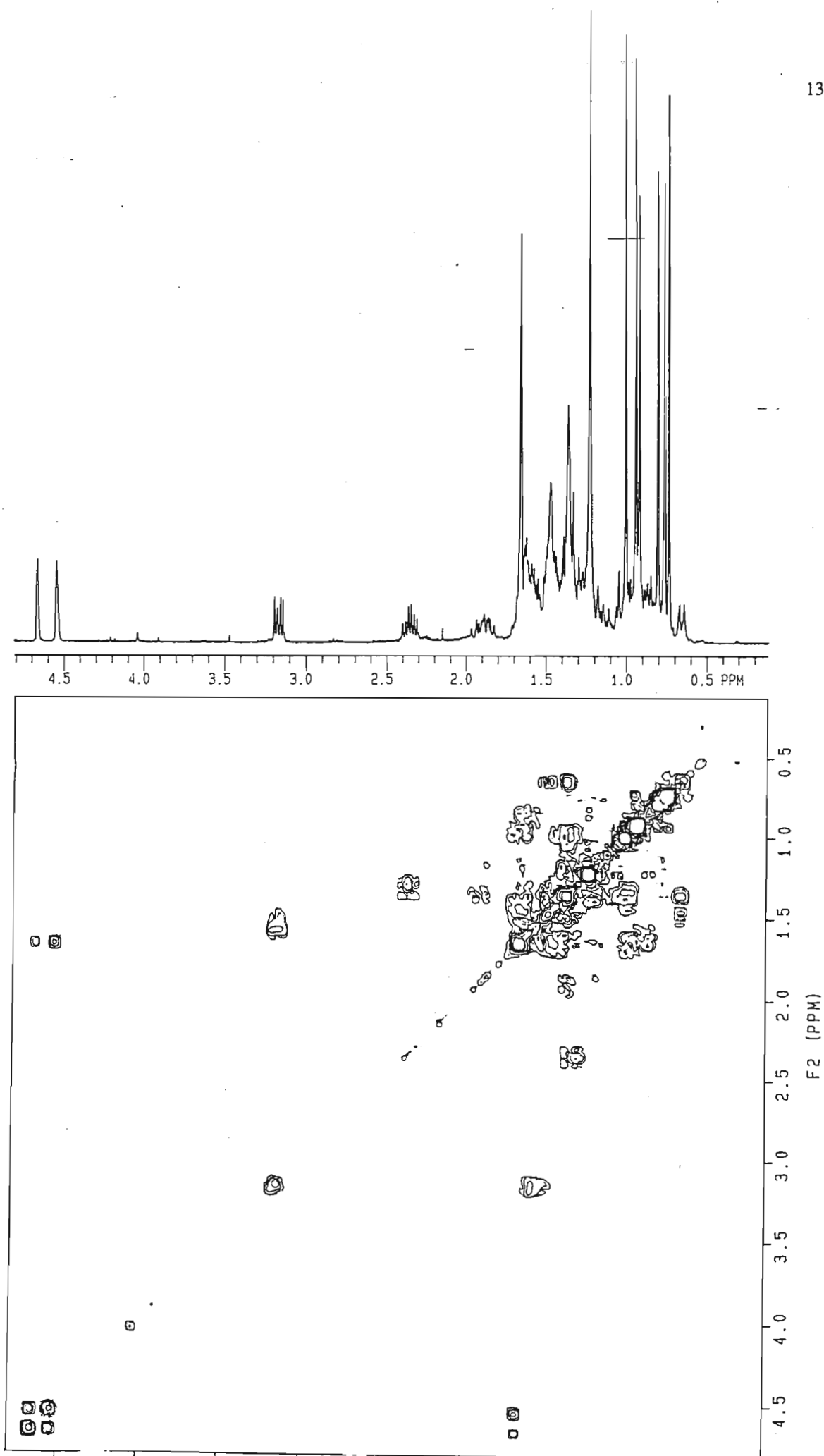
Spectrum 6a: ^1H NMR spectrum of compound VI.



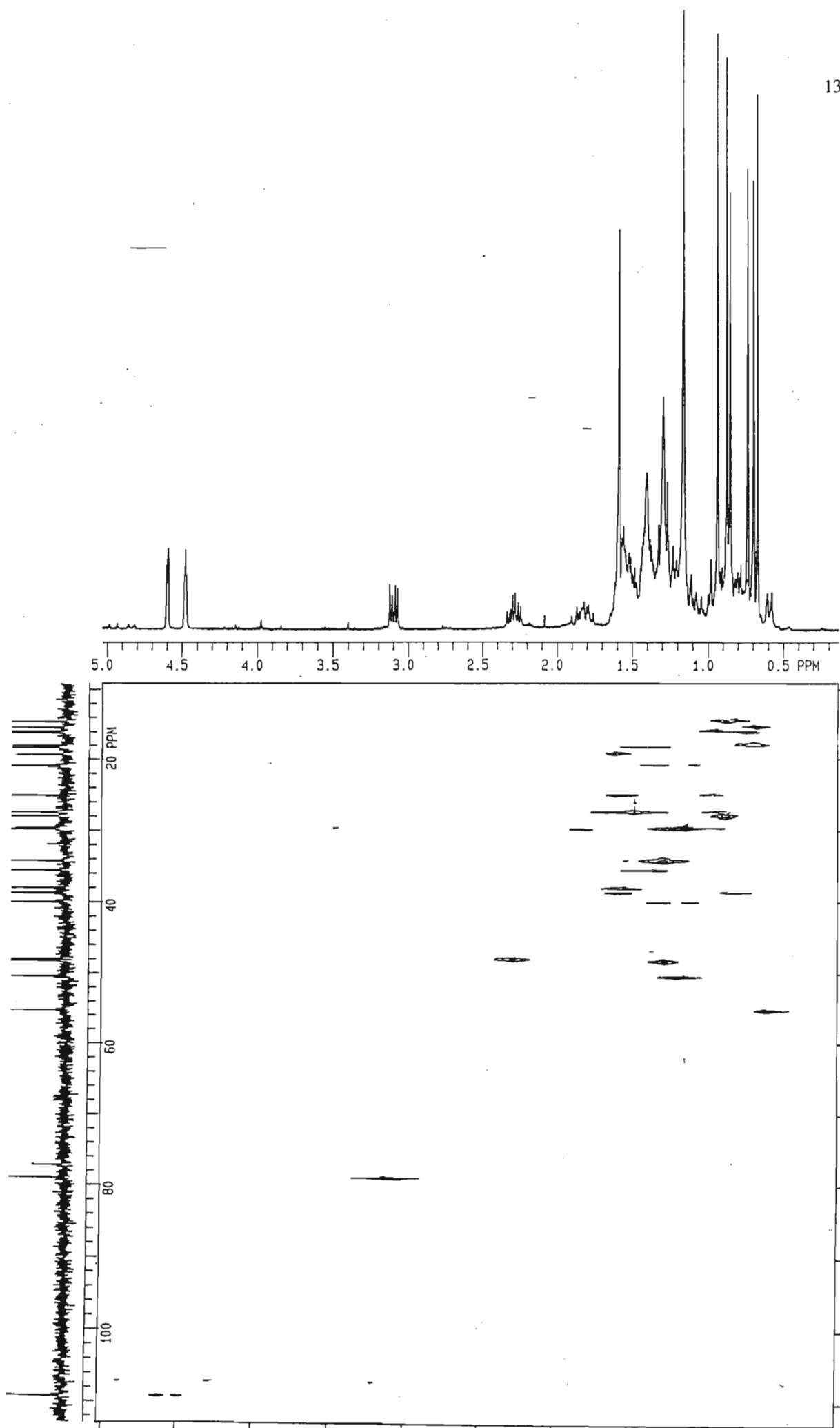
Spectrum 6b: ^1H NMR spectrum of acetylated compound VI.



Spectrum 6c: ^{13}C NMR spectrum of compound VI.

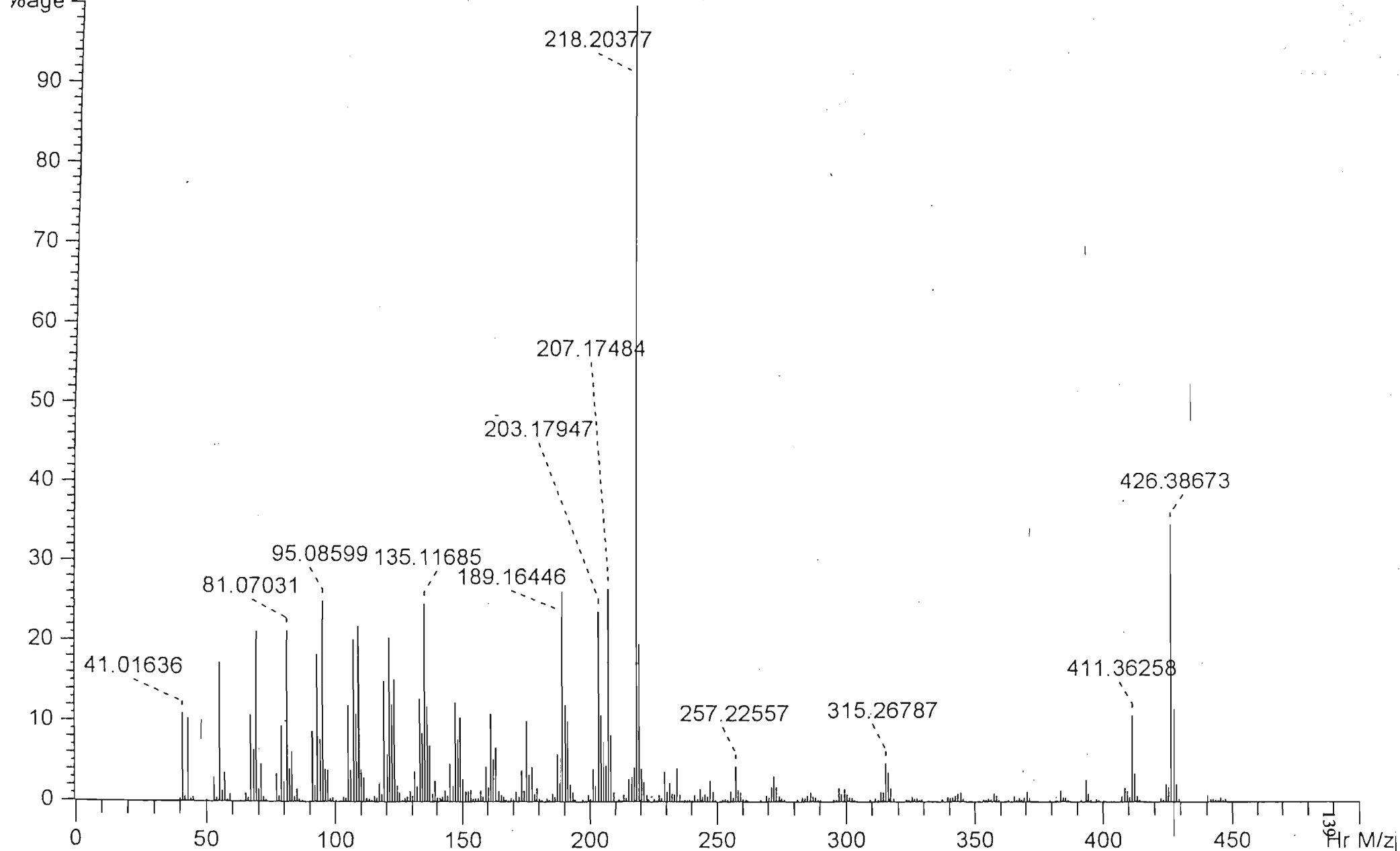


Spectrum 6d: COSY spectrum of compound VI.

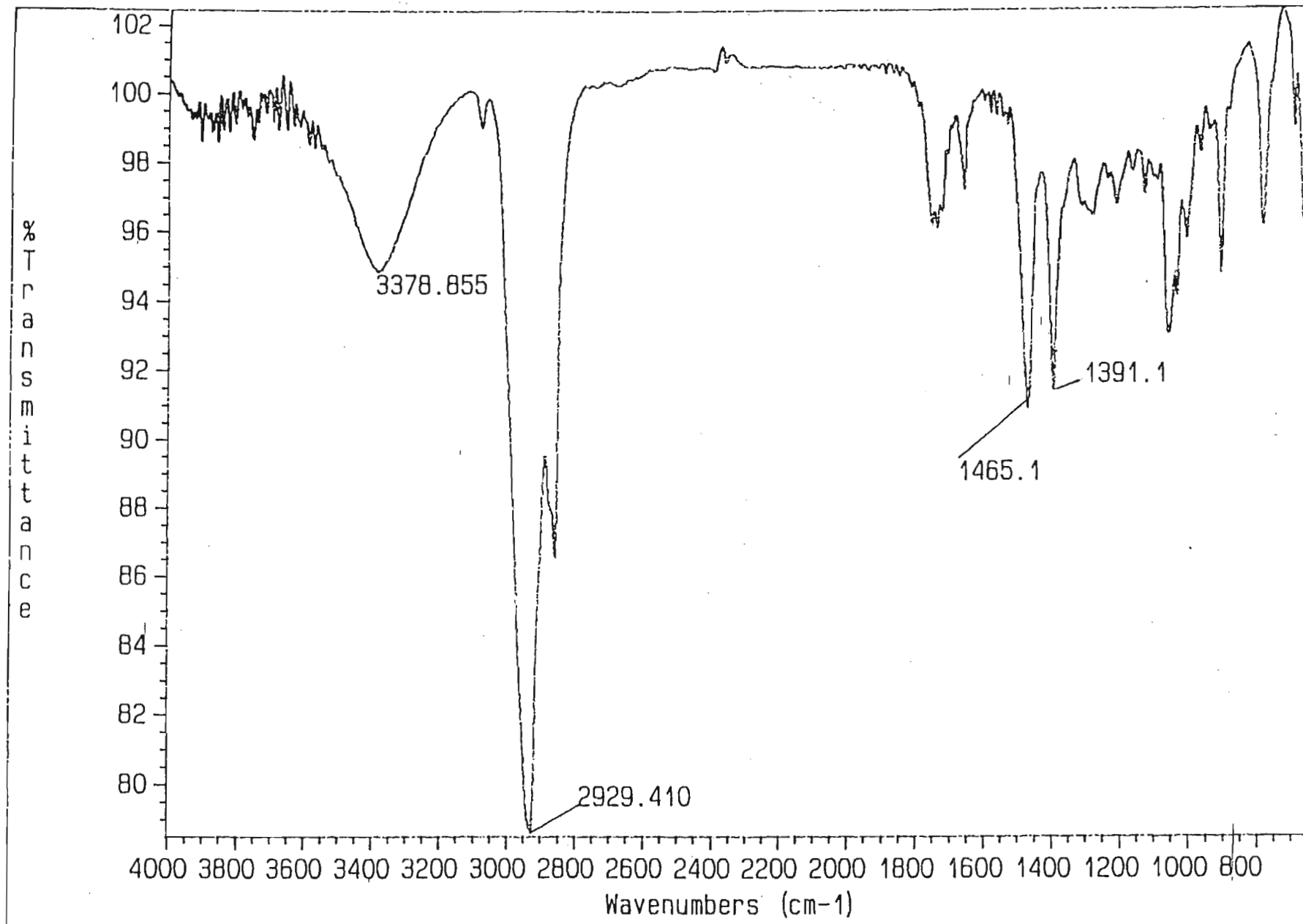


Spectrum 6e: HETCOR spectrum of compound VI.

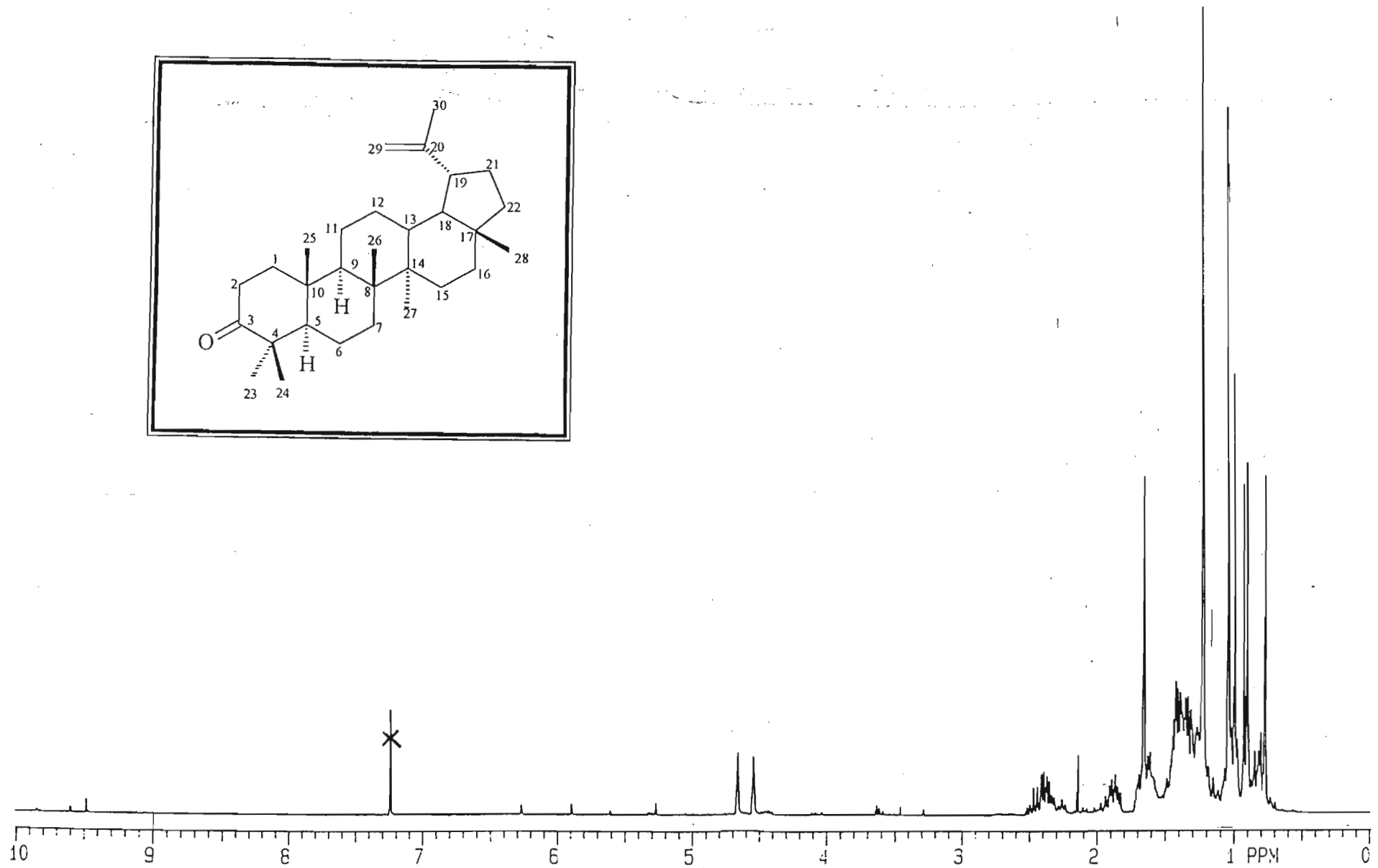
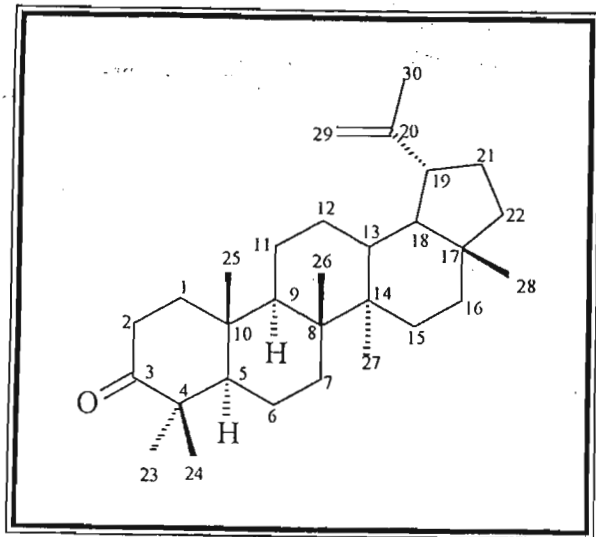
Scan 28#6:43 - 33#7:52. Entries=353. Base M/z=218.20377. 100% Int.=4.01493. EI. POS.



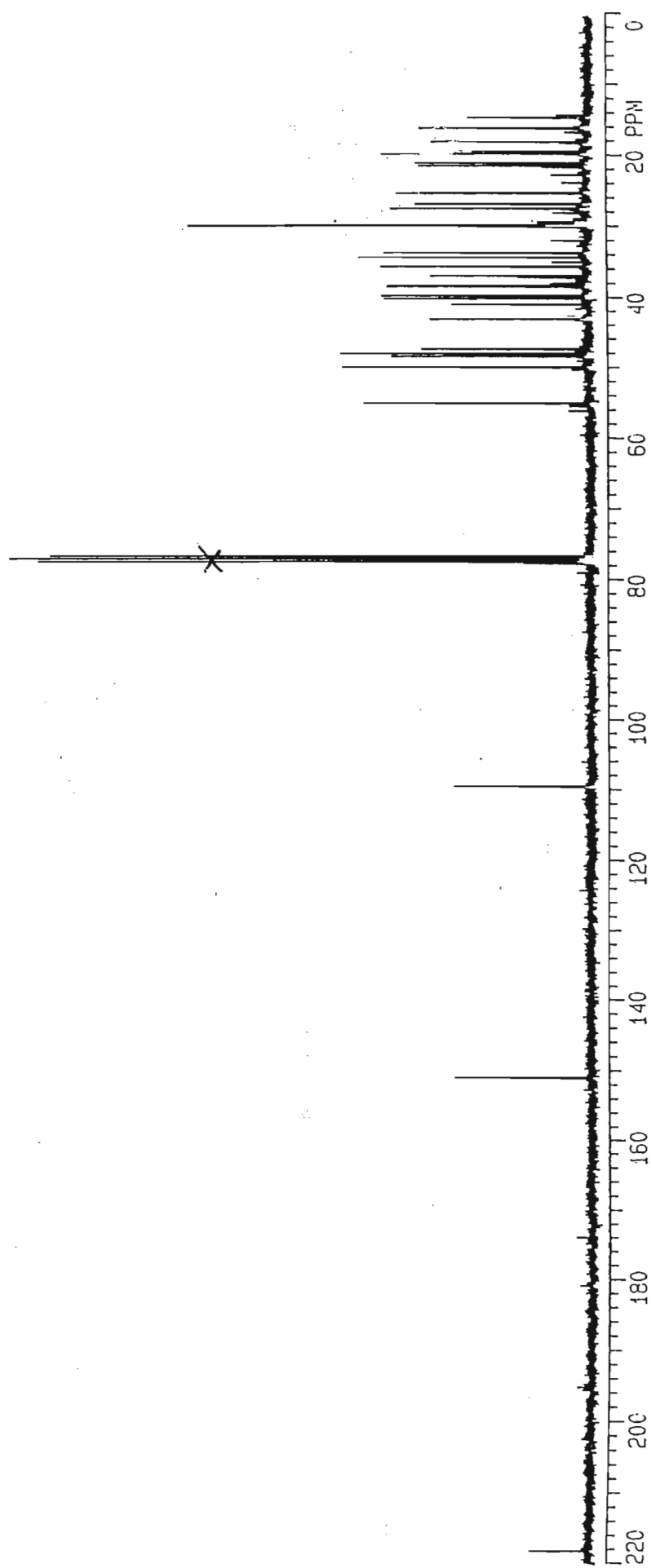
Spectrum 6f: High resolution mass spectrum of compound VI.



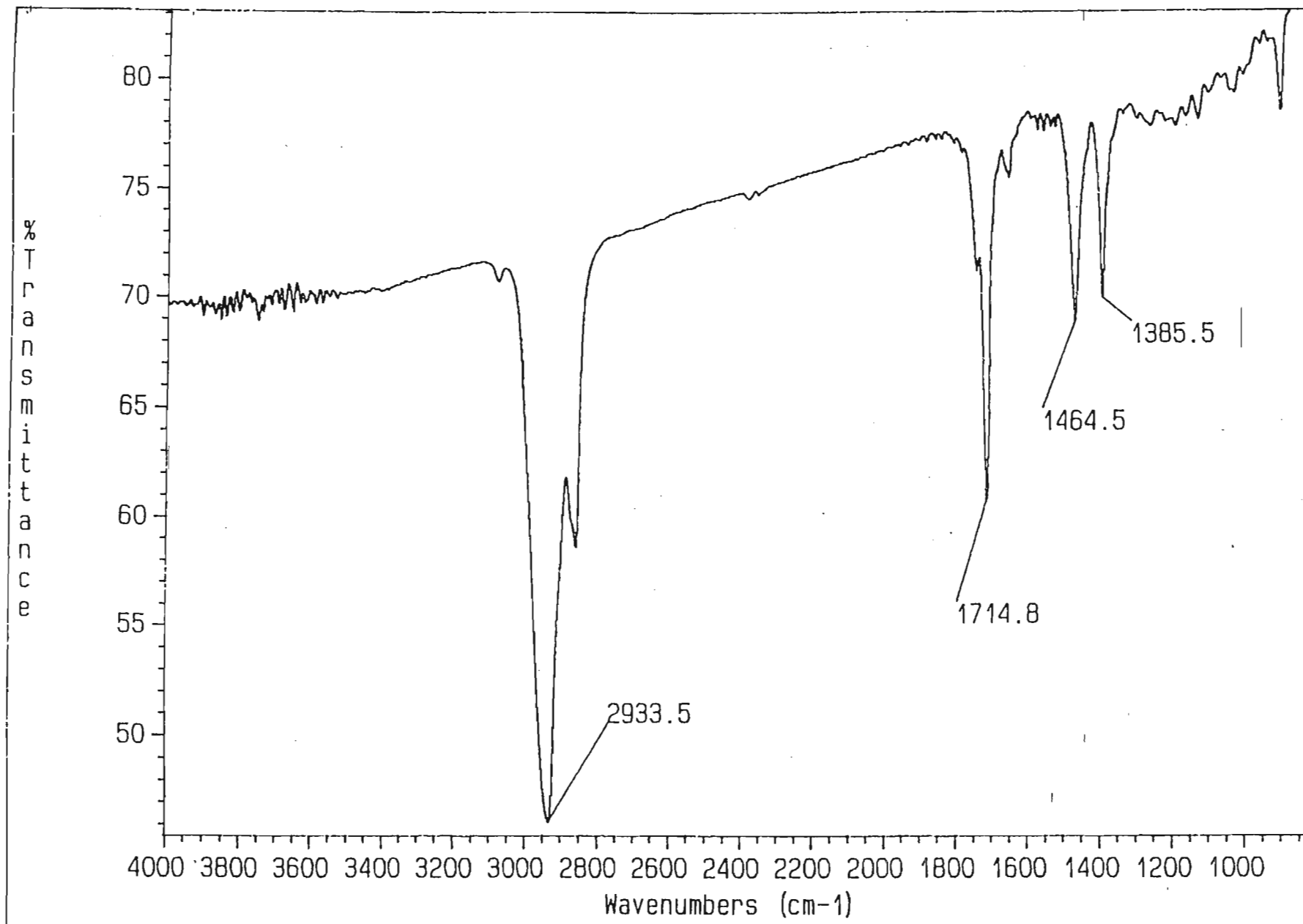
Spectrum 6g: Infra red spectrum of compound VI.



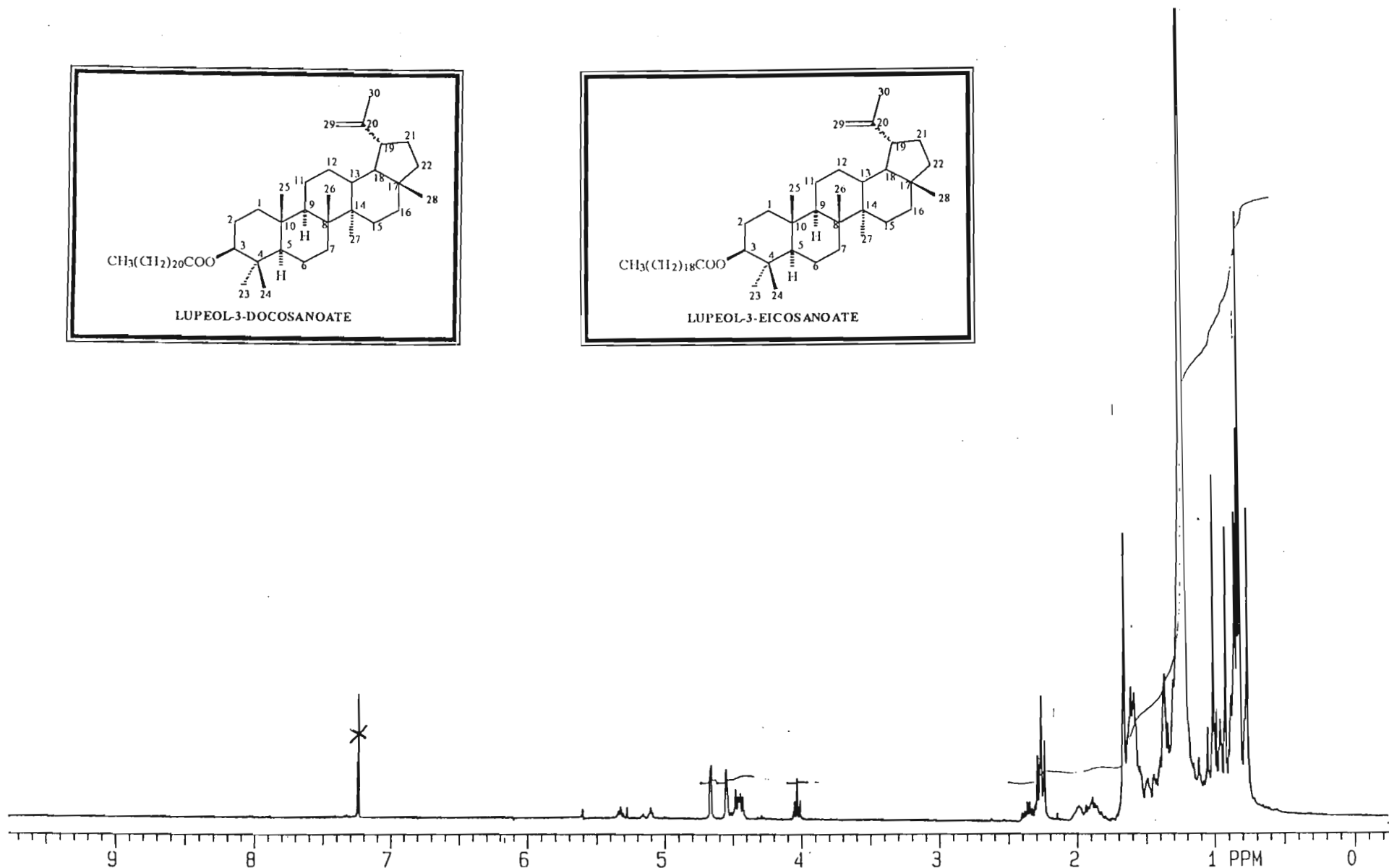
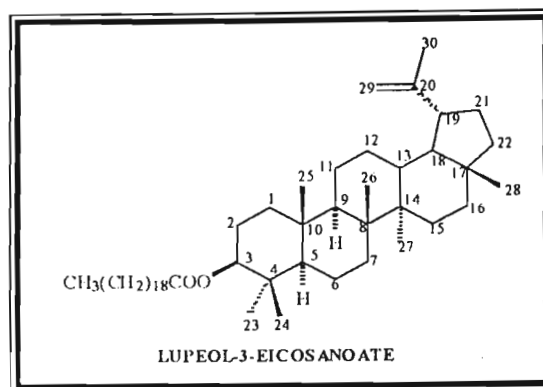
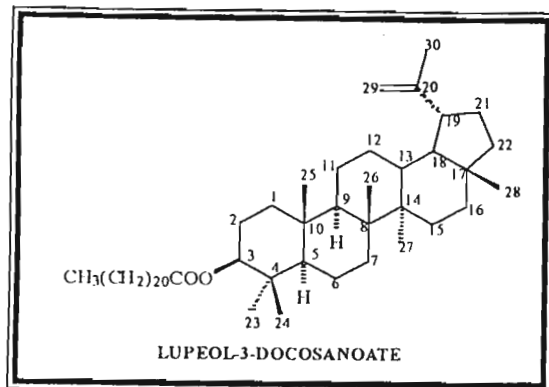
Spectrum 7a: ^1H NMR spectrum of compound VII.



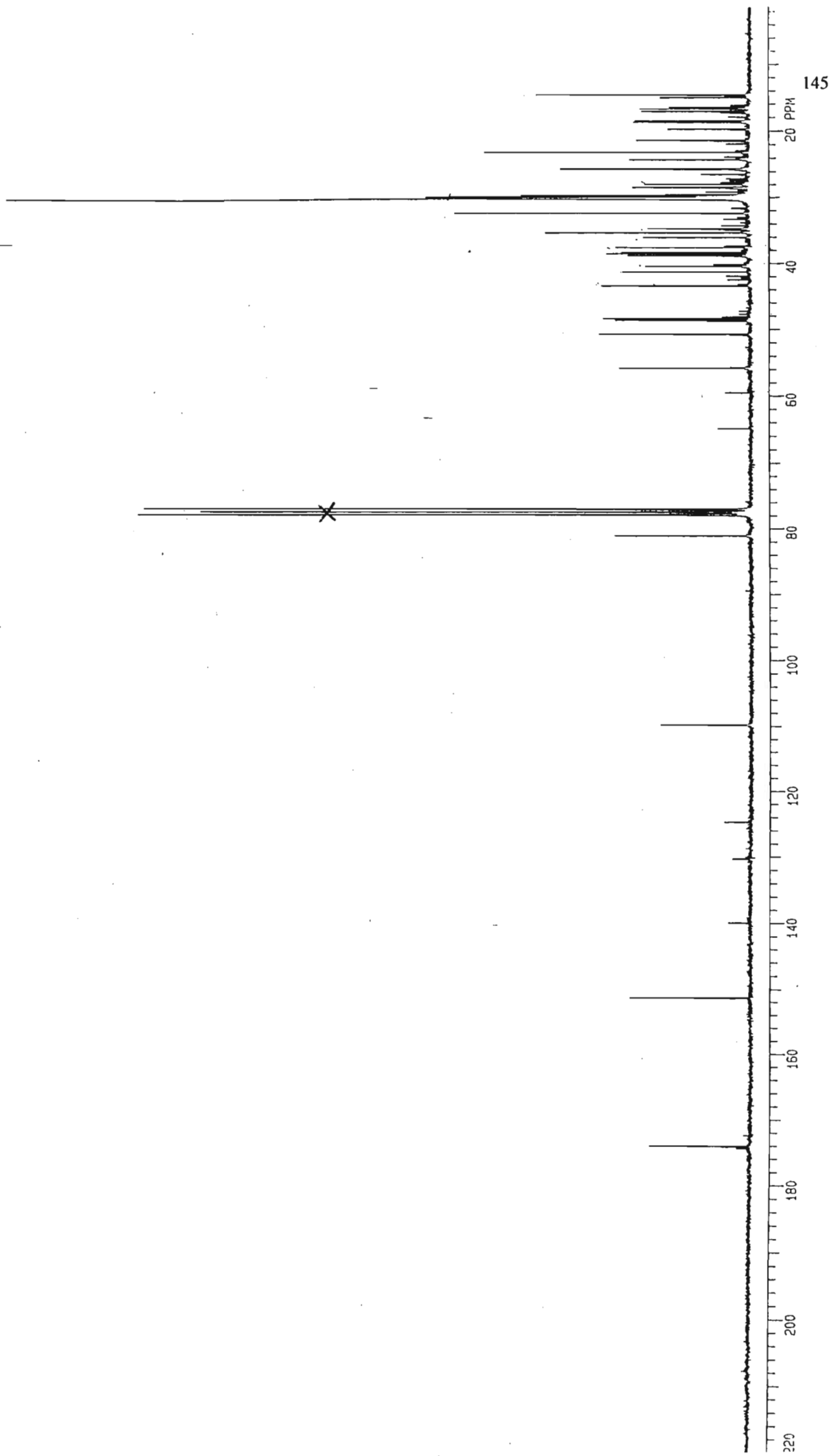
Spectrum 7b: ^{13}C NMR spectrum of compound VII.



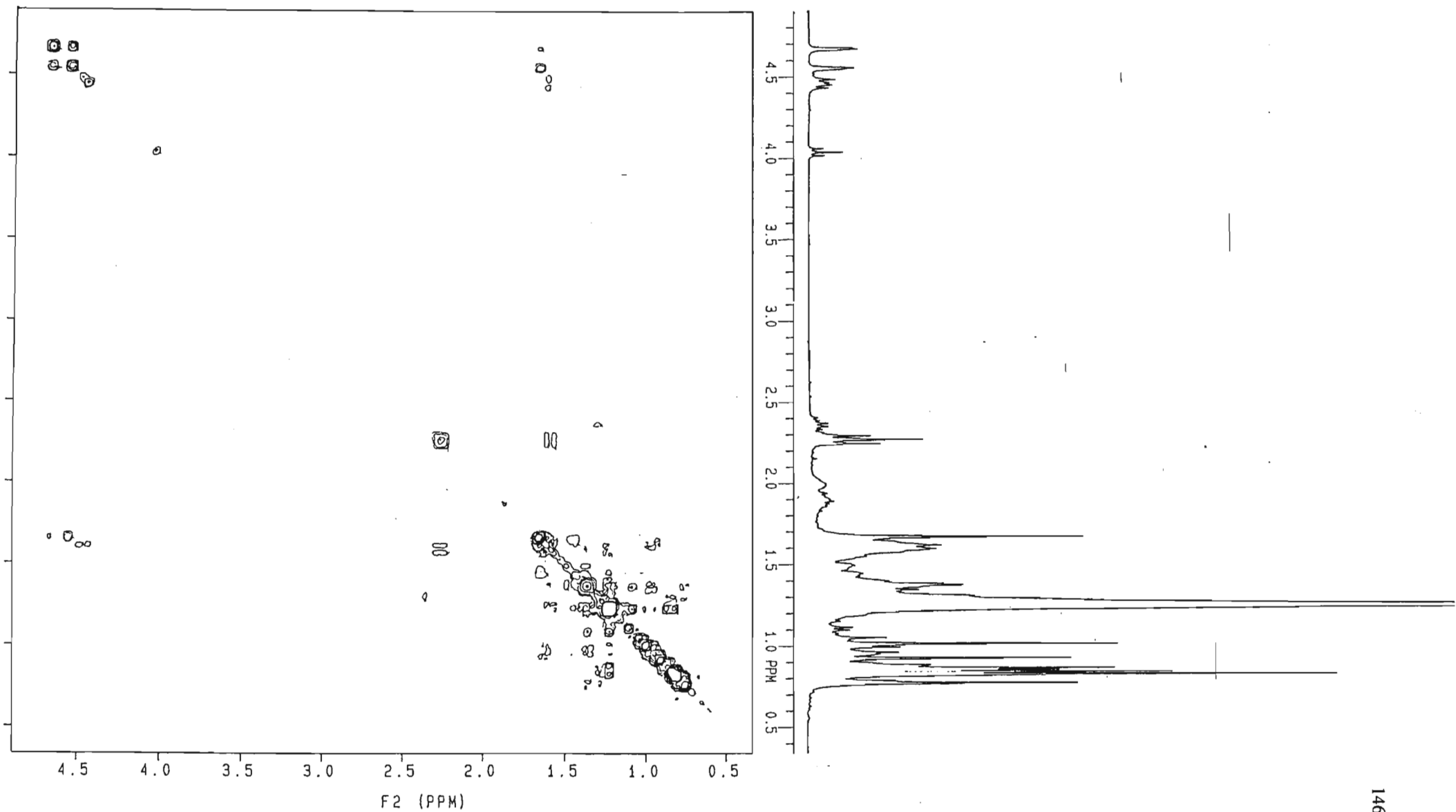
Spectrum 7c: Infra red spectrum of compound VII.



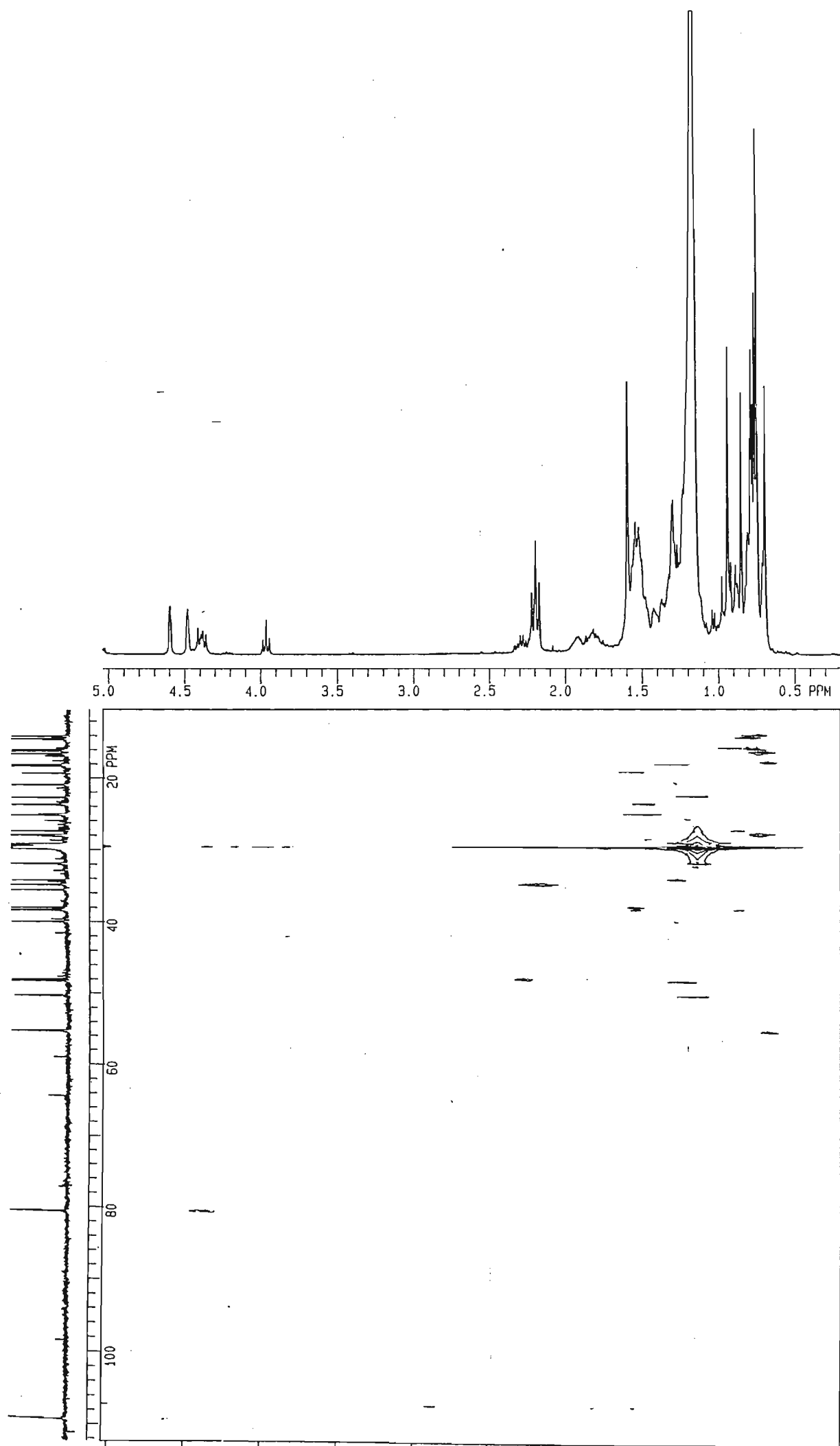
Spectrum 8a: ¹H NMR spectrum of compound VIII and IX.



Spectrum 8b: ^{13}C NMR spectrum of compound VIII and IX.

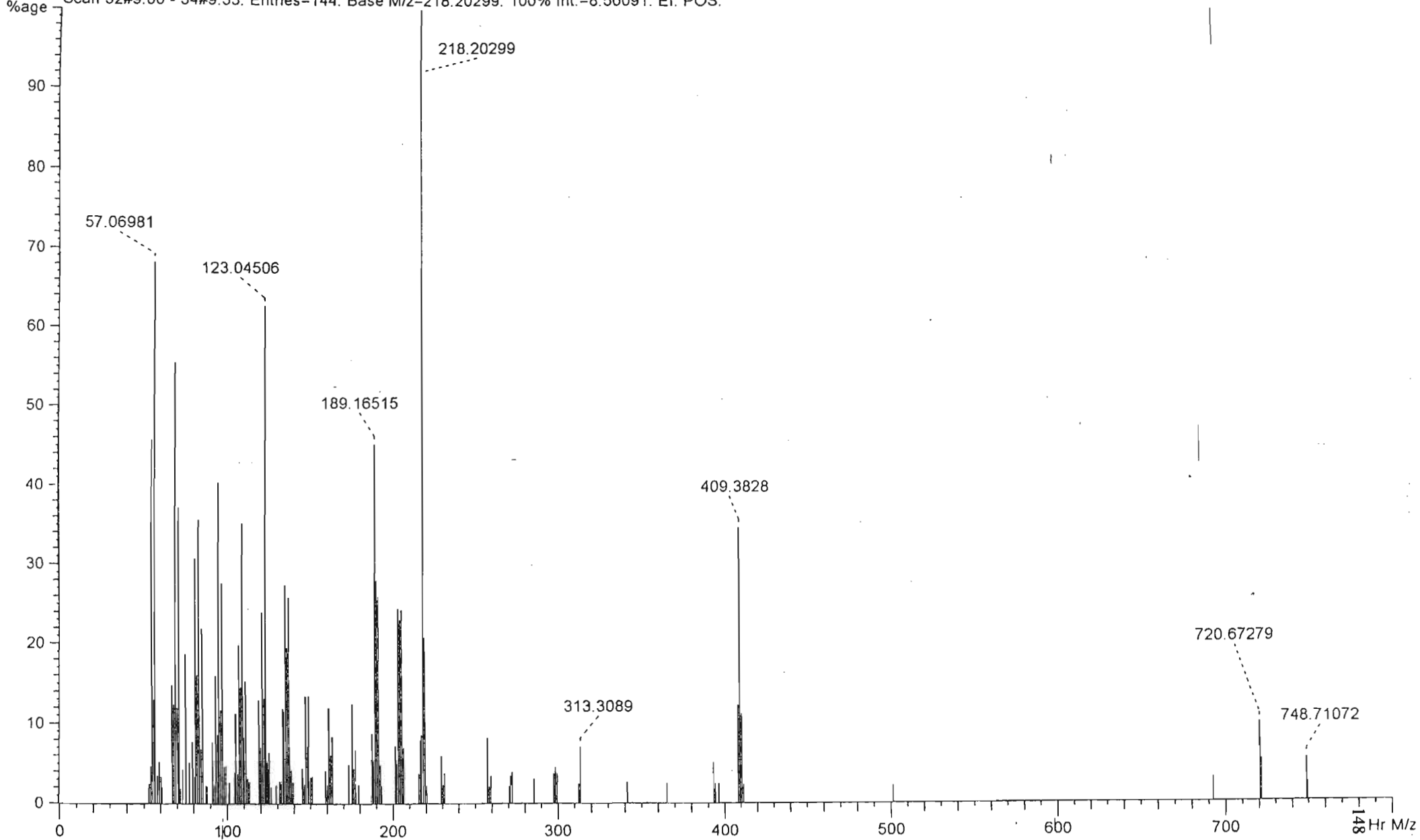


Spectrum 8c: COSY spectrum of compound VIII and IX.

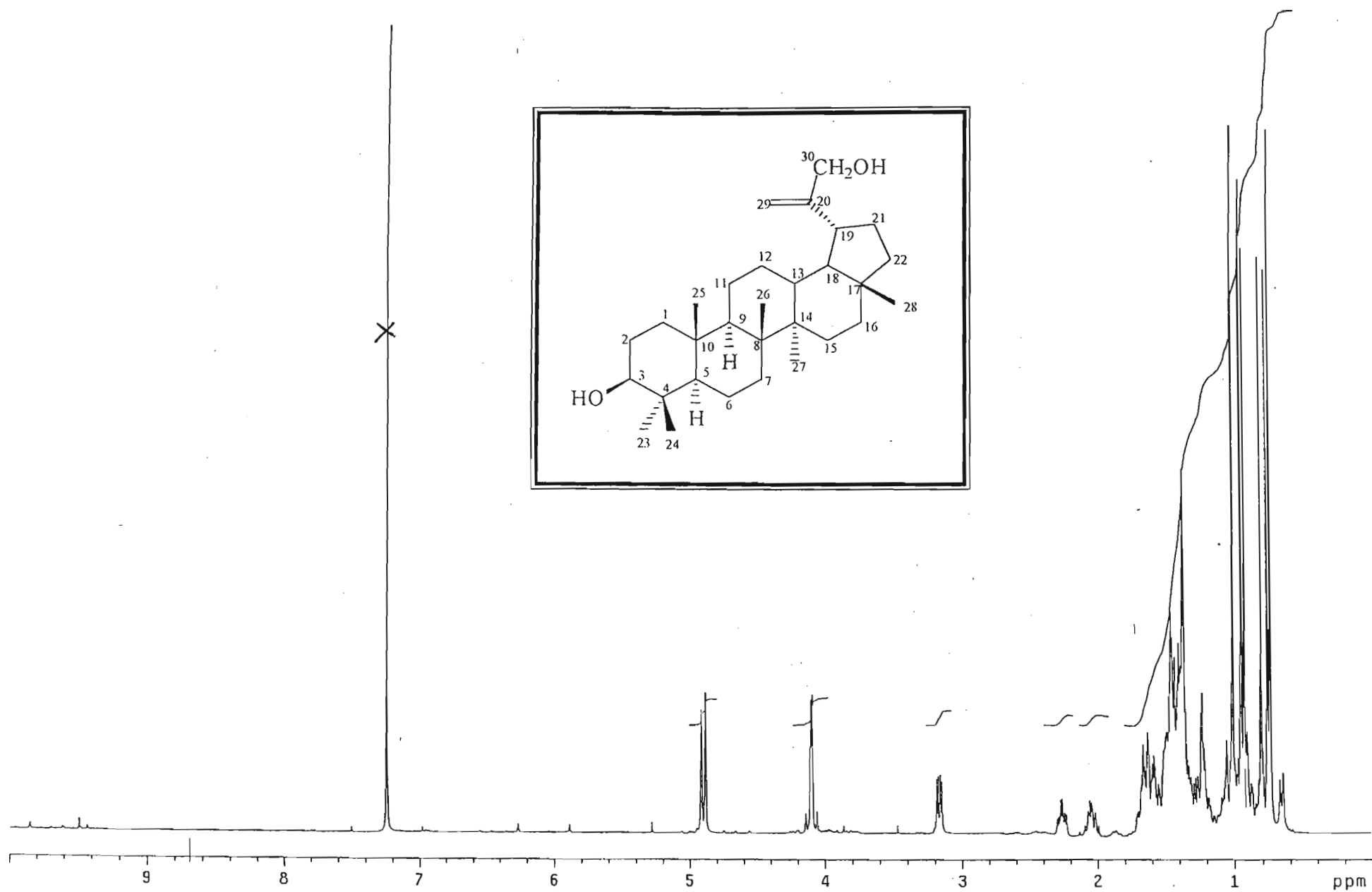


Spectrum 8d: HETCOR spectrum of compound VIII and IX.

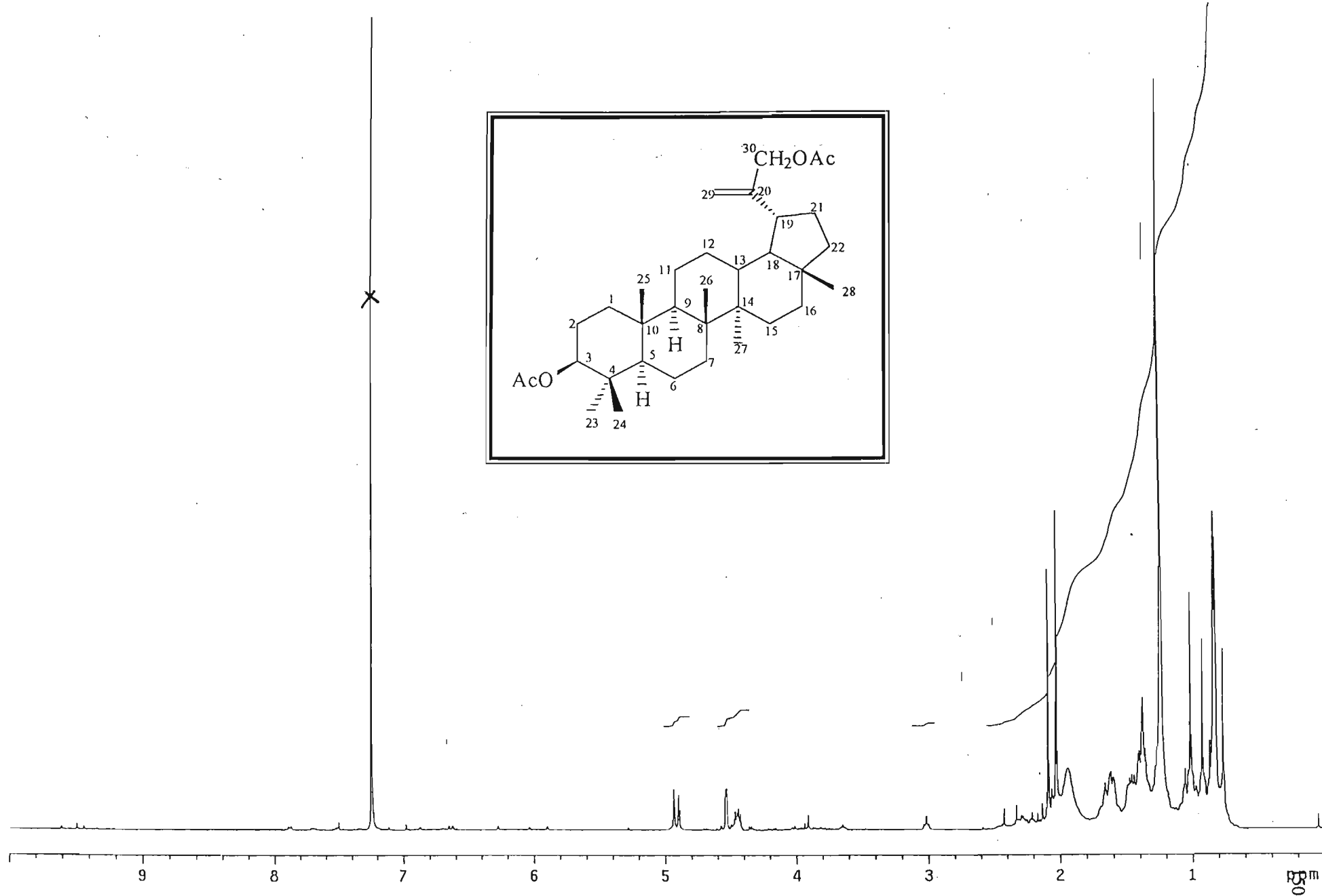
Scan 32#9:00 - 34#9:33. Entries=144. Base M/z=218.20299. 100% Int.=8.50091. EI. POS.



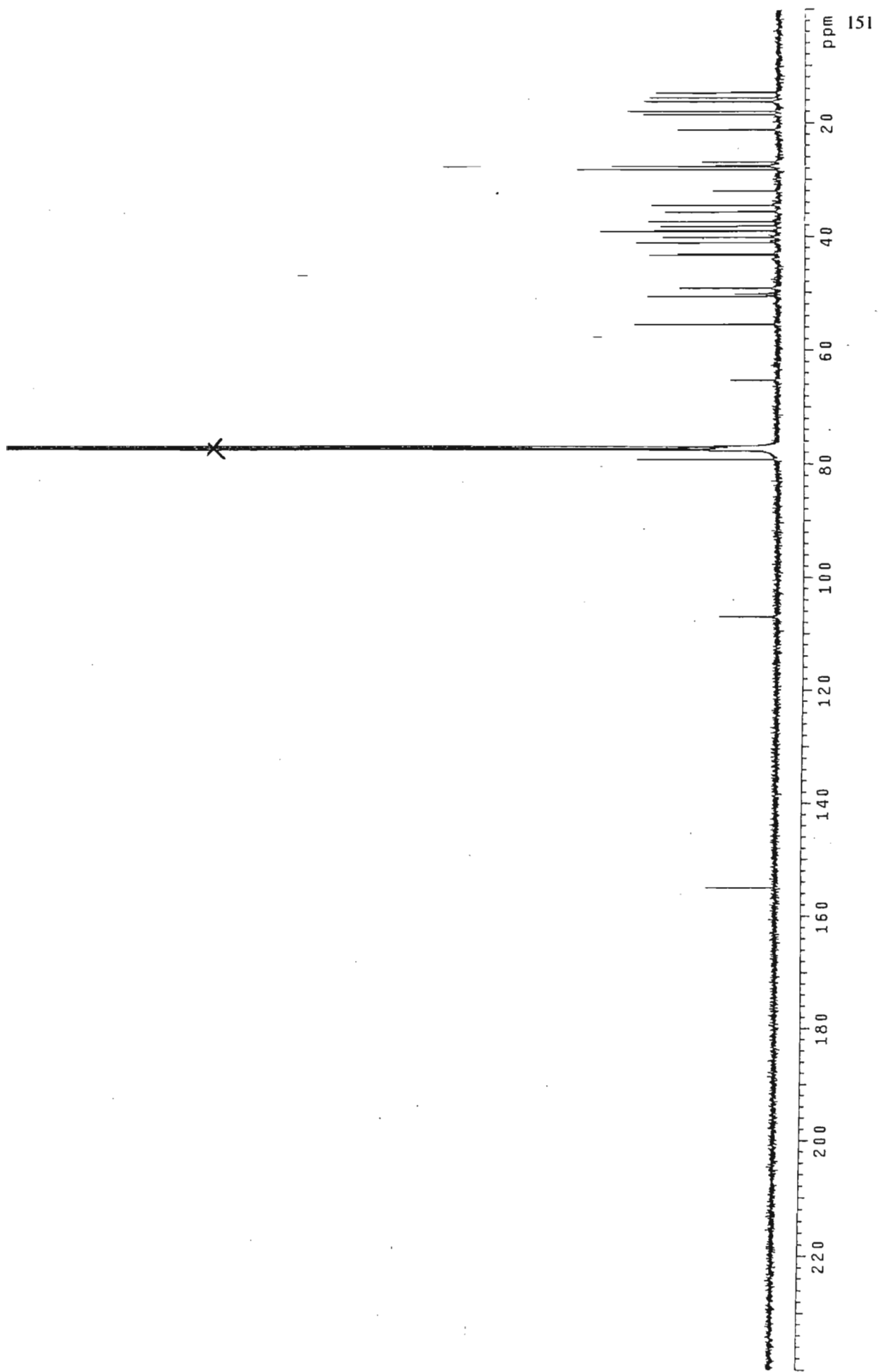
Spectrum 9a: High resolution mass spectrum of compound VIII and IX.



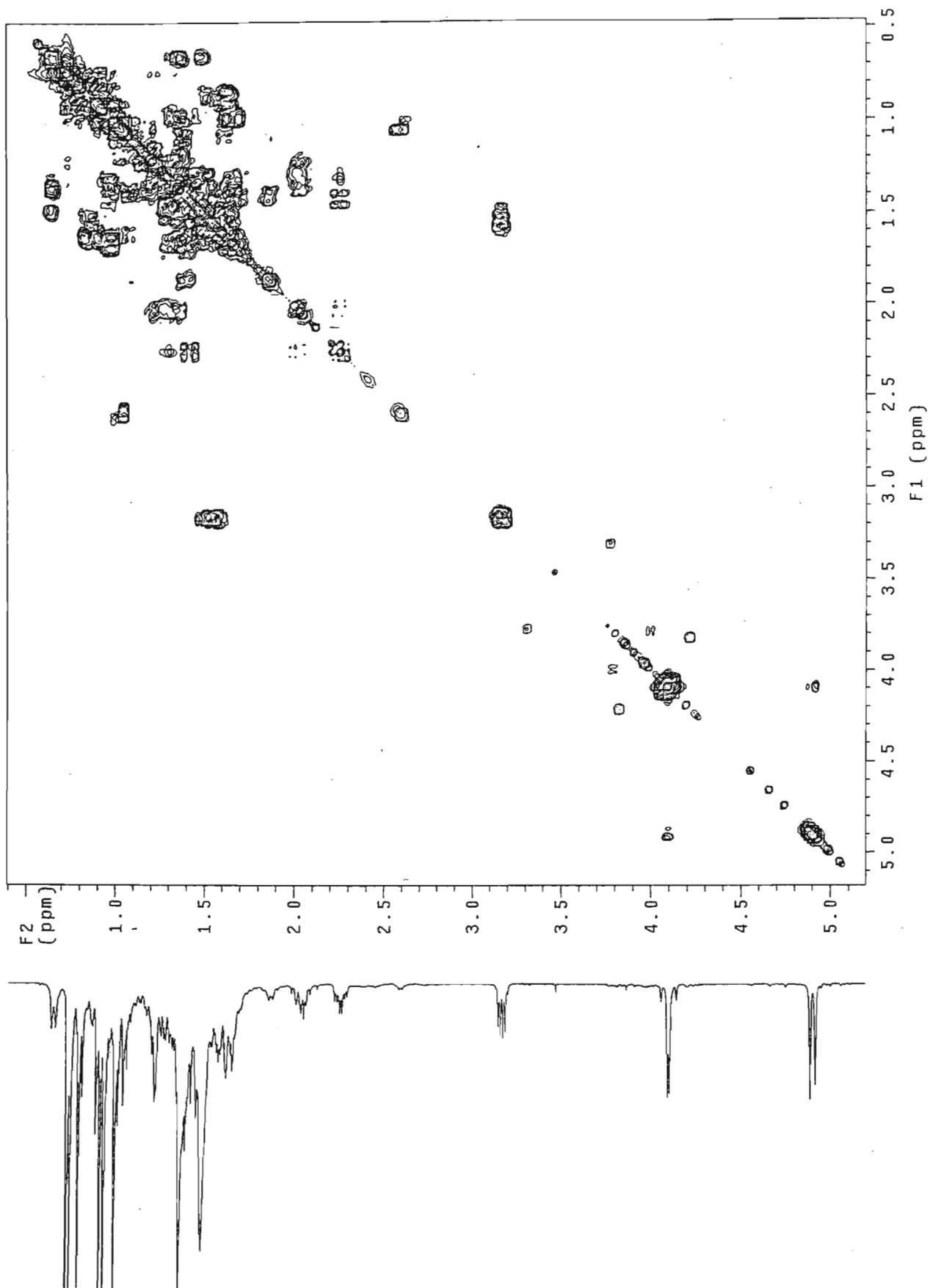
Spectrum 10a: ^1H NMR spectrum of compound X.



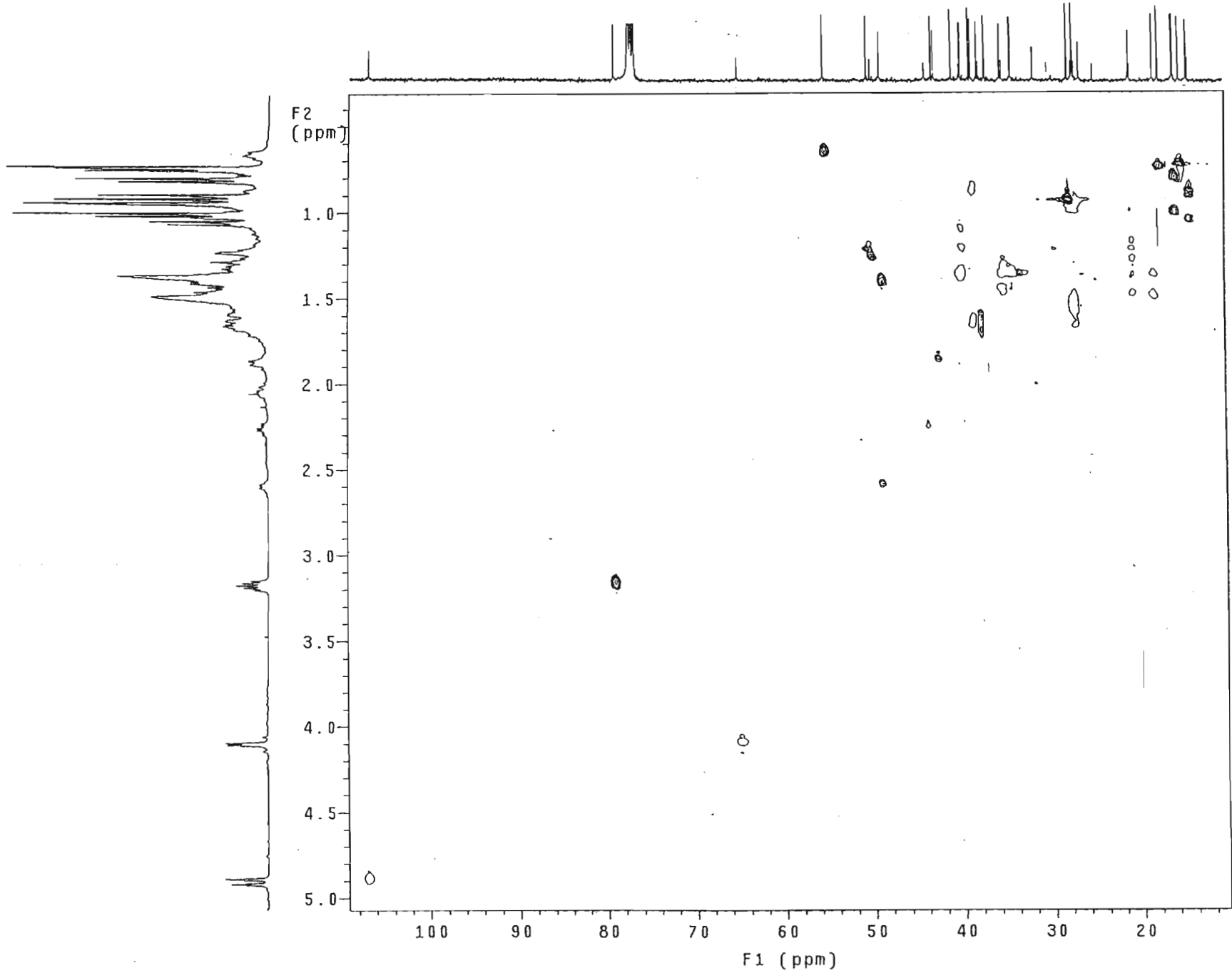
Spectrum 10b: ¹H NMR spectrum of acetylated compound X.



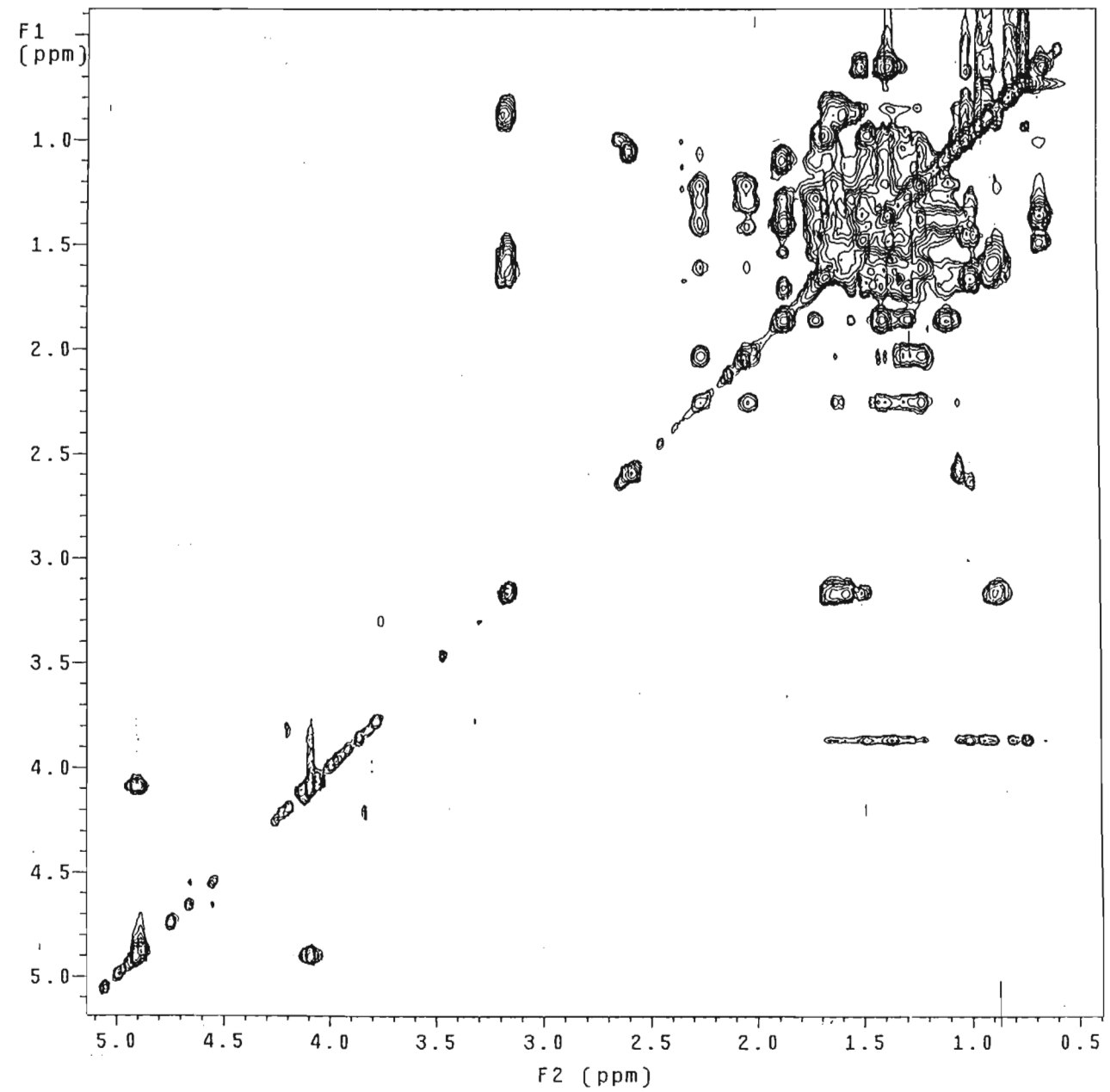
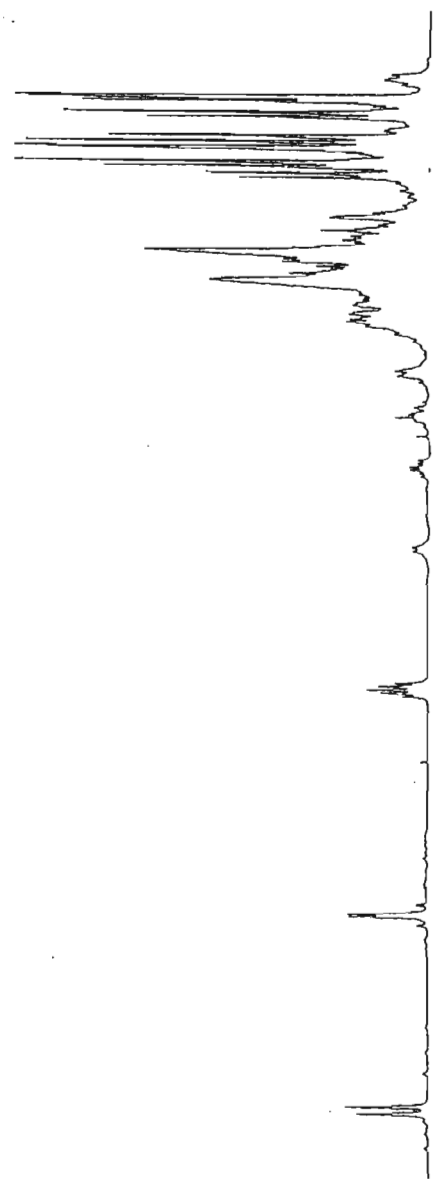
Spectrum 10c: ^{13}C NMR spectrum of compound X.



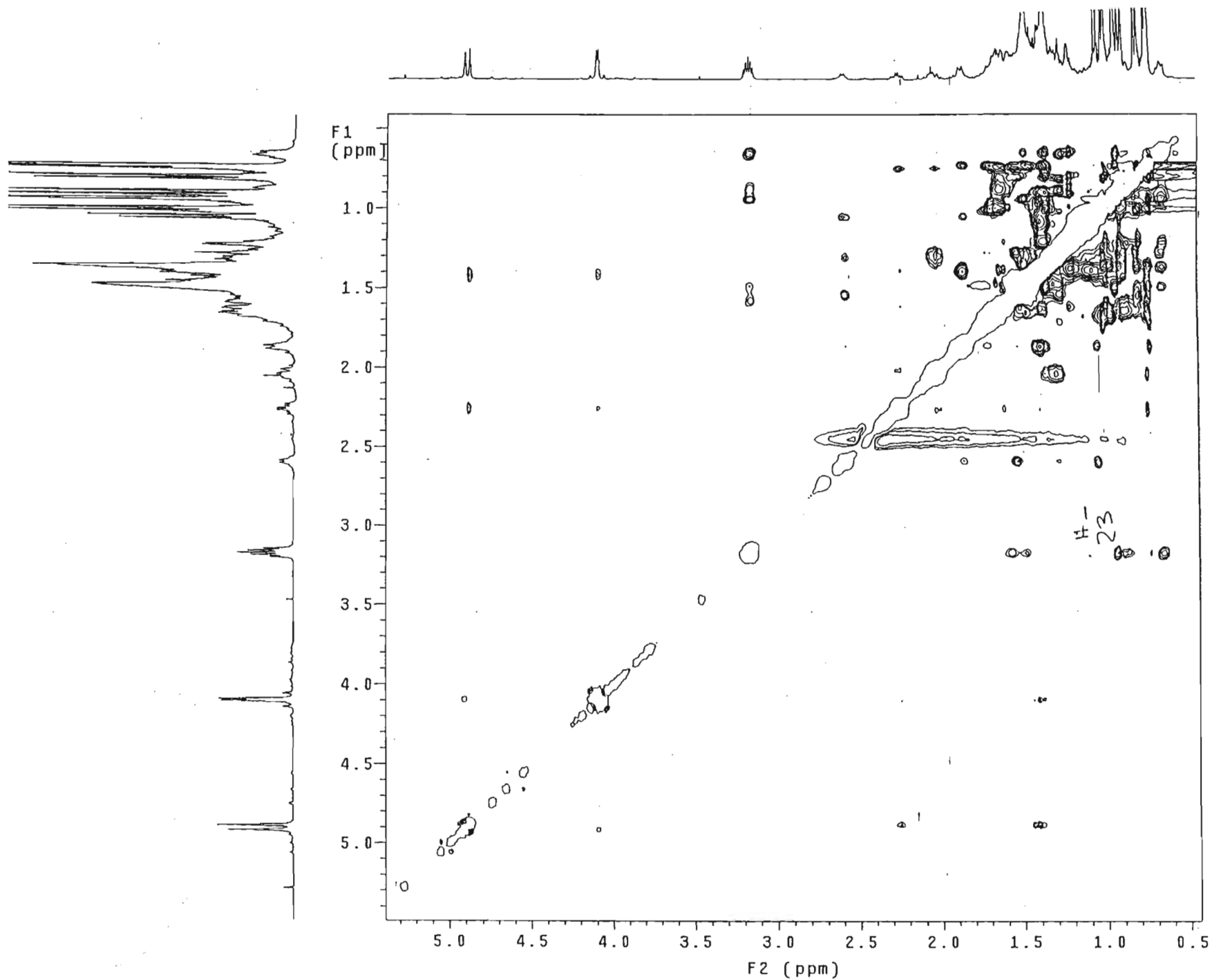
Spectrum 10d: COSY spectrum of compound X.



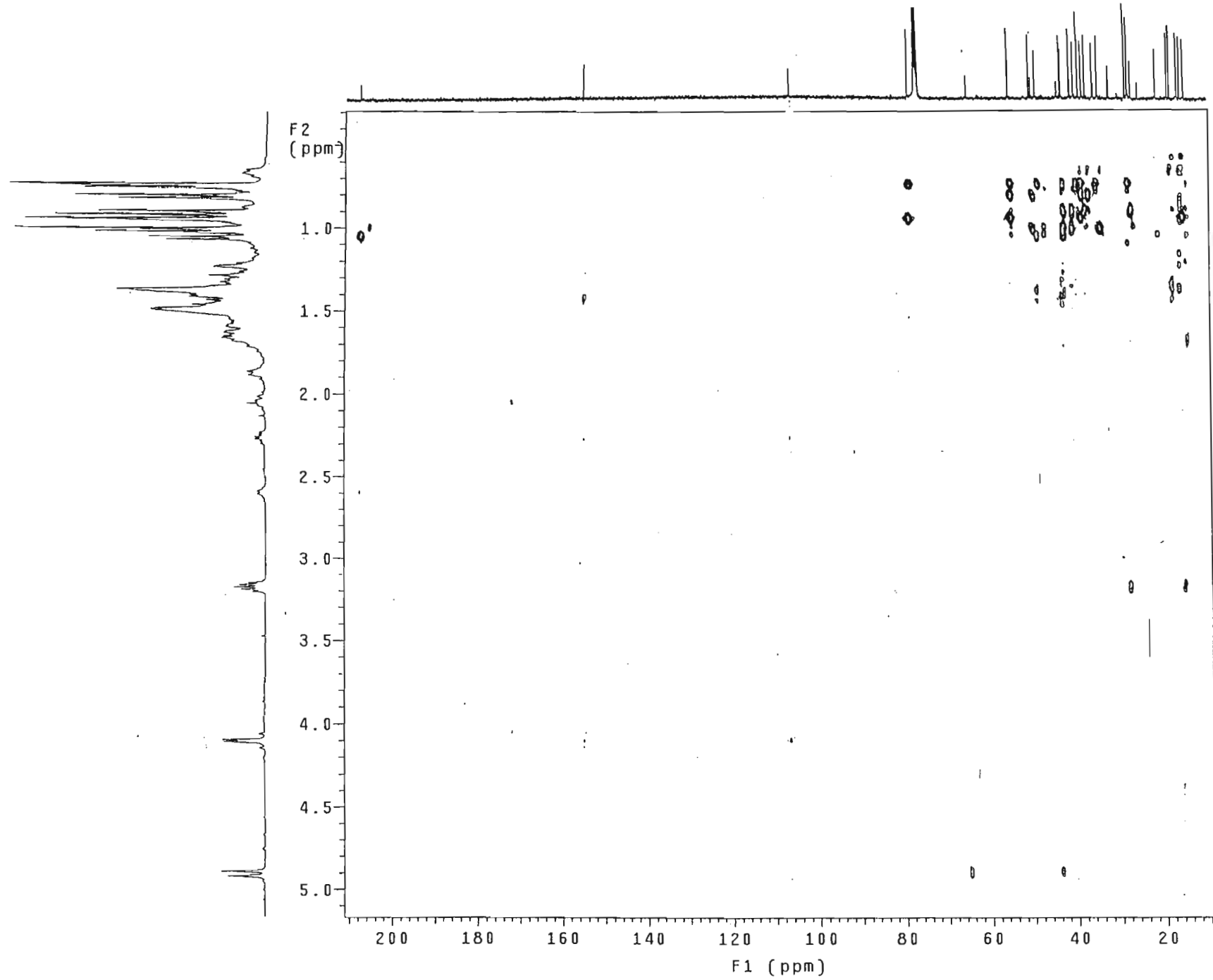
Spectrum 10e: HSQC spectrum of compound X.



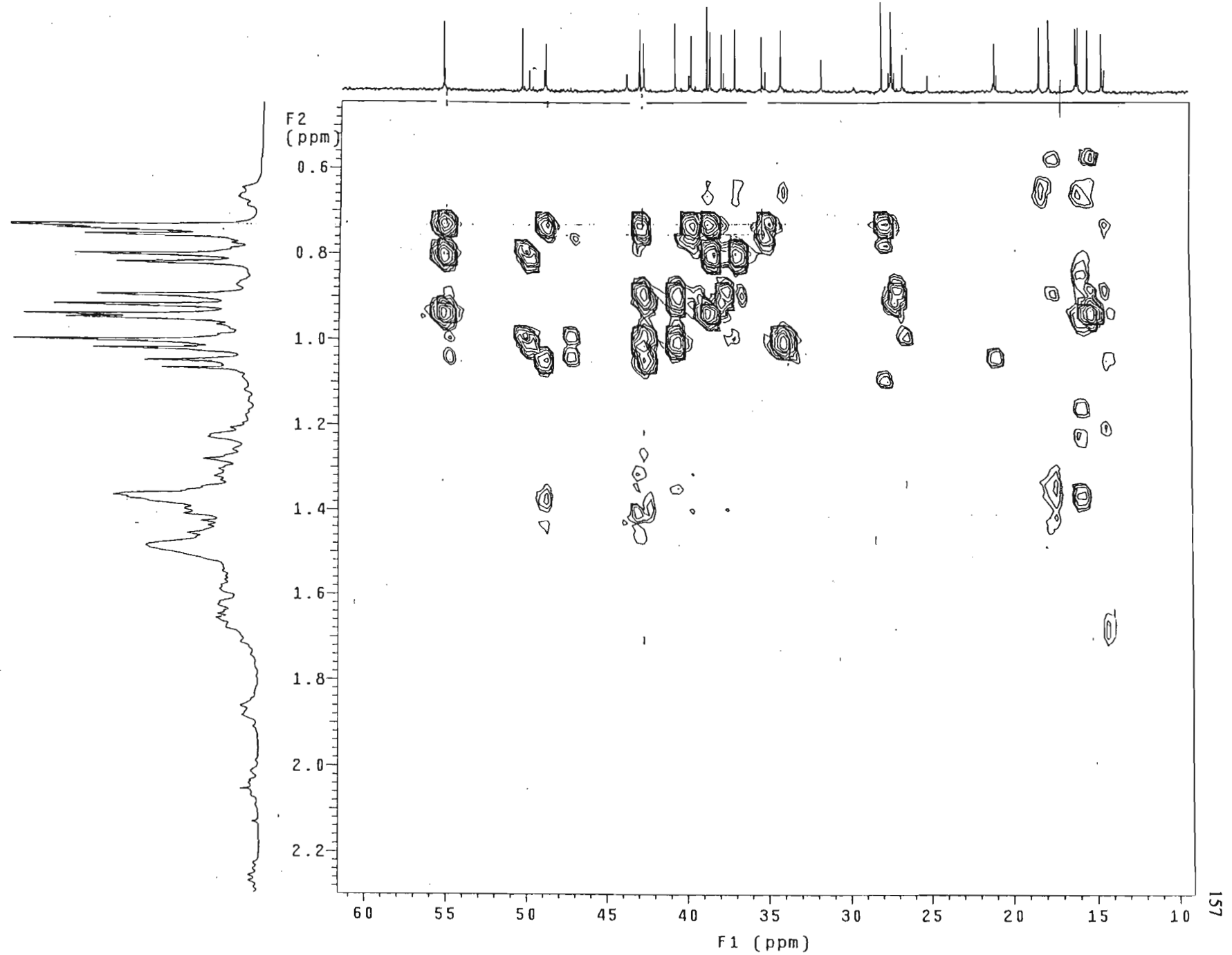
Spectrum 10f: TOCSY spectrum of compound X.



Spectrum 10g: NOESY spectrum of compound X.

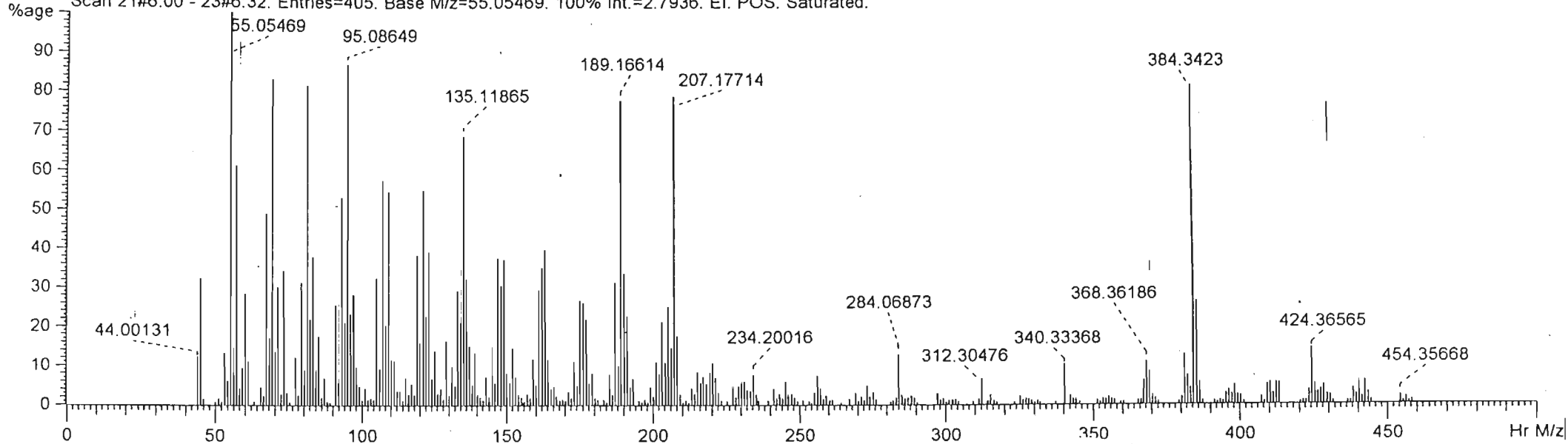


Spectrum 10h: HMBC spectrum of compound X.

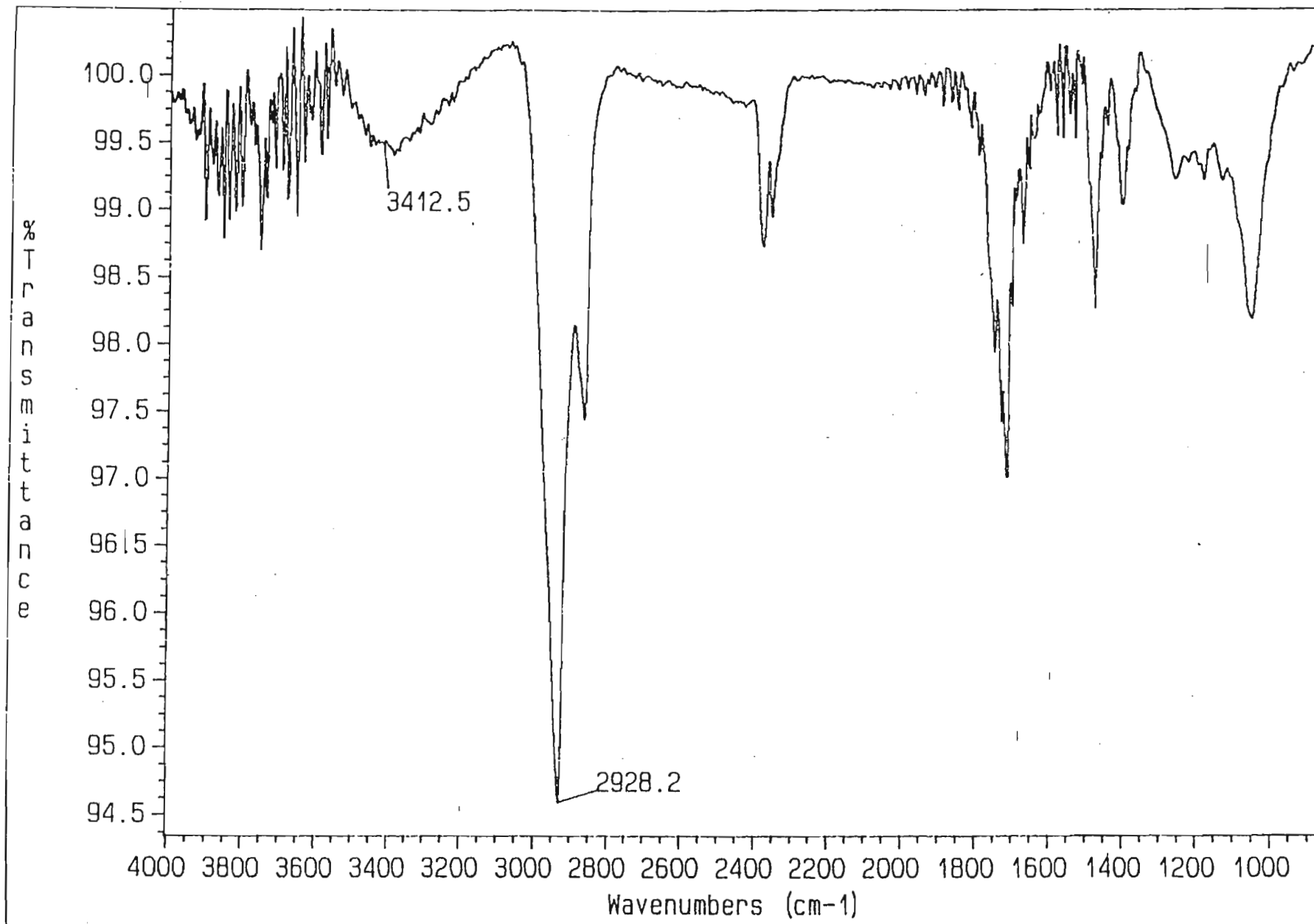


Spectrum 10i: Expanded HMBC spectrum of compound X.

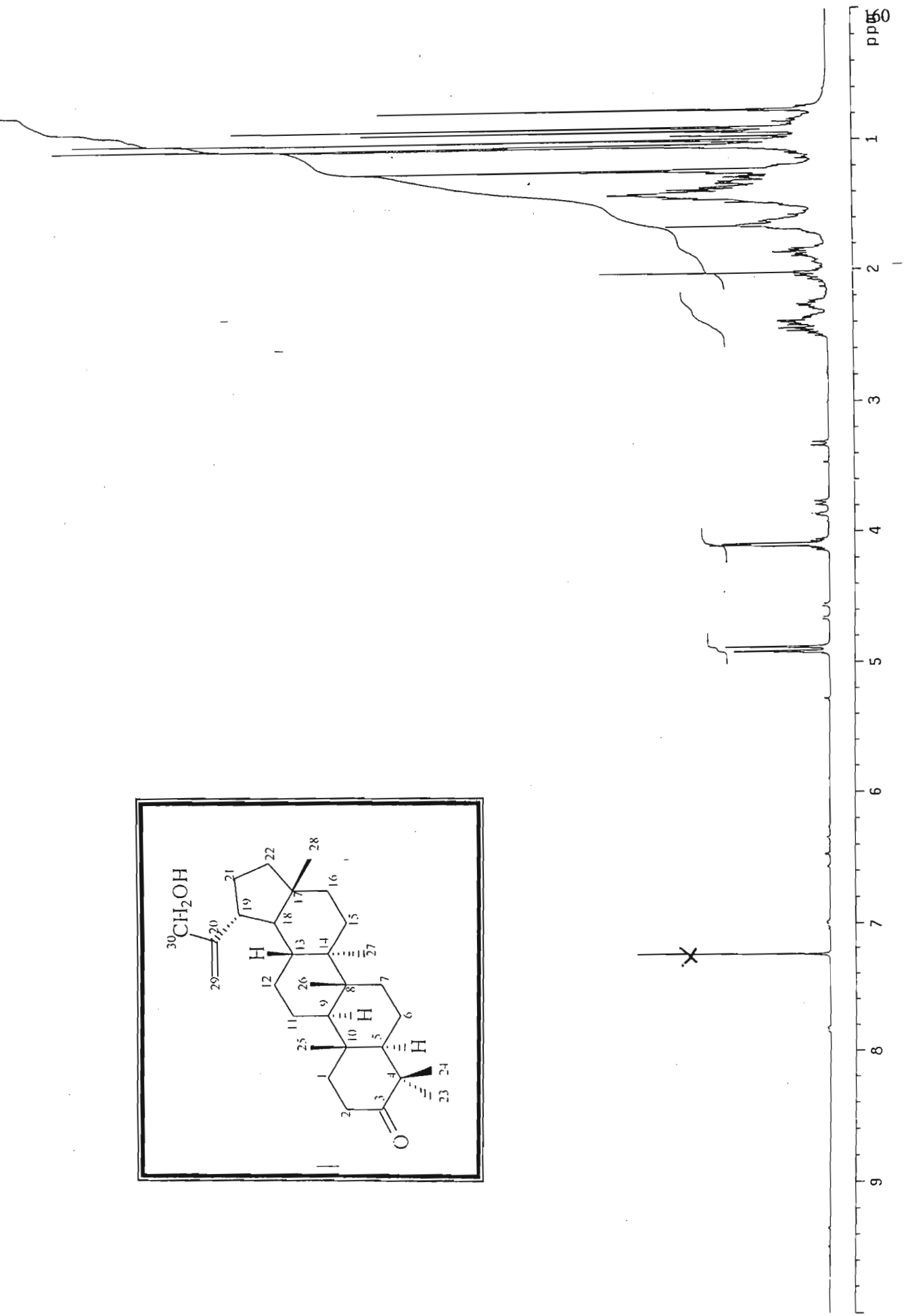
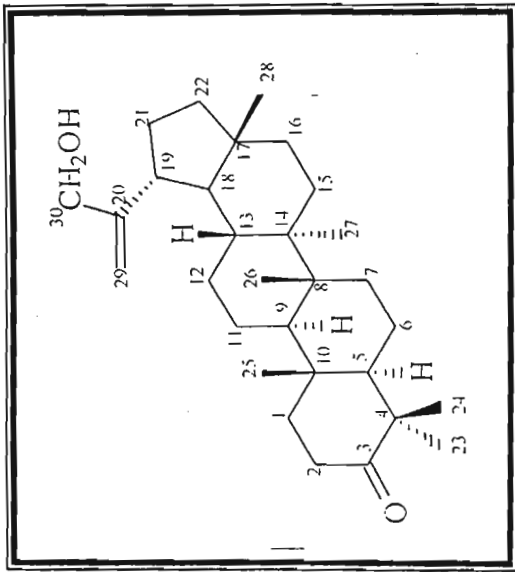
SCAN GRAPH. Flagging=Hr M/z. Filter=[Int:0.5%. Range:0-460. Excl: Ref/Ex.].
Scan 21#6:00 - 23#6:32. Entries=405. Base M/z=55.05469. 100% Int.=2.7936. EI. POS. Saturated.



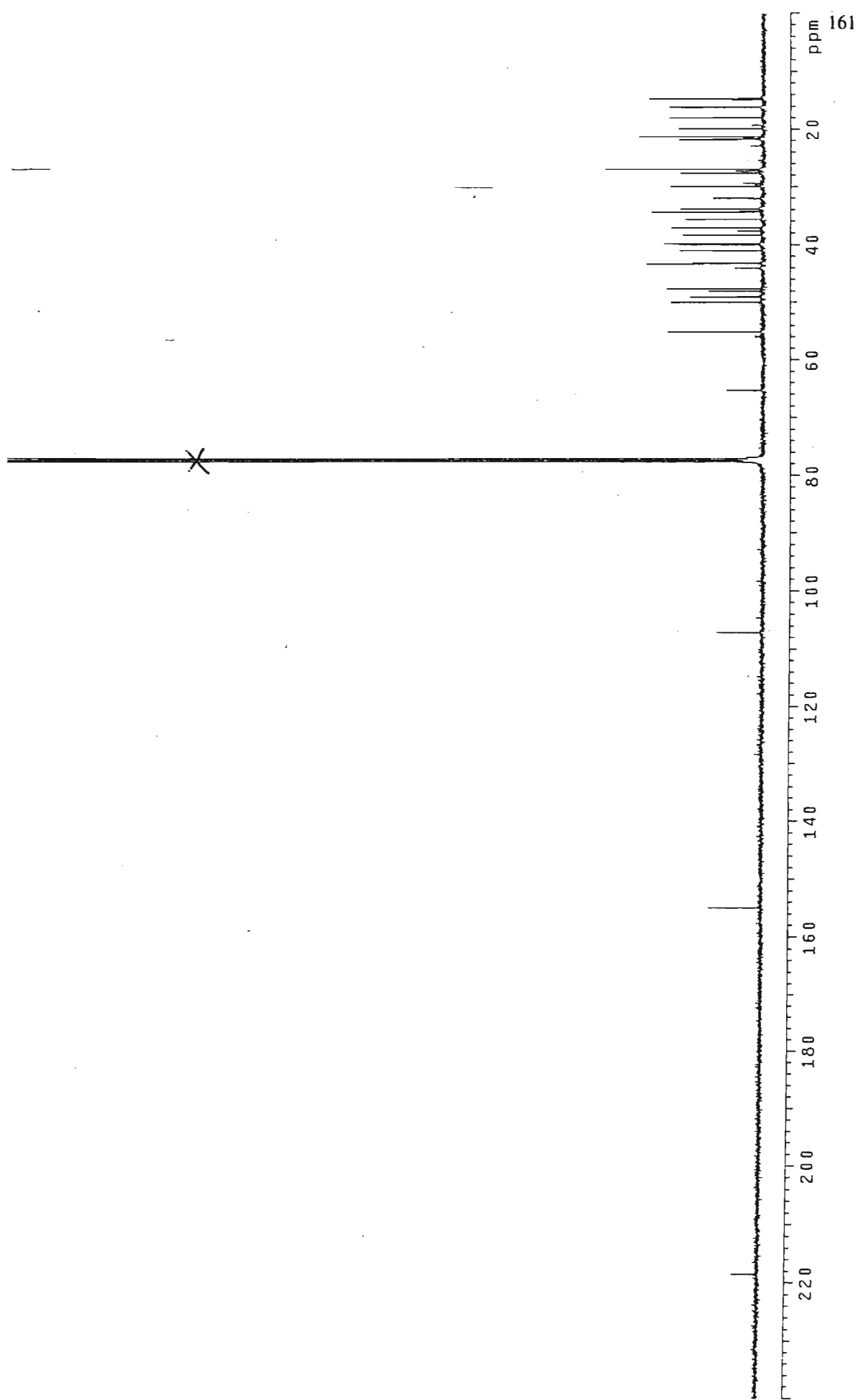
Spectrum 10j: High resolution mass spectrum of compound X.



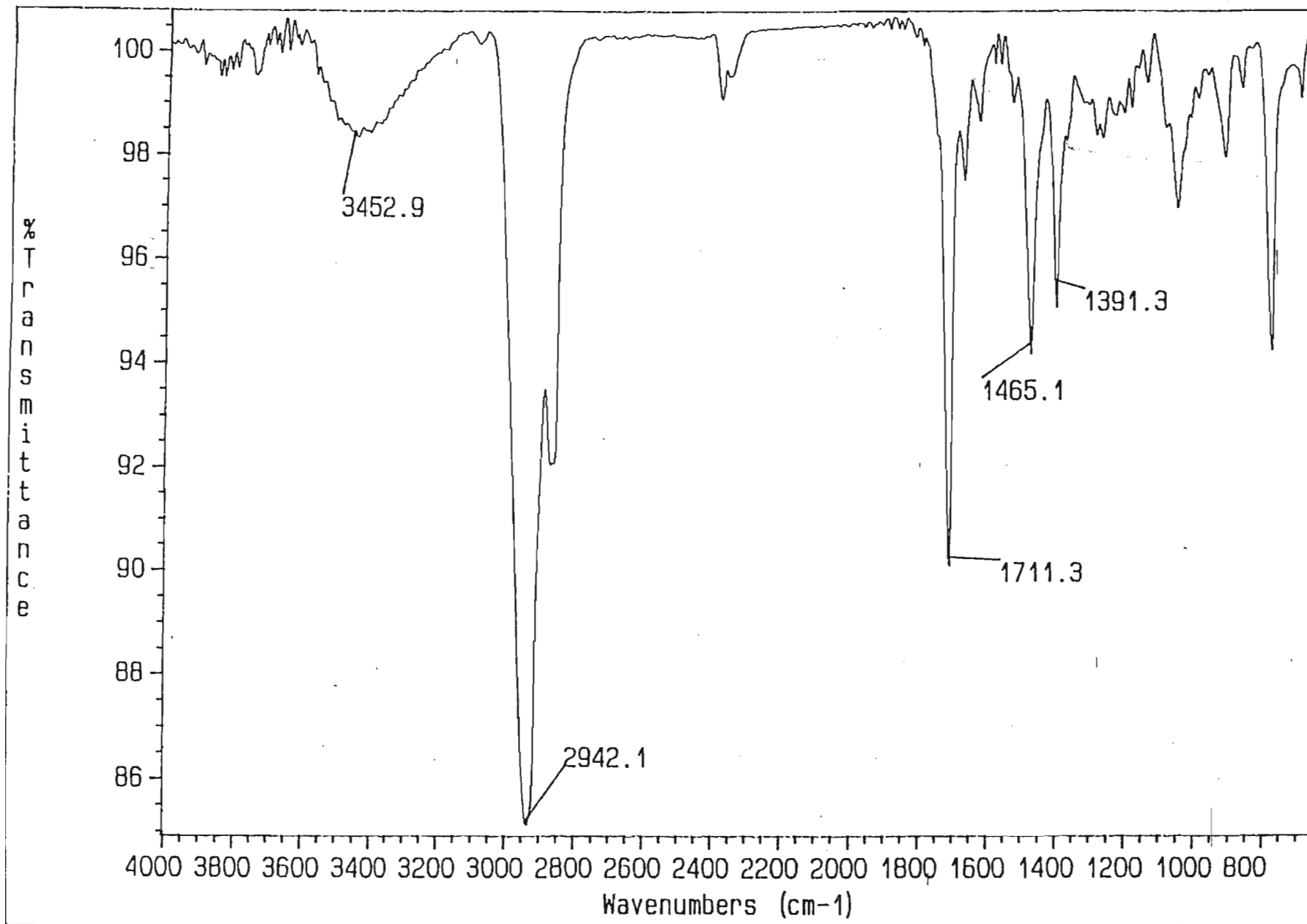
Spectrum 10k: Infra red spectrum of compound X.



Spectrum 11a: ^1H NMR spectrum of compound XI.



Spectrum 11b: ^{13}C NMR spectrum of compound XI.



Spectrum 11c: Infra red spectrum of compound XI.